Soil organic matter dynamics in the Siberian Kulunda steppe

Von der Naturwissenschaftlichen Fakultät der

Gottfried Wilhelm Leibniz Universität Hannover

zur Erlangung des Grades

Doktor der Naturwissenschaften (Dr. rer. nat.)

genehmigte Dissertation

von

Norbert Eberhard Stefan Bischoff, Diplom-Geograph

[2017]

Referent: Prof. Dr. rer. nat. Georg Guggenberger

Korreferent: Prof. Dr. rer. nat. Robert Mikutta

Tag der Promotion: 06. Juli 2017

Acknowledgements

First, I would like to thank both of my supervisors, Prof. Dr. Georg Guggenberger and Prof. Dr. Robert Mikutta, for teaching me scientific working and giving me the opportunity to dive into science. They showed me what a good scientist is and were always open for discussions. I am thankful to Prof. Dr. Gerald Kuhnt for filling in the function of a chairman. I thank the KULUNDA project in whose framework this thesis was accomplished and I am grateful to the entire project team for great team spirit, good collaboration and unforgettable experiences during field work. Thanks to all my colleagues from the Institute of Soil Science at the Leibniz University Hannover, who made my life at the institute a wonderful experience. I particularly acknowledge Hilal Alemdar, Silke Bokeloh, Elke Eichmann-Prusch, Ulrieke Pieper, Heike Steffen, Roger-Michael Klatt, Pieter Wiese, and "Herr Walther" for their great assistance in the laboratory. Dr. Leopold Sauheitl is acknowledged for his excellent guidance in the lab. I am thankful to my PhD colleagues for fruitful discussions and nice coffee breaks or evenings at the barbecue with nice conversations. Special thanks go to my office mates, Norman Gentsch and Robert Strey, who were just like close friends and with whom I always fell into discussions about the latest scientific articles or new statistical methods. I also appreciate the wonderful and traditional lunch breaks with the "Kellerkinder". I am grateful to Dr. Frank Schaarschmidt for taking the time to show me statistics and discuss methodological approaches and problems. Thank you to Janine, Ksenia, Susi, and Daniel for proofreading certain parts of this thesis. Particularly acknowledged are my flatmates at home who spend relaxed times with me and accompanied me during great experiences beside work. I thank all my good friends for being there when I needed them and which therefore supported this work importantly. I am grateful to my dear girlfriend Ksenia for making me feel home and making me laugh after a hard day. I am deeply grateful to my lovely parents for supporting me during my life and making all of that possible. I am much obliged to everybody who helped me to realize that work!

Abstract

The Kulunda steppe is situated within the West Siberian Plain and part of the greatest conversion areas of the world, where 420,000 km^2 grassland were converted into cropland between 1954 and 1963. The area is under intensive agricultural management as it includes some of the most fertile soils worldwide, i.e. mainly Chernozems and Kastanozems, but also salt-affected soils such as Solonchaks occur frequently. Research on soil organic matter (OM) dynamics in the Siberian steppes yet attained little attention, while most of the studies dealing with OM stabilization mechanisms in steppe soils focused on the North American Great Plains. This is surprising, as the Siberian conversion areas are even larger than those of the Great Plains. Moreover, given the growing importance of salt-affected soils due to the expansion of arid and semi-arid environments in the course of climate change, more attention should be paid to the study of OM dynamics in these soils. Soil OM is an important repository in the global carbon (C) cycle and the sequestration of soil organic C (OC) was proposed as an effective strategy to mitigate climate change and enhance food security. On the other hand, inorganic C (IC) may significantly contribute to the total C storage particularly in steppe soils. Declining OC stocks due to land-use change (LUC) from grassland to cropland were observed in the North American prairies, but little is known about the effect of grassland to cropland conversion on soil OM in the Siberian steppes and particularly how these effects will be affected by climate change. This thesis, therefore, was set out to elucidate the effect of grassland to cropland conversion on the quantity and quality of soil OM under various climatic conditions in the Siberian steppes and highlight OM stabilization mechanisms which control the potential loss of soil OM upon LUC. Moreover, OM dynamics in salt-affected soils were studied and the role of IC in terms of C sequestration was discussed. This was achieved by means of three studies dealing with OM dynamics and an additional analysis considering IC.

In the first study, typical arable soils (Chernozems and Kastanozems) of the Kulunda steppe under different land-use (grassland *vs.* cropland) were investigated in a paired plot design along a climatic gradient from the forest steppe over the typical steppe to the dry steppe. We determined OC stocks down to 60cm depth and the amount and ^{14}C activity of OC stored in density-separated OM fractions (light fraction < 1.6 g cm^{-3} < heavy fraction), while the analysis of phospholipid fatty acids (PLFA) elucidated microbial community compositions and fungi : bacteria ratios which were related to estimations of aggregate stability.

In a second study, we tested the potential stabilization of macro-aggregate occluded OM under varying land-use duration and intensity by comparing OC mineralization rates of dry-sieved intact (250–2000 µm) and crushed (<250 µm) macro-aggregates along two agricultural chronosequences in a long-term incubation (401 days, 20°C, 60% water holding capacity). Additionally, bulk soil (<2000 µm) was incubated to identify the effect of increasing land-use

duration on a fast and slow soil OC pool, as determined by fitting exponential decay models to incubation data.

The third study was performed to elucidate the effect of increasing salinity and sodicity on soil OM dynamics by assessing OC stocks and the quantity and quality of particulate and mineral-associated OM along a soil salinity gradient in the dry steppe. Neutral sugar contents and C isotopic compositions (δ^{13}C, ^{14}C activity) were measured in density-separated OM fractions (ρ = 1.6 g cm^{-3}), while above-ground biomass measurements indicated plant growth and PLFA analysis elucidated microbial community compositions.

In an additional analysis of the entire data set across all three studies the percentage of IC was calculated in the total C stocks and its role in terms of C sequestration was discussed.

The overall hypotheses were: (i) OC stocks decrease with aridity, while the percentage of particulate OC increases concurrently, (ii) LUC from grassland to cropland reduces soil OC stocks, with greater losses under arid conditions because of the larger proportion of mineralizable particulate OM, (iii) the LUC-induced decline of soil OC is mostly attributed to the destruction of macro-aggregates by tillage and the subsequent mineralization of previously occluded particulate OM, since macro-aggregate occluded OM is protected against decomposition, (iv) aggregate stability increases with fungal abundance, and (v) OC stocks decrease with salinity due to limited plant growth and consequently small soil OC inputs.

The results show that OC stocks decreased with aridity whereas the percentage of particulate OC increased concomitantly, thus confirming the first hypothesis. Land-use change from grassland to cropland reduced soil OC stocks by 31% in 0–25 cm (95% confidence interval: 17–43%) but this decline was independent from climate, hence, rejecting the second hypothesis. This was assigned to the fact that under all climatic conditions >90% of OC was stored in mineral-organic associations, while maximally 10% of OC existed in particulate OM. At the same time, most of the OC loss (80–90%) originated from mineral-bound OM and this loss was independent from climate. Together with high ^{14}C ages of mineral-bound OC in croplands (500–2,900 years B.P.) this result suggests that mineral-organic associations are heterogeneous and comprise both, labile OM components vulnerable to LUC but also stable OM protected against decomposition. In contrast to the third hypothesis, the LUC-induced decline of soil OC was not attributed to the break-down of macro-aggregates and the subsequent liberation and mineralization of macro-aggregate occluded OM, since OM mineralization rates of crushed macro-aggregates were similar to those of intact macro-aggregates during the incubation. This was assigned to the small proportion of particulate OM in the Siberian soils, which is supposed to be the dominant OM fraction protected by occlusion within macro-aggregates, while most of the LUC-induced OC loss originated from mineral-bound OM. Moreover, OM stabilization in mineral-organic associations or by occlusion of OM within micro-aggregates appeared to be more decisive than protection of OM within macro-aggregates. Contrary to the fourth hypotheses, fungal abundance was not related to aggregate stability, which was attributed to large OM and relatively high clay

contents in the Kulunda soils and a strong rooting of plants which all together stabilizes soil aggregates. PLFA-based microbial community compositions were more affected by climate than by LUC, while the relative abundance of fungi decreased with aridity with a concurrent increase of gram-positive bacteria. Remarkably, microbial community compositions were more similar under croplands than grasslands along the climatic gradient. These results indicate that climate change will alter microbial community compositions more than LUC, while the climatic effect is more pronounced in grasslands than in croplands. The fifth hypothesis was rejected since, surprisingly, OC stocks increased with salinity. This was ascribed to an adaptive plant community whose productivity, as determined by above-ground biomass, was unaffected by salinity, suggesting that soil OM inputs were not reduced under saline conditions. Similarly, PLFA-based microbial community compositions were nearly unaffected by salt occurrence and microbes appeared capable of decomposing OM in salt-affected soils at the same rate as in non-salt-affected soils, thus inhibiting the accumulation of particulate OM. At the same time, salinity-induced high ionic strength conditions fostered the formation of mineral-organic associations which consequently resulted in large soil OC stocks. High salinity superimposed the effect of sodicity, i.e. a dispersing effect of Na^+ on OM and mineral components was not detected, since large salt concentrations prompted the flocculation of soil constituents. Particularly in salt-affected soils IC contributed significantly to total C stocks and the largest total C stocks were observed in salt-affected soils. Based on theoretical considerations, IC corresponds to a C sink once it is dissolved by carbonate dissolution, discharged into the groundwater and subsequently translocated into the oceans. Under future drier climate conditions, dissolution of carbonates and subsequent groundwater recharge decreases in the region, hence, reducing the C sequestration potential via carbonate dissolution.

In conclusion, climate change will (i) reduce the C sequestration potential of the region by lowering OC stocks and limiting C sequestration via carbonate dissolution, (ii) not alter the negative effect of LUC on soil OM stocks, and (iii) shift microbial community compositions more than LUC. The loss of OC upon LUC is not assigned to the disruption of macro-aggregates by tillage and the subsequent release and mineralization of macro-aggregate occluded particulate OM but most of the lost OC originated from mineral-organic associations. A significant portion of OC in Siberian steppes is stored in salt-affected soils.

Keywords: Soil organic matter, Soil microbial community, Land-use change, Climate, Steppe soil, Salt-affected soil

Zusammenfassung

Die Kulundasteppe liegt in der Westsibirischen Tiefebene und ist Teil einer der größten Konversionsregionen der Erde. Zwischen 1954 und 1963 wurde hier etwa 420,000 km² Grasland in Ackerland umgebrochen. Die Region steht unter intensiver landwirtschaftlicher Nutzung da in ihr, mit Chernozemen und Kastanozemen, einige der fruchtbarsten Böden weltweit vorkommen. Auch salzbeeinflusste Böden, wie z. B. Solonchaks, treten aufgrund des trockenen Klimas häufig auf. Forschungen zur Dynamik der organischen Bodensubstanz (OBS) in Steppen fokussierten bisher vor allem die nordamerikanischen Prärien der Great Plains, während wenig über Stabilisierungsmechanismen der OBS in den sibirischen Steppen bekannt ist. Dies ist überraschend, da die sibirischen Konversionsregionen größer sind als jene der nordamerikanischen Prärien. Darüber hinaus werden Forschungen zur Dynamik der OBS in salzbeeinflussten Böden zunehmend wichtiger, da prognostiziert wird, dass diese Böden im Zuge des Klimawandels an Fläche gewinnen werden.

Die OBS ist ein wichtiger Speicher im globalen Kohlenstoffkreislauf und die Sequestrierung organischen Kohlenstoffs (OC) im Boden ist eine bedeutende Strategie zur Abschwächung des Klimawandels sowie zur Sicherung der globalen Nahrungsmittelproduktion. Insbesondere in Steppengebieten kann aber auch anorganischer Kohlenstoff (IC) einen großen Anteil am gesamten im Boden gespeicherten Kohlenstoff (C) ausmachen. Eine Abnahme der OBS infolge des Landnutzungswechsels von Grasland zu Ackerland wurde in den nordamerikanischen Prärien beobachtet, jedoch ist wenig darüber bekannt, wie sich dieser Landnutzungswechsel in den sibirischen Steppen auswirkte und im Zuge des Klimawandels weiter auswirken wird. Ziel dieser Arbeit war daher zu ermitteln, welchen Effekt der Graslandumbruch auf die Quantität und die Qualität der OBS in den sibirischen Steppen hat und inwieweit dieser Effekt durch klimatische Bedingungen beeinflusst wird. Weiterhin wurden Stabilisierungsmechanismen der OBS beleuchtet, welche den Verlust an OC infolge des Landnutzungswechsels entscheidend beeinflussen. In salzbeeinflussten Böden wurde die Dynamik der OBS untersucht, während für die gesamte Region die Rolle von IC für das C-Sequestrierungspotential diskutiert wurde. Umgesetzt wurde dies anhand von drei Studien welche quantitative und qualitative Parameter der OBS untersuchten sowie einer zusätzlichen Analyse welche die Rolle von IC aufzeigte.

In der ersten Studie wurden typische Ackerböden der Kulundasteppe (Chernozeme und Kastanozeme) unter verschiedener Landnutzung (Grasland vs. Ackerland) in einem *paired plot design* untersucht. Dies geschah entlang eines klimatischen Gradienten von der Waldsteppe über die Typische Steppe bis hin zur Trockensteppe. Es wurden OC-Vorräte bis 60cm Tiefe bestimmt sowie der Anteil und die ^{14}C-Aktivität des OC in verschiedenen dichteseparierten Fraktionen der OBS (leichte Fraktion < 1.6 g cm^{-3} < schwere Fraktion) ermittelt. Die Zusammensetzung der mikrobiellen Gemeinschaft wurde mittels Phospholipid-

Fettsäuren (PLFA) untersucht. Anhand der PLFA wurden Pilz : Bakterien Verhältnisse berechnet und diese in Zusammenhang mit Messungen der Aggregatstabilität gebracht.

In der zweiten Studie wurde die Stabilisierung der in Makroaggregaten okkludierten OBS in Abhängigkeit von Landnutzungsdauer und -intensität getestet. Dies erfolgte indem OC-Mineralisierungsraten trockengesiebter intakter (250–2000 µm) und zerstörter (<250 µm) Makroaggregate von zwei landwirtschaftlichen Chronosequenzen in einer Langzeitinkubation (401 Tage, 20°C, 60% Wasserhaltekapazität) miteinander verglichen wurden. Zusätzlich wurde Gesamtboden (<2000 µm) inkubiert, um den Effekt der Landnutzungsdauer auf einen rasch und einen langsam abbaubarer OC-Pool zu untersuchen, welche mittels Modellen des exponentiellen Abbaus der OBS gefittet wurden.

Eine dritte Studie wurde durchgeführt, um den Effekt zunehmender Salinität und Sodizität auf die Dynamik der OBS zu ermitteln. Es wurden OC-Vorräte sowie die Menge und Qualität partikulärer und mineral-assoziierter OBS entlang eines Salinitätsgradienten in der Trockensteppe bestimmt. Weiterhin wurden Neutralzuckergehalte und die isotopische Zusammensetzung (δ^{13}C, ^{14}C-Aktivität) der OBS in dichteseparierten OBS-Fraktionen (ρ = 1.6 g cm^{-3}) ermittelt. Messungen der oberirdischen pflanzlichen Biomasse gaben Aufschlüsse über das Pflanzenwachstum und die Analyse von PLFA erlaubte Einblicke in die Zusammensetzung der mikrobiellen Gemeinschaft.

In einer vierten zusätzlichen Analyse des Gesamtdatensatzes wurde der Anteil von IC am Gesamt-C entlang des klimatischen Gradienten und in den verschiedenen Bodentypen bestimmt, sowie dessen Rolle hinsichtlich des C-Sequestrierungspotentials aufgezeigt.

Die allgemeinen Hypothesen lauteten: (i) OC-Vorräte nehmen mit zunehmender Aridität ab, bei gleichzeitiger Erhöhung des relativen Anteils an partikulärem OC, (ii) der Landnutzungswechsel von Grasland zu Ackerland führt zu einer Abnahme der OC-Vorräte, wobei die Verluste größer unter ariden Bedingungen sind, da dort auch die Anteile leicht mineralisierbarer partikulärer OBS größer sind, (iii) die Abnahme der OBS infolge des Landnutzungswechsels ist vor allem auf die Zerstörung der Makroaggregate durch Bodenbearbeitung sowie die bevorzugte Mineralisierung der dabei frei werdenden makroaggregat-okkludierten OBS zurückzuführen, da die in Makroaggregaten okkludierte OBS vor Mineralisierung geschützt vorliegt, (iv) die Aggregatstabilität erhöht sich mit der Abundanz von Pilzen, und (v) OC-Vorräte nehmen mit zunehmender Salinität ab, da erhöhte Salzgehalte das Pflanzenwachstum einschränken und so zu einer Verringerung des Streueintrags führen.

Die Ergebnisse zeigen, dass, entsprechend der ersten Hypothese, die OC-Vorräte mit zunehmender Aridität abnehmen, während gleichzeitig der Anteil an partikulärem OC steigt. Der Landnutzungswechsel von Grasland zu Ackerland verringerte die OC-Vorräte um 31% in 0–25 cm (95% Konfidenzintervall: 17–43%), wobei diese Verluste unabhängig von den klimatischen Bedingungen waren, sodass die zweite Hypothese abgelehnt werden muss.

Grund dafür war, dass der Anteil an partikulärem OC unter allen klimatischen Bedingungen nur maximal 10% betrug, während >90% des OC in Form von mineral-assoziierter OBS vorlag. Dabei stammte der Großteil (80–90%) des durch den Landnutzungswechsel verloren gegangenen OC aus mineral-organischen Assoziationen und der Verlust aus dieser Fraktion war klimaunabhängig. Zusammen mit dem hohen ^{14}C-Alter mineral-assoziierter OBS unter Ackerland (500–2,900 Jahre) deuten diese Ergebnisse darauf hin, dass mineral-organische Assoziationen hinsichtlich ihrer Zusammensetzung heterogen sind und labile sowie stabile Komponenten der OBS beinhalten.

Entgegen der dritten Hypothese war die Zerstörung von Makroaggregaten und das damit verbundene Freiwerden makroaggregat-okkludierter OBS nicht ursächlich für die Abnahme der OC-Vorräte infolge des Landnutzungswechsels von Grasland zu Ackerland. Das zeigte sich darin, dass im Inkubationsexperiment die zerstörten Makroaggregate nur unwesentlich oder gar keine erhöhten Mineralisierungsraten gegenüber den intakten Makroaggregaten aufwiesen. Dies wurde mit den geringen Gehalten partikulärer OBS in den Böden der Kulundasteppe erklärt, welche die dominierende aggregat-okkludierte Fraktion darstellt. Zudem stammte der Großteil des durch den Landnutzungswechsel verloren gegangenen OC aus mineral-organischen Assoziationen. Darüber hinaus erschien die Stabilisierung der OBS an mineralischen Oberflächen oder durch Okklusion in Mikroaggregaten entscheidender als der Schutz der OBS in Makroaggregaten.

Im Gegensatz zur vierten Hypothese zeigte sich kein Zusammenhang zwischen der Abundanz von Pilzen und der Aggregatstabilität. Dies wurde auf die hohen OBS-Gehalte und die relativ hohen Tongehalte in den Kulundaböden zurückgeführt, sowie auf die aggregatstabilisierende Wirkung von Pflanzenwurzeln. Die PLFA-basierte Zusammensetzung der mikrobiellen Gemeinschaft wurde stärker durch das Klima beeinflusst als durch den Effekt des Landnutzungswechsels, wobei mit zunehmender Aridität die Abundanz von Pilzen (bei gleichzeitiger Zunahme von grampositiven Bakterien) abnahm. Bemerkenswerterweise war die Zusammensetzung der mikrobiellen Gemeinschaft unter Äckern verschiedener Steppenklimate ähnlicher als unter Grasländern. Diese Ergebnisse zeigen, dass infolge des Klimawandels eine stärkere Änderung der mikrobiellen Zusammensetzung zu erwarten ist als durch den Graslandumbruch. Die Änderungen aufgrund des Klimas werden dabei stärker in den Grasländern als unter Acker sein.

Die fünfte Hypothese wurde abgelehnt, da die OC-Vorräte mit zunehmender Salinität stiegen. Dies wurde mit einer anpassungsfähigen Pflanzengemeinschaft erklärt, deren Produktivität (gemessen anhand der oberirdischen pflanzlichen Biomasse) unbeeinflusst von der Salzkonzentration im Boden war, sodass die Menge des Streueintrags entlang des Salinitätsgradienten, entgegen der Annahme, vermutlich nicht abnahm. Ähnlich unbeeinflusst von der zunehmenden Salzkonzentration im Boden zeigte sich die PLFA-basierte mikrobielle Zusammensetzung. Die Mikroorganismen konnten die OBS in salzbeeinflussten Böden vermutlich mit der gleichen Rate zersetzen wie in nicht salzbeeinflussten Böden, sodass sich

partikuläre OBS entlang des Salinitätsgradienten nicht anreicherte. Gleichzeitig förderte die hohe Ionenstärke in der Bodenlösung der salzbeeinflussten Böden die Bildung mineral-organischer Assoziationen, was wahrscheinlich zu den hohen OC-Vorräten in diesen Böden führte. Die hohe Salinität überlagerte den Effekt der Sodizität; das heißt, dass die dispergierende Wirkung hoher Na^+-Konzentrationen nicht auftrat, da die hohe Salzkonzentration das Ausflocken der Bodenbestandteile bewirkte.

Insbesondere in den salzbeeinflussten Böden machte IC einen Großteil der gesamten C-Vorräte aus, wobei die größten Gesamt-C-Vorräte auch in den salzbeeinflussten Böden gemessen wurden. Basierend auf theoretischen Überlegungen lässt sich feststellen, dass IC als C-Senke fungiert, sobald IC durch Karbonatlösung gelöst, in das Grundwasser ausgewaschen und in die Ozeane transportiert wird. Da die Karbonatlösung und das Auswaschen von IC ins Grundwasser unter einem zukünftig trockeneren Klima abnehmen werden, sinkt das durch Karbonatlösung verursachte C-Sequestrierungspotential der Region.

Zusammenfassend lässt sich sagen, dass der Klimawandel (i) zu einer Abnahme des C-Sequestrierungspotentials der Region führen wird, da die OC-Vorräte der Region abnehmen werden und die Lösung von IC aus der Karbonatverwitterung unwahrscheinlicher wird, (ii) den negativen Effekt des Landnutzungswechsels von Grasland zu Ackerland auf die OC-Vorräte nicht verändern wird, und (iii) die mikrobielle Zusammensetzung stärker verändern wird als der Graslandumbruch. Die OC-Verluste infolge des Landnutzungswechsels werden nicht durch die Zerstörung der Makroaggregate sowie die anschließende Mineralisierung der darin enthaltenen partikulären OBS verursacht, sondern der Großteil des verlorenen OC stammt aus mineral-organischen Assoziationen. Ein signifikanter Teil an OC ist in den sibirischen Steppen in Salzböden gespeichert.

Schlagworte: Organische Bodensubstanz, Mikrobielle Bodengemeinschaft, Landnutzungswechsel, Klima, Steppenboden, Salzbeeinflusste Böden

Content

List of Tables

List of Figures

Abbreviations

ATP	adenosine triphosphate
BD	bulk density
C	carbon
CH_4	methane
CO_2	carbon dioxide
DIC	dissolved inorganic carbon
DNA	deoxyribonucleic acid
EC	electrical conductivity
Fe_d	dithionite-extractable iron
Fe_o	oxalate-extractable iron
fPOM	free particulate organic matter
HF	heavy fraction
IC	inorganic carbon
LF	light fraction
LUC	land-use change
MAP	mean annual precipitation
MAT	mean annual temperature
N	nitrogen
NPP	net primary production
OBS	organische Bodensubstanz
OC	organic carbon
OM	organic matter
oPOM	occluded particulate organic matter

PLFA phospholipid fatty acids

rRNA ribosomal ribonucleic acid

SCM soil continuum model

TN total nitrogen

Research highlights

- Global warming will decrease soil organic carbon stocks in the Kulunda region

- Climate change will not alter losses of soil organic matter after land-use change

- Mineral-organic associations were susceptible to land-use change

- Macro-aggregate protected organic carbon was almost absent

- Climate rather than land-use change affected soil microbial community compositions

- Salt-affected soils held significant organic carbon stocks in Siberian steppes

- Particulate organic matter was not preferentially stabilized in salt-affected soils

- The formation of mineral-associated organic matter was enhanced in salt-affected soils

- Increasing salinity did not inhibit the microbial transformation of organic matter

1   Introduction

1.1   The global carbon cycle

The global carbon (C) cycle is, conceptually, distinguished into two domains: (i) a slow domain with turnover times >10,000 years, comprising mostly C stored in rocks and sediments (geological reservoir), and (ii) a fast domain with relatively rapid turnover times ranging from days over decades to some millennia (Ciais *et al.*, 2013). Carbon exchanges between the two domains occur by volcanic eruptions, chemical weathering, erosion and sediment formation, and are relatively small and approximately constant over time (Ciais *et al.*, 2013). Carbon cycling inside the fast domain, also termed the contemporary C cycle, refers to the exchanges of C within and between the atmosphere, the ocean, the terrestrial biosphere, i.e. soils and vegetation, and fossil fuels (Houghton, 2003; Ciais *et al.*, 2013). In this thesis, the focus is on the contemporary C cycle, as it has strong impacts on climate change with soil C playing an important role. Given that (i) C forms the structure of all life on planet and makes up about 50% of all living things, (ii) the cycling of C approximates the flows of energy around the earth, and (iii) C constitutes two of the most important greenhouse gases, i.e. carbon dioxide (CO_2) and methane (CH_4), the understanding of the global C cycle is of utmost importance (Houghton, 2003). Anthropogenic C sources have increased the amount of greenhouse gases in the atmosphere and, hence, accelerate global warming. The rate and extend of this warming depend, in part, on the global C cycle (Houghton, 2003).

Carbon occurs principally either in form of organic C (OC) or as inorganic C (IC). Biomass in terrestrial ecosystems, for example, consists primarily of OC, whereas calcareous shells of oceanic organisms are mainly composed of IC (Houghton, 2003). In the atmosphere, C is largely found in the form of CO_2 and CH_4, while the CO_2 concentration exceeds that of CH_4 approximately by a factor of 200 (Ciais *et al.*, 2013).

Figure 1 shows a simplified schematic of the contemporary global C cycle. The largest C reservoir is the ocean with about 40,500 Pg C stored, mostly in the form of dissolved IC (DIC), followed by about 1,500–2,400 Pg C stored in soils. Permafrost, sometimes included in soil C, contains 1,700 Pg C, while fossil fuels amount for 1,000–1,950 Pg C. Atmospheric C is estimated to about 830 Pg C, while the vegetation holds the smallest C reservoir with ca. 450–650 Pg C.

Though soils comprise only the second largest C reservoir, they are thought to be the largest repository of actively cycling C, i.e. with comparatively fast turnover rates (Ciais *et al.*, 2013; Castellano *et al.*, 2015). As evident from Figure 1, soils contain more than twice as much C as the atmosphere and vegetation combined. Thus, small relative changes of the soil C reservoir can result in large changes of the atmospheric C concentration and, hence, impact climate

change (Myhre *et al.*, 2013). In this regard, one may refer to the ´red´ numbers and arrows in Figure 1, indicating the human contribution to C fluxes and reservoirs. Besides the additional atmospheric C input due to the combustion of fossil fuels, C released to the atmosphere by land-use changes (LUC), i.e. mainly deforestation and cultivation of virgin soils, comprises the main source of additional atmospheric C. Albeit of the recognized importance of the soil C repository, estimations about the size of this reservoir yet remain uncertain, which is evident from the wide range of calculated values (1,500–2,400 Pg C). Though more recent studies presented more accurate estimations of the soil C repository (including permafrost C) of 1,325 Pg OC in the upper 1 m (Köchy *et al.*, 2015) and 2,060 ± 215 Pg OC in 0–2 m depth (Batjes, 2016), many of these studies included only OC. This gives rise to the need of additional studies concerning the amount of C, both OC and IC, stored in soils.
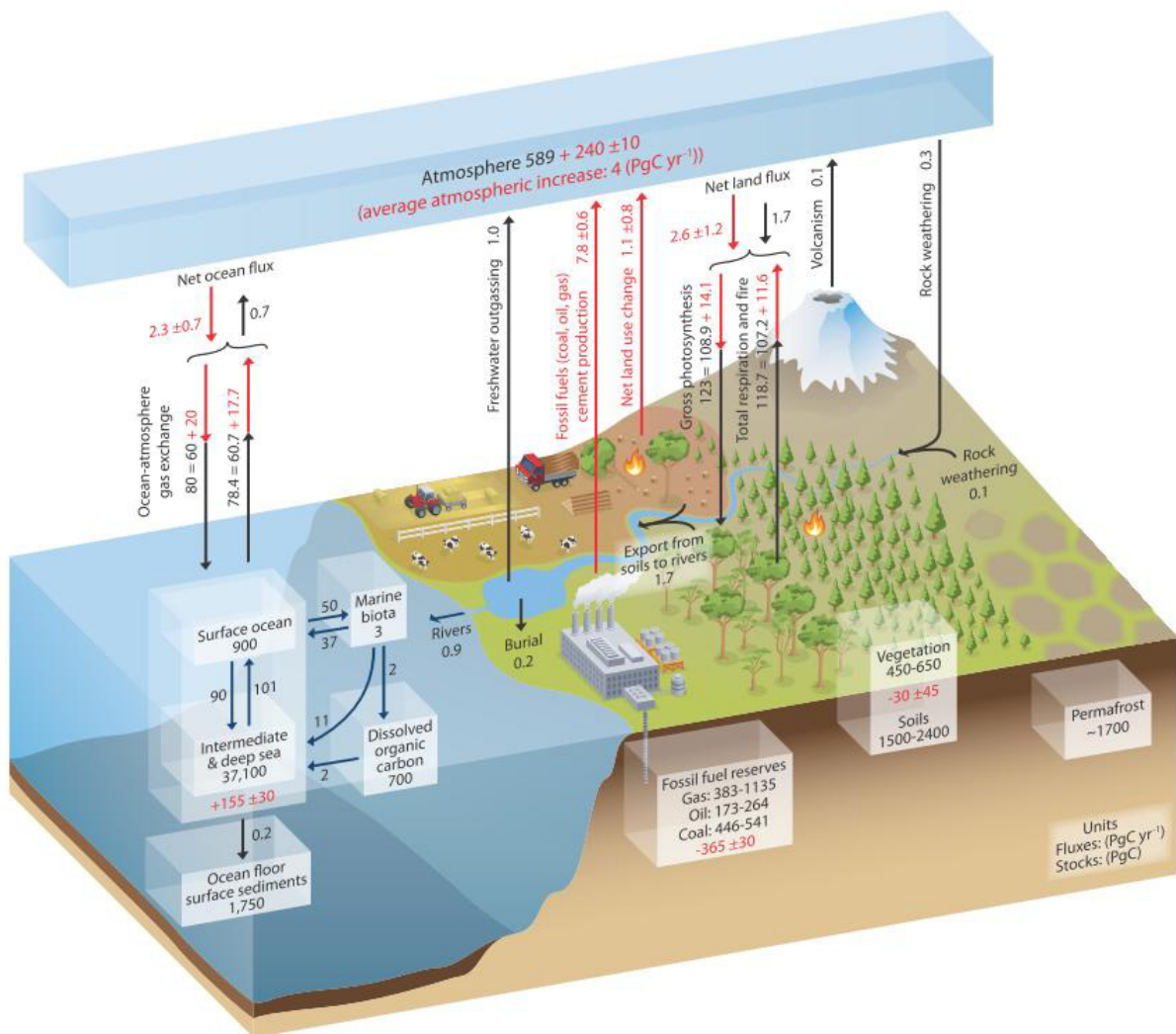
Figure 1: Simplified schematic of the global C cycle. Numbers in boxes represent C stocks (Pg C, 1 Pg C = 10^{15} g C) and numbers along arrows indicate annual C fluxes (Pg C yr^{-1}). Black numbers and arrows denote stocks and exchange fluxes prior to the Industrial Era, about 1750, while red arrows and numbers show annual anthropogenic fluxes averaged over the 2000–2009 time period and red numbers in the reservoirs highlight cumulative changes of anthropogenic C over the industrial Period 1750–2011. Source: Ciais *et al.* (2013)

1.2 Soil organic matter

Most of OC in soils is stored in form of soil organic matter (OM). Conceptually, soil OM refers to all plant, animal and microbial residues at various stages of decomposition, while living roots or organisms are not assigned to soil OM (Blume *et al.*, 2010). About 58% of soil OM is made up of OC (Essington, 2004). In the previous section (Sect. 1.1) we recognized the quantitative relevance of soil C within the global C cycle. In order to predict the response of the soil C repository to disturbances, such as climate change or human land-use, the study of soil OM formation and decomposition is indispensable.

The primary source of all soil OM are plant residues, entering the soil either above-ground as leaf litter or woody plant parts, or below-ground as root litter or rhizodeposits (Kögel-Knabner, 2002). When incorporated into the soil, plant residues are colonized by soil organisms, which use the organic substrate as energy and nutritional source. The soil macro-, meso-, and microfauna (e.g. earthworms, springtails, mites, or nematodes) disintegrate larger organic components into smaller pieces, thus, increasing the surface and contact area of the organic substrate for soil microorganisms (Wolters, 2000). While the soil fauna contributes mostly indirectly to soil OM mineralization by comminution of the organic material, most of soil OM is mineralized by microorganisms (Persson, 1989).

The mineralization of soil OM requires two steps (Maire *et al.*, 2013). First, the organic substrate is broken down via microbial extracellular enzymes until it is small enough (<600 Da; Lehmann & Kleber, 2015) to be assimilated by microorganisms (Burns & Dick, 2002). Thereby, no molecule of CO_2 is released. In the second step, the organic substrate is assimilated and further processed by endoenzymes with the aim to produce energy in form of adenosine triphosphate (ATP), either to generate biomass (anabolism) or to provide energy for various metabolic processes (catabolism). During this step, which refers to heterotrophic respiration, CO_2 is released (Maire *et al.*, 2013). In the course of OM mineralization the organic substrate becomes depolymerized and oxidized, hence, OM mineralization also refers to "oxidative depolymerization" (ten Have & Teunissen, 2001). After microbial death, previously assimilated OC is returned into the fraction of soil OM as microbial residues. Thus, the parent materials for soil OM formation are both, plant and microbial residues, respectively (Kögel-Knabner, 2002).

Because microbes are the primary decomposers of soil OM, recent research on soil OM decomposition has focused on the understanding of microbial functioning and microbial-related processes. Some studies indicate that microbial community composition affects the fate of OM and also its decomposition rate (Six *et al.*, 2006; Fontaine *et al.*, 2011), thus different microbial groups are considered to carry distinct functions in the decomposition process. Evidence suggests that fungi rather grow on coarser plant residues with high C to nitrogen (N) ratios, while bacteria prefer low C : N substrates (Frey *et al.*, 2000; Bossuyt *et al.*, 2001; Six *et al.*, 2006). Moreover, Schimel & Schaeffer (2012) conclude that microbial community composition is likely to be important for the rate of OM breakdown in the

rhizosphere and in detritus. However, they note that microbial community composition is not likely to be important in the mineral soil, where the accessibility of soil OM is the rate-limiting process. But, also in the mineral soil they indicate the importance of microbial community composition for the fate of C.

The accessibility of soil OM is either restricted by the occlusion of the organic substrate within aggregates or the sorption of OM to mineral surfaces (reviewed by von Lützow *et al.*, 2006). Aggregate-occluded OM is protected from microbial decomposition, as the organic substrate is spatially inaccessible to microorganisms, since the pores of the surrounding soil matrix are too small to be passed by microbes. The association of OM with mineral components restricts microbial access due to the strong adsorption of organic compounds to mineral surfaces which results in low desorbability and, hence, little microbial availability, while the binding and inactivation of enzymes on mineral surfaces may add to this effect (Kleber *et al.*, 2015). The decomposition of OM can also be restricted by its indigenous molecular composition, termed chemical recalcitrance, meaning that substrates with high bonding energies or unfavorable stoichiometric ratios (e.g. lignin due to its N deficiency) require more microbial energy input and, hence, are selectively preserved in soils (von Lützow *et al.*, 2006). However, Klotzbücher *et al.* (2011) demonstrated that lignin was easily mineralized in the presence of bioavailable C sources, while Yang *et al.* (2014) showed that bacteria were capable of mineralizing even plastics, indicating that chemical recalcitrance is not as important as assumed.

Besides limited microbial accessibility, soil OM decomposition is controlled by abiotic factors, such as water, temperature, soil pH or the nutritional state of the soil solution, which all affects the functioning of microbial communities. Microbial functioning demands a sufficient moisture content and either water stress or water saturation can attenuate the functionality of the microbial community (Moyano *et al.*, 2013). A water deficit hampers the movement of microbes within the soil and their interaction with the organic substrate, while water saturation limits oxygen availability. Temperature increases the rate of chemical reactions and, hence, also the rate of OM decomposition, given that sufficient water is available. Soil pH affects the decomposition rate as it partly controls the availability of nutrients, while severely acid or alkaline environments are unfavorable for most soil microorganisms. The pH was also shown to select for certain microbial groups, as the relative abundance of soil fungi increased at low pH (Frostegård & Bååth, 1996). Overall, the rate of soil OM decomposition is mainly controlled by microbial substrate accessibility and the conditions for microbial functioning which are mostly dependent on abiotic factors.

The given insights into the functioning of soil OM formation and decomposition have led to the development of various decomposition models (Powlson *et al.*, 1996; Schimel & Weintraub, 2003). By far the most attractive and innovative model was recently proposed by Lehmann & Kleber (2015), termed the soil continuum model (SCM). Herein, the view of soil OM decomposition as an "oxidative depolymerization" process married with the finding,

physicochemical stabilization of OM by occlusion within aggregates and sorption to mineral surfaces are the most important OM stabilization processes. According to the SCM, plant, animal and microbial residues are progressively processed towards smaller molecular size (depolymerization), while the oxidation of the organic substrates leads to polar or even ionizable molecular groups, thus increasing the reactivity and the solubility of soil OM in water. Due to the greater reactivity, OM is increasingly stabilized on mineral surfaces and continuous OM processing leads to greater incorporation of OM into aggregates. The model includes the view that soil OM turnover slows down with enhanced OM stabilization by minerals or aggregates.

For scientific purpose soil OM is conceptually divided into functionally different OM fractions: (i) particulate OM, (ii) mineral-associated OM, and (iii) dissolved OM. Various fractionation methods have been developed to isolate these OM fractions. Most common for isolation of particulate and mineral-associated OM is density-fractionation, where the soil is immersed into a liquid with a specific density to separate a light fraction (LF), floating on top of the liquid, from a heavy fraction (HF) settling on the bottom (reviewed by Christensen, 1992; detailed method description see Study I of this thesis). At a density between 1.6–1.8 g cm^{-3} the LF usually corresponds to particulate OM, while HF material includes both mineral-associated OM and minerals free of OM. Particulate OM comprises decomposing plant and animal residues (but it is primarily of plant origin) with a relatively high C : N ratio and a rapid turnover (Christensen, 1992). In soils were fires occur occasionally also charcoal can be present in particulate OM which significantly lowers its turnover rates. Particulate OM can be further divided into free particulate OM (fPOM) and occluded particulate OM (oPOM), where fPOM refers to unprotected inter-aggregate particulate OM, while oPOM is found occluded within soil aggregates. Mineral-associated OM is primarily of microbial origin and refers to OM adsorbed to mineral surfaces, with usually narrow C : N ratios and slow turnover times. Dissolved OM is not isolated by density fractionation but corresponds to OM dissolved in the aqueous phase of soils with a size <0.45µm (Kalbitz *et al.*, 2000). Since steppe soils are oftentimes dry with little surplus of water, dissolved OM is generally thought to be of less importance in these soils. Thus, in this thesis it was focused on the partitioning of OM between particulate and mineral-associated OM.

1.3 Steppe biomes

The steppe biomes on earth are principally located in three areas: (i) within the Eurasian loess belt extending from the Ukraine across southern Siberia until the north of China, (ii) within the North American prairies, and (iii) within the Argentinian Pampas (Figure 2). The primary parent material is loess, which was deposited as aeolian sediment during the last ice-age (Pleistocene) (FAO, 2001). The climate is semi-arid to semi-humid and continental with dry, hot summers and cold, snowy winters. The vegetation includes grasslands and only in the wetter parts forested areas are present, referred to as forest steppes. Under these climatic conditions fertile soils are formed with usually thick mollic epipedons, resulting from the

slow soil OM decomposition as the climate is dry in summers and cold in winters. Typical steppe soils are Kastanozems, Chernozems, and Phaeozems (FAO, 2001). These loess-derived, calcareous, siltic soils have a large water holding capacity and a usually high availability of nutrients, making them favorable for agricultural use. According to IUSS Working Group WRB (2014) steppe biomes encompass the best farmland soils in the world. Thus, they comprise about 14% of agricultural land globally (FAO, 2013), though, they cover only some 6% of terrestrial land worldwide. Due to their large OC stocks they contribute with 7% significantly to the terrestrial OC storage down to one meter (see Study II). Since steppe soils are weakly weathered due to the semi-arid to semi-humid climate, OM stabilization by mineral-organic associations is considered to be of less importance than in more humid climates (Kleber *et al.*, 2015). In contrast, protection of OM via occlusion within aggregates is thought to be more decisive in steppe soils.
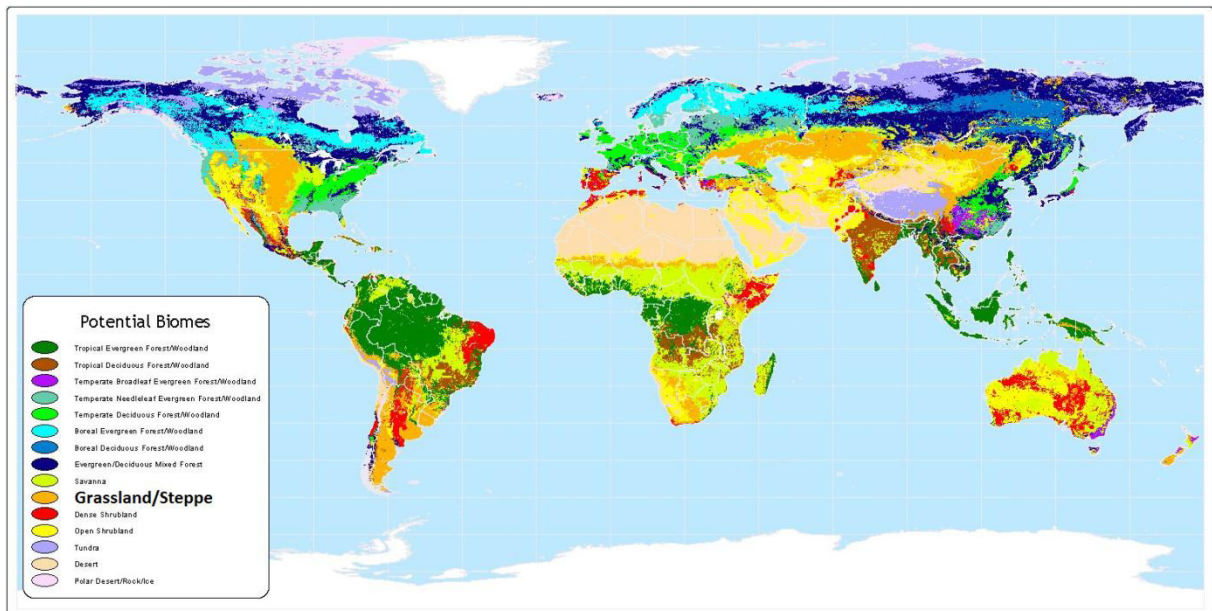
Figure 2: Potential biomes on earth, with emphasis on the grassland/steppe biome. Map slightly modified from Ramankutty & Foley (1999).

At shallow groundwater depth, the dry conditions cause capillary rise of groundwater and the accumulation of salts within the soil. As a consequence, Solonchaks develop which are characterized by large contents of water-soluble salts, usually determined by an electrical conductivity (EC) of the soil solution >4 dS m^{-1} (IUSS Working Group WRB, 2014). If the salts are rich in sodium, Na^+ becomes a dominant cation on the soil exchange sites and soil particles tend to disperse which results in a downward translocation of clay and OM; a typical characteristic for Solonetzes (FAO, 2001). Both soil types belong to the group of salt-affected soils but differ considerably in their physico-chemical properties: while Solonchaks have a compact soil aggregation, Solonetzes have a poor soil structure due to the dispersing effect of Na^+ and a usually high pH (Sumner, 1993; Qadir & Schubert, 2002). However, both soils

have in common that they are harsh environments for plants, since the large salt contents reduce the osmotic potential and thus limit plant water uptake, while ion competition hampers the uptake of nutrients (Qadir & Schubert, 2002; Läuchli & Grattan, 2007). Consequently, plant growth is restricted on these soils, subsequently lowering soil OM inputs and soil OM storage (Wong *et al.*, 2010). Thus, the contribution of salt-affected soils to the overall soil OM storage in steppe biomes is considered to be small when compared to the OM-rich Chernozems and Kastanozems.

In this thesis, soils of the south-western Siberian Kulunda steppe were studied. The region is located in the Russian Federation (Altaysky Kray) and represents a typical example of a Siberian steppe biome, including an aridity gradient with three steppe types: forest steppe, typical steppe and dry steppe. The Kulunda steppe belongs to the West Siberian Plain, which is the greatest conversion area in the world with 420,000 km² natural steppe being converted into cropland between 1954 and 1963 in the frame of the so-called "Virgin Lands Campaign" (Russian: *Zelina*). This comprises an area greater than that of the conversion areas of the North American Great Plains (Frühauf, 2011). However, little is known about the past, present, and future impacts of LUC on OM dynamics in the Siberian soils, since previous research on soil OM in steppe biomes focused on the North American prairies. Moreover, research on OM dynamics in the salt-affected soils of steppe biomes is scarce, though the area of these soils is predicted to increase as a result of climate change (Amini *et al.*, 2016). To highlight that research gap about soil OM in Siberian steppe biomes, Figure 3 shows the distribution of ca. 21,000 soil profiles which were used by Batjes (2016) to calculate the global soil OC storage. From that figure, it is apparent that data from North American prairie soils is highly abundant, while information about steppe soils in Central Asia, particularly the south-western Siberian steppe soils, is scarce if not absent. Thus, estimates about the amount of OC stored in these soils are very uncertain. This study is a first attempt to resolve the poor data basis in this region. In addition, IC is considered at the end of this thesis, since several studies revealed that particularly in steppic climates IC contributes significantly to the total C storage, though estimates about the quantity of this fraction remain highly uncertain (Lal, 2004a; Mi *et al.*, 2008; Shaoxuan *et al.*, 2016).
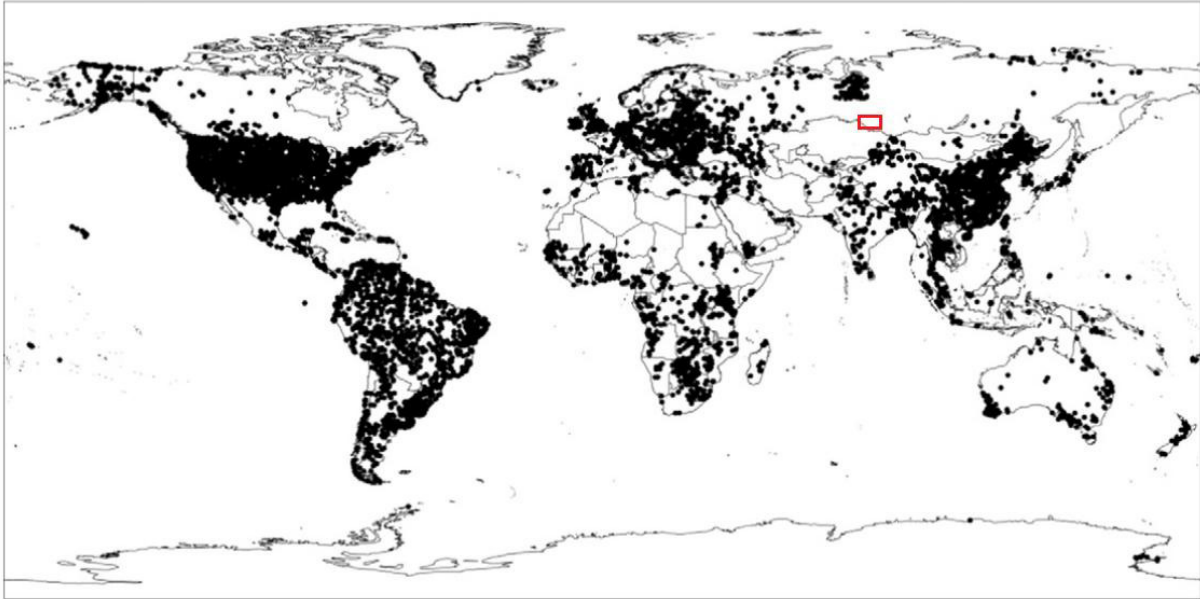
Figure 3: Soil profiles considered for analysis of global soil OC stocks (~21,000) in a meta-analysis of Batjes (2016). The red rectangle was added to the original figure and indicates the Kulunda steppe.

1.4   Climate change

The IPCC (2014) defines climate change as "a change in the state of the climate that can be identified by changes in the mean and/or the variability of its properties and that persists for an extended period, typically decades or longer". As such, it is not distinguished between human or natural causes but solely referred to the change of the system itself. The global mean annual temperature (MAT) increased since 1880 (start of the industrial era) by about 0.85 °C, while an increase of ca. 0.65 °C was solely observed since 1951 (IPCC, 2014). This is related to an increase of greenhouse gas emissions like CO_2, CH_4, and N_2O, which are thought to be the primary cause of global warming. Primary anthropogenic sources of these gases are fossil fuel combustion and LUC, such as deforestation or the cultivation of virgin soils (Ciais *et al.*, 2013). Until the 1970s, more CO_2 was released to the atmosphere by LUC than via combustion of fossil fuels, but this has been reversed due to the increasing demand of fossil fuels for energy production in the last decades (Lal, 2004a and Figure 4). A reduction of greenhouse gases in the atmosphere would attenuate the observed temperature increase and, thus, limit climate change. A possible mitigation strategy is to sequester C in the soil and, hence, reduce the atmospheric CO_2 concentration (Lal, 2004a, 2004b; Lal *et al.*, 2007). Lal (2004a) estimated that soil C sequestration has the potential to offset fossil fuel emissions by 5–15%. Therefore, research increasingly focused on understanding the mechanisms of C stabilization and sequestration in soil.
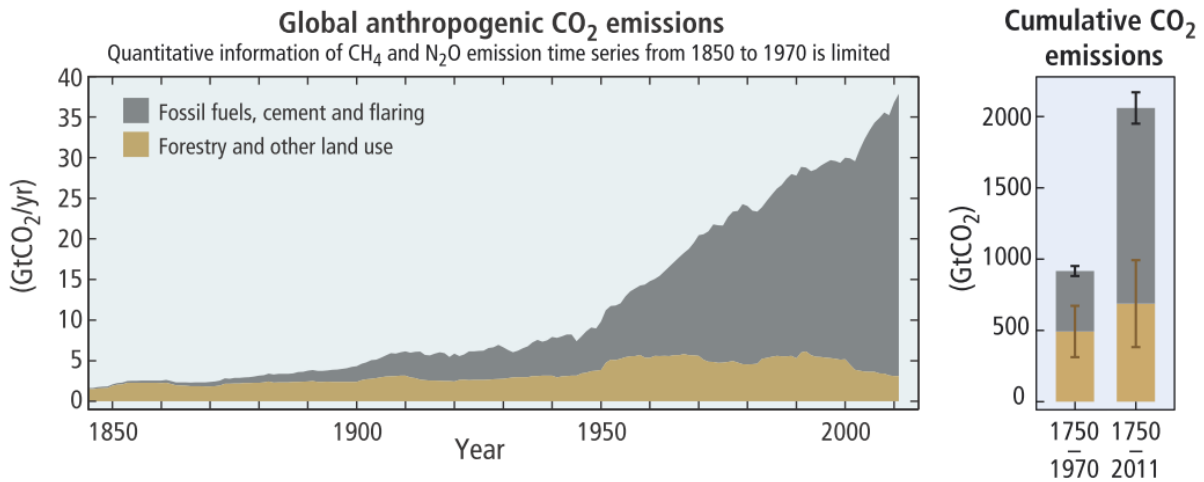
Figure 4: Time course of global anthropogenic CO₂ emissions from 1850 until 2010 separated by source (left panel), and cumulative CO₂ emissions since 1750 (right panel). The category "Forestry and other land use" includes deforestation and cultivation of virgin soils. Source: IPCC (2014).

In the Kulunda steppe, Kharlamova & Revyakin (2006) observed a MAT increase of 2.8 °C from 1838 till 2004 which was accompanied by an increase of aridity. Thus, the effect of climate change is even more severe in the Kulunda steppe than on a global scale. Hijoka *et al.* (2014) predicted in south-western Siberia a further temperature increase of 2–6 °C until the late 21st century, coming along with more frequent drought events and more aridity. However, the general response of terrestrial ecosystems to these climatic changes is still in debate and particularly in the Siberian steppes little is known about the consequences. Wu *et al.* (2011) suggested the necessity of studies assessing the interaction of temperature and precipitation on the C balance of terrestrial ecosystems. Particularly the effect of a changing climate on soil OC stocks remains uncertain (Trumbore, 1997). Thus, studies are needed which address the potential effect of climate change on the quantity and quality of soil OC. This thesis, hence, dealt with the effect of a predicted drier climate on OM in Siberian steppe soils by investigating soil OM dynamics along a climatic gradient in the Kulunda steppe.

1.5 Land-use change

Land-use change refers to a change in the use or management of land induced by humans, which may lead to a change in land cover (IPCC, 2014). In this thesis, LUC from grassland to cropland was explicitly investigated, because this was the predominant LUC in the study area since the 1950s (Frühauf, 2011).

Grassland to cropland conversion generally lowers soil OM inputs by plant residues, as crops are harvested and remaining crop residues have smaller biomass quantities than observed under natural grassland (Kuzyakov & Domanski, 2000). On the other hand, soil management, such as tillage, aims at enhancing soil OM mineralization rates to provide crops with

sufficient nutrients. The combination of both effects generally results in a decline of soil OM. Cambardella & Elliot (1992) and Six *et al.* (1998) observed a predominant loss of particulate OM after cultivation of prairie soils in the Great Plains and concluded that this is the OM fraction most vulnerable to LUC, while mineral-associated OM appeared more stable. Moreover, previous studies showed that the break-down of macro-aggregates and the increased mineralization of previously occluded particulate OM reduced soil OC levels in agricultural soils (Elliott, 1986; Cambardella & Elliott, 1993, 1994). In this regard an important role is dedicated to soil fungi, as they enhance macro-aggregate stability due to the enmeshment of soil particles and, thus, increase the fraction of aggregate-occluded soil OM. Six *et al.* (2000a) investigated micro-aggregates within macro-aggregates under no-tillage and conventional tillage systems and concluded, that the increased macro-aggregate turnover in tilled soils attenuates the formation of OC-protecting micro-aggregates which leads to smaller OC contents in tilled soils. Thus, both macro- and micro-aggregates, respectively, contribute to OM protection in arable soils, but macro-aggregates are supposed to play a greater role in the course of LUC as they disintegrate more readily upon soil disturbance (Tisdall & Oades, 1982; Six *et al.*, 2000b).

Most research underpinned the negative effect of LUC from grassland to cropland on soil OC levels. Based on a global meta-analysis of 74 studies, Guo & Gifford (2002) concluded that the conversion of pasture to cropland caused average soil OC losses of 59%. In a more recent study, Poeplau *et al.* (2011) analyzed 95 studies dealing with soils of the temperate zone, and calculated average soil OC losses of 36% due to conversion of grassland to cropland. Though, many studies focused on the effect of LUC on the quantity and quality of soil OC, little is known, about the effect of LUC on soil OC under a changing climate. Burke *et al.* (1989) and Guo & Gifford (2002) observed larger OC losses with increasing mean annual precipitation (MAP) until MAP of ca. 600 mm but could not find reasons for that. Poeplau *et al.* (2011) detected a positive relationship between MAT and the LUC-induced soil OC losses, but found no effect with MAP. Thus, how the effect of LUC on soil OC may change under different climatic conditions is very uncertain and possible explanations are rare. This points to the necessity of studies dealing with the effect of LUC on soil OC under different climatic conditions. This thesis, therefore, aimed in Study I at elucidating LUC-induced effects on soil OC under different climatic conditions by investigating the effect of grassland to cropland conversion along a climatic gradient in soils of the Kulunda steppe.

Two reasons are mentioned why we should matter about the effect of LUC on soil OM: (i) as outlined in previous sections, soil OM mineralization is a major source of CO_2 and, hence, provokes global warming, while (ii) soil OM resembles the most important reservoir for plant-available nutrients and, thus, significantly controls soil fertility. As shown in Figure 4, LUC belongs to the most important CO_2 sources, however, accurate determinations about the percentage of CO_2 emitted solely by cultivation of virgin soils remain uncertain, hence complicating future projections (Lal, 2004a). Moreover, given the projected world population increase by 3.5 billion people until the year 2100 (United Nations, 2015) and the concomitant

rising demand for food, maintaining soil fertility becomes one of the crucial tasks of mankind (Lal *et al.*, 2007). Lal (2004b) estimated that the sequestration of 1 Mg soil C in degraded croplands may increase crop yields of wheat by 20–40 kg ha^{-1}. Among the possibilities for sequestering C in agricultural soils are improved soil management, e.g. conservative tillage practices such as mini-tillage or no-tillage (Lal, 2004b). These management strategies reduce soil disturbance, e.g. the break-down of aggregates, and thus minimize the loss of OC, while crop residues remain on the field and thus elevate soil OM inputs, which consequently increases soil OM levels. Many studies revealed the positive effect of conservative tillage practices over conventional ones with respect to soil OM storage (reviewed by West & Post, 2002). In this thesis, however, the main purpose was not to deal with the effect of different soil management strategies on soil OM but to assess the effect of LUC. Yet, the effect of different tillage practices was studied along two transects in the dry steppe type.

1.6 Motivation, objectives, hypotheses, and scientific approach

The previous sections were outlined to demonstrate the motivation of this thesis. To summarize, I showed that soils are the largest reservoir of actively cycling C, thus, small changes in the quantity of soil C may severely affect the concentration of atmospheric CO_2 and consequently impact climate change. The majority of soil C exists in form of OM, hence, the understanding of soil OM formation and decomposition is crucial for assessing the dynamics of this C repository. Microorganisms are the driver of OM decomposition and, therefore, control the CO_2 release from soil to the atmosphere. It was suggested, that microbial community composition is critical for the fate of OM and its decomposition rate (Schimel & Schaeffer, 2012). Thus, the determination of microbial community compositions is indispensable when analyzing soil OM dynamics.

Steppe biomes contain worldwide significant OC stocks (ca. 7% of OC globally) as the climatic conditions of these ecosystems result in the development of OM-rich soils, such as Chernozems and Kastanozems. Moreover, the area of salt-affected soils, which frequently occur in steppe biomes, is predicted to increase as a result of climate change, however, little is known about OM dynamics in these soils. When considering the large quantities of IC in steppe soils, steppe biomes gain even larger importance in the global C cycle. Thus, the study of OM dynamics in steppe biomes and the consideration of IC is of utmost importance for the global C budget.

While most research on OM dynamics in steppes focused on steppe soils in the North American prairies, little is known about soils in the Siberian steppes, though they cover an area that is larger than that of the North American prairies. The Kulunda steppe is a typical example of a Siberian steppe biome, covering a climatic gradient with increasing aridity from the forest steppe over the typical steppe to the dry steppe. Due to their large fertility most steppe soils are subject to intensive agricultural use. In the Kulunda steppe, the majority of grassland was converted into agricultural land between 1954 and 1963 in the frame of the so-

called "Virgin Lands Campaign". However, little is known about the past, present, and future impacts of these LUC activities on soil OM, particularly under a predicted drier climate in the course of climate change. Moreover, uncertainty remains about the relative importance of OM stabilization mechanisms in the Siberian steppe soils, such as occlusion of OM within aggregates or association of OM with mineral surfaces.

Steppe soils were shown to contain large quantities of particulate OM, of which some is occluded within aggregates and, hence, protected from decomposition (Elliott, 1986; Flessa *et al.*, 2008). Previous studies revealed that much of this particulate OM was lost upon soil cultivation due to the break-down of macro-aggregates and the subsequent mineralization of previously occluded OM (Elliott, 1986; Cambardella & Elliott, 1993, 1994). Some authors observed a positive relation between fungal abundance and aggregate formation and stability, suggesting that fungi increase the quantity of occluded and thus protected particulate OM, hence, promoting soil C sequestration (Guggenberger *et al.*, 1999; Bossuyt *et al.*, 2001). On the other hand, it was suggested that mineral-organic associations play a minor role for OM stabilization in weakly weathered steppe soils (Kleber *et al.*, 2015).

In order to gain insights about OM dynamics and C stabilization mechanisms in Siberian steppe soils, this thesis has the following overall objectives and hypotheses:

Overall Objectives:

O1: Determination of OC stocks in characteristic soils of the Kulunda steppe

O2: Assessing the relative proportion of OC in functionally different OM fractions (particulate *vs.* mineral-associated OM) as a function of soil type, land use and climate

O3: Estimation of the contribution of aggregation to soil OM stabilization

O4: Elucidation of microbial community compositions along climatic, land-use, and salinity gradients, and determination of the contribution of fungi to aggregate stability

O5: Determination of the percentage of IC in the total C stocks and its role in terms of C sequestration

Overall Hypotheses:

H1: OC stocks decrease with aridity, while the percentage of particulate OC increases concurrently, since the formation of mineral-organic associations is reduced due to limited water availability (Kleber *et al.*, 2015)

H2: Land-use change from grassland to cropland reduces soil OC stocks, with greater soil OC losses under arid conditions because of the larger proportion of mineralizable particulate OM

H3:   The LUC-induced decline of soil OC is mostly attributed to the destruction of macro-aggregates and the liberation and subsequent mineralization of previously occluded particulate OM, since macro-aggregate occluded OM is protected against decomposition by separation of the substrate from microbial decomposers

H4:   Aggregate stability increases with fungal abundance, as the hyphal network of fungi enmeshes soil particles into stable aggregates

H5:   OC stocks decrease with salinity due to limited plant growth and consequently small soil OC inputs, thus, salt-affected soils contribute little to the soil OC storage in steppe biomes

To address the overall objectives and hypotheses three studies and an additional analysis of the entire data set across all sites were conducted:

Study I: "Land-use change under different climatic conditions: Consequences for organic matter and microbial communities in Siberian steppe soils"

The first study aimed at investigating the climate-dependent effect of LUC from grassland to cropland on OM in Chernozems and Kastanozems, which are the typical agricultural soils in the Siberian steppes. This was approached by determining OC stocks along a climatic gradient (forest steppe, typical steppe, dry steppe) and comparing sites under different land use (grassland *vs.* cropland) in a paired plot design. The determination of OC in density-separated OM fractions indicated the proportion of OC stored in functionally different OM fractions (particulate *vs.* mineral-associated OM), while the determination of ^{14}C activities provided insights to the stabilization of OM in these fractions. By analyzing phospholipid fatty acid (PLFA) profiles we elucidated microbial community compositions and calculated fungi : bacteria ratios which were related to measurements of soil aggregate stability. Thus, this study focused on objectives O1–O4 and addressed hypotheses H1, H2, and H4.

Study II: "Limited protection of macro-aggregate occluded organic carbon in Siberian steppe soils"

The main goal of the second study was to determine the quantity of macro-aggregate protected OC in grassland and cropland soils of increasing time since cultivation and of varying land-use intensity to elucidate the amount of macro-aggregate protected OC which was lost as a result of LUC. This was done by comparing OC mineralization rates between dry-sieved intact macro-aggregates (250–2000 µm) and crushed macro-aggregates (<250 µm) in a long-term incubation (401 days, 20°C, and 60% water holding capacity) along two agricultural chronosequences. The potentially increased OC mineralization in crushed macro-aggregates was attributed to previously protected OC which was occluded within macro-

aggregates. By investigating intact *vs.* crushed macro-aggregates in different plots along the two agricultural chronosequences, we aimed at elucidating the quantity of macro-aggregate protected OC which was lost after LUC in the time course of cultivation. Additionally, bulk soil (<2000 µm) was incubated along both chronosequences to assess the effect of LUC and subsequent agricultural use on a fast and slow soil OC pool, as determined by fitting exponential decay models to incubation data. This study addressed objective O3 and hypotheses H3.

Study III: "Organic matter dynamics along a salinity gradient in Siberian steppe soils"

The third study was designed to examine the effect of salinity and sodicity on soil OM dynamics by comparing soil OC stocks and the quantity and quality of density-separated OM fractions (particulate *vs.* mineral-associated OM) along a salinity and sodicity transect of characteristic soils of the dry steppe (Kastanozem, Non-sodic Solonchak, Sodic Solonchak). By measuring above-ground biomass amounts we estimated plant growth and the quantity of soil OM inputs. Quality parameters of OM fractions comprised the composition of C isotopes ($\delta^{13}C$, ^{14}C activity) and non-cellulosic neutral sugars. Via analyzing PLFA we estimated microbial community compositions and assessed the relative abundance of fungi *vs.* bacteria, and related these results to the properties of the functionally different OM fractions. The determination of aggregate stability provided insights to the adverse effect of Na^+ on soil structure. The third study encompassed objectives O1, O2, and O4 and hypothesis H5.

Additional analysis: "Contribution of IC to total C stocks and its role in terms of C sequestration"

An additional analysis was carried out on the entire data set across all sites of the three studies to determine soil IC stocks as function of soil type and climate. Soil IC stocks were compared to OC stocks and total C stocks were calculated. A brief method description is presented in section 5.7. Based on theoretical considerations, the role of IC in terms of C sequestration in steppe biomes was discussed. The additional analysis concerned objective O5.

2 Study I

Land-use change under different climatic conditions: Consequences for organic matter and microbial communities in Siberian steppe soils

Contribution: I did half of the field work, conducted about half of the laboratory analyses, collected and analyzed the data, compiled tables and graphs and wrote the manuscript. As the corresponding author I performed the review process of the paper.

Research paper

Land-use change under different climatic conditions: Consequences for organic matter and microbial communities in Siberian steppe soils

Norbert Bischoff[a,*], Robert Mikutta[a,1], Olga Shibistova[a,b], Alexander Puzanov[c], Evgeny Reichert[d], Marina Silanteva[d], Anna Grebennikova[d], Frank Schaarschmidt[e], Steffen Heinicke[f], Georg Guggenberger[a]

[a] Institute of Soil Science, Leibniz Universität Hannover, Herrenhäuser Straße 2, 30419 Hannover, Germany
[b] VN Sukachev Institute of Forest, Siberian Branch of the Russian Academy of Sciences, Akademgorodok 50, 660036 Krasnoyarsk, Russian Federation
[c] Institute for Water and Environmental Problems, Siberian Branch of the Russian Academy of Sciences, Molodezhnaya Street 1, 656038 Barnaul, Russian Federation
[d] Faculty of Biology, Altai State University, Prospekt Lenina 61a, 656049 Barnaul, Russian Federation
[e] Institute of Biostatistics, Leibniz Universität Hannover, Herrenhäuser Straße 2, 30419 Hannover, Germany
[f] Institute of Biology, Martin Luther University Halle-Wittenberg, Am Kirchtor 1, 06108 Halle (Saale), Germany

ARTICLE INFO

ABSTRACT

The Kulunda steppe is part of the greatest conversion areas of the world where 420,000 km^2 grassland have been converted into cropland between 1954 and 1963. However, little is known about the recent and future impacts of land-use change (LUC) on soil organic carbon (OC) dynamics in Siberian steppe soils under various climatic conditions. By investigating grassland vs. cropland soils along a climatic gradient from forest to typical to dry steppe types of the Kulunda steppe, our study aimed to (i) quantify the change of OC stocks (0–60 cm) after LUC from grassland to cropland as function of climate, (ii) elucidate the concurrent effects on aggregate stability and different functional soil organic matter (OM) fractions (particulate vs. mineral-bound OM), and (iii) assess climate- and LUC-induced changes in the microbial community composition and the contribution of fungi to aggregate stability based on phospholipid fatty acid (PLFA) profiles. Soil OC stocks decreased from the forest steppe (grassland: 218 ± 17 Mg ha^{-1}) over the typical steppe (153 ± 10 Mg ha^{-1}) to the dry steppe (134 ± 11 Mg ha^{-1}). Across all climatic regimes, LUC caused similar OC losses of 31% (95% confidence interval: 17–43%) in 0–25 cm depth and a concurrent decline in aggregate stability, which was not related to the amount of fungal PLFA. Density fractionation revealed that the largest part of soil OM (>90% of total OC) was associated with minerals and <10% of C existed in particulate OM. While LUC induced smaller relative losses of mineral-associated OC than particulate OC, the absolute decline in total OC stocks was largely due to losses of OM bound to minerals. This result together with the high ^{14}C ages of mineral-bound OM in croplands (500–2900 yrs B.P.) suggests that mineral-bound OM comprises, in addition to stable OC, also management-susceptible labile OC. The steppe type had a larger impact on microbial communities than LUC, with a larger relative abundance of gram-positive bacteria and less fungi under dry conditions. Our results imply that future drier climate conditions in the Siberian steppes will (i) result in smaller OC stocks on a biome scale but (ii) not alter the effect of LUC on soil OC, and (iii) change the microbial community composition more than the conversion from grassland to cropland.

© 2016 Elsevier B.V. All rights reserved.

1. Introduction

Global soils hold a substantial proportion of the earth's carbon with about 1325 Pg organic carbon (OC) being stored in the upper first meter and almost 3000 Pg OC when deeper soil layers are included (Köchy et al., 2015). Past research found soil OC to be very sensitive to land-use changes (LUC) (Guo and Gifford, 2002; Murty et al., 2002; Poeplau et al., 2011), and its role to regulate climate

change and food security is considered to be crucial (Lal, 2004). This particularly concerns steppe soils as they are rich in organic matter (OM) and commonly under intensive agricultural use. Nowadays, about 14% of agricultural land globally consists of steppe soils, typically Chernozems and Kastanozems (FAO, 2013).

Land-use change from grassland to cropland usually involves a loss of OC due to smaller residue inputs into the soil and larger soil OM decomposition as triggered by soil tillage (Mann, 1986; Poeplau et al., 2011). Previous studies observed a break-down of soil macroaggregates due to soil tillage and a subsequent release of occluded particulate OM which is then mineralized by micro-organisms (reviewed by Bronick and Lal, 2005). The formation and stabilization of macroaggregates depend on the abundancy and functioning of soil fungi, since their extensive hyphae network generally supports aggregate formation and stabilization (Guggenberger et al., 1999). Besides the stabilization of soil OM by occlusion within aggregates, soil OM can be chemically stabilized by its association with mineral surfaces. Mean residence times of mineral-associated OM are in the range of >100yr, while particulate OM has a turnover of years (Kleber et al., 2015).

Research on LUC effects in steppe soils predominantly focused on American prairie soils. For this region the OC stock decline after conversion from grassland to cropland was estimated to be 24–32% for conventional soil tillage practices (Beniston et al., 2014; Doran et al., 1998; VandenBygaart et al., 2003). Some studies were conducted in steppe soils of the European part of Russia where the decrease of OC stocks after conversion from grassland to cropland ranged from 27% to more than 40% (Mikhailova et al., 2000; Rodionov et al., 1998). Apart from that, there is no study dealing with the effects of LUC on soil OC in steppe soils of Siberia, despite the region belongs to the greatest agricultural production areas in the world and occupies an area greater than that in the Great Plains (Frühauf, 2011). Moreover, little is known about the effects of LUC on soil OM under different climatic conditions, which is particularly important in the course of climate change. For south-western Siberia, Hijoka et al. (2014) predicted a temperature increase of 2–6 °C until the late 21st century coming along with more frequent drought events, which translates into a higher degree of aridity. As this will change the environmental conditions there is an increasing demand for understanding how LUC impacts are affected by climate change. Studies on the climate-dependent effect of LUC on soil OM have not come to a clear conclusion yet. Burke et al. (1989) and Guo and Gifford (2002) found a positive relationship between relative OC loss and precipitation (until a mean annual precipitation of ca. 600 mm), but did not have an explanation for this finding. Poeplau et al. (2011) identified temperature being positively correlated to the relative soil OC loss due to LUC, but not the mean annual precipitation (MAP). Considering processes of carbon stabilization in soil, we believe that soil OC losses should be larger under dry conditions, as the formation of OM-protecting mineral-organic associations is reduced under dry conditions (Kleber et al., 2015). Thus, larger proportions of readily decomposable particulate OM are expected in arid regions, as evidenced by Amelung et al. (1998), which would lead to larger losses of soil OC upon LUC. To elucidate the effects of LUC on soil OM in Siberian steppe soils under different climatic conditions we investigated the effect of LUC from grassland to cropland in soils of the south-western Siberian Kulunda steppe along a climatic gradient. The region is part of the greatest conversion area of the world, where 420,000 km^2 of grassland were converted into cropland between 1954 and 1963 as part of the so-called "Virgin Lands Campaign" (Russian: "zelina"). The main objectives of our study were to (i) investigate the climate-dependent effect of LUC from grassland to cropland on soil OC stocks, (ii) account for the concurrent effects on aggregate stability and different functional soil OM fractions (particulate *vs.* mineral-

bound OM), and (iii) determine changes in the microbial community composition along the climatic gradient and the two land use types and the contribution of fungi to aggregate stability. We approached this by quantifying soil OC stocks under different land use (grassland *vs.* cropland) in a paired plot design along a climatic gradient with sites in the forest, typical and dry steppe types and assessing the concurrent changes in aggregate stability and density-separated soil OM fractions. The apparent stability of particulate and mineral-bound OM was estimated based on ^{14}C measurements. Based on phospholipid fatty acid (PLFA) profiles we elucidated the amount of bacterial and fungal PLFA and separated the microbial community into six microbial groups. We hypothesize that the response of soils to LUC depends on the climatic conditions with larger OC losses in arid regions. Moreover, we expect that the loss of OC relates to a decrease in aggregate stability which itself is associated to a reduction in the amount of fungal PLFA.

2. Material and methods

2.1. Study sites and soil sampling

The Kulunda steppe is situated in the Altai Krai region of the Russian Federation, between 51°N and 54°N and 78°E and 84°E, and belongs to the Eurasian loess belt (Fig. 1). The area is separated into three distinct steppe types: the forest steppe (FS) with a MAP of 350–450 mm, the typical steppe (TS) with a MAP of 300–350 mm and the dry steppe (DS) with a MAP of 250–300 mm. The mean annual temperature (MAT) increases from FS (MAT 1 °C) to DS (MAT 2 °C) by around 1 °C (climate data from "WorldClim" data base; Hijmans et al., 2005). As a result, aridity increases in the order FS < TS < DS and the vegetation cover changes from partially forested areas in FS to mostly grassland areas in DS with the largest biomass production in FS and the smallest one in DS. Dominant plant species in the grasslands of FS were *Bromopsis inermis* and *Stipa capilata*, while *Festuca valesiaca* and *Bromopsis inermis* dominated in grasslands of TS. Grasslands of DS were characterized by *Festuca valesiaca* and *Artemisia frigida*. The agricultural production in the entire area focuses mainly on wheat and sunflower, but also rape seed and peas are common. In FS and TS, soils were mostly classified as Chernozems, reflecting the wetter climate as compared to DS, where Kastanozems are more frequent.

For assessing the impact of LUC on soil, we used a paired plot design (Poeplau and Don, 2013). Nine sites were selected, three sites in FS, two sites in TS and four sites in DS, with a total of 21 plots (Table S1). Each site consisted of at least two plots, one reference plot, representing the soil conditions before LUC and one or more conversion plots, representing the soil conditions at a certain time after LUC. Seven sites consisted of one reference and one conversion plot, while two sites (in DS) consisted of one reference and two conversion plots (triple plot), giving a total of eleven pairs (reference and conversion plot). The grasslands chosen as reference plots were either in pristine state or in use as extensive pastures. As further criteria, soils had to be unaffected by erosion and LUC should have occurred at least 20 years ago, as several studies showed most soils establish a new equilibrium approximately after that time (e.g. Murty et al., 2002; Poeplau et al., 2011). For a LUC chronosequence in FS, we also included one plot with <20 yrs since LUC. Per plot one key profile was established for soil description and sampled according to generic horizons down to a depth of ca. 160 cm. Subhorizons (e.g. A1, A2) were treated separately in the laboratory, but the measurements were bulked according to the proportion of a subhorizon in the main horizon to obtain one value per horizon (A, AC, C). Additionally, per plot three randomly chosen soil profiles were excavated around the key profile and sampled in 0–10, 10–25 and
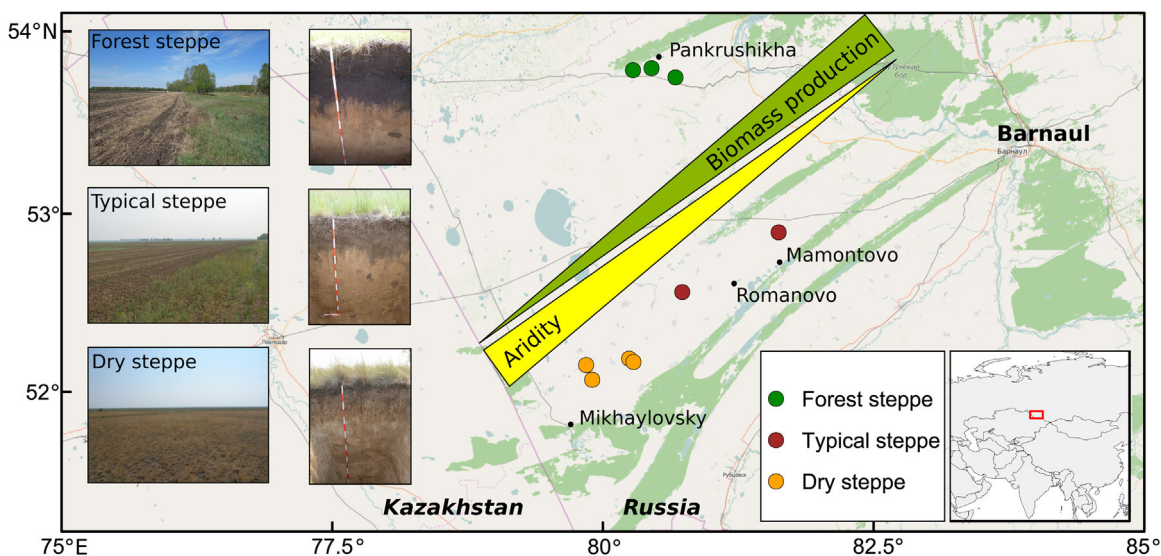
Fig. 1. Map of the Kulunda steppe with sampling sites according to the steppe types forest steppe, typical steppe and dry steppe. Biomass and aridity gradients are shown schematically. For each steppe type a representative landscape picture and soil profile is shown. Map modified from © OpenStreetMap-contributors, for copyright see www. openstreetmap.org/copyright.

25–60 cm depth increments (hereafter referred to as increment profiles). This gave a total of 60 horizon samples from the key profiles and 180 samples from increment profiles.

The horizon samples from the key profiles were analyzed for basic soil parameters as texture, bulk density, pH, electrical conductivity, carbonate content ($CaCO_3$), dithionite- and oxalate-extractable Fe, as well as particulate and mineral-associated OM contents as determined by density fractionation. The latter OM fractions were also analyzed for their ^{14}C activities. For both, horizons from key profiles and samples from increment profiles, we determined soil OC content, total nitrogen and aggregate stability (aggregate stability only in 0–10 cm or the topmost horizon). Phospholipid fatty acid profiles were analyzed in 0–10 cm of the increment profiles.

2.2. Sample preparation and basic soil analyses

Soil samples were air-dried, gently crushed in a mortar to break down clods, and sieved to <2 mm. All visible roots and plant residues were removed and an aliquot of 5 g fine soil was dried at 105 °C to determine the residual soil water content. Soil bulk density was determined in triplicate for generic horizons of the key profile and calculated for the corresponding depths of the increment profiles. Soil pH was measured at a soil-to-water ratio of 1:2.5 (w:v), while the electrical conductivity (EC) was measured at a ratio of 1:5 (w:v). Dithionite- and oxalate-extractable Fe was measured according to the method in McKeague & Day (1966). Soil texture was determined with the standard sieve-pipette method (DIN ISO 11277, 2002) for generic horizons to a depth of 100 cm. Carbonate content was analyzed by the Scheibler volumetric method (Schlichting et al., 1995).

2.3. Soil organic carbon analysis

An aliquot of the <2-mm fraction was homogenized in a ball mill, treated with HCl fume to remove carbonates (Walthert et al., 2010), and analyzed for OC and total nitrogen (TN) by dry combustion in an Elementar vario MICRO cube C/N Analyzer (Elementar Analysensysteme GmbH, Hanau, Germany).

2.4. Density fractionation and ^{14}C analysis

We used density fractionation (modified after Golchin et al., 1994) to isolate a light fraction (LF) mostly containing particulate OM (POM) from a heavy fraction (HF) representing mineral-associated OM (MOM). As POM is generally most abundant in the topsoil, generic horizons deeper than 80 cm depth were not considered for analysis. In brief, 25 g of air-dried sample was given in duplicate in a beaker and 125 ml of sodiumpolytungstate ($1.6\,g\,cm^{-3}$) was added. After stirring the suspension with a glass rod, ultrasonification with an energy input of $60\,J\,ml^{-1}$ was applied for 8 min to disperse the soil. The sample was centrifuged at 3,000 g for 20 min and LF, floating on top of the suspension, was decanted on polyethersulfone filters, and washed with deionized water until the washing solution had an electrical conductivity $<60\,\mu S\,cm^{-1}$. The procedure was repeated if the separation between LF and HF was insufficient. The HF was washed with deionized water until the electrical conductivity was $<100\,\mu S\,cm^{-1}$ or, for samples which contained pedogenic salts, at maximum four times. The washing solutions of both fractions were collected, passed through 0.45-μm syringe filters (PVDF), and analyzed for dissolved OC (DOC) with a LiquiTOC (Elementar Analysensysteme GmbH, Hanau, Germany). This mobilized DOC accounted for 5–31% of total OC (Table S2). The isolated LF and HF were freeze-dried, weighted, and carefully homogenized in a mortar. All fractions were analyzed for OC and TN (after removal of carbonates). DOC mobilized during the washing procedure was added to the OC content of the corresponding fraction.

A subset of OM fractions was analyzed for ^{14}C activities at the Max Planck Institute for Biogeochemistry Jena (Germany). Inorganic C was removed by 2 M HCl until pH remained <3.5. After neutralization with 2 M NaOH to pH 6, samples were freeze-dried, and measured for ^{14}C using a 3 MV Tandetron™ AMS ^{14}C system (Steinhof et al., 2011). [14]C isotope ratios were converted to pMC (percent modern carbon) according to Steinhof (2013). Percent modern carbon is defined according to Stuiver and Polach (1977):

$$pMC = \frac{A_{SN}}{A_{abs}} \times 100\% \tag{1}$$

18

where A_{SN} is the normalized sample activity and A_{abs} is the activity of the absolute international standard, both activities background-corrected and $\delta^{13}C$-normalized. Conventional ^{14}C ages were estimated using OxCal 4.2 software (University of Oxford). The IntCal13 calibration curve (Reimer et al., 2013) was selected if pMC was <100% while the calibration curve calculated by Hua et al. (2013) was used if pMC was >100%.

2.5. Phospholipid fatty acid analysis

1.0–1.5 g field-moist soil was cleaned from visible roots, weighted into cryovials and stabilized in RNAlater® to prevent sample degradation (Schnecker et al., 2012). An aliquot was dried at 105 °C to determine the soil water content. The cryovials were kept cool and frozen to −20 °C within 72 h. We used a modified method of Gunina et al. (2014) to analyze the phospholipid fatty acids (PLFA). Briefly, the samples were transferred from the cryovials into test tubes and washed with ultrapure water to remove residual RNAlater®. Lipids were extracted twice using a chloroform-methanol-citrate buffer (1:2:0.8 v/v/v) and separated by solid phase extraction with activated Silica gel (Sigma Aldrich, pore size 60 Å, 70–230 mesh) into glycolipids, neutral lipids, and phospholipids. Only phospholipids were used for further analysis and converted into fatty acid methyl esters (FAME) using BF_3 as a catalyst. FAMES were analyzed by gas chromatography using an Agilent Technologies 7890A GC system equipped with a 60 m Zebron capillary GC column (0.25 mm diameter and 0.25 μm film thickness; Phenomenex, Germany) and a flame ionization detector, using He as a carrier gas. Nonadecanoic acid (FA 19:0) was used as an internal standard. Seventeen PLFA were analyzed in total and the sum of all PLFA was used as a proxy of the microbial biomass and expressed as PLFA biomass. A principal components analysis (PCA) was conducted on data of the relative abundance of all 17 PLFA (%) to separate the microbial community into distinct microbial groups. The PCA-based classification of the PLFA into the microbial groups was in good agreement with literature data (Frostegård et al., 2011; Ruess and Chamberlain, 2010; Zelles, 1999), and we used the following markers to distinguish the microbial community: i15:0, a15:0, i16:0, i17:0, a17:0 and 18:1ω9c for gram-positive bacteria (Gram+), 16:1ω5c, 18:1ω7c and Cy19:0 for gram-negative bacteria (Gram−), 10Me16:0 for actinomycetes, 18:2ω6,9 for fungi, 20:4ω6c for protozoa, and 14:0, 15:0, 16:1ω7c, 17:0, and 18:0 for unspecific bacteria. We did not use PLFAs 18:1ω9c and 16:1ω5c as markers for fungi or arbuscular mycorrhiza, respectively, as they are also common in bacteria and, hence, had no good indicator function in arable soils (Frostegård et al., 2011). The ratio of the fungal PLFA to the bacterial PLFAs was used to estimate the fungi : bacteria ratio (Frostegård and Bååth, 1996). The ratio of PLFAs representing gram-positive bacteria and actinomycetes to those representing gram-negative bacteria was calculated to estimate the Gram+ : Gram− ratio (Wixon and Balser, 2013).

2.6. Aggregate stability

Aggregate stability was determined according to Hartge and Horn (1989) in combination of a dry- and wet sieving method. In brief, the field-moist soil was sieved to <8 mm to remove big clods and subsequently air-dried. About 120 g of the air-dry soil was placed on top of a stack of sieves with 4, 2, and 1 mm mesh size, rotated vertically 60 times, and the aggregate size fraction in each sieve was recovered and weighted. An aliquot of the air-dry soil was dried at 105 °C to determine the residual soil water content. The three isolated fractions from the dry sieving were pooled and gently wetted to 15% of their soil mass. The wetted aggregates were placed on a stack of sieves with 4, 2, 1, 0.5, and 0.2 mm mesh size, slowly submerged in water, and vertically rotated during 5 min with a frequency of 35 rpm. Each recovered aggregate size fraction was dried at 105 °C and the difference of aggregate size distributions between the dry- and the wet sieving method was calculated as difference between the masses (on a sand-free basis) of the corresponding aggregate size fractions according to Eq. (2):

$$\Delta MWD = \frac{\Sigma(n_{i1} \times d_i) - (n_{i2} \times d_i)}{\Sigma n_{i1}} \tag{2}$$

where ΔMWD is the difference of the mean weight diameter between the dry- and wet sieving method, d is the mean of an aggregate size fraction i (mm), and n_{i1} and n_{i2} are the weights of the ith aggregate size fraction as proportion of all aggregate size fractions (%) after the dry- and wet sieving, respectively. The higher is ΔMWD the lower is the aggregate stability (Hartge and Horn, 1989).

2.7. Calculation of organic carbon stocks

Organic C stocks ($Mg\,ha^{-1}$) were calculated according to Poeplau and Don (2013) for all depth increments and horizons using Eq. (3):

$$OC\ stock = \Sigma_{i=1}^{n} \frac{FSM_i}{V_i} \times C_i \times D_i \tag{3}$$

where n is the number of depth increments or horizons, FSM is the fine soil mass (g), V is the volume (cm^3), C is the OC content (% of soil mass) and D is the length of the depth increment or horizon (cm). As LUC generally implies a change in soil bulk density, OC stocks were corrected to account for different soil masses, according to Ellert and Bettany (1995). The soil with the least mass was used as reference.

2.8. Statistical analyses

2.8.1. Linear mixed effects models

Data analysis was performed in R 3.1.2 (R Core Team, 2015). Linear mixed models (package lme4, Bates et al., 2012) were fitted to test for the effect of steppe type and land-use type on response variables (e.g., OC stock, aggregate stability, PLFA biomass) where possible with respect to different horizons or depth increments. We thereby accounted for the nested structure of sampling, i.e. main effects of steppe type and land-use type as well as their interaction and, where possible, the mean depth were included as fixed effects, while sites and plots within sites were included as random effects. After fitting initial models, residuals and random effect estimates were visually checked for deviations from normality, using Q-Q-normal plots. If these showed right-skewed distribution or heterogeneity of variances, models were re-fitted with log-transformed response variables. Based on the linear mixed model fit, the differences of the response variable between steppe type and land-use type classification were tested including corrections for multiple comparisons (analogous to the Tukey test), with Satterthwaite degrees of freedom, based on the R packages lsmeans (Lenth and Herve, 2015), lmerTest (Kuznetsova et al., 2015), and multcomp (Hothorn et al., 2008). To estimate the proportion of variance explained by steppe type and land-use type with respect to OC stocks, an intercept-only linear mixed effects model was fitted for each depth increment including steppe type, land-use type, sites and plots within sites as random effects and calculating the relative proportion of each component to the total variance (variance components analysis). Graphs were made using ggplot2 (Wickham, 2009) and the map of the survey area was

Table 1

Summary of soil parameters for different horizons depending on land-use type and steppe type. Values are given as arithmetic mean ± standard error of the mean. Abbreviations: FS = forest steppe, TS = typical steppe, DS = dry steppe, BD = bulk density, EC = electrical conductivity, Fe_o = oxalate-extractable Fe, Fe_d = dithionite-extractable Fe, OC = organic carbon.

Steppe type	Horizon	Land-use type	n	Depth cm	BD g cm⁻³	pH –	EC µS cm⁻¹	CaCO₃ mg g⁻¹	Fe_o mg g⁻¹	Fe_d mg g⁻¹	Clay mg g⁻¹	OC mg g⁻¹	C : N –
FS	A	grassland	3	32.7 ± 2.2	1.20 ± 0.10	7.0 ± 0.3	83.8 ± 28.0	0.3 ± 0.3	0.9 ± 0.2	5.2 ± 0.4	283.5 ± 42.4	37.6 ± 4.7	11.5 ± 0.2
		cropland	3	27.7 ± 1.9	1.24 ± 0.09	6.8 ± 0.2	50.6 ± 5.4	0.3 ± 0.3	0.7 ± 0.1	5.5 ± 0.9	288.2 ± 49.1	33.2 ± 5.3	11.2 ± 0.2
	AC	grassland	3	59.0 ± 4.7	1.43 ± 0.09	8.0 ± 0.3	93.2 ± 32.5	41.7 ± 41.2	0.4 ± 0.2	5.9 ± 0.7	307.3 ± 35.8	8.1 ± 2.2	10.3 ± 1.8
		cropland	3	57.0 ± 8.9	1.43 ± 0.06	7.5 ± 0.2	72.3 ± 31.1	4.0 ± 4.0	0.7 ± 0.1	5.8 ± 0.9	318.3 ± 44.6	13.0 ± 1.8	10.2 ± 0.3
	C	grassland	3	160.0 ± 11.5	1.55 ± 0.06	8.9 ± 0.3	149.1 ± 37.1	89.0 ± 28.2	0.3 ± 0.1	4.0 ± 0.3	275.5 ± 41.4	2.6 ± 0.6	6.6 ± 0.4
		cropland	3	150.0 ± 5.8	1.54 ± 0.06	8.6 ± 0.2	95.4 ± 17.4	89.0 ± 32.2	0.2 ± 0.0	4.1 ± 0.8	266.5 ± 55.3	2.9 ± 0.6	7.4 ± 0.7
TS	A	grassland	2	37.5 ± 9.5	1.14 ± 0.02	7.4 ± 0.2	1500.1 ± 1434.8	1.0 ± 1.0	0.5 ± 0.0	6.1 ± 0.0	338.5 ± 35.9	28.4 ± 2.8	11.6 ± 0.4
		cropland	2	29.0 ± 6.0	1.27 ± 0.05	7.6 ± 0.6	358.4 ± 244.4	2.5 ± 2.5	0.9 ± 0.3	6.5 ± 0.3	318.3 ± 35.3	24.8 ± 12.4	10.5 ± 1.4
	AC	grassland	2	58.3 ± 12.4	1.24 ± 0.03	8.4 ± 0.2	1332.9 ± 1218.5	50.7 ± 38.3	0.4 ± 0.1	6.0 ± 0.4	327.2 ± 12.6	11.4 ± 2.6	9.4 ± 0.2
		cropland	2	56.0 ± 6.7	1.36 ± 0.04	8.3 ± 0.3	713.9 ± 556.6	37.3 ± 28.8	0.5 ± 0.1	5.5 ± 0.4	305.1 ± 25.4	8.8 ± 2.0	9.3 ± 0.7
	C	grassland	2	144.0 ± 16.0	1.45 ± 0.03	8.5 ± 0.0	2005.4 ± 355.4	104.3 ± 9.2	0.3 ± 0.0	5.1 ± 0.0	300.0 ± 10.1	2.3 ± 0.4	5.8 ± 0.6
		cropland	2	156.7 ± 3.3	1.45 ± 0.02	8.7 ± 0.2	1003.1 ± 637.1	79.3 ± 9.9	0.4 ± 0.1	5.0 ± 0.4	276.0 ± 22.2	2.9 ± 0.7	6.4 ± 1.6
DS	A	grassland	4	23.3 ± 3.7	1.29 ± 0.06	7.0 ± 0.2	43.5 ± 2.3	0.0 ± 0.0	0.5 ± 0.1	6.6 ± 0.4	274.1 ± 19.8	25.3 ± 5.1	11.2 ± 0.2
		cropland	6	25.7 ± 2.2	1.33 ± 0.02	7.4 ± 0.2	62.4 ± 9.3	1.5 ± 1.5	0.3 ± 0.1	6.4 ± 0.2	258.1 ± 13.3	17.7 ± 1.8	10.7 ± 0.4
	AC	grassland	4	53.0 ± 5.8	1.34 ± 0.05	7.9 ± 0.2	88.9 ± 28.0	24.5 ± 21.0	0.5 ± 0.2	5.7 ± 0.5	278.9 ± 24.4	10.9 ± 1.7	9.1 ± 0.6
		cropland	6	51.7 ± 5.6	1.30 ± 0.03	8.0 ± 0.2	93.1 ± 25.0	18.5 ± 14.5	0.2 ± 0.1	6.5 ± 0.2	280.4 ± 11.3	9.6 ± 0.8	9.2 ± 0.4
	C	grassland	4	152.5 ± 2.5	1.43 ± 0.03	8.8 ± 0.0	427.3 ± 325.6	85.8 ± 9.8	0.2 ± 0.1	4.9 ± 0.8	262.5 ± 51.3	3.2 ± 0.4	6.7 ± 0.7
		cropland	6	155.0 ± 2.2	1.43 ± 0.04	8.8 ± 0.1	572.6 ± 292.5	91.7 ± 11.9	0.1 ± 0.0	5.0 ± 0.2	252.0 ± 17.1	2.6 ± 0.1	6.2 ± 0.4

generated using ggmap (Kahle and Wickham, 2013) and the open source software Inkscape.

2.8.2. ADONIS and Nonmetric multidimensional scaling

After separating the microbial community into six microbial groups by PCA (see Section 2.5), Permutational Multivariate Analysis of Variance Using Distance Matrices (ADONIS; 999 permutations) was used to investigate the effect of steppe type and land-use type as well as their interaction on the microbial community composition, thereby using the Bray-Curtis dissimilarity index as distance metric. Pairwise comparisons between steppe types were tested in ADONIS by using subsets of the data with two corresponding factor levels and correcting p-values for multiple comparisons by Bonferroni correction. For graphical data presentation Nonmetric Multidimensional Scaling (NMDS) was chosen as it retains major parts of the entire variation and complexity of the data set and reflects similarities or dissimilarities within the microbial community with respect to site effects. To improve interpretation in NMDS, we chose a two-dimensional ordination which yielded a stress of 0.10. Confidence regions (95%) for the group centroids were added for steppe types and land-use types. All multivariate analysis was done in R package vegan (Oksanen et al., 2015).

3. Results

3.1. Basic soil characteristics

The soil parameters are characteristic for Chernozems and Kastanozems, with neutral to slightly alkaline pH, accumulation of carbonates in the subsoil, partial occurrence of pedogenic salts as indicated by high EC values, and low oxalate- and dithionite-extractable Fe contents as chemical weathering is limited due to the dry climate (Table 1). Comparable clay contents in the respective horizons of grassland and cropland soils suggest same substrate at the paired plots. The thickness of the A horizons tended to decrease in the order FS > TS > DS, and was greater for grassland than for cropland soils in FS and TS. Concurrently, the OC contents were larger in grasslands than in croplands, and soils of

the FS had larger OC contents than those of the TS and DS (Table 1). The C : N ratios did not differ considerably between grassland and arable soils or steppe types.

3.2. Soil and organic matter properties as function of steppe type and land-use type

3.2.1. Soil organic carbon stocks

Soil OC stocks decreased significantly with decreasing MAP in the order FS > TS > DS for both land-use types (p < 0.05), while differences between TS and DS were smaller as compared to the differences to FS (Fig. 2). The conversion from grassland to cropland reduced soil OC stocks in all steppe types (p < 0.01). The relative decline of OC due to LUC was generally most pronounced in the topsoil increment (0–10 cm) and decreased when subsoil is included (0–60 cm). The proportional OC stock change was similar for FS and DS, while TS tended to have larger proportional OC losses, though statistically not significant (p = 0.54). On average, conversion from grassland to cropland decreased soil OC stocks by 37% in 0–10 cm, 31% in 0–25 cm, and 28% in 0–60 cm independently from steppe type (Fig.S1). Chronosequence data from FS showed that already after five years following grassland to cropland conversion, OC stocks declined by 29% and 22% in 0–10 and 0–25 cm, respectively, while during the following 25 years the total OC decline was much less (Fig. 3). While OC stocks in 0–10 cm depth were mainly controlled by land-use type (50% explained variance), we found that effects of steppe type and land-use type were virtually equal when considering 0–25 cm depth (each 33% explained variance, Table S3). Over the depth of 0–60 cm, OC stocks were more affected by steppe type (36% explained variance) than by land-use type (23% explained variance).

3.2.2. Organic matter fractions

Density fractionation was performed on the horizon samples in order to separate functionally different OM. The HF was the dominant OM fraction in soils of all steppe types and land-use types in all considered soil horizons (>90% of total OC; Table 2). The LF contributed <10% to the total OC pool and tended to have larger contribution under arid conditions (Table 2). Grassland to cropland
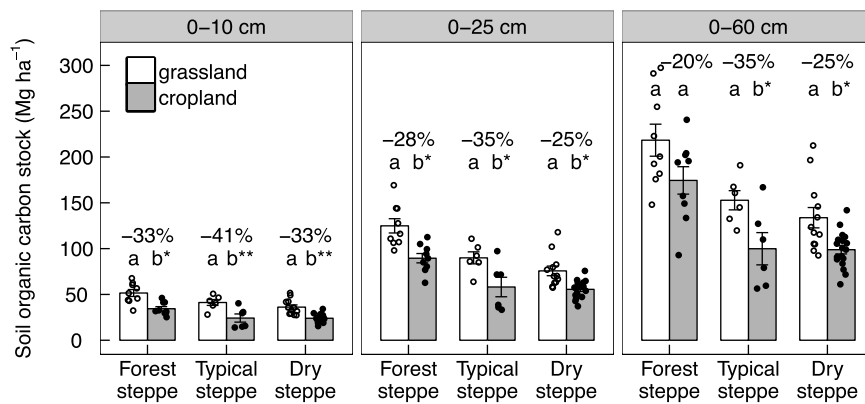
Fig. 2. Soil organic carbon stocks (Mg ha^{-1}) depending on land-use type for 0–10 cm, 0–25 cm, and 0–60 cm in different steppe types. Values are given as arithmetic mean ± standard error of the mean. Points show individual measurements and lowercase letters indicate significant differences between land-use types, tested within steppe type and depth increment (p-value, $0 < *** < 0.001 < ** < 0.01 < * < 0.05$). Numbers above bars indicate the relative soil OC stock decline due to grassland to cropland conversion.
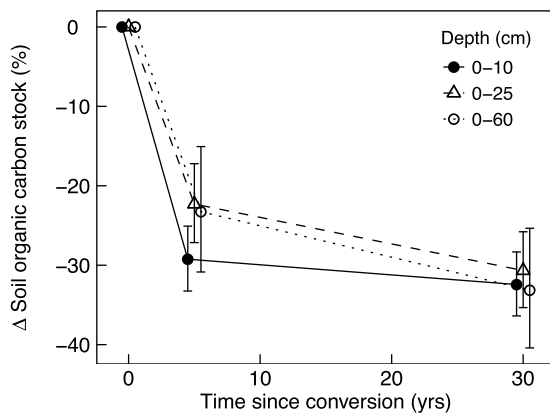

Fig. 3. Time-dependent decline of soil organic carbon stocks (%) for three depths at a chronosequence site in the forest steppe (n = 3 per depth and time interval), time intervals are 5 and 30 yrs for all three depths. Position shifting was done to avoid overlapping of error bars.

conversion caused a reduction of the OC content per g soil with respect to both OM fractions, most pronounced in A horizons. The OC content of the HF decreased with increasing aridity from about 30 mg OC g^{-1} fraction in A horizons of FS to about 15–20 mg OC g^{-1} fraction in topsoils of DS, while no differences between steppe types were apparent with respect to the LF. Conversion from grassland to cropland caused a small decrease of the OC content in the HF of A horizons under all climatic conditions, while no consistent trend was apparent regarding the LF. However, A horizons of grasslands had larger amounts of LF material per g soil than croplands (ca. 9–10 mg LF g^{-1} soil in grasslands vs. ca. 5–6 mg LF g^{-1} soil in croplands). Land-use change induced a larger relative decline of LF-OC stocks than HF-OC stocks (Fig. 4). However, given the much larger contribution of HF-OC to total OC, HF-OC accounted for most of the soil OC losses (80–90%; Fig.S2). Radiocarbon analysis revealed that OC in the HF contained less modern C than LF-OC (Fig.S3), with estimated ^{14}C ages of 500–2900 years B.P. for HF-OC and ages mostly <400 years B.P. for LF-OC. The ^{14}C activities tended to increase with increasing aridity and

Table 2
OC content and C: N ratio of soil organic matter fractions and contribution of each fraction to the bulk soil mass and the soil OC pool depending on steppe type, horizon and land-use type. Values are given as arithmetic mean ± standard error of the mean. Abbreviations: FS = forest steppe, TS = typical steppe, DS = dry steppe.

| Steppe type	Horizon	Land-use type	n	Light fraction (LF)					Heavy fraction (HF)				
				mg OC g^{-1} fraction	C : N	mg LF g^{-1} soil	mg OC g^{-1} soil	% OC of total soil OC	mg OC g^{-1} fraction	C : N	mg HF g^{-1} soil	mg OC g^{-1} soil	% OC of total soil OC
FS	A	grassland	3	267.8 ± 22.0	18.8 ± 0.5	9.7 ± 1.7	2.5 ± 0.2	6.9 ± 0.9	33.3 ± 4.4	12.8 ± 0.7	990.3 ± 1.7	35.0 ± 4.6	93.1 ± 0.9
		cropland	3	245.4 ± 19.0	17.6 ± 0.4	6.1 ± 1.3	1.6 ± 0.3	5.2 ± 1.6	29.6 ± 5.9	12.2 ± 0.2	993.9 ± 1.3	31.6 ± 5.6	94.8 ± 1.6
	AC	grassland	3	264.4 ± 6.7	19.6 ± 0.5	1.2 ± 0.5	0.4 ± 0.2	4.5 ± 0.5	6.7 ± 2.3	8.4 ± 0.7	998.8 ± 0.5	7.7 ± 2.1	95.5 ± 0.5
		cropland	3	266.6 ± 21.3	23.0 ± 1.3	2.8 ± 0.9	0.8 ± 0.2	6.7 ± 2.2	10.4 ± 2.3	11.0 ± 0.7	997.2 ± 0.9	12.2 ± 2.0	93.3 ± 2.2
	C	grassland	3	224.3 ± 12.5	11.7 ± 2.0	0.5 ± 0.2	0.1 ± 0.0	4.9 ± 1.2	2.4 ± 0.4	6.0 ± 0.2	999.5 ± 0.2	2.5 ± 0.6	95.1 ± 1.2
		cropland	3	224.2 ± 3.1	17.1 ± 1.1	1.1 ± 0.5	0.1 ± 0.0	4.8 ± 1.7	2.4 ± 0.5	6.3 ± 0.1	998.9 ± 0.5	2.7 ± 0.6	95.2 ± 1.7
TS	A	grassland	2	244.6 ± 31.6	18.1 ± 0.4	9.0 ± 0.4	2.3 ± 0.0	8.1 ± 0.7	23.4 ± 3.5	11.5 ± 0.1	991.0 ± 0.4	26.1 ± 2.8	91.9 ± 0.7
		cropland	2	250.3 ± 28.7	15.1 ± 2.0	5.4 ± 2.8	1.5 ± 0.9	5.8 ± 0.7	20.5 ± 9.7	10.6 ± 1.5	994.6 ± 2.8	23.2 ± 11.5	94.2 ± 0.7
	AC	grassland	2	256.0 ± 7.6	16.3 ± 0.4	2.9 ± 0.9	0.8 ± 0.2	6.5 ± 0.6	10.1 ± 2.3	9.8 ± 0.3	997.1 ± 0.9	10.7 ± 2.4	93.5 ± 0.6
		cropland	2	282.3 ± 31.9	15.4 ± 2.5	1.5 ± 0.2	0.5 ± 0.1	5.5 ± 0.6	7.8 ± 1.9	9.0 ± 1.0	998.5 ± 0.2	8.3 ± 1.9	94.5 ± 0.6
	C	grassland	2	258.3 ± 12.8	15.9 ± 1.2	1.6 ± 0.3	0.3 ± 0.1	10.2 ± 2.9	3.4 ± 0.6	6.6 ± 0.1	998.5 ± 0.3	2.5 ± 0.0	89.8 ± 2.9
		cropland	2	208.1 ± 4.5	11.9 ± 0.4	1.1 ± 0.6	0.2 ± 0.1	7.3 ± 3.1	3.1 ± 0.7	5.6 ± 0.9	998.9 ± 0.6	2.7 ± 0.7	92.7 ± 3.1
DS	A	grassland	4	221.4 ± 22.2	17.2 ± 1.0	10.2 ± 2.4	2.5 ± 0.7	9.8 ± 0.9	20.1 ± 4.1	10.5 ± 0.3	989.8 ± 2.4	22.8 ± 4.4	90.2 ± 0.9
		cropland	6	263.7 ± 20.8	15.9 ± 1.0	6.3 ± 1.5	1.7 ± 0.4	9.7 ± 1.7	14.6 ± 1.3	10.9 ± 0.3	993.7 ± 1.5	16.0 ± 1.6	90.3 ± 1.7
	AC	grassland	4	230.5 ± 13.7	17.4 ± 1.2	3.0 ± 0.6	0.7 ± 0.1	6.8 ± 1.3	9.6 ± 1.7	8.4 ± 0.2	997.1 ± 0.6	10.2 ± 1.6	93.2 ± 1.3
		cropland	6	213.4 ± 11.8	16.1 ± 1.8	2.2 ± 0.6	0.5 ± 0.1	4.7 ± 0.7	8.5 ± 0.8	8.5 ± 0.4	997.8 ± 0.6	9.1 ± 0.8	95.3 ± 0.7
	C	grassland	4	212.8 ± 16.9	16.0 ± 0.6	1.8 ± 0.1	0.3 ± 0.0	8.8 ± 0.8	3.8 ± 0.5	7.0 ± 0.3	998.2 ± 0.1	2.9 ± 0.4	91.2 ± 0.8
		cropland	6	223.0 ± 20.6	13.6 ± 0.5	1.6 ± 0.4	0.2 ± 0.0	8.6 ± 1.3	3.4 ± 0.3	8.6 ± 1.2	998.4 ± 0.4	2.4 ± 0.1	91.4 ± 1.3
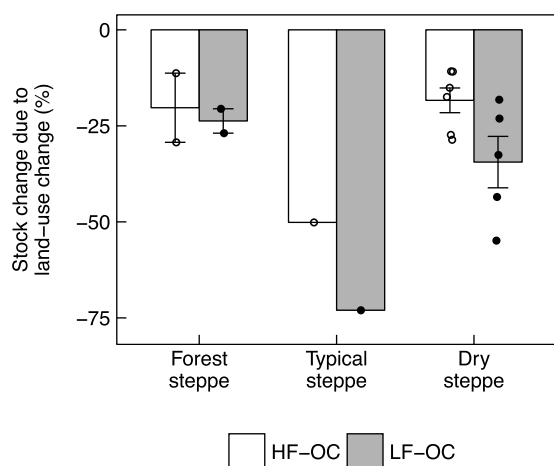
Fig. 4. Change of the mass-corrected stocks of heavy fraction OC (HF-OC) and light fraction OC (LF-OC) in A horizons of three steppe types due to LUC from grassland to cropland. Bars indicate arithmetic means ± standard error of the mean and points show individual measurements.

grasslands contained more modern C in both fractions than croplands.

3.2.3. Phospholipid fatty acids

Grassland to cropland conversion decreased the microbial PLFA biomass significantly in the topsoil (0–10 cm) of all three steppe types (p < 0.05, Table 3). The largest amounts of PLFA biomass were found in grasslands of FS with ca. 225 nmol PLFA g^{-1} soil, while grassland soils in TS and DS had a similar level containing ca. 175 nmol PLFA g^{-1} soil. Cropland soils had a similar PLFA biomass of ca. 115 nmol PLFA g^{-1} soil irrespectively of steppe type. The amount of PLFA biomass relative to soil OC was largest in grassland and cropland soils of DS. It decreased with increasing humidity (p < 0.05, Table 3), and the smallest values were detected in grasslands of FS and TS and croplands of FS (Table 3). Land-use change from grassland to cropland has not significantly changed the OC-based PLFA biomass in any steppe type. However, grassland soils of FS tended to have higher PLFA biomass relative to total OC than cropland soils. Fungal PLFA biomass decreased significantly due to grassland to cropland conversion in soils of FS and TS (p < 0.05), while this decrease was not significant in DS. The fungal PLFA biomass tended to decline with increasing aridity from FS to DS, though not significant. The fungi : bacteria ratio was significantly larger in grasslands than in croplands of FS (p < 0.01), while the difference between grasslands and croplands was smaller in TS (p = 0.2) and no difference was found in DS (Table 3). Drier climate increased the Gram+ : Gram− ratio significantly in

grasslands (p < 0.001), while no trend was apparent for croplands. The conversion from grassland to cropland reduced the Gram+ : Gram− ratio only in DS significantly (p < 0.05, Table 3).

Nonmetric Multidimensional Scaling showed PLFAs assigned to Gram− and fungi were slightly more abundant in FS, whereas PLFAs attributed to Gram+ and protozoa were relatively more abundant in DS (Fig. 5a). The effect of land-use type on the PLFA-based microbial community composition, on the other hand, was less clear. Only the group of unspecific bacterial PLFA tended to a larger relative abundance in croplands, while fungal PLFA tended to be slightly more abundant under grasslands (Fig. 5b). Results from ADONIS showed that steppe type (R^2 = 0.22, p = 0.001) had a stronger effect on the microbial community composition than land-use type (R^2 = 0.10, p = 0.001; Fig. 5a,b). The largest difference between the microbial communities existed between forest steppe and dry steppe (Table S4; R^2 = 0.25, p = 0.003), while the difference between typical steppe and dry steppe was smaller (R^2 = 0.15, p = 0.024) and no significant difference was evident between forest steppe and typical steppe (R^2 = 0.07, p = 0.381). Conversion from grassland to cropland had a different effect on microbial communities depending on steppe type, as indicated by the significant interaction between steppe type and land-use type (R^2 = 0.11, p = 0.01; Fig. 5c). Accordingly, LUC caused a decrease of PLFA assigned to fungi only in FS, while PLFA representing Gram+ decreased only in DS, as is also shown by the fungi : bacteria ratio and Gram+ : Gram− ratio in Table 3. It is important to note that the effect of steppe type and land-use type on the microbial community was small, as R^2 values range between 0.10 and 0.22.

3.2.4. Aggregate stability

Soil aggregate stability decreased significantly after conversion from grassland to cropland in all three steppe types to a similar extent (p < 0.05, Table S5). Grassland soils had a ΔMWD between 0.28 ± 0.17 (FS) and 0.40 ± 0.05 (TS), while ΔMWD values of croplands ranged between 1.37 ± 0.08 (FS) and 1.62 ± 0.17 (DS). Lower aggregate stability was related to lower OC contents (Fig. 6). In the studied soils, aggregate stability was not related to the amount of fungal PLFA (Table S6). Land-use change from grassland to cropland caused a change in the aggregate size class distribution in all steppe types, with a preferential decrease of aggregates >1 mm and a subsequent increase of aggregates <1 mm (Fig.S4).

4. Discussion

4.1. Climate-dependent effect of LUC from grassland to cropland on soil OC stocks

Soil OC stocks of the Kulunda steppe decreased from FS to DS, and thus followed a precipitation gradient (Fig. 2). As shown by

Table 3

PLFA data in 0–10 cm depending on land-use type and steppe type. Values are given as arithmetic mean ± standard error of the mean. As one sample from TS grassland and two samples from DS cropland were discarded during measurement, the sample size n is 57 instead of 60.

Steppe type	Land-use type	No. plots	n	PLFA biomass	PLFA biomass relative to soil OC	fungal PLFA biomass	fungi : bacteria ratio	Gram+ : Gram− ratio
				nmol g^{-1} soil	mmol g^{-1} soil OC	nmol g^{-1} soil	–	–
FS	grassland	3	9	224.8 ± 41.4aA	4.62 ± 0.24aA	8.51 ± 3.22aA	0.037 ± 0.009aA	2.33 ± 0.21aA
	cropland	3	9	114.4 ± 28.2b***A	3.48 ± 0.37aA	2.39 ± 0.94b***A	0.020 ± 0.003b**A	2.75 ± 0.25aA
TS	grassland	2	5	174.6 ± 25.8aA	4.56 ± 0.26aA	5.05 ± 0.69aA	0.030 ± 0.000aA	3.04 ± 0.16aAB
	cropland	2	6	116.8 ± 9.3b*A	6.05 ± 1.98aB*	2.56 ± 0.43b*A	0.023 ± 0.006aA	2.51 ± 0.37aA
DS	grassland	4	12	178.7 ± 20.6aA	6.21 ± 0.37aA	4.39 ± 0.88aA	0.025 ± 0.002aA	3.53 ± 0.07aB***
	cropland	6	16	117.6 ± 10.9b**A	6.15 ± 0.35aB**	2.88 ± 0.16aA	0.026 ± 0.002aA	3.02 ± 0.06b*A

Lowercase letters indicate significant differences between land-use types within steppe type, and uppercase letters indicate significant differences between steppe types within land-use type (p-value, 0 < *** < 0.001 < ** < 0.01 < * < 0.05). Abbreviations: FS = forest steppe, TS = typical steppe, DS = dry steppe.
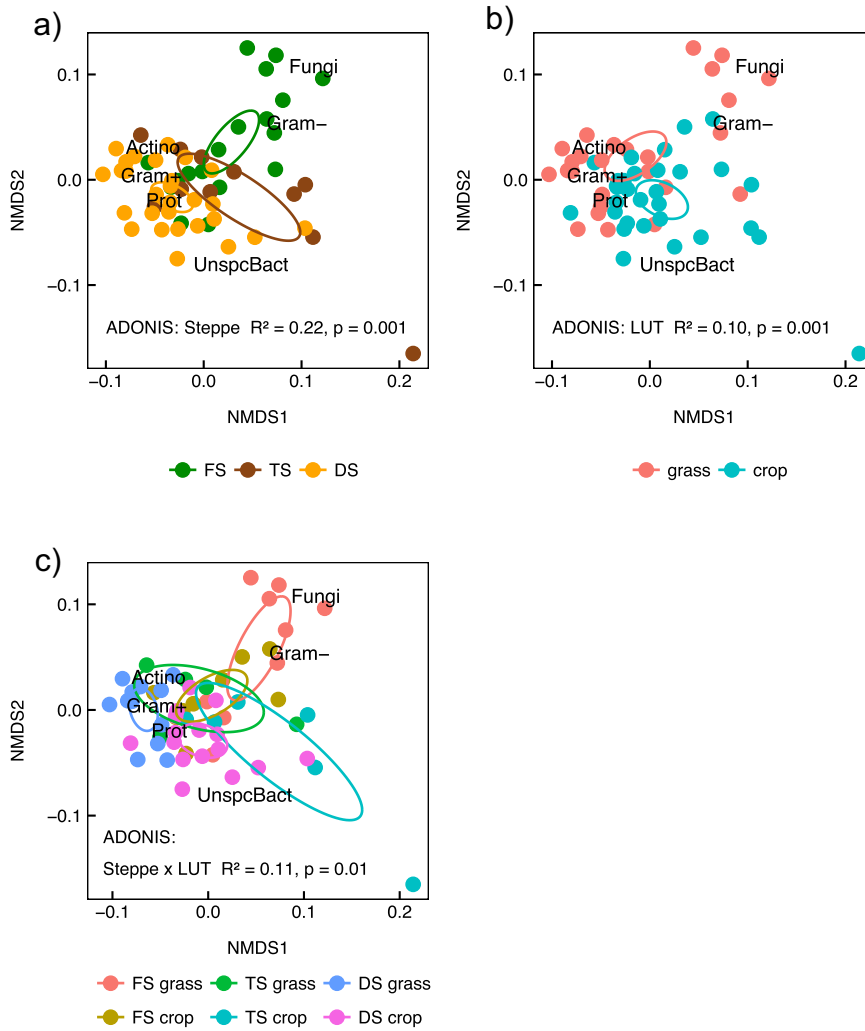
Fig. 5. Two-dimensional Nonmetric Multidimensional Scaling (NMDS), showing the effect of a) steppe type, b) land-use type and c) the interaction between steppe type and land-use type on the microbial community composition in 0–10 cm. The stress value of the NMDS is 0.10. Ellipses indicate 95% confidence regions for the group centroids. Results from ADONIS show that steppe type has a stronger effect than land-use type. Land-use change has a different effect in each steppe type as the interaction between steppe type and land-use type (Steppe x LUT) is significant. As one sample from TS grassland and two samples from DS cropland had to be discarded during measurement, the sample size n is 57 instead of 60. Abbreviations: LUT = land-use type, FS = forest steppe, TS = typical steppe, DS = dry steppe, grass = grassland, crop = cropland, Actino = actinomycetes, Gram– = gram-negative bacteria, Gram+ = gram-positive bacteria, UnspcBact = unspecific bacteria, Prot = protozoa.

Fig. 6. Relation between aggregate stability (ΔMWD) and $\log_e$(soil organic carbon) (%) for topsoils in the three different steppe types. The points show arithmetic means ± standard error of the mean of each plot. The dashed lines connect all paired plots within one site. The solid line corresponds to the trend line over all plots within one steppe type.

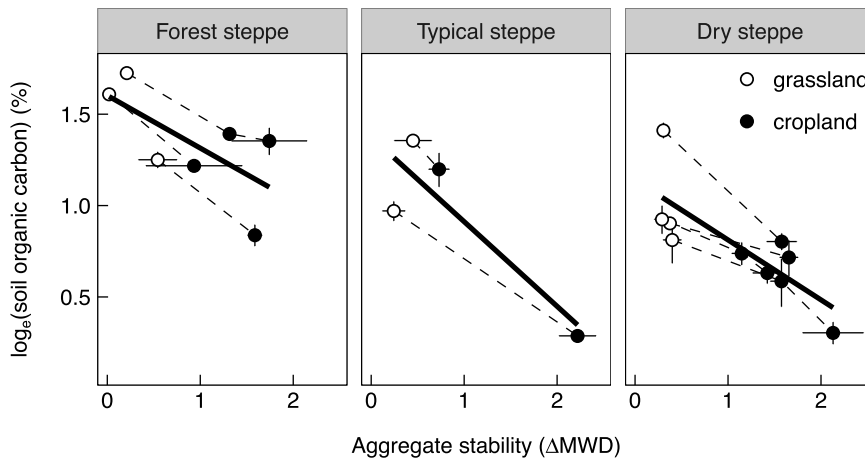Saparov et al. (2007) for steppe soils of Kazakhstan, there is a strong impact of plant residue input on OC stocks. Larger precipitation enhances net primary productivity and thus increases biomass input into the soil which eventually elevates soil OC stocks.

Conversion from grassland to cropland caused an average decline in the OC stock of roughly one third for the upper 25 cm, which was independent from climate (Fig. 2). For a site in FS, this decline occurred fast within the first five years, demonstrating the tremendous impact of soil disturbance (Fig. 3). The magnitude of the soil OC loss after conversion from grassland to cropland in the Kulunda steppe is in line with data from previous studies of similar soils. In North American prairies grassland to cropland conversion caused a soil OC stock decline of 24–32% (Beniston et al., 2014; Doran et al., 1998; VandenBygaart et al., 2003). In Chernozems of European Russia topsoil OC stocks decreased by 27–40% due to LUC from grassland to cropland (Mikhailova et al., 2000; Rodionov et al., 1998). Modelling results for temperate soils (MAT 0–18 °C) showed a soil OC decrease of $36 \pm 5\%$ in 0–27 cm due to conversion from grassland to cropland with ca. 80% of OC being lost within the first five years (Poeplau et al., 2011). Thus, the OC stock declines observed for Siberian steppe soils as a result of LUC were comparable to those previously reported for steppe soils of European Russia and prairie soils of North America.

The aim of our study was not only to elucidate the effect of LUC on soil OC stocks, but particularly how this effect changes under different climatic conditions. In contrast to our hypothesis, we did not find larger OC losses upon LUC in drier climate (Fig. 2). Surprisingly, the LUC-induced decline of soil OC stocks was independent from climatic conditions, though we showed that the proportion of labile POM tended to increase with drier climate ($6.9 \pm 0.9\%$ OC of total soil OC in A horizons of grasslands in FS vs. $9.8 \pm 0.9\%$ in DS; Table 2). A possible reason is that in the Chernozems and Kastanozems under study POM comprised only a small proportion (<10%) of total OC and contributed little to the overall LUC-induced decline of OC stocks. Thus, it is not the stability of POM but rather that of mineral-associated OM, which dictates the relative loss of OC upon LUC. The stability of MOM was obviously not climate-dependent in the studied region (Fig. 4; same HF-OC stock change due to LUC in FS and DS), wherefore neither the decline of total soil OC stocks showed a climate dependence. In this regard, our results are different from what was found in previous work from other regions of the world. Burke et al. (1989) and Guo and Gifford (2002) found relative OC losses after grassland to cropland conversion positively correlated to precipitation until a MAP of 600 mm in soils from North America. On the other hand, Poeplau et al. (2011) found no correlation between precipitation and relative OC loss as a result of LUC but an attenuating effect of clay in temperate soils.

Regardless of parameters which determined the decline of soil OC due to LUC, we encountered clay content, pH and bulk density as significant environmental factors for the OC content in the studied Kulunda soils (Section S1; Table S8). This is in agreement with previous work (e.g. Schimel et al., 1994) and supports conclusions about the primary importance of these variables on soil OC contents along climate and land use gradients.

In summary, our results suggest that drier climate in the course of climate change is not expected to change the magnitude of LUC on soil OC levels in the soils under study.

4.2. Protection of soil OM on mineral surfaces and within aggregates

Particulate OM is supposed to be a labile fraction with fast turnover rates whereas mineral-associated OM is considered more stable with slower turnover rates (Kleber et al., 2015; von Lützow et al., 2006). In steppe soils, POM is believed to play an important quantitative role in terms of soil OM dynamics as it contributes substantially to total OC (>20%) in Chernozems of Canada (Plante et al., 2010), European Russia (Breulmann et al., 2014; Kalinina et al., 2011), or China (Steffens et al., 2010). However, astonishingly, in soils of the Siberian Kulunda steppe POM was of minor relevance as it accounted for maximally 10% of total OC (Table 2). Land-use change from grassland to cropland reduced particulate OC relatively more than mineral-associated OC, which is in line with previous reports from soils of the temperate zone (Poeplau and Don, 2013). However, due to its small contribution to total OC, the absolute contribution of particulate OC to the total OC stock decline was small. About 80–90% of lost OC has been associated with minerals (Fig. S2). In fact, a considerable part (20–50%, see Fig. 4) of mineral-associated OC is vulnerable to soil-management and possibly part of a labile OM pool. Thus, OC bound to minerals in the soils under study is not necessarily stabilized against decomposition by microorganisms. Weaker mineral-organic associations may result from the higher soil pH, absence of reactive minerals, or generally weaker bondings of OM to minerals (e.g. OM held by "Ca^{2+} bridges"; Mikutta et al., 2007; Kleber et al., 2015). However, ^{14}C ages from mineral-bound OC of 500–2900 years B.P. in cropland soils also show that a considerable part of this fraction remained protected from decomposition. This suggests that mineral-associated OC is a heterogeneous fraction, which at the same time comprises labile and stable OC components, with the labile forms being also vulnerable to LUC.

Besides the protection of OC on mineral surfaces, aggregates are known to protect OM against microbial decomposition over decadal or even centennial time scales due to the physical separation of the aggregate-occluded organic substrate from the microbial community (Stockmann et al., 2013; von Lützow et al., 2008). Particularly in agro-ecosystems, aggregate stability was found to be a major determinant for OC contents (Bronick and Lal, 2005). Like reported in studies from other regions (e.g., Follett et al., 2015; Six et al., 1998), aggregate stability decreased significantly due to LUC from grassland to cropland also in the soils under study and this effect did not depend on the climatic conditions (Table S5). The reduction of aggregate stability is possibly related to a decreased OM input in agricultural systems, as the input of fresh OM would favor the formation of stable aggregates (Bossuyt et al., 2001; Steffens et al., 2009). This matches our finding that aggregate stability and OC were positively correlated (Fig. 6). In addition, an increased macroaggregate (250–2000 μm) turnover in croplands and the concurrent decrease of the formation of stable microaggregates (53–250 μm) within macroaggregates was shown to reduce the potential of arable soils to store OC (Six et al., 2000). The correlation between aggregate stability and OC was therefore also shown in previous studies (Al-Kaisi et al., 2014; Follett et al., 2015).

The formation of stable macroaggregates is supported by the presence of soil fungi wherefore they play a major role in the sequestration of OM in agricultural systems (Frey et al., 1999; Guggenberger et al., 1999). Unlike expected, we did neither find aggregate stability to be correlated to the amount of fungal PLFA (as a proxy for the fungal biomass; Table S6) nor was the amount of PLFA biomass related to aggregate stability (data not shown). This could be due to the large clay contents in soils of the Kulunda steppe, with average clay contents of 26–34%. Kiem and Kandeler (1997) reported that microbial-induced aggregate stabilization is of less importance in clayey soils, as minerals already act as strong binding agents. Thus, soil fungi seemingly do not mediate aggregate stability in the soils under study. In soils of FS, grassland to cropland conversion reduced the fungi : bacteria ratio significantly (Table 3). This can be explained by the destruction of fungal hyphae due to soil tillage (Bronick and Lal, 2005; Six et al., 2006) or by different residue placement under grassland as

compared to cropland (Six et al., 2006). Frey et al. (2000) showed that the presence of surface residues under grassland favors fungal communities, as fungi are able to bridge the interspace between residues and bulk soil and translocate N-rich compounds to the C-rich, but N-depleted surface litter. However, the fungi : bacteria ratio did not decrease after grassland to cropland conversion in DS. This is assigned to initially lower fungi abundance under grasslands in DS, therefore diminishing the negative effect of LUC on fungi (Calderón et al., 2000).

Summing up, mineral-associated OM was the dominant OM fraction in the soils under study and the main source of declining OC stocks upon LUC. The decline of soil OC was associated to a concurrent decrease in aggregate stability, which in turn was not related to the amount of fungal PLFA.

4.3. Microbial abundance and community composition as affected by land-use change along the climatic gradient

Microbial biomass and OM contents of soils are intimately connected (e.g. Ingram et al., 2008), as OM serves as carbon and energy source for most soil microorganisms (Drenovsky et al., 2004). The larger microbial PLFA biomass in topsoils of the Kulunda steppe under grassland than under cropland can therefore, largely be explained by the larger OC stocks in grasslands. However, irrespective of steppe type and initial microbial biomass in grasslands, the PLFA biomass decreased to a similar level in cropland soils (Table 3). Thus, higher OC contents in arable soils of FS do not result in a larger abundance of microbes. Moll et al. (2015) showed that the abundance of fungi is largely dependent on the amount of residue inputs in arable topsoils, while Xiao et al. (2015) found this for the whole microbial community in steppe soils of Inner Mongolia. The similar amount of PLFA biomass in croplands along the climatic gradient could therefore be attributed to similar plant residue inputs across croplands throughout the Kulunda steppe.

The composition of the microbial community is sensitive to changes in environmental conditions, such as climate or the quantity and quality of litter inputs (Fanin et al., 2014; Frey et al., 2008). Also LUC-related soil disturbance was found to change microbial communities significantly (Li et al., 2014; Zhang et al., 2014). PLFA is a rapid and sensitive method to detect changes in the microbial community composition, however, it cannot compete with rRNA methods in the phylogenetic resolution by which a microbial community can be characterized (Frostegård et al., 2011). Nevertheless, PLFA analysis of soils of the Kulunda steppe revealed that the microbial community composition was more controlled by steppe type than by land-use type and the climatic effect on microbial communities was different in each land-use type (Fig. 5). Changes in the microbial community composition due to climatic shifts were more pronounced under grassland than under cropland, as indicated by a sharp increase in the Gram+ : Gram− ratio from wet to dry climate under grassland, while no trend was apparent under cropland (Table 3). The relative amount of fungal PLFA was lower under dry than wet climate (Fig. 5). Hence, drier conditions are expected to cause a relative decrease of fungi, while gram-positive bacteria would relatively increase. This is in contrast to some studies that concluded fungal biomass being superior to bacteria at conditions of water stress (Schimel et al., 2007; Drenovsky et al., 2004; Zhang et al., 2005). But our finding is supported by Zogg et al. (1997) and Frey et al. (2008), who found a smaller contribution of fungi and a larger contribution of Gram+ with increasing temperature in warming experiments, i.e. drier soil conditions. Billings and Ballantyne (2013) hypothesized that the thicker cell walls of Gram+ makes them more resistant to dry conditions than Gram−. In addition, De Vries and Shade (2013) noted, that the ability of Gram+ to sporulate allows them to

withstand disturbances, including drought. In summary, our data emphasize a small but significant climatic effect on PLFA-based microbial groups, which is more pronounced in grassland than in cropland soils. Drier climate in the future is expected to change the microbial community more than the conversion of the soils from grasslands to croplands.

5. Conclusions

The main goal of the current study was to determine the climate-dependent effect of land-use change from grassland to cropland on soil OM in a semi-arid steppe ecosystem of Siberia. Cultivation of grassland soils decreased OC stocks by about 31% in the upper 25 cm, which was independent from climate. The loss of OC went along with a reduction of aggregate stability but this was not related to the amount of fungal PLFA. Unlike expected, POM accounted generally for only <10% of the total OC pool, and the majority of OC across all steppe types was bound to minerals (>90%). Despite the low ^{14}C age of POM (< 400 yrs B.P.) and large relative losses due to soil cultivation (up to 70%), most management-induced OC losses (80–90%) could be assigned to a decrease of mineral-bound OC. Stocks of mineral-associated OC decreased in A horizons by 20–50% due to cultivation of grasslands. This demonstrates that a considerable portion of mineral-bound OM is vulnerable to LUC, while other mineral-associated OC components are stable and largely unaffected by LUC, as can be inferred from the high ^{14}C ages (500–2900 yrs B.P.) of mineral-bound OM in croplands. PLFA-based soil microbial communities varied along the climatic gradient with larger relative abundance of fungal PLFA and Gram− bacterial PLFA in moist climate and a larger relative abundance of PLFA assigned to gram-positive bacteria under dry conditions. The climate had a larger impact on microbial communities than LUC, and communities under grassland were more affected by climatic shifts than those under cropland.

We conclude that at the predicted drier climate in the semi-arid steppes of southern Siberia there will be a pronounced OC loss under both, grassland and cropland, due to generally reduced biomass inputs under dry conditions. Converting grassland to cropland under drier conditions will keep the LUC-induced OC losses at the same critical level as is observed in soils at present. Soil microbial communities are expected to change more as a result of drier climate than due to the conversion from grassland to cropland.

Appendix A. Supplementary data

Supplementary data associated with this article can be found, in the online version, at http://dx.doi.org/10.1016/j.agee.2016.10.022.

References

Al-Kaisi, M.M., Douelle, A., Kwaw-Mensah, D., 2014. Soil microaggregate and macroaggregate decay over time and soil carbon change as influenced by different tillage systems. J. Soil Water Conserv. 69, 574–580. doi:http://dx.doi.org/10.2489/jswc.69.6.574.

Amelung, W., Flach, K.W., Zhang, X., Zech, W., 1998. Climatic effects on C pools of native and cultivated prairie. Adv. GeoEcology 31, 217–224.

Bates, D., Mächler, M., Bolker, B., 2012. Fitting linear mixed-effects models using lme4. J. Stat. Software 1–51.

Beniston, J.W., DuPont, S.T., Glover, J.D., Lal, R., Dungait, J.A.J., 2014. Soil organic carbon dynamics 75 years after land-use change in perennial grassland and annual wheat agricultural systems. Biogeochemistry 120, 37–49. doi:http://dx.doi.org/10.1007/s10533-014-9980-3.

Billings, S.A., Ballantyne, F., 2013. How interactions between microbial resource demands, soil organic matter stoichiometry, and substrate reactivity determine the direction and magnitude of soil respiratory responses to warming. Glob. Chang. Biol. 19, 90–102. doi:http://dx.doi.org/10.1111/gcb.12029.

Bossuyt, H., Denef, K., Six, J., Frey, S., Merckx, R., Paustian, K., 2001. Influence of microbial populations and residue quality on aggregate stability. Appl. Soil Ecol. 16, 195–208. doi:http://dx.doi.org/10.1016/S0929-1393(00)00116-5.

Breulmann, M., Masyutenko, N.P., Kogut, B.M., Schroll, R., Dörfler, U., Buscot, F., Schulz, E., 2014. Short-term bioavailability of carbon in soil organic matter fractions of different particle sizes and densities in grassland ecosystems. Sci. Total Environ. 497–498, 29–37. doi:http://dx.doi.org/10.1016/j.scitotenv.2014.07.080.

Bronick, C.J., Lal, R., 2005. Soil structure and management: a review. Geoderma 124, 3–22. doi:http://dx.doi.org/10.1016/j.geoderma.2004.03.005.

Burke, I.C., Yonker, C.M., Parton, W.J., Cole, C.V., Flach, K., Schimel, D.S., 1989. Texture, climate, and cultivation effects on soil organic matter content in US grassland soils. Soil Sci. Soc. Am. J. 53, 800–805. doi:http://dx.doi.org/10.2136/sssaj1989.03615995005300030029x.

Calderón, F.J., Jackson, L.E., Scow, K.M., Rolston, D.E., 2000. Microbial responses to simulated tillage in cultivated and uncultivated soils. Soil Biol. Biochem. 32, 1547–1559. doi:http://dx.doi.org/10.1016/S0038-0717(00)00067-5.

Core Team, R., 2015. R: A Language and Environment for Statistical Computing. .

DIN ISO 11277, 2002. Soil Quality −determination of Particle Size Distribution in Mineral Soil Material −method by Sieving and Sedimentation. .

De Vries, F.T., Shade, A., 2013. Controls on soil microbial community stability under climate change. Front. Microbiol. 4, 1–16. doi:http://dx.doi.org/10.3389/fmicb.2013.00265.

Doran, J., Elliott, E., Paustian, K., 1998. Soil microbial activity, nitrogen cycling, and long-term changes in organic carbon pools as related to fallow tillage management. Soil Tillage Res. 49, 3–18. doi:http://dx.doi.org/10.1016/S0167-1987(98)00150-0.

Drenovsky, R.E., Vo, D., Graham, K.J., Scow, K.M., 2004. Soil water content and organic carbon availability are major determinants of soil microbial community composition. Microb. Ecol. 48, 424–430. doi:http://dx.doi.org/10.1007/s00248-003-1063-2.

Ellert, B.H., Bettany, J.R., 1995. Calculation of organic matter and nutrients stored in soils under contrasting management regimes. Can. J. Soil Sci. doi:http://dx.doi.org/10.4141/cjss95-075.

FAO, 2013. FAO Statistical Yearbook 2013. World food and agriculture, Rome.

Fanin, N., Hättenschwiler, S., Fromin, N., 2014. Litter fingerprint on microbial biomass, activity, and community structure in the underlying soil. Plant Soil 379, 79–91. doi:http://dx.doi.org/10.1007/s11104-014-2051-7.

Follett, R.F., Stewart, C.E., Pruessner, E.G., Kimble, J.M., 2015. Great Plains climate and land-use effects on soil organic carbon. Soil Sci. Soc. Am. J. 79, 261. doi:http://dx.doi.org/10.2136/sssaj2014.07.0282.

Frühauf, M., 2011. Landnutzungs- und Ökosystementwicklung in den südsibirischen Agrarsteppen. Geogr. Rundschau 1, 46–53.

Frey, S.D., Elliott, E.T., Paustian, K., 1999. Bacterial and fungal abundance and biomass in conventional and no-tillage agroecosystems along two climatic gradients. Soil Biol. Biochem. 31, 573–585. doi:http://dx.doi.org/10.1016/S0038-0717(98)00161-8.

Frey, S.D., Elliott, E.T., Paustian, K., Peterson, G.A., 2000. Fungal translocation as a mechanism for soil nitrogen inputs to surface residue decomposition in a no-tillage agroecosystem. Soil Biol. Biochem. 32, 689–698. doi:http://dx.doi.org/10.1016/S0038-0717(99)00205-9.

Frey, S.D., Drijber, R., Smith, H., Melillo, J., 2008. Microbial biomass, functional capacity, and community structure after 12 years of soil warming. Soil Biol. Biochem. 40, 2904–2907. doi:http://dx.doi.org/10.1016/j.soilbio.2008.07.020.

Frostegård, Å., Bååth, E., 1996. The use of phospholipid fatty acid analysis to estimate bacterial and fungal biomass in soil. Biol. Fertil. Soils 22, 59–65. doi:http://dx.doi.org/10.1007/BF00384433.

Frostegård, Å., Tunlid, A., Bååth, E., 2011. Use and misuse of PLFA measurements in soils. Soil Biol. Biochem. 43, 1621–1625. doi:http://dx.doi.org/10.1016/j.soilbio.2010.11.021.

Golchin, A., Oades, J.M., Skjemstad, J.O., Clarke, P., 1994. Study of free and occluded particulate organic matter in soils by solid state 13C CP/MAS NMR spectroscopy and scanning electron microscopy. Aust. J. Soil Res. 32, 285–309. doi:http://dx.doi.org/10.1071/SR9940285.

Guggenberger, G., Elliott, E.T., Frey, S.D., Six, J., Paustian, K., 1999. Microbial contributions to the aggregation of a cultivated grassland soil amended with starch. Soil Biol. Biochem. 31, 407–419. doi:http://dx.doi.org/10.1016/S0038-0717(98)00143-6.

Gunina, A., Dippold, M.A., Glaser, B., Kuzyakov, Y., 2014. Fate of low molecular weight organic substances in an arable soil: from microbial uptake to utilisation and stabilisation. Soil Biol. Biochem. 77, 304–313. doi:http://dx.doi.org/10.1016/j.soilbio.2014.06.029.

Guo, L.B., Gifford, R.M., 2002. Soil carbon stocks and land use change: a meta analysis. Glob. Chang. Biol. 8, 345–360. doi:http://dx.doi.org/10.1046/j.1354-1013.2002.00486.x.

Hartge, K.H., Horn, R., 1989. Die Physikalische Untersuchung Von Böden, 2. ed. F. Enke Verlag, Stuttgart.

Hijmans, R.J., Cameron, S.E., Parra, J.L., Jones, P.G., Jarvis, A., 2005. Very high resolution interpolated climate surfaces for global land areas. Int. J. Climatol. 25, 1965–1978. doi:http://dx.doi.org/10.1002/joc.1276.

Hijoka, Y., Lin, E., Pereira, J.J., Corlett, R.T., Cui, X., Insarov, G.E., Lasco, R.D., Lindgren, E., Surjan, A., 2014. Asia. In: Barros, V.R., Field, C.B., Dokken, D.J., Mastrandrea, M. D., Mach, K.J., Bilir, T.E., Chatterjee, M., Ebi, K.L., Estrada, Y.O., Genova, R.C., Girma, B., Kissel, E.S., Levy, A.N., MacCracken, S., Mastrandrea, P.R., White, L.L. (Eds.), Climate Change 2014: Impacts, Adaptation, and Vulnerability. Part B: Regional Aspects. Contribution of Working Group II to the Fifth Assessment Report of the Intergovernmental Panel on Climate Change. Cambridge University Press Cambridge, United Kingdom and New York, NY USA, pp. 1327–1370.

Hothorn, T., Bretz, F., Westfall, P., 2008. Simultaneous inference in general parametric models. Biometrical J. 50, 346–363. doi:http://dx.doi.org/10.1002/bimj.200810425.

Hua, Q., Barbetti, M., Rakowski, A.Z., 2013. Atmospheric radiocarbon for the period 1950–2010. Radiocarbon 55, 2059–2072. doi:http://dx.doi.org/10.2458/azu_js_rc.v55i2.16177.

Ingram, L.J., Stahl, P.D., Schuman, G.E., Buyer, J.S., Vance, G.F., Ganjegunte, G.K., Welker, J.M., Derner, J.D., 2008. Grazing impacts on soil carbon and microbial communities in a mixed-grass ecosystem. Soil Sci. Soc. Am. J. 72, 939. doi:http://dx.doi.org/10.2136/sssaj2007.0038.

Köchy, M., Hiederer, R., Freibauer, A., 2015. Global distribution of soil organic carbon −Part 1: Masses and frequency distributions of SOC stocks for the tropics, permafrost regions, wetlands, and the world. Soil 1, 351–365. doi:http://dx.doi.org/10.5194/soil-1-351-2015.

Kahle, D., Wickham, H., 2013. ggmap: spatial visualization with ggplot2. R. J. 5, 144–161.

Kalinina, O., Krause, S.-E., Goryachkin, S.V., Karavaeva, N.A., Lyuri, D.I., Giani, L., 2011. Self-restoration of post-agrogenic chernozems of Russia: soil development, carbon stocks, and dynamics of carbon pools. Geoderma 162, 196–206. doi:http://dx.doi.org/10.1016/j.geoderma.2011.02.005.

Kiem, R., Kandeler, E., 1997. Stabilization of aggregates by the microbial biomass as affected by soil texture and type. Appl. Soil Ecol. 5, 221–230. doi:http://dx.doi.org/10.1016/S0929-1393(96)00132-1.

Kleber, M., Eusterhues, K., Keiluweit, M., Mikutta, C., Mikutta, R., Nico, P.S., 2015. Mineral-organic associations: formation, properties, and relevance in soil environments. Adv. Agron. 130, 1–140. doi:http://dx.doi.org/10.1016/bs.agron.2014.10.005.

Kuznetsova, A., Brockhoff, P.B., Christensen, R.H.B., 2015. lmerTest: tests in linear mixed effects models. R Package Version 2, , pp. 0–25.

Lal, R., 2004. Soil carbon sequestration impacts on global climate change and food security. Science (80) 304, 1623–1627. doi:http://dx.doi.org/10.1126/science.1097396.

Lenth, R.V., Herve, M., 2015. lsmeans: least-squares means. R Package Version 2, , pp. 17.

Li, N., Yao, S.-H., You, M.-Y., Zhang, Y.-L., Qiao, Y.-F., Zou, W.-X., Han, X.-Z., Zhang, B., 2014. Contrasting development of soil microbial community structure under no-tilled perennial and tilled cropping during early pedogenesis of a Mollisol. Soil Biol. Biochem. 77, 221–232. doi:http://dx.doi.org/10.1016/j.soilbio.2014.07.002.

Mann, L.K., 1986. Changes in soil carbon storage after cultivation. Soil Sci. 142 doi:http://dx.doi.org/10.1097/00010694-198611000-00006.

McKeague, J.A., Day, J.H., 1966. Dithionite- and oxalate-extractable Fe and Al as aids in differentiating various classes of soils. Can. J. Soil Sci. 46.

Mikhailova, E.A., Bryant, R.B., Vassenev, I.I., Schwager, S.J., Post, C.J., 2000. Cultivation effects on soil carbon and nitrogen contents at depth in the Russian Chernozem. Soil Sci. Soc. Am. J. 64, 738. doi:http://dx.doi.org/10.2136/sssaj2000.642738x.

Mikutta, R., Mikutta, C., Kalbitz, K., Scheel, T., Kaiser, K., Jahn, R., 2007. Biodegradation of forest floor organic matter bound to minerals via different binding mechanisms. Geochim. Cosmochim. Acta 71, 2569–2590. doi:http://dx.doi.org/10.1016/j.gca.2007.03.002.

Moll, J., Goldmann, K., Kramer, S., Hempel, S., Kandeler, E., Marhan, S., Ruess, L., Krüger, D., Buscot, F., 2015. Resource type and availability regulate fungal communities along arable soil profiles. Microb. Ecol. 70, 390–399. doi:http://dx.doi.org/10.1007/s00248-015-0569-8.

Murty, D., Kirschbaum, M.U.F., McMurtrie, R.E., McGilvray, H., 2002. Does conversion of forest to agricultural land change soil carbon and nitrogen? A review of the literature. Glob. Chang. Biol. 8, 105–123. doi:http://dx.doi.org/10.1046/j.1354-1013.2001.00459.x.

Oksanen, J., Blanchet, F.G., Kindt, R., Legendre, P., Minchin, P.R., O'Hara, R.B., Simpson, G.L., Solymos, P., Henry, M., Stevens, H., Wagner, H., 2015. Vegan: community ecology package. R Package Version 2, 2–1.

Plante, A.F., Virto, I., Malhi, S.S., 2010. Pedogenic, mineralogical and land-use controls on organic carbon stabilization in two contrasting soils. Can. J. Soil Sci. doi:http://dx.doi.org/10.4141/cjss09052.

Poeplau, C., Don, A., 2013. Sensitivity of soil organic carbon stocks and fractions to different land-use changes across Europe. Geoderma 192, 189–201. doi:http://dx.doi.org/10.1016/j.geoderma.2012.08.003.

Poeplau, C., Don, A., Vesterdal, L., Leifeld, J., Van Wesemael, B., Schumacher, J., Gensior, A., 2011. Temporal dynamics of soil organic carbon after land-use change in the temperate zone − carbon response functions as a model approach. Glob. Chang. Biol. 17, 2415–2427. doi:http://dx.doi.org/10.1111/j.1365-2486.2011.02408.x.

Reimer, P.J., Bard, E., Bayliss, A., Beck, J.W., Blackwell, P.G., Ramsey, C.B., 2013. IntCal13 and Marine13 radiocarbon age calibration curves 0–50,000 years cal BP. Radiocarbon 55, 1869–1887. doi:http://dx.doi.org/10.2458/azu_js_rc.55.16947.

Rodionov, A., Amelung, W., Urusevskaja, I., Zech, W., 1998. Beziehungen zwischen Klimafaktoren und C-, N-Pools in Partikelgrössen-Fraktionen zonaler Steppenböden Russlands. Zeitschrift Fur Pflanzenernahrung Und Bodenkd. 161, 563–569.

Ruess, L., Chamberlain, P.M., 2010. The fat that matters: soil food web analysis using fatty acids and their carbon stable isotope signature. Soil Biol. Biochem. 42, 1898–1910. doi:http://dx.doi.org/10.1016/j.soilbio.2010.07.020.

Saparov, A., Pachikin, K., Erokhina, O., Nasyrov, R., 2007. Dynamics of soil carbon and recommendations on effective sequestration of carbon in the steppe zone of Kazakhstan. In: Lal, R., Suleimenov, M., Stewart, B.A., Hansen, D.O., Doraiswamy, P. (Eds.), Climate Change and Terrestrial Carbon Sequestration in Central Asia.. Taylor & Francis/Balkema, Leiden, pp. 177–188 (368.700958—dc22 2007009819).

Schimel, D.S., Braswell, B.H., Holland, E.A., McKeown, R., Ojima, D.S., Painter, T.H., Parton, W.J., Townsend, A.R., 1994. Climatic, edaphic, and biotic controls over storage and turnover of carbon in soils. Glob. Biogeochem. Cycl. 8, 279. doi:http://dx.doi.org/10.1029/94GB00993.

Schimel, J., Balser, T.C., Wallenstein, M., 2007. Microbial stress-response physiology and its implications for ecosystem function. Ecology 88, 1386–1394. doi:http://dx.doi.org/10.1890/06-0219.

Schlichting, E., Blume, H.-P., Stahr, K., 1995. Bodenkundliches Praktikum −Eine Einführung in Pedologisches Arbeiten für Ökologen, Insbesondere Land- Und Forstwirte, Und für Geowissenschaftler, 2nd ed. Blackwell Wissenschafts-Verlag, Berlin, Wien.

Schnecker, J., Wild, B., Fuchslueger, L., Richter, A., 2012. A field method to store samples from temperate mountain grassland soils for analysis of phospholipid fatty acids. Soil Biol. Biochem. 51, 81–83. doi:http://dx.doi.org/10.1016/j.soilbio.2012.03.029.

Six, J., Elliott, E.T., Paustian, K., Doran, J.W., 1998. Aggregation and soil organic matter accumulation in cultivated and native grassland soils. Soil Sci. Soc. Am. J. 62, 1367. doi:http://dx.doi.org/10.2136/sssaj1998.03615995006200050032x.

Six, J., Elliott, E., Paustian, K., 2000. Soil macroaggregate turnover and microaggregate formation: a mechanism for C sequestration under no-tillage agriculture. Soil Biol. Biochem. 32, 2099–2103. doi:http://dx.doi.org/10.1016/S0038-0717(00)00179-6.

Six, J., Frey, S.D., Thiet, R.K., Batten, K.M., 2006. Bacterial and fungal contributions to carbon sequestration in agroecosystems. Soil Sci. Soc. Am. J. 70, 555–569. doi:http://dx.doi.org/10.2136/sssaj2004.0347.

Steffens, M., Kölbl, A., Kögel-Knabner, I., 2009. Alteration of soil organic matter pools and aggregation in semi-arid steppe topsoils as driven by organic matter input. Eur. J. Soil Sci. 60, 198–212. doi:http://dx.doi.org/10.1111/j.1365-2389.2008.01104.x.

Steffens, M., Kölbl, A., Schörk, E., Gschrey, B., Kögel-Knabner, I., 2010. Distribution of soil organic matter between fractions and aggregate size classes in grazed semiarid steppe soil profiles. Plant Soil 338, 63–81. doi:http://dx.doi.org/10.1007/s11104-010-0594-9.

Steinhof, A., Baatzsch, A., Hejja, I., Wagner, T., 2011. Ion source improvements at the Jena 14C-AMS facility. Nucl. Instrum. Methods Phys. Res. Sect. B Beam Interact. Mater. Atoms 269, 3196–3198. doi:http://dx.doi.org/10.1016/j.nimb.2011.04.018.

Steinhof, A., 2013. Data analysis at the Jena ^{14}C laboratory. Radiocarbon 55, 282–293. doi:http://dx.doi.org/10.2458/azu_js_rc.55.16350.

Stockmann, U., Adams, M.A., Crawford, J.W., Field, D.J., Henakaarchchi, N., Jenkins, M., Minasny, B., McBratney, A.B., De Courcelles, V.D.R., Singh, K., Wheeler, I., Abbott, L., Angers, D.A., Baldock, J., Bird, M., Brookes, P.C., Chenu, C., Jastrow, J.D., Lal, R., Lehmann, J., O'Donnell, A.G., Parton, W.J., Whitehead, D., Zimmermann, M., 2013. The knowns, known unknowns and unknowns of sequestration of soil organic carbon. Agric. Ecosyst. Environ. 164, 80–99. doi:http://dx.doi.org/10.1016/j.agee.2012.10.001.

Stuiver, M., Polach, H.A., 1977. Reporting of ^{14}C data. Radiocarbon 19, 355–363. doi:http://dx.doi.org/10.1016/j.forsciint.2010.11.013.

VandenBygaart, A.J., Gregorich, E.G., Angers, D.A., 2003. Influence of agricultural management on soil organic carbon: a compendium and assessment of Canadian studies. Can. J. Soil Sci. 83, 363–380. doi:http://dx.doi.org/10.4141/s03-009.

von Lützow, M., Kögel-Knabner, I., Ekschmitt, K., Matzner, E., Guggenberger, G., Marschner, B., Flessa, H., 2006. Stabilization of organic matter in temperate soils: mechanisms and their relevance under different soil conditions − a review. Eur. J. Soil Sci. 57 (4), 426–445. doi:http://dx.doi.org/10.1111/j.1365-2389.2006.00809.x.

von Lützow, M., Kögel-Knabner, I., Ludwig, B., Matzner, E., Flessa, H., Ekschmitt, K., Guggenberger, G., Marschner, B., Kalbitz, K., 2008. Stabilization mechanisms of organic matter in four temperate soils: development and application of a conceptual model. J. Plant Nutr. Soil Sci. 171, 111–124. doi:http://dx.doi.org/10.1002/jpln.200700047.

Walthert, L., Graf, U., Kammer, A., Luster, J., Pezzotta, D., Zimmermann, S., Hagedorn, F., 2010. Determination of organic and inorganic carbon, δ^{13}C, and nitrogen in soils containing carbonates after acid fumigation with HCl. J. Plant Nutr. Soil Sci. 173, 207–216. doi:http://dx.doi.org/10.1002/jpln.200900158.

Wickham, H., 2009. ggplot2: Elegant graphics for data analysis. .

Wixon, D.L., Balser, T.C., 2013. Toward conceptual clarity: PLFA in warmed soils. Soil Biol. Biochem. 57, 769–774. doi:http://dx.doi.org/10.1016/j.soilbio.2012.08.016.

Xiao, C., Guenet, B., Zhou, Y., Su, J., Janssens, I.A., 2015. Priming of soil organic matter decomposition scales linearly with microbial biomass response to litter input in steppe vegetation. Oikos 124, 649–657. doi:http://dx.doi.org/10.1111/oik.01728.

Zelles, L., 1999. Fatty acid patterns of phospholipids and lipopolysaccharides in the characterisation of microbial communities in soil: a review. Biol. Fertil. Soils 29, 111–129. doi:http://dx.doi.org/10.1007/s003740050533.

Zhang, W., Parker, K.M., Luo, Y., Wan, S., Wallace, L.L., Hu, S., 2005. Soil microbial responses to experimental warming and clipping in a tallgrass prairie. Glob. Chang. Biol. 11, 266–277. doi:http://dx.doi.org/10.1111/j.1365-2486.2005.00902.x.

Zhang, B., Li, Y., Ren, T., Tian, Z., Wang, G., He, X., Tian, C., 2014. Short-term effect of tillage and crop rotation on microbial community structure and enzyme activities of a clay loam soil. Biol. Fertil. Soils 50, 1077–1085. doi:http://dx.doi.org/10.1007/s00374-014-0929-4.

Zogg, G.P., Zak, D.R., Ringelberg, D.B., White, D.C., MacDonald, N.W., Pregitzer, K.S., 1997. Compositional and functional shifts in microbial communities due to soil warming. Soil Sci. Soc. Am. J. 61, 475. doi:http://dx.doi.org/10.2136/sssaj1997.03615995006100020015x.

Supplement of

Land-use change under different climatic conditions: Consequences for organic matter and microbial communities in Siberian steppe soils

N. Bischoff et al.

Correspondence to: N. Bischoff (bischoff@ifbk.uni-hannover.de)

Supplements - Tables

Steppe type	Site code	Plot code	Land-use type	Time since grassland conversion	Coordinates latitude	Coordinates longitude	Soil type	Vegetation in grasslands, dominant species (from least to most dominant)
Forest steppe	Pan M	Pan M1	cropland	>20 yrs	53°47'22.01"N	80°16'40.82"E	Protocalcic Chernozem (Aric, Loamic)	
		Pan M2	grassland		53°47'22.60"N	80°16'39.54"E	Protocalcic Chernozem (Loamic)	Fragaria viridis - Bromopsis inermis
	Pan K	Pan K1	cropland	>20 yrs	53°48'4.46"N	80°27'1.17"E	Protocalcic Chernozem (Aric, Loamic)	
		Pan K2	grassland		53°48'1.08"N	80°26'55.76"E	Hypocalcic Chernozem (Loamic)	Stipa capilata - Gallium ruthenicum - Bromopsis inermis
	Zit	Zit 00	cropland	>20 yrs	53°45'3.32"N	80°40'2.97"E	Protocalcic Chernozem (Aric, Siltic)	
		Zit 01	cropland	5 yrs	53°45'0.19"N	80°40'12.68"E	Protocalcic Chernozem (Aric, Siltic)	
		Zit 02	grassland		53°44'19.53"N	80°41'2.88"E	Protocalcic Chernozem (Siltic)	Bromopsis inermis - Fillipendula vulgaris - Festuca valesiaca
Typical steppe	Per	PerWei	grassland		52°53'52.83"N	81°37'24.51"E	Protocalcic Chernozem (Siltic)	Festuca valesiaca - Bromopsis inermis - Peucedanum morisonii
		Per Ack	cropland	>20 yrs	52°53'47.38"N	81°37'21.01"E	Protocalcic Chernozem (Aric, Siltic)	
	Sido L	Sido L1	cropland	>20 yrs	52°33'50.30"N	80°43'51.09"E	Protocalcic Kastanozem (Aric, Siltic)	
		Sido L2	grassland		52°33'47.79"N	80°43'56.63"E	Protocalcic Chernozem (Siltic)	Thymus marschallianus - Artemisia frigida - Festuca valesiaca
Dry steppe	Kom S + Marv	Kom S1	cropland	>20 yrs	52°11'18.06"N	80°14'31.41"E	Protocalcic Kastanozem (Aric, Siltic)	
		Kom S2	grassland		52°11'21.64"N	80°15'0.42"E	Protocalcic Kastanozem (Siltic)	Artemisia frigida - Koeleria glauca - Festuca valesiaca - Stipa capillata
	Kom F	Kom F1	cropland	>20 yrs	52°10'7.86"N	80°16'53.21"E	Protocalcic Chernozem (Aric, Siltic)	
		Kom F2	grassland		52°10'9.27"N	80°16'56.18"E	Protocalcic Chernozem (Siltic)	Galium ruthenicum - Thymus marschallianus - Festuca valesiaca - Stipa pennata - Spiraea hypericifolia

Site	Plot	Land use	Age	Latitude	Longitude	Soil classification	Vegetation
PT N	PT N1	cropland	>20 yrs	52°9'7.04"N	79°50'46.44"E	Protocalcic Kastanozem (Aric, Loamic)	
	PT N2	grassland		52°9'8.14"N	79°50'43.41"E	Protocalcic Kastanozem (Loamic)	Artemisia frigida - Festuca valesiaca-Stipa capillata
	PT N3	cropland	>20 yrs	52°9'8.53"N	79°50'40.29"E	Protocalcic Kastanozem (Aric, Siltic)	
PT D	PT D1	cropland	>20 yrs	52°3'26.23"N	79°53'37.90"E	Haplic Chernozem (Aric, Loamic)	
	PT D2	grassland		52°3'26.49"N	79°53'35.11"E	Protocalcic Chernozem (Loamic)	Koeleria glauca - Phleum phleoides - Festuca valesiaca
	PT D3	cropland	>20 yrs	52°3'26.50"N	79°53'32.69"E	Protocalcic Chernozem (Aric, Loamic)	

Table S 1   Site description and soil classification according to IUSS Working Group **WRB** (2014). Codes for site and plot are internally given field identifications.

Steppe type	Horizon	Land-use type	n	LF-OC mg g^{-1} SOC			HF-OC mg g^{-1} SOC			DOC-LF mg g^{-1} SOC			DOC-HF mg g^{-1} SOC			mean number of washing procedures LF	HF
FS	A	grassland	3	66	±	9	887	±	14	3	±	1	44	±	6	2	2
		cropland	3	50	±	14	902	±	29	3	±	1	46	±	13	2	2
	AC	grassland	3	39	±	8	796	±	49	7	±	3	159	±	54	2	4
		cropland	3	65	±	21	842	±	43	3	±	2	91	±	22	2	3
	C	grassland	3	36	±	13	772	±	52	13	±	4	179	±	54	2	4
		cropland	3	47	±	10	725	±	126	15	±	9	214	±	107	2	4
TS	A	grassland	2	76	±	8	834	±	8	6	±	0	85	±	15	2	2
		cropland	2	51	±	9	834	±	11	7	±	2	107	±	18	2	2
	AC	grassland	2	49	±	16	749	±	83	13	±	7	190	±	91	2	4
		cropland	2	49	±	3	749	±	50	11	±	1	190	±	52	2	4
	C	grassland	1	60	±	-	752	±	-	13	±	-	176	±	-	2	4
		cropland	2	24	±	5	715	±	78	18	±	5	243	±	68	2	4
DS	A	grassland	4	91	±	10	829	±	11	7	±	1	73	±	10	2	2
		cropland	6	90	±	17	812	±	22	6	±	1	91	±	11	2	2
	AC	grassland	4	58	±	10	803	±	32	9	±	3	129	±	20	2	3
		cropland	6	40	±	8	786	±	19	7	±	1	167	±	16	2	3
	C	grassland	4	71	±	8	702	±	43	17	±	4	210	±	38	2	4
		cropland	6	67	±	13	629	±	26	20	±	1	285	±	20	2	4

Table S 2   Summary of fractions isolated during density fractionation. Values are given as arithmetic mean ± standard error of the mean. DOC-LF and DOC-HF refers to dissolved organic carbon (DOC) which was mobilized from the light fraction (LF) or heavy fraction (HF), respectively, during the fractionation procedure. Increasing portions of DOC-HF from topsoil to subsoil are not necessarily due to increasing quantities of the mobilizable fraction, as also the number of washing procedures increased from topsoil to subsoil due to larger retention of sodium-polytungstate in the subsoil. Abbreviation: SOC = soil organic carbon.

Depth (cm)	Factor	Soil OC stock			
		NumDF	DenDF	p-value	Variance explained (%)
0-10	steppe type	2	5.85	0.129	14
	land-use type	1	9.77	<0.001	50
	residual				36
0-25	steppe type	2	5.97	0.035	33
	land-use type	1	9.90	<0.001	33
	residual				34
0-60	steppe type	2	6.01	0.037	36
	land-use type	1	9.93	<0.01	23
	residual				41

Table S 3   Effect of steppe type and land-use type on soil organic carbon stocks for different depth increments estimated by variance components analysis. Residual variance names the sum of variance components for sites, plots nested within sites and the residual variance. Abbreviations: NumDF = numerator degrees of freedom, DenDF = denominator degrees of freedom.

Pairs	F-value	R²	p-value
forest steppe vs. typical steppe	2.01	0.07	0.381
forest steppe vs. dry steppe	14.89	0.25	0.003
typical steppe vs. dry steppe	6.38	0.15	0.024

Table S 4   Pairwise comparisons in a Permutational Multivariate Analysis of Variance Using Distance Matrices (ADONIS) between steppe types with respect to their PLFA-based microbial community composition (see Fig.5a).

Steppe type	Land-use type	No. of plots	n	Aggregate stability ΔMWD		
Forest steppe	grassland	3	6	0.28 ± 0.17	a	A
	cropland	3	8	1.37 ± 0.08	b*	A
Typical steppe	grassland	2	4	0.40 ± 0.05	a	A
	cropland	2	6	1.46 ± 0.77	b*	A
Dry steppe	grassland	4	12	0.36 ± 0.04	a	A
	cropland	6	18	1.62 ± 0.17	b***	A

Table S 5   Aggregate stability in 0-10 cm depending on land-use type and steppe type. Values are given as arithmetic mean± standard error of the mean. As some samples from FS grassland and cropland as well as TS grassland had to be discarded during measurement, the sample size n differs from the general sample size. Lowercase letters indicate significant differences between land-use types within steppe type, and uppercase letters indicate significant differences between steppe types within land-use type (p-value, 0 < *** < 0.001 < ** < 0.01 < * < 0.05).

Variable	Mean Sums of Squares	Degrees of Freedom		F-value	p-value
		Numerator	Denominator		
steppe type	0.03	2	5.90	0.348	0.72
land-use type	4.15	1	10.11	43.429	< 0.001
fungal PLFA biomass	0.00	1	42.95	0.004	0.95

Table S 6 Results of an Analysis of Variance (ANOVA) Type III after fitting a linear mixed effects model with aggregate stability as response variable and the specified variables as fixed effects, while plots nested within sites were a random effect. The following interactions were not significant, thus not reported in the ANOVA-table: land-use type x fungal biomass, steppe type x fungal biomass, steppe type x land-use type x fungal biomass.

S1 Factors controlling soil OC contents in the Kulunda steppe (Annotation to Table S8)

To determine factors controlling soil OC contents in the Kulunda steppe we used additional information from sites and plots which did not meet our assumptions for the paired plot design to determine LUC effects. This concerned sites which were slightly affected by erosion or single plots under arable land which had no proper reference plot. Also plots with a time since grassland conversion <20 yrs were included in the analysis. Table S7 lists the additionally included plots. Together with the sites and plots considered for the effect of LUC on soil OC (Table S1) this gave a total of 14 sites with 28 plots. The statistical analysis was carried out on samples from the key profiles (horizons) as most soil parameters were measured on these samples. Subhorizons were also included in the analysis (this was only possible with respect to A and C horizons), giving a total of 46, 28 and 44 samples in the A, AC and C horizon, respectively.

Steppe type	Site code	Plot code	Land-use type	Time since grassland conversion	Reference plot?	Erosion	Coordinates		Soil type	Vegetation in grasslands, dominant species (from least to most dominant)
							latitude	longitude		
Forest steppe	Kom Amaz	Kom Amaz	cropland	>20 yrs	no	no	53°19'27.29"N	83°2'15.10"E	Protocalcic Chernozem (Aric, Siltic)	
Typical steppe	Per Amaz	Per Amaz	cropland	>20 yrs	no	no	52°54'7.35"N	81°43'47.14"E	Protocalcic Chernozem (Aric, Siltic)	
	Tam L	Tam L0	cropland	>20 yrs	yes	yes	52°36'26.87"N	80°54'38.16"E	Petrocalcic Chernozem (Aric, Loamic)	
		Tam L1	cropland	5 yrs	yes	yes	52°36'24.97"N	80°54'46.25"E	Protocalcic Chernozem (Aric, Siltic)	
		Tam L2	grassland		yes	yes	52°36'22.98"N	80°54'50.92"E	Protocalcic Chernozem (Siltic)	Motley grasses - Carex stenophylla
	Tam ND	Tam ND1	cropland	>20 yrs	no	no	52°41'8.86"N	81°0'25.35"E	Protocalcic Chernozem (Aric, Siltic)	
Dry steppe	Pol Amaz	Pol Amaz	cropland	>20 yrs	no	no	52°4'7.25"N	79°54'3.41"E	Protocalcic Kastanozem (Aric, Loamic)	

Table S 7   Sites which were additionally included in the multiple regression analysis to determine environmental factors controlling soil OC contents in the Kulunda steppe. Soil classification according to IUSS Working Group WRB (2014). Codes for site and plot are internally given field identifications.

To test for the effect of environmental variables on soil OC a multiple linear regression analysis was performed (in R 3.1.2.; R Core Team, 2015)using the following predictors: steppe type, land-use type, depth, bulk density, pH, electrical conductivity (EC), C : N ratio, oxalate-extractable Fe, dithionite-extractable Fe, clay content, silt content and $CaCO_3$. Numerical predictor variables (bulk density, pH, etc.) were visually assessed using histograms and scatter plot matrices for their distributional properties. Variables showing right-skewed distribution, extremely high but plausible observations or variation over several orders of magnitude were log-transformed to reduce influence of single extreme observations in subsequent analyses (i.a., EC, $CaCO_3$, C : N ratio). Further, Principal Components Analysis on the numerical predictor variables was used to identify sets of highly correlated variables and to assess the potential for reducing the dimensions of the covariates. Additionally, the variance inflation factor (package car; Fox & Weisberg, 2011) was used to assess the extent of multicollinearity among predictor variables.A linear mixed model was fitted for each horizon (A, AC, C), thereby differentiating between possible distinct effects of predictors within each horizon. The response variable (OC) was log-transformed due to a very clear mean-variance dependency along with a right skewed distribution. For the initial model, all predictors were added as fixed effects (except of those showing multicollinearity) and steppe type, land-use type and depth were used as covariates.We accounted for the nested structure of sampling and included sites and plots within sites as random effects in the model. Non-significant variables were removed from the initial model to reduce the number of predictors. Whether effects of significant predictors were significantly different between horizons, was tested in a separate linear mixed model including all horizons and testing for significance of interactions. Model assumptions were assessed by residuals vs. fitted plots and Q-Q-plots for the residual errors and random effect estimates, revealing a slight variance heterogeneity in the residuals that could not be explained by any of the predictor variables. $R^2_{marginal}$ and

$R^2_{conditional}$ were calculated according to Nakagawa and Schielzeth(2013). Results are shown in

Table S8.

Horizon	Bulk Density	Clay content	Electrical Conductivity	pH	$R^2_{marginal}$	$R^2_{conditional}$	n
A	10.8**	29.2***	n.s.	37.3***	0.86	0.95	46
AC	13.2**	5.9*	n.d.	9.8**	0.65	0.65	28
C	4.0*	27.4***	20.2***	n.s.	0.67	0.67	44
Interaction with horizon	n.s.	n.s.	n.s.	significant**			

Table S 8   F-values and significance (p-value, $0 < *** < 0.001 < ** < 0.01 < * < 0.05$) for significant predictors (bulk density, clay content, electrical conductivity, pH) of soil organic carbon content in multiple regression analysis using linear mixed effects models and ANOVA type III sums of squares. For each horizon a separate model was fitted, thus we tested whether different F-values in different horizons are significant by testing whether each predictor has a significant interaction with the horizon. The steppe type and land-use type are covariates in the models, thus the interpretation of each predictor is given the same steppe type and land-use type. $R^2_{marginal}$ corresponds to the variance explained by the fixed effects, while $R^2_{conditional}$ corresponds to the variance explained by the entire model (fixed + random effects). The statistical approach is described above, while a detailed model description is found below. Abbreviations: n.s. = not significant, n.d. = not determined.

Model description for Table S8:

Bold face indicates categorial predictor variables, normal face indicates numerical predictor variables, the term (1|site/plot) indicates random intercepts for site and plots nested within sites, x indicates an interaction term.

A horizon, including 6 predictors:

$\log_2(OC)$ = **Steppe type** + **Land-use type** + Depth^2 + Bulk density + pH + Clay content + (1|site/plot)

AC horizon, including 6 predictors (the effect of electrical conductivity could not be determined, because of multicollinearity):

$\log_2(OC)$ = **Steppe type** + **Land-use type** + Depth + Depth^2 + Bulk density + pH + Clay content + (1|site)

C horizon, including 6 predictors:

$\log_2(OC)$ =**Steppe type** + **Land-use type** + $\log_2(\text{Depth})$ + Bulk density + $\log_2(\text{Electrical conductivity})$ + Clay content + (1|site/plot)

To test for interactions between significant predictors and horizons, a full model (including all horizons) was fitted.

Full model (null model), including 8 predictors:

$\log_2(\text{OC})$ = **Steppe type** + **Land-use type** + **Horizon** + Depth² + Bulk density + pH + $\log_2$(Electrical conductivity) + Clay content + (1|site/plot)

Interactions were tested against the null model by ANOVA:

For the predictor *pH* the model with interaction is for example:

$\log_2(\text{OC})$ = **Steppe type** + **Land-use type** + **Horizon** + Depth² + Bulk density + pH + $\log_2$(Electrical conductivity) + Clay content + pH x **Horizon** + (1|site/plot)
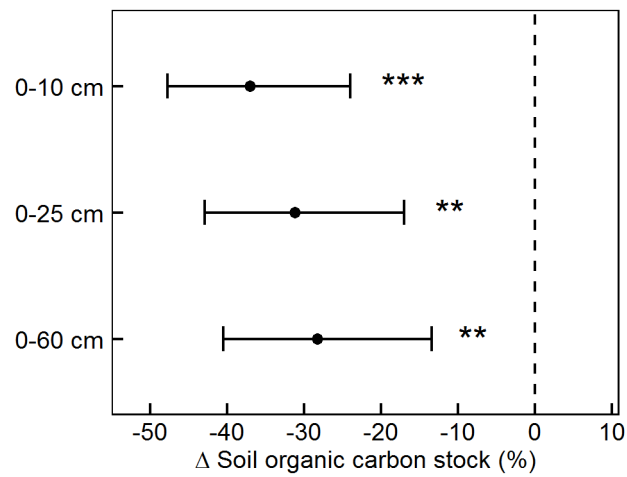
Fig. S 1 Soil organic carbon stock decline (%) due to land-use change from grassland to cropland as a function of depth in the entire Kulunda steppe. Shown are means and 95% confidence intervals. n = 60 per depth. Asterisks indicate significance (p-value, *** < 0.001 < ** < 0.01).
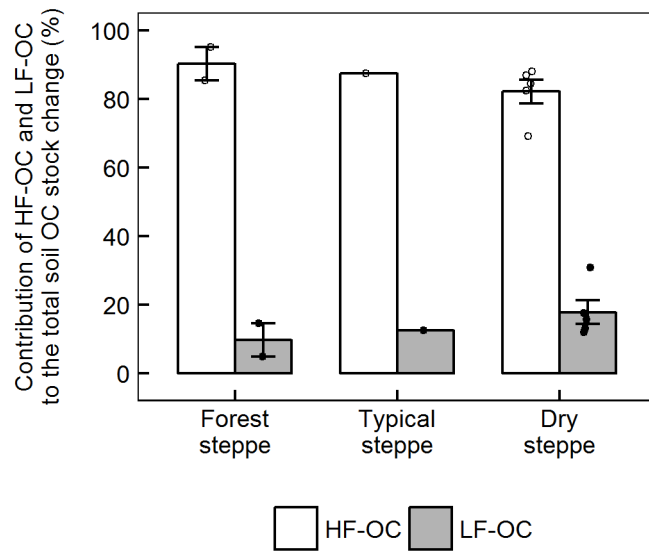
Fig. S 2 Contribution of heavy fraction OC (HF-OC) and light fraction OC (LF-OC) to the total soil OC stock change due to LUC from grassland to croplandin A horizons of the three steppe types. Bars indicate the arithmetic mean ± standard error of the mean whereas points show individual measurements.

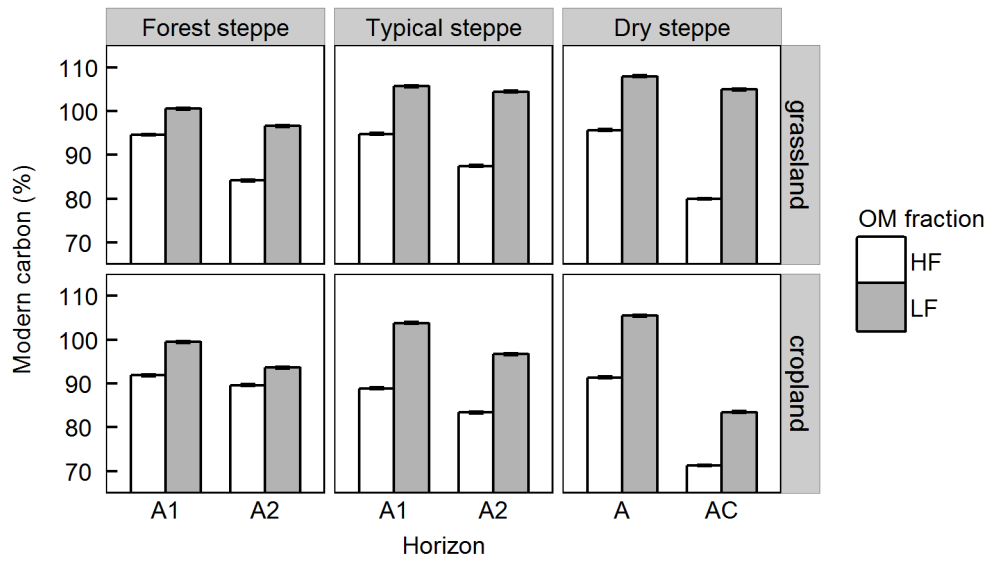**Fig. S 3**   Percent modern C as determined by ^{14}C measurement depending on horizon, steppe type, and land-use type in the heavy fraction (HF) and light fraction (LF); n = 1 per bar, error bars indicate measurement error.
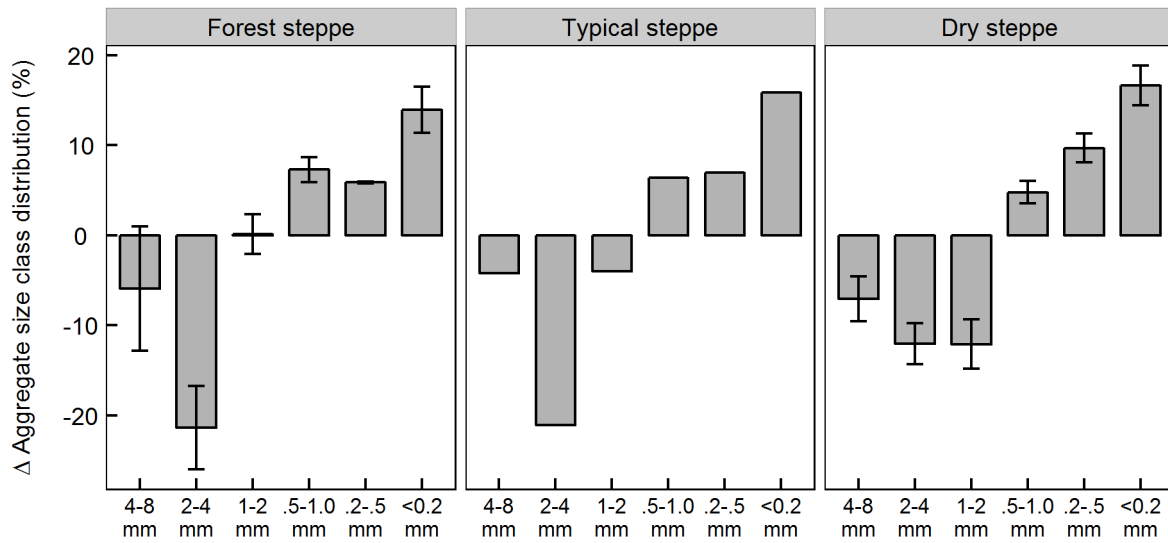
Fig. S 4   Change of the aggregate size class distribution (%) due to grassland to cropland conversion. Shown are the arithmetic mean ± standard error of the mean for pairwise comparisons of grassland and cropland plots. Forest steppe n = 3, typical steppe n = 2, dry steppe n = 6.

References

Fox, J., Weisberg, S., 2011. An R Companion to Applied Regression, 2. ed. Thousand Oaks, SAGE, CA.

IUSS Working Group WRB, 2014. World reference base for soil resources 2014. International soil classification system for naming soils and creating legends for soil maps, World Soil Resources Reports No. 106. doi:10.1017/S0014479706394902

Nakagawa, S., Schielzeth, H., 2013. A general and simple method for obtaining R2 from generalized linear mixed-effects models. Methods Ecol. Evol. 4, 133–142. doi:10.1111/j.2041-210x.2012.00261.x

R Core Team, 2015. R: A language and environment for statistical computing.

3 Study II

Limited protection of macro-aggregate occluded organic carbon in Siberian steppe soils

Contribution: I performed about half of the laboratory work and the incubation experiment, collected and analyzed the data, compiled tables and graphs, and wrote the manuscript. As the corresponding author I performed the (ongoing) review process of the paper.

Limited protection of macro-aggregate occluded organic carbon in Siberian steppe soils

Norbert Bischoff[1], Robert Mikutta[2], Olga Shibistova[1,3], Alexander Puzanov[4], Marina Silanteva[5], Anna Grebennikova[5], Roland Fuß[6], Georg Guggenberger[1,3]

[1]Institute of Soil Science, Leibniz Universität Hannover, Hannover, 30419, Germany

[2]Soil Science and Soil Protection, Martin-Luther University Halle-Wittenberg, Halle, 06120, Germany

[3]VN Sukachev Institute of Forest, Siberian Branch of the Russian Academy of Sciences, Krasnoyarsk, 660036, Russian Federation

[4]Institute for Water and Environmental Problems, Siberian Branch of the Russian Academy of Sciences, Barnaul, 656038, Russian Federation

[5]Faculty of Biology, Altai State University, Barnaul, 656049, Russian Federation

[6]Institute of Climate-Smart Agriculture, Johann Heinrich von Thünen Institute, Braunschweig, 38116, Germany

Correspondence to: Norbert Bischoff (bischoff@ifbk.uni-hannover.de)

Abstract.

Macro-aggregates especially in agricultural steppe soils are supposed to play a vital role for soil organic carbon (OC) stabilization at a decadal time scale. While most research on soil OC stabilization in steppes focused on North American

5 prairie soils of the Great Plains with information mainly provided by short-term incubation experiments, little is known about the agricultural steppes in south-western Siberia, though they belong to the greatest conversion areas in the world and occupy an area larger than that in the Great Plains. To quantify the proportion of macro-aggregate protected OC under different land-use and as function of land-use duration and intensity in Siberian steppe soils, we determined OC mineralization rates of intact (250–2000 µm) and crushed (<250 µm) macro-aggregates in long-term incubations over 401

10 days (20°C; 60% water holding capacity) along two agricultural chronosequences in the Siberian Kulunda steppe. Additionally we incubated bulk soil (<2000 µm) to determine the effect of land-use change (LUC) and subsequent agricultural use on a fast and a slow soil OC pool (labile *vs.* more stable OC), as derived from fitting exponential decay models to incubation data. We hypothesized that (i) macro-aggregate crushing leads to increased OC mineralization due to an increasing microbial accessibility of a previously occluded labile macro-aggregate OC fraction, and (ii) bulk soil OC

15 mineralization rates and the size of the fast OC pool are higher in pasture than in arable soils with decreasing bulk soil OC mineralization rates and size of the fast OC pool as land-use duration and intensity increase. Against our hypothesis, OC mineralization rates of crushed macro-aggregates were similar to those of intact macro-aggregates under all land-use regimes. Macro-aggregate protected OC was almost absent and accounted for <1% of the total macro-aggregate OC content and to maximally 8 ± 4% of mineralized OC. In accordance to our second hypothesis, highest bulk soil OC mineralization

20 rates and sizes of the fast OC pool were determined under pasture, but mineralization rates and pool sizes were unaffected by the duration and intensity of land-use. However, mean residence times of the fast and slow OC pool tended to become shorter along one chronosequence. We conclude, that the tillage-induced break-down of macro-aggregates has not reduced the OC contents in the soils under study. The decline of OC after LUC is probably attributed to the faster soil OC turnover under arable land as compared to pasture at a reduced plant residue input.

25

Introduction

Steppe soils comprise about 7% of the terrestrial soil organic carbon (OC) storage down to 1m (Calculation see supplementary material) and cover about 885 million ha worldwide (FAO, 2001). As they are rich in organic matter (OM) and well-suited for agriculture they encompass about 14% of agricultural land globally (FAO, 2013). Intensive management

5 of steppe soils reduced their OC stocks significantly, with estimated OC losses between 24 and 40% associated with conversion of grassland to cropland (Beniston et al., 2014; Mikhailova et al., 2000; Rodionov et al., 1998; VandenBygaart et al., 2003). As the stabilization of OC in agricultural steppe soils is crucial for maintaining soil fertility and to reduce the emission of CO_2 to the atmosphere, further insights into the processes that govern OC stabilization in steppe soils are needed. For temperate soils chemical stabilization by formation of mineral-organic associations and physical disconnection

10 of OM from microorganisms by occlusion of OM in aggregates, were identified as main factors stabilizing soil OC (von Lützow et al., 2006). For dry steppe ecosystems the role of aggregation might be more decisive for OC stabilization than the one of mineral-organic associations, as the latter requires sufficient water for the formation of pedogenic minerals and the interaction of OM with mineral surfaces (Kleber et al., 2015).

The mean residence time of aggregate-occluded OC ranges from decades to several hundreds of years (Six et al.,

15 2002). Tisdall and Oades (1982) proposed a concept in which aggregates are structured hierarchically with respect to their size and binding agents. According to this aggregate hierarchy concept, free primary particles or silt-sized aggregates (<20 µm) are bound together to micro-aggregates (<250 µm) by persistent binding agents, e.g. humified OM, polyvalent metal cations or oxides. The micro-aggregates, in turn, are linked together to form larger macro-aggregates (>250 µm) by temporary (e.g. fungal hyphae, roots) or transient binding agents (e.g. microbial and plant-derived polysaccharides). Due to

20 the hierarchical order of aggregate structure and the different persistence of the involved binding agents, macro-aggregates are less stable and more vulnerable to soil management than micro-aggregates (Tisdall and Oades, 1982). Accordingly, Six et al. (2000b) showed that macro-aggregates disintegrated more readily upon disturbance than micro-aggregates, particularly in soils with increasing cultivation intensity. By that, macro-aggregate occluded OC becomes available to microbial decomposition, hence, this fraction is supposed to play an important role for the decline of soil OC in intensively managed

25 steppe soils (Cambardella and Elliott, 1993, 1994; Elliott, 1986).

One way to quantify the proportion of macro-aggregate protected soil OC is to compare mineralization rates from intact and crushed macro-aggregates. Previous studies found an increase of soil OC mineralization after macro-aggregate crushing (Beare et al., 1994; Bossuyt et al., 2002; Elliott, 1986; Gupta and Germida, 1988; Pulleman and Marinissen, 2004), though not all studies revealed consistent results (Garcia-Oliva et al., 2004; Goebel et al., 2009; Plante et al., 2009; Tian et

30 al., 2015). Moreover, OC mineralization after macro-aggregate crushing differed also with respect to land-use. Pulleman and Marinissen (2004) found larger mineralization after crushing of macro-aggregates in croplands than in grasslands and ascribed this to the physicogenic nature of macro-aggregates in arable soils, which have smaller pore sizes than biogenic macro-aggregates in grasslands, and therefore larger protection capacity. Also Elliott (1986) observed the increase of OC

3

mineralization with macro-aggregate crushing to be more pronounced in arable than in grassland soils, while Gupta and Germida (1988) observed the opposite effect. A shortcoming of previous studies is the short incubation period of only few weeks resulting in non-equilibrium mineralization rates, which complicates an accurate assessment of the size of the macro-aggregate protected OC fraction and its turnover time. This fact, therefore, asks for long-term incubation experiments to

5   address the vulnerability of macro-aggregate protected OC.

The majority of research on OC protection in aggregates of steppe soils focused on prairie soils of the Great Plains, while little is known for Siberian steppe soils. This is surprising as the semi-arid steppe ecosystems in Siberia belong to the greatest agricultural production areas in the world with an area greater than that of the Great Plains and cover some of the most intensively managed soils globally (Frühauf, 2011). In the West Siberian Plain 420,000 km² natural steppe was

10   converted into cropland between 1954 and 1963 in the frame of the so-called "Virgin Lands Campaign" (Russian: *Zelina*). Conversion from grassland to cropland reduced soil OC stocks by about 31% in 0-25 cm, of which most occurred within the first years after land conversion and was associated with a decline in aggregate stability (Bischoff et al., 2016). This indicated an interrelation between aggregate stability and OC storage also in these soils. Moreover, Bischoff et al. (2016) found about 10% of OC in the studied soils was existent in particulate OM of which some is probably occluded within

15   aggregates. In the present study we aimed to quantify the proportion of macro-aggregate protected OC under different land-use and as function of land-use duration and intensity in Siberian steppe soils by comparing OC mineralization rates of intact (250–2000 µm) and crushed (<250 µm) macro-aggregates in long-term incubations over 401 days along two agricultural chronosequences of the south-western Siberian Kulunda steppe. In addition, bulk soil samples (<2000 µm) were incubated to determine the effect of land-use change (LUC) from pasture to arable land on a fast and a slow soil OC pool (labile *vs.* more

20   stable OC), as derived from fitting exponential decay models to incubation data. We hypothesized that (i) crushing of macro-aggregates leads to increased OC mineralization due to an increasing microbial accessibility of a previously occluded labile macro-aggregate OC fraction, and (ii) bulk soil OC mineralization rates and the size of the fast soil OC pool are higher in pasture than in arable soils with decreasing bulk soil OC mineralization rates and size of the fast OC pool as land-use duration and intensity increase. In this study, we refer to fractions as physically separated soil OC components (macro-

25   aggregate occluded soil OC), while pools refer to mathematically derived OC constituents from fitting exponential decay models to incubation data (fast and slow soil OC pool).

Material & Methods

Study sites and soil sampling

The Kulunda steppe is part of the Russian Federation (Altayskiy Kray) and located within the semi-arid steppes of south-western Siberia. We selected two sites in two different steppe types under different climate with soils of different textures
5 (Fig. 1). The first site is located in the forest steppe (FS) near Pankrushikha (53°44'19.53"N, 80°41'2.88"E) with a mean annual precipitation (MAP) of 368 mm and a mean annual temperature (MAT) of 1.1°C (Table 1). The second site is situated near Sidorovka (52°30'1.43"N, 80°44'41.68"E) and part of the more arid typical steppe (TS) with a MAP of 339 mm and a MAT of 2.0°C (climate data from "WorldClim" data base; Hijmans *et al.*, 2005). At each site we identified a land-use chronosequence with four plots. At FS, we also included two plots with varying land-use intensity (extensive pasture *vs.*
10 arable land with forage crops). The FS site comprised an extensive pasture (vegetation: *Festuca valesiaca - Fillipendula vulgaris - Bromopsis inermis*), an arable land with forage crops and arable land after five and ten years of cultivation (arable 5 yr, arable 10 yr). Crop rotations on the arable 5 yr and arable 10 yr included summer wheat, summer barley and peas. The soils were classified as Protocalcic Chernozems (Siltic) according to IUSS Working Group WRB (2014). The TS site consisted of four plots which were all cultivated since the 1950s (*Zelina*) but left as fallow since 1983 because of low
15 agricultural productivity. After 1983 all plots were used extensively as pasture but three of the four plots were recultivated at different points in time, allowing for a chronosequence with a 30-year old fallow (meanwhile used as pasture) and plots with one, three, and ten years arable land-use (arable 1 yr, arable 3 yr , arable 10 yr). The 30-year old fallow (pasture) is characterized by *Agropyron pectinatum*, *Bromopsis inermis* and *Artemisia glauca*. The absence of some typical steppe species like *Stipa sp.* or *Festuca sp.* pointed to the fact that the vegetation of this plot was degraded from grazing. The site
20 was located on a small hillslope with <2° inclination, where the fallow 30 yr was located at the highest point and the arable 10 yr at the base level. Though the inclination was very small, we measured larger soil OC contents in the arable 10 yr plot than in the upslope arable 1 yr and arable 3 yr plots, which we attributed to erosion. Nevertheless, we decided to include this site in our study, as chronosequences are very sparse in the study area and the possible effect of macro-aggregate crushing on soil OC mineralization, if existent, will be also evident on slightly eroded plots. Soils at the TS site were classified as
25 Protocalcic Kastanozem (Loamic). At both sites one characteristic key profile was established from 0-150 cm on the pasture plots for soil description and sampled in generic horizons. As the arable 5 yr and arable 30 yr at the FS site were >500 m distant from the other two plots, we additionally established a key profile on each of these two plots. Key profile samples were analyzed for pH, soil texture, and electrical conductivity (EC). Further, on all plots three additional soil samples (field replicates) were randomly collected in 0-10 cm depth for determination of soil OC and total nitrogen (TN) content and for
30 use in the soil incubation experiment. Geographical coordinates of all plots are summarized in Table S1.

5

Sample preparation and basic soil analyses

Soil samples were air-dried and sieved to <2 mm. Big clods were gently broken apart to pass the 2 mm sieve and all visible plant residues were removed. A subsample was dried at 105°C for 24 h to determine the residual soil water content. Another subsample was homogenized with a ball mill (Retsch MM200, Haan, Germany) and measured for OC and TN via dry

5   combustion with an Elementar vario MICRO cube C/N Analyzer (Elementar Analysensysteme GmbH, Hanau, Germany). Traces of inorganic carbon ($CaCO_3$-content <0.1%) were previously removed by HCl fumigation (Walthert et al., 2010). Soil pH was measured at a 1:2.5 (w:v) soil-to-water$_{deion}$ ratio after leaving the suspensions for one day to reach equilibrium, and soil EC was measured at a soil-to-water$_{deion}$ ratio of 1:5 (w:v). The texture of the soils was determined according to the standard sieve-pipette method (DIN ISO 11277, 2002).

10 **Aggregate crushing and incubation of soil samples**

Each of the samples from 0-10 cm was divided into three fractions: (i) bulk soil (<2000 µm), (ii) intact macro-aggregates (250–2000 µm), and (iii) crushed macro-aggregates (<250 µm). Intact macro-aggregates were isolated by gently sieving the air-dry bulk soil through a 250-µm sieve and using the fraction remaining on the sieve. A subsample from the intact macro-aggregates was crushed in a mortar and sieved again through the 250-µm sieve to obtain the fraction of crushed macro-

15 aggregates (<250 µm). We decided to use dry-sieved aggregates for soil incubation as wet-sieving releases soluble OM, which is bioavailable and thus a critical fraction for soil OC mineralization (Sainju, 2006). Further, microbial activity is less affected by dry-sieving than by wet-sieving (Sainju, 2006). All samples of the three fractions were divided into three analytical replicates, giving a total of 216 samples for soil incubations (8 plots x 3 field replicates x 3 fractions x 3 analytical replicates).

20   To determine whether the crushed macro-aggregates consisted of intact micro-aggregates or free primary particles, a subsample of crushed macro-aggregates was sieved through a 63-µm sieve and obtained fractions were imaged by a JEOL JSM-6390A scanning electron microscope (JEOL Ltd., Tokyo, Japan). Our analysis revealed that 62.1 ± 3.2% of crushed macro-aggregates still existed as large micro-aggregates (>63 µm), while 37.9 ± 3.2% were found in the fraction <63 µm, which mainly consisted of small micro-aggregates and only few free primary particles (Fig. S1).

25   Soil laboratory incubations were carried out under aerobic conditions in the dark, at constant temperature of 20°C and 60% of water holding capacity (WHC). An amount of 7.5 g soil sample was mixed with 12.5 g combusted (1000°C for 24 h) quartz powder (Roth, Karlsruhe, Germany; >99% pulverized, <125 µm) and filled into 120-ml glass jars. Quartz powder was used to increase the sample volume and prevent the formation of aggregates in the crushed samples. Three jars were solely filled with quartz and used as control. Soil moisture was regulated during the experiment by periodically

30 weighing the glass jars and adding ultrapure water. All samples were pre-incubated for 14 days and respiration measurements were subsequently taken at days 1, 3, 8, 14, 21, 28, 57, 98, 127, 196, 268, and 401 by sampling the headspace

of each jar using a syringe through a septum, which was installed in the jar lids prior to sampling. Gas samples were analyzed for CO_2 concentrations with a Shimadzu GC-2014 modified after Loftfield et al. (1997).

Determination of microbial biomass

After the laboratory incubations all samples were analyzed for microbial biomass C using the chloroform-fumigation-extraction method (Vance et al., 1987). Briefly, 6 g soil were kept at 60% WHC and weighed in duplicate into glass jars. One sample was fumigated with ethanol-free $CHCl_3$ during 24 h while the other sample was left unfumigated. Both, fumigated and unfumigated samples, were extracted with 0.5 M K_2SO_4 at a soil-to-solution ratio of 1:10 (w:v), shaken for 30 min, and subsequently centrifuged at 2700 g. The extracts were filtered (Whatman filter paper, ashless, Grade 42) and measured for non-purgeable organic carbon (NPOC) by a LiquiTOC (Elementar Analysensysteme GmbH, Hanau, Germany). Microbial biomass C was calculated as the difference between fumigated and unfumigated soil samples and expressed as mg C g OC^{-1}.

Calculations and statistical analyses

All data analyses were carried out in R 3.1.2 (R Core Team, 2015). To calculate cumulative respiration rates, data of CO_2 measurements per day was interpolated by spline interpolation for each sample (i.e. analytical replicate) separately. Cumulative respiration rates were analyzed by fitting three different exponential-decay models to the data and choosing the model with the best fit by AIC selection (Akaike Information Criterion). The first model was a first-order exponential decay model with one pool (one-pool model; Eq. 1):

$$C_{remain} = C_1 \times e^{(-k_1 \times t)} \tag{Eq. 1}$$

The second model consisted of two pools (two-pool model; Eq. 2):

$$C_{remain} = C_1 \times e^{(-k_1 \times t)} + C_2 \times e^{(-k_2 \times t)} \tag{Eq. 2}$$

The third model was an asymptotic first-order exponential decay model with two pools (asymptotic two-pool model; Eq. 3):

$$C_{remain} = C_2 + C_1 \times e^{(-k_1 \times t)} \tag{Eq. 3}$$

where C_{remain} is the amount of OC remaining in the sample, C_1 and C_2 are the sizes of the fast and the slow pool, respectively, k_1 and k_2 the rate constant of the fast and the slow pool, respectively, and t the time. For the majority of samples the two-pool model showed the best fit. Only for the pasture plot at FS the incubation time was too short to calculate the rate constant k

7

for the slow pool, thus the asymptotic two-pool model fitted the data best. The mean residence time (MRT) was calculated as $1/k$. The modelled parameters were used in linear mixed effects models (package lme4; Bates et al., 2012) to test for significant differences between soil fractions within plots, accounting for the nested structure of sampling by using the field replicates within each plot as random effects. Moreover, random slopes were included by allowing field replicates within

5   each plot to have random slopes for the effect of soil fraction. Based on the linear mixed model fit, we tested whether differences of the dependent variable between soil fractions within plots were significant, including corrections for multiple comparisons (analogous to the Tukey test) with Satterthwaite degrees of freedom, using the R packages lsmeans (Lenth and Herve, 2015), lmerTest (Kuznetsova et al., 2015) and multcomp (Hothorn et al., 2008). Model assumptions were checked using residuals *vs.* fitted plots and Q-Q-plots for the residual errors and random effect estimates. The proportion of the

10   macro-aggregate protected OC fraction to the total macro-aggregate OC content was calculated by Eq. 4:

$$C_{macro,\,total\,aggrC} = C_{min,crushed} - \frac{1}{n}\ \sum_{i=1}^{n} C_{min,intact} \qquad\qquad\qquad \text{(Eq. 4)}$$

where $C_{macro,total\,aggrC}$ is the proportion of macro-aggregate protected OC to the total macro-aggregate OC (%), $C_{min,crushed}$ is

15   the proportion of OC mineralized in the crushed macro-aggregates (%) and $C_{min,intact}$ is the proportion of OC mineralized in the intact macro-aggregates (%), while n is the number of analytical replicates per field replicate for the treatment of intact macro-aggregates and i is the ith analytical replicate per field replicate. The proportion of the macro-aggregate protected OC fraction to the total mineralized OC as function of time was calculated by Eq. 5:

20   $$C_{macro,\,mineralizableC}\ (t) = \frac{C_{min,crushed}\ (t) - \frac{1}{n}\sum_{i=1}^{n} C_{min,intact}\ (t)}{C_{min,crushed}\ (t)} \times 100 \qquad\qquad \text{(Eq. 5)}$$

where $C_{macro,mineralizableC}\ (t)$ is the proportion (%) of macro-aggregate protected OC to the total mineralized OC at time t (days). Graphs were generated using ggplot2 (Wickham, 2009). Boxplots show the median, the first and the third quartile and the whiskers extend from the box to the highest or lowest value, respectively, that is within $1.5 \times$ inter-quartile range.

25   Individual measurements are plotted as points.

8

Results

Soil organic carbon contents along the chronosequences

In FS, soil OC contents decreased as a result of LUC from pasture to arable land from 55 ± 5 mg g^{-1} under extensive pasture to 39 ± 1 mg g^{-1} and 40 ± 2 mg g^{-1} under arable 5 yr and arable 30 yr, respectively (Table 1). Thus, increasing duration of

5   agricultural land-use caused no further decrease of soil OC contents in arable soils. C : N ratios were around 12 and slightly higher for non-arable than for arable soils. Soil OC contents in TS were smaller than in FS and did not follow the gradient over time since cultivation as the site was affected by erosion (Sect. 2.1). In TS, soil C : N ratios did not vary considerably between the plots.

Effect of macro-aggregate crushing on the mineralization of soil organic carbon

10   Mass balance calculations revealed, that in both steppe types about 70% of OC was associated with macro-aggregates, indicating the importance of macro-aggregates for the OC dynamics in these soils. Organic C and TN contents did not vary considerably between intact and crushed macro-aggregates (Table S2). As is typically for soil incubations, respiration rates were higher at the beginning and decreased with increasing incubation time (Fig. S2). The amount of OC remaining in the sample during incubation was described by either two-pool or asymptotic two-pool models (Fig. 2). The variability of the

15   amount of OC remaining in the samples within one plot decreased with increasing time since cultivation (Fig. 2). Thus, soil samples belonging to the plots with the longest cultivation history were more similar to each other than samples from plots in more pristine state. The amount of soil OC mineralized was slightly larger in the bulk soil fraction (<2000 µm) than in the intact and crushed macro-aggregates in most of the studied plots, though significant differences were only observed in soils of FS ($p<0.05$, Fig. 3).

20   There was no significant difference in soil OC mineralization between intact and crushed macro-aggregates after 401 days of incubation in all plots under study (Fig. 2 and 3). The fraction of macro-aggregate protected OC was practically not existent and accounted for <1% of the total macro-aggregate OC content in all plots (data not shown). Furthermore, macro-aggregate crushing did not increase the size of the fast soil OC pool, which was determined by fitting exponential decay models to the incubation data (Fig. 4). Also the MRT of the fast and the slow OC pool was unaffected by macro-

25   aggregate crushing (Table 2). However, we could determine a small contribution of the macro-aggregate protected OC fraction to the total OC mineralization during the beginning of the incubation in seven out of eight plots, where macro-aggregate protected OC contributed to about 10% to the total mineralized OC d^{-1} (Fig. 5). Cumulated over the entire incubation period, the contribution of the macro-aggregate protected OC fraction to the total OC mineralization was not existent or very small and amounted between zero and 8 ± 4% in seven out of eight plots with no clear trend with respect to

30   the land-use duration (Table 3). The arable 3 yr plot in TS had clearly negative values of macro-aggregate protected OC, which resulted from a lower OC mineralization in crushed than in intact macro-aggregates. For most plots, the negligible

9

fraction of macro-aggregate protected OC was depleted between 100 and 400 days, while the arable 30 yr in FS and the fallow 30 yr (pasture) in TS showed a constant but small (ca. 5%) mineralization rate of macro-aggregate protected OC during the complete incubation period (Fig. 5).

Soil organic carbon mineralization along the chronosequences

5   The bulk soil OC mineralization declined after LUC from pasture to arable land in both steppe types, but only in TS we observed also a trend of decreasing soil OC mineralization with increasing duration of land-use (Fig. 3). Likewise, the proportion of the fast soil OC pool decreased as a result of LUC, but it was unaffected by the duration or intensity of arable land-use (Fig. 4). The MRT of the fast OC pool became shorter in the course of LUC in both steppe types, but only in FS we observed also a trend towards shorter MRTs with increasing intensity and duration of land-use (Table 2). With respect to the

10   slow soil OC pool, only in FS we detected shorter MRTs due to conversion of pasture to arable land and with increasing intensity and duration of land-use, while no trend was apparent along the chronosequence in TS (Table 2). In general, the amount of soil OC mineralized was slightly larger in TS than in FS, while the differences were most pronounced between the pasture plots (Fig. 3). Remarkable was the pasture in TS, which had clearly the largest OC mineralization and proportion of the fast OC pool but, at the same time, also the highest variability (Fig. 3 and 4).

15   **Microbial biomass carbon**

The share of microbial biomass C in the total OC was similar in both steppe types and ranged between 1.5 and 4.0 mg C g^{-1} OC, as indicated by the first and third quartile of the boxplots (Fig. 6). Crushing of macro-aggregates caused a small decrease of microbial biomass C, which was significant when considering all plots ($p<0.05$), while bulk soil samples and intact macro-aggregates had similar amounts of microbial biomass C. There was no correlation between the amount of OC

20   mineralized and the share of microbial biomass C in total OC (Fig. S3). Moreover, the quantity of OC mineralization was not related to the amount of microbial biomass C per gram soil (Fig. S4).

Discussion

Limited protection of macro-aggregate occluded organic carbon

Previous studies showed higher OC mineralization following macro-aggregate crushing (e.g. Beare et al., 1994; Bossuyt et

25   al., 2002; Pulleman and Marinissen, 2004), while some studies showed no such effect (Garcia-Oliva et al., 2004; Goebel et al., 2009; Plante et al., 2009). In our study, the macro-aggregate occluded OC fraction contributed only marginally to the OC mineralization during the entire incubation (Fig. 5, Table 3). Against our hypothesis, macro-aggregate occluded OC is not protected against decomposition in the studied soils. In turn, the break-down of macro-aggregates due to soil tillage and the subsequent release of soil OC is not the reason for a decrease of soil OC contents due to soil management, as observed along

30   the chronosequence in FS (Table 1). Plante et al. (2009) suspected that the disruption treatments used in their experiments

10

(crushing of 2–4 mm aggregates to <0.5 mm) was insufficient to release large amounts of physically protected OC for decomposition, and that a considerable amount of OC was stabilized in micro-aggregates. Also Balesdent et al. (2000) provided some evidence that the proportion of physically protected OC is larger in micro-aggregates than in macro-aggregates. In our study, the majority of crushed macro-aggregates (62 ± 3%) consisted of micro-aggregates with 63–250

5   µm size (See Material & Methods), and as the OC mineralization of the crushed aggregate fraction was not enhanced, we suggest that most of the OC was stabilized in the micro-aggregates. However, micro-aggregates are less sensitive to soil tillage (Tisdall and Oades, 1982), therefore, in light of LUC-induced OC losses, the soil OC in macro-aggregates is generally considered to be more vulnerable for destabilization than OC in micro-aggregates. This could not be confirmed for the soils under study. Nevertheless, we cannot rule out that an increased macro-aggregate turnover due to agricultural management

10 leads to a reduced formation of micro-aggregates within macro-aggregates and, as a result, to lower OC contents in arable as compared to pasture soils (Six et al., 2000a).

Only few studies determined the share of the macro-aggregate protected OC fraction in the total OC mineralization or the total macro-aggregate OC, respectively. Beare et al. (1994) showed that macro-aggregate protected OC accounted for about 1% of total aggregate OC and to about 8–23% of total mineralizable OC during 20 days of incubation. They detected a

15 smaller macro-aggregate protected OC mineralization in more intensively managed soils. In our study, <1% of total macro-aggregate OC was stored as macro-aggregate protected OC, while this fraction accounted for max. 8 ± 4% of total OC mineralization (Table 3). Thus, our values are in the same order of magnitude as observed by Beare et al. (1994), who suggested that an increased macro-aggregate turnover in tilled soils is one reason for the small macro-aggregate protected OC fraction. According to Beare et al. (1994), the physically protected but relatively labile macro-aggregate occluded OC is

20 released for microbial decomposition due to the frequent tillage-induced macro-aggregate break-down. As a result, macro-aggregates contain only little or no labile OC. This can be a reason in arable soils, but is unlikely in pasture soils where the macro-aggregate turnover is slower due to the absence of tillage (Six et al., 2002). In the untilled soils, therefore, other factors are probably responsible for the absence of labile macro-aggregate protected OC.

The mineralization of OC is driven by microorganisms and, thus, can be affected by disturbances of their physical

25 environment (Schimel and Schaeffer, 2012). Garcia-Oliva et al. (2004) observed lower OC mineralization in crushed than in intact macro-aggregates and attributed this finding to a reduced microbial activity in crushed samples, what they explained by a disturbed soil environment with possibly anaerobic conditions. Balesdent et al. (2000) reviewed the effect of aggregate-crushing on the mineralization of soil OM and indicated a reduced microbial biomass in crushed aggregates as a possible reason for similar OC mineralization rates in intact and crushed aggregates. In our study, crushed macro-aggregates

30 contained slightly but significantly less microbial biomass C than intact macro-aggregates (Fig. 6). This may have contributed to the missing effect of aggregate crushing on OC mineralization.

Besides stabilization of OC by physical occlusion within aggregates, formation of mineral-organic associations can be an important mechanism for OC stabilization (von Lützow et al., 2006). Bischoff et al. (2016) showed that a large OC fraction (>90% of total OC) is associated with mineral surfaces in soils of the Kulunda steppe, which is much more than

generally observed in steppe soils (Kalinina et al., 2011; Plante et al., 2010). In our study, about 38 ± 3% of the crushed macro-aggregate fraction were particles <63 µm, in which the proportion of particulate OC is usually very low (Christensen, 2001). Based on the similar OC mineralization rates of intact and crushed macro-aggregates, this suggests that a considerable OC proportion is stabilized by mineral surfaces. As a result, OC in crushed aggregates became not available to

5   microorganisms and thus did not enhance soil OC mineralization.

Summing up, our results suggest that the tillage-induced break-down of macro-aggregates and the subsequent release of OM is not the key factor driving OC losses due to LUC in the studied soils. In contrast, most OC in steppe soils of Siberia appears protected by occlusion within micro-aggregates and/or association with minerals. This, in part, contrasts with previous research of prairie soils from the North American Great Plains. Elliott (1986) and Cambardella and Elliott (1993,

10   1994) found that macro-aggregate occluded OC was rapidly lost after conversion of grassland to cropland due to the break-down of macro-aggregates and concluded that this fraction is protected from decomposition. Though, more recent research (e.g. Six et al., 2000) indicated that micro-aggregates which are formed within existing macro-aggregates are decisive for OC stabilization in agroecosystems, it is still widely accepted that the decomposition of previously occluded macro-aggregate OC is another key factor controlling the decline of OC after grassland to cropland conversion. Our results imply,

15   that this is not the case in the Siberian steppe soils. A possible explanation for the observed differences are smaller soil OC inputs by crop residues and rhizodeposits in the Siberian soils, resulting in smaller proportions of particulate OC (Castellano et al., 2015) and, thus, less possibilities for the formation of macro-aggregate occluded OC.

Effect of land management and soil characteristics on the mineralization potential of soil organic carbon

As shown in previous studies the conversion from grassland to arable land caused a decrease of labile soil OC (Plante et al.,

20   2011; Poeplau and Don, 2013), which corresponds to OC with fast turnover rates. In line with this, we found a larger fast OC pool under pasture than under arable land, while the proportion of the fast OC pool was unaffected by the intensity and duration of agricultural use (Fig. 4). This means, that the fast OC pool is highly vulnerable to LUC as the majority of this pool was rapidly lost within 1–5 yrs after grassland to cropland conversion. At the same time higher intensity or duration of agricultural land-use tended to shorten MRTs in the fast and slow OC pool of the soils in FS (Table 2), thus reducing the

25   potential to sequester soil OC. This is in line with Beare et al. (1994) and Grandy and Robertson (2007) who reported that the MRT of soil OC pools from laboratory incubations were shorter under high than under low land-use intensity. Beare et al. (1994) argued that the frequent soil disturbance in tilled soils impedes a strong association of OC with mineral surfaces, which in turn leads to a low protection of OC against microbial decomposition and thus fast turnover rates. Moreover, McLauchlan (2006) showed that the MRT of the fast OC pool was shorter in arable soils than in soils which were left as

30   fallow, which is supported by our results. We should consider that our observations were derived from long-term laboratory incubations and that we expect the difference of MRTs between arable and pasture soils to be even more pronounced under field conditions, as soil tillage generally accelerates the turnover of soil OC. Moreover, soil OC inputs by plant residues are

probably reduced in arable soils. This, together with faster soil OC turnover times would lead to a decrease of total soil OC as a result of agricultural land management.

We observed differences in the amount of mineralized soil OC between the two sites. Mineralization rates were smaller in the clayey soils of FS than in the soils of TS with larger sand content. Many studies showed smaller OC

5 mineralization rates in clayey soils as compared to sandy soils, as OC is stabilized by clay-sized minerals and thus protected against decomposition by microorganisms (Franzluebbers, 1999; Franzluebbers and Arshad, 1997; Harrison-Kirk et al., 2013). Moreover, Bischoff et al. (2016) showed that the proportion of labile particulate OC tended to increase with aridity in the soils under study. This means, that soils in TS would have larger amounts of bioavailable and easily decomposable particulate OC than soils in FS, which in turn leads to increased OC mineralization in the soils of TS. The differences

10 between both sites with respect to their soil OC mineralization rates could therefore be attributed to a different contribution of mineral-organic associations, with less mineral-bound OC in TS as compared to FS.

Interestingly, we found a smaller variation of the percentage of OC mineralized (i.e. OC mineralization rates) between samples from plots with long land-use duration (Fig. 2). This is possibly due to the fact that tillage homogenizes the soil within plough depth and consequently minimizes the heterogeneity of soil OC at the field scale. This idea is supported

15 by Schrumpf et al. (2011), who showed that soil OC contents are less variable under cropland as compared to grassland. We, therefore, conclude that continuous agricultural management obliterates differences of soil OC properties across a field.

Conclusion

This study set out to determine the quantity of macro-aggregate protected OC in Siberian steppe soils under different land-use and as function of land-use duration and intensity by crushing of dry-sieved macro-aggregates (250–2000 µm) to <250

20 µm and subsequent incubation of crushed and intact macro-aggregates at 20°C and 60% WHC during 401 days along two agricultural chronosequences of the Kulunda steppe. The effect of macro-aggregate crushing on OC mineralization was negligible along the two chronosequences. Macro-aggregate protected OC accounted for <1% of the total macro-aggregate OC content and for maximally 8 ± 4% of total mineralized OC. The majority of macro-aggregate protected OC was mineralized during the beginning of the incubation, showing that this represents a labile fraction with fast turnover rates. Our

25 results imply that the tillage-induced break-down of macro-aggregates has not reduced the OC contents in the studied soils. In contrast, our data suggest that mainly OC occluded within micro-aggregates and/or associated with mineral-surfaces is decisive for OC stabilization in these soils. Long-term incubations of bulk soil samples revealed that LUC from pasture to arable land but also the cultivation with forage crops caused a rapid decrease of a fast soil OC pool within 1–5 yrs of agricultural management. At the same time the MRT tended to become shorter in the fast and slow OC pool with increasing

30 land-use duration and intensity at one of the investigated sites. This suggests that the potential of the soils to sequester OC is reduced under agricultural management, as OC which enters the soil from above- or belowground is released to the atmosphere within few decades. The difference of turnover times between arable and pasture soils is probably even more

pronounced under field conditions, as soil tillage leads to a frequent disturbance of the soil environment which additionally accelerates soil OC mineralization. Thus, we conclude that the decrease of soil OC contents in the course of LUC is attributed to faster soil OC turnover under arable land as compared to pasture at a reduced plant residue input but not to the tillage-induced release of macro-aggregate occluded soil OC.

References

Balesdent, J., Chenu, C. and Balabane, M.: Relationship of soil organic matter dynamics to physical protection and tillage, Soil Tillage Res., 53(3–4), 215–230, doi:10.1016/S0167-1987(99)00107-5, 2000.

Bates, D., Mächler, M. and Bolker, B.: Fitting linear mixed-effects models using lme4, J. Stat. Softw., 1–51 [online]
5 Available from: http://arxiv.org/abs/1406.5823%5Cnhttp://listengine.tuxfamily.org/lists.tuxfamily.org/eigen/2011/06/pdfKU_S0z6LjT.pdf, 2012.

Beare, M. H., Hendrix, P. F., Cabrera, M. L. and Coleman, D. C.: Aggregate-protected and unprotected organic matter pools in conventional- and no-tillage soils, Soil Sci. Soc. Am. J., 58(3), 787, doi:10.2136/sssaj1994.03615995005800030021x,
10 1994.

Beniston, J. W., DuPont, S. T., Glover, J. D., Lal, R. and Dungait, J. A. J.: Soil organic carbon dynamics 75 years after land-use change in perennial grassland and annual wheat agricultural systems, Biogeochemistry, 120(1–3), 37–49, doi:10.1007/s10533-014-9980-3, 2014.

Bischoff, N., Mikutta, R., Shibistova, O., Puzanov, A., Reichert, E., Silanteva, M., Grebennikova, A., Schaarschmidt, F.,
15 Heinicke, S. and Guggenberger, G.: Land-use change under different climatic conditions: Consequences for organic matter and microbial communities in Siberian steppe soils, Agric. Ecosyst. Environ., 235, 253–264, doi:10.1016/j.agee.2016.10.022, 2016.

Bossuyt, H., Six, J. and Hendrix, P. F.: Aggregate-protected carbon in no-tillage and conventional tillage agroecosystems using carbon-14 labeled plant residue, Soil Sci. Soc. Am. J., 66(6), 1965, doi:10.2136/sssaj2002.1965, 2002.

20 Cambardella, C. A. and Elliott, E. T.: Carbon and nitrogen distribution in aggregates from cultivated and native grassland soils, Soil Sci. Soc. Am. J., 57, 1071–1076, doi:10.2136/sssaj1993.03615995005700040032x, 1993.

Cambardella, C. A. and Elliott, E. T.: Carbon and nitrogen dynamics of soil organic matter fractions from cultivated grassland soils, Soil Sci. Soc. Am. J., 58, 123–130, doi:10.2136/sssaj1994.03615995005800010017x, 1994.

Castellano, M. J., Mueller, K. E., Olk, D. C., Sawyer, J. E. and Six, J.: Integrating plant litter quality, soil organic matter
25 stabilization, and the carbon saturation concept, Glob. Chang. Biol., 21(9), 3200–3209, doi:10.1111/gcb.12982, 2015.

Christensen, B. T.: Physical fractionation of soil and structural and functional complexity in organic matter turnover, Eur. J. Soil Sci., 52(3), 345–353, doi:10.1046/j.1365-2389.2001.00417.x, 2001.

DIN ISO, 11277: Soil quality – determination of particle size distribution in mineral soil material – method by sieving and sedimentation, 2002.

30 Elliott, E. T.: Aggregate structure and carbon, nitrogen, and phosphorus in native and cultivated soils, Soil Sci. Soc. Am. J.,

15

50, 627–633, doi:10.2136/sssaj1986.03615995005000030017x, 1986.

FAO: Lecture notes on the major soils of the world, edited by P. Driessen, J. Deckers, O. Spaargaren, and F. Nachtergaele, World soil Resour. reports, 94, 336, doi:10.1136/gut.27.11.1400-b, 2001.

FAO: FAO Statistical yearbook 2013 - World food and agriculture, Rome., 2013.

5   Franzluebbers, A. J.: Potential C and N mineralization and microbial biomass from intact and increasingly disturbed soils of varying texture, Soil Biol. Biochem., 31, 1083–1090, doi:10.1016/S0038-0717(99)00022-X, 1999.

Franzluebbers, A. J. and Arshad, M. A.: Soil microbial biomass and mineralizable carbon of water-stable aggregates, Soil Sci. Soc. Am. J., 61(4), 1090–1097, doi:10.2136/sssaj1997.03615995006100040015x, 1997.

Frühauf, M.: Landnutzungs- und Ökosystementwicklung in den südsibirischen Agrarsteppen, Geogr. Rundschau, 1, 46–53, 10   2011.

Garcia-Oliva, F., Oliva, M. and Sveshtarova, B.: Effect of soil macroaggregates crushing on C mineralization in a tropical deciduous forest ecosystem, Plant Soil, 259(1–2), 297–305, doi:10.1023/B:PLSO.0000020978.38282.dc, 2004.

Goebel, M.-O., Woche, S. K. and Bachmann, J.: Do soil aggregates really protect encapsulated organic matter against microbial decomposition?, Biologia (Bratisl)., 64(3), 443–448, doi:10.2478/s11756-009-0065-z, 2009.

15   Grandy, A. S. and Robertson, G. P.: Land-use intensity effects on soil organic carbon accumulation rates and mechanisms, Ecosystems, 10(1), 58–73, doi:10.1007/s10021-006-9010-y, 2007.

Gupta, V. V. S. R. and Germida, J. J.: Distribution of microbial biomass and its activity in different soil aggregate size classes as affected by cultivation, Soil Biol. Biochem., 20(6), 777–786, doi:10.1016/0038-0717(88)90082-X, 1988.

Harrison-Kirk, T., Beare, M. H., Meenken, E. D. and Condron, L. M.: Soil organic matter and texture affect responses to 20   dry/wet cycles: Effects on carbon dioxide and nitrous oxide emissions, Soil Biol. Biochem., 57, 43–55, doi:10.1016/j.soilbio.2012.10.008, 2013.

Hijmans, R. J., Cameron, S. E., Parra, J. L., Jones, P. G. and Jarvis, A.: Very high resolution interpolated climate surfaces for global land areas, Int. J. Climatol., 25(15), 1965–1978, doi:10.1002/joc.1276, 2005.

Hothorn, T., Bretz, F. and Westfall, P.: Simultaneous inference in general parametric models, Biometrical J., 50(3), 346–363, 25   doi:10.1002/bimj.200810425, 2008.

IUSS Working Group WRB: World reference base for soil resources 2014. International soil classification system for naming soils and creating legends for soil maps, World Soil Resour. Reports No. 106, 1–191, doi:10.1017/S0014479706394902, 2014.

Kalinina, O., Krause, S.-E., Goryachkin, S. V., Karavaeva, N. A., Lyuri, D. I. and Giani, L.: Self-restoration of post-

16

agrogenic chernozems of Russia: Soil development, carbon stocks, and dynamics of carbon pools, Geoderma, 162(1–2), 196–206, doi:10.1016/j.geoderma.2011.02.005, 2011.

Kleber, M., Eusterhues, K., Keiluweit, M., Mikutta, C., Mikutta, R. and Nico, P. S.: Mineral-organic associations: formation, properties, and relevance in soil environments, Adv. Agron., 130, 1–140, doi:10.1016/bs.agron.2014.10.005, 2015.

5 Kuznetsova, A., Brockhott, P. B. and Christensen, R. H. B.: lmerTest: Tests in linear mixed effects models. R package version 2.0-25, [online] Available from: http://cran.r-project.org/package=lmerTest, 2015.

Lenth, R. V. and Herve, M.: lsmeans: Least-squares means. R package version 2.17, [online] Available from: http://cran.r-project.org/package=lsmeans, 2015.

Loftfield, N., Flessa, H., Augustin, J. and Beese, F.: Automated gas chromatographic system for rapid analysis of the

10 atmospheric trace gases methane, carbon dioxide, and nitrous oxide, J. Environ. Qual., 26(2), 560, doi:10.2134/jeq1997.00472425002600020030x, 1997.

von Lützow, M., Kögel-Knabner, I., Ekschmitt, K., Matzner, E., Guggenberger, G., Marschner, B. and Flessa, H.: Stabilization of organic matter in temperate soils: Mechanisms and their relevance under different soil conditions - A review, Eur. J. Soil Sci., 57(4), 426–445, doi:10.1111/j.1365-2389.2006.00809.x, 2006.

15 McLauchlan, K. K.: Effects of soil texture on soil carbon and nitrogen dynamics after cessation of agriculture, Geoderma, 136(1–2), 289–299, doi:10.1016/j.geoderma.2006.03.053, 2006.

Mikhailova, E. A., Bryant, R. B., Vassenev, I. I., Schwager, S. J. and Post, C. J.: Cultivation effects on soil carbon and nitrogen contents at depth in the russian Chernozem, Soil Sci. Soc. Am. J., 64, 738, doi:10.2136/sssaj2000.642738x, 2000.

Plante, A. F., Six, J., Paul, E. A. and Conant, R. T.: Does physical protection of soil organic matter attenuate temperature

20 sensitivity?, Soil Sci. Soc. Am. J., 73(4), 1168, doi:10.2136/sssaj2008.0351, 2009.

Plante, A. F., Virto, I. and Malhi, S. S.: Pedogenic, mineralogical and land-use controls on organic carbon stabilization in two contrasting soils, Can. J. Soil Sci., 90(1), 15–26, doi:10.4141/CJSS09052, 2010.

Plante, A. F., Fernández, J. M., Haddix, M. L., Steinweg, J. M. and Conant, R. T.: Biological, chemical and thermal indices of soil organic matter stability in four grassland soils, Soil Biol. Biochem., 43(5), 1051–1058,

25 doi:10.1016/j.soilbio.2011.01.024, 2011.

Poeplau, C. and Don, A.: Sensitivity of soil organic carbon stocks and fractions to different land-use changes across Europe, Geoderma, 192, 189–201, doi:10.1016/j.geoderma.2012.08.003, 2013.

Pulleman, M. M. and Marinissen, J. C. Y.: Physical protection of mineralizable C in aggregates from long-term pasture and arable soil, Geoderma, 120(3–4), 273–282, doi:10.1016/j.geoderma.2003.09.009, 2004.

17

R Core Team: R: A language and environment for statistical computing, [online] Available from: http://www.r-project.org/, 2015.

Rodionov, A., Amelung, W., Urusevskaja, I. and Zech, W.: Beziehungen zwischen Klimafaktoren und C-, N-Pools in Partikelgrössen-Fraktionen zonaler Steppenböden Russlands, Zeitschrift für Pflanzenernährung und Bodenkd., 161(1981), 563–569, 1998.

Sainju, U. M.: Carbon and nitrogen pools in soil aggregates separated by dry and wet sieving methods, Soil Sci., 171(12), 937–949, doi:10.1097/01.ss0000228062.30958.5a, 2006.

Schimel, J. P. and Schaeffer, S. M.: Microbial control over carbon cycling in soil, Front. Microbiol., 3(SEP), 1–11, doi:10.3389/fmicb.2012.00348, 2012.

Schrumpf, M., Schulze, E. D., Kaiser, K. and Schumacher, J.: How accurately can soil organic carbon stocks and stock changes be quantified by soil inventories?, Biogeosciences, 8(5), 1193–1212, doi:10.5194/bg-8-1193-2011, 2011.

Six, J., Elliott, E. . and Paustian, K.: Soil macroaggregate turnover and microaggregate formation: a mechanism for C sequestration under no-tillage agriculture, Soil Biol. Biochem., 32(14), 2099–2103, doi:10.1016/S0038-0717(00)00179-6, 2000a.

Six, J., Paustian, K., Elliott, E. T. and Combrink, C.: Soil structure and organic matter: I. Distribution of aggregate-size classes and aggregate-associated carbon, Soil Sci. Soc. Am. J., 64, 681–689, doi:10.2136/sssaj2000.642681x, 2000b.

Six, J., Feller, C., Denef, K., Ogle, S. M. and Moraes, J. C., Albrecht, A.: Soil organic matter, biota and aggregation in temperate and tropical soils - effects of no-tillage, Agronomie, 22, 755–775, doi:10.1051/agro:2002043, 2002.

Tian, J., Pausch, J., Yu, G., Blagodatskaya, E., Gao, Y. and Kuzyakov, Y.: Aggregate size and their disruption affect 14C-labeled glucose mineralization and priming effect, Appl. Soil Ecol., 90, 1–10, doi:10.1016/j.apsoil.2015.01.014, 2015.

Tisdall, J. and Oades, J.: Organic matter and water-stable aggregates in soils, J. soil Sci., 33, 141–163, doi:10.1111/j.1365-2389.1982.tb01755.x, 1982.

Vance, E. D., Brookes, P. C. and Jenkinson, D. S.: An extraction method for measuring soil microbial biomass C, Soil Biol. Biochem., 19(6), 703–707, doi:10.1016/0038-0717(87)90052-6, 1987.

VandenBygaart, A. J., Gregorich, E. G. and Angers, D. A.: Influence of agricultural management on soil organic carbon: A compendium and assessment of Canadian studies, Can. J. Soil Sci., 83, 363–380, doi:10.4141/S03-009, 2003.

Walthert, L., Graf, U., Kammer, A., Luster, J., Pezzotta, D., Zimmermann, S. and Hagedorn, F.: Determination of organic and inorganic carbon, δ13 C, and nitrogen in soils containing carbonates after acid fumigation with HCl, J. Plant Nutr. Soil Sci., 173(2), 207–216, doi:10.1002/jpln.200900158, 2010.

Wickham, H.: ggplot2: Elegant graphics for data analysis, [online] Available from: papers2://publication/uuid/DE806F9A-5AD0-450B-AC68-5164EDBA8787, 2009.

19

Tables

Table 1: Land-use and soil properties in A horizons (pH, EC, sand, silt, clay) and in 0-10 cm (OC, TN, C : N) of investigated sites with mean annual temperature (MAT) and mean annual precipitation (MAP). Soil type classification according to IUSS Working Group WRB (2014). Abbreviation: n.d. = not determined.

Steppe	MAT	MAP	Soil type	Land use	pH	EC	Sand	Silt	Clay	OC			TN			C : N		
	°C	mm			-	µS cm^{-1}	mg g^{-1}	mg g^{-1}	mg g^{-1}	mg g^{-1}			mg g^{-1}			-		
Forest steppe	1.1	368	Protocalcic Chernozem	extensive pasture	7.6	116.6	28	609	363	54.6	±	5.4	4.5	±	0.4	12.2	±	0.2
				forage crop	n.d.	n.d.	n.d.	n.d.	n.d.	49.3	±	1.7	4.1	±	0.2	12.1	±	0.0
				arable 5 yr	7.1	58.6	39	600	360	39.1	±	1.4	3.3	±	0.1	11.7	±	0.1
				arable 30 yr	7.0	60.4	34	598	369	40.4	±	1.6	3.4	±	0.1	11.8	±	0.1
Typical steppe	2.0	339	Protocalcic Kastanozem	fallow 30 yr (pasture)	7.1	34.8	292	472	236	21.6	±	2.3	2.0	±	0.2	10.9	±	0.1
				arable 1 yr	n.d.	n.d.	n.d.	n.d.	n.d.	13.3	±	0.3	1.3	±	0.0	10.0	±	0.1
				arable 3 yr	n.d.	n.d.	n.d.	n.d.	n.d.	14.9	±	1.6	1.5	±	0.2	9.8	±	0.2
				arable 10 yr	n.d.	n.d.	n.d.	n.d.	n.d.	18.8	±	1.5	1.8	±	0.1	10.6	±	0.2

Table 2: Mean residence times of the fast and slow OC pool (years) as arithmetic mean ± SE, as derived from least-square fitting of incubation data, for two steppe types and as function of land-use and soil fraction. Significant differences (p<0.05) between fractions within land-use were not detected, which is indicated by same lowercase letters.

| Steppe	Land-use	Fraction	Mean residence time (years)					
			Fast OC pool			Slow OC pool		
Forest steppe	extensive pasture	bulk	0.73	± 0.07	a	62.8	± 18.6	a
		intact	0.74	± 0.09	a	54.5	± 1.6	a
		crushed	0.69	± 0.06	a	89.5	± 19.2	a
	forage crop	bulk	0.46	± 0.07	a	53.5	± 7.6	a
		intact	0.68	± 0.11	a	65.2	± 13.6	a
		crushed	0.42	± 0.06	a	48.3	± 3.3	a
	arable 5 yr	bulk	0.51	± 0.07	a	45.2	± 8.0	a
		intact	0.51	± 0.06	a	48.1	± 6.4	a
		crushed	0.33	± 0.02	a	42.4	± 3.1	a
	arable 30 yr	bulk	0.38	± 0.02	a	36.5	± 1.6	a
		intact	0.41	± 0.03	a	41.5	± 1.9	a
		crushed	0.33	± 0.01	a	36.9	± 1.7	a
Typical steppe	fallow 30 yr (pasture)	bulk	0.79	± 0.11	a	21.7	± 7.1	a
		intact	0.79	± 0.10	a	25.8	± 2.4	a
		crushed	0.80	± 0.10	a	25.9	± 9.0	a
	arable 1 yr	bulk	0.33	± 0.06	a	26.2	± 4.9	a
		intact	0.43	± 0.05	a	30.9	± 3.2	a
		crushed	0.32	± 0.05	a	30.3	± 6.6	a
	arable 3 yr	bulk	0.68	± 0.11	a	29.5	± 4.0	a
		intact	0.64	± 0.14	a	20.6	± 1.3	a
		crushed	0.88	± 0.16	a	22.7	± 2.7	a
	arable 10 yr	bulk	0.55	± 0.08	a	24.4	± 1.4	a
		intact	0.86	± 0.18	a	33.2	± 7.2	a
		crushed	0.58	± 0.10	a	25.9	± 1.6	a

5

Table 3: Proportion of macro-aggregate protected OC (% of mineralized OC) for two steppe types and the respective land-use. Since the proportion of macro-aggregate protected OC was calculated by subtracting the amount of OC mineralized in intact macro-aggregates from that in crushed macro-aggregates, negative values occur when the OC mineralization was smaller in crushed than in intact macro-aggregates.

Steppe	Land-use	Macro-aggregate protected OC (% of mineralized OC)		
Forest steppe	extensive pasture	1.4	±	2.4
	forage crop	-0.4	±	8.4
	arable 5 yr	2.6	±	4.3
	arable 30 yr	7.7	±	4.2
Typical steppe	fallow 30 yr (pasture)	4.7	±	0.8
	arable 1 yr	0.7	±	1.8
	arable 3 yr	-8.8	±	5.7
	arable 10 yr	4.3	±	3.1

5

Figures
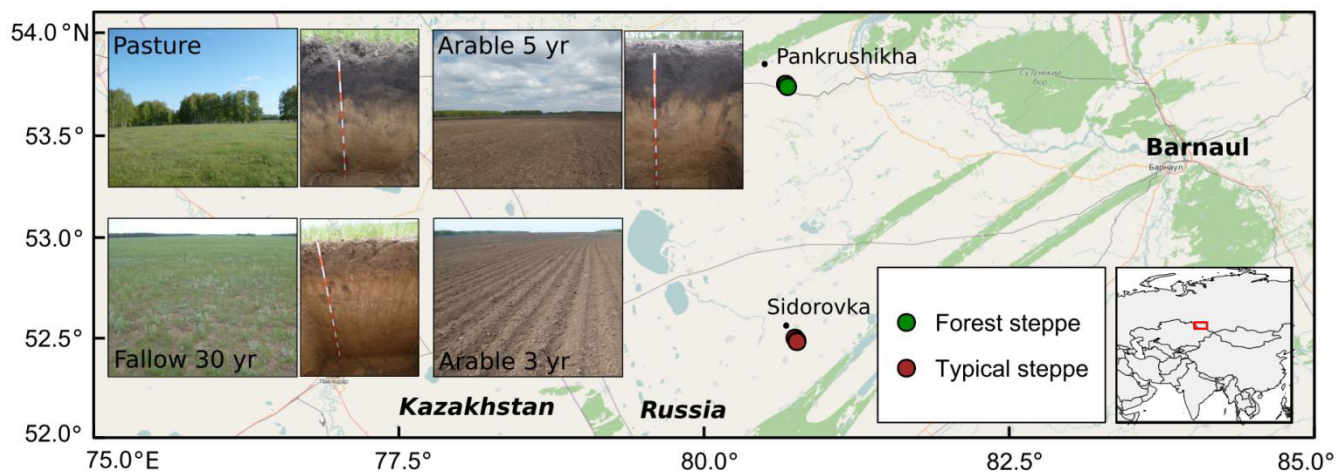
Figure 1: Map of the study area and pictures from the two sites near Pankrushikha and Sidorovka. Map modified from
5   **©OpenStreetMap contributors, for copyright see www.openstreetmap.org/copyright.**
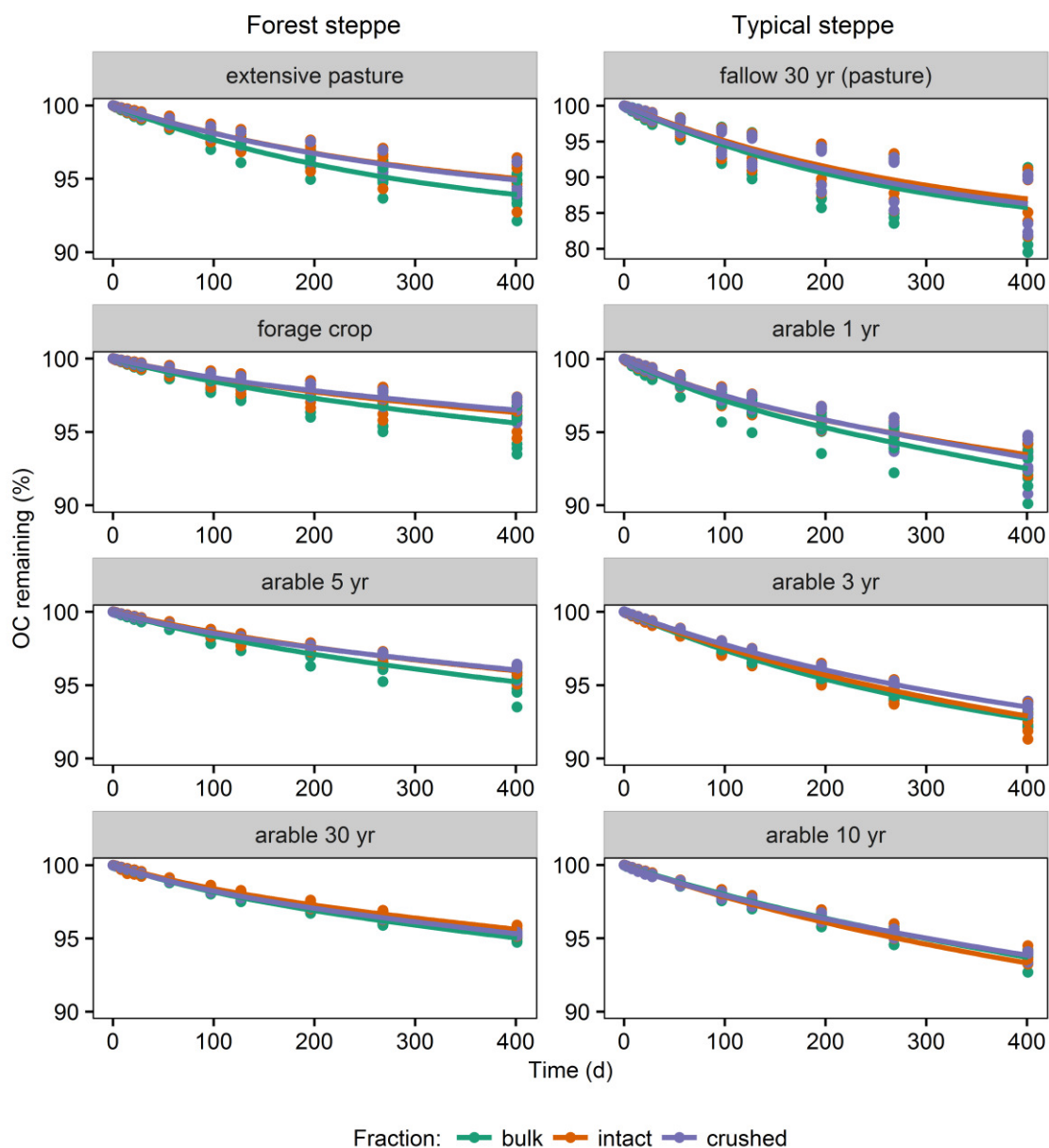
23

Figure 2: Percentage of soil OC remaining in the samples during 401 days of incubation for eight plots within two steppe types and for the three fractions bulk soil, intact macro-aggregates, and crushed macro-aggregates. For all plots a two-pool model (Eq. 2) was fitted, except for the extensively managed plots (extensive pasture and the fallow 30 yr (pasture)), where an asymptotic two-pool model was fitted (Eq. 3). Note the different scale for the fallow 30 yr (pasture).
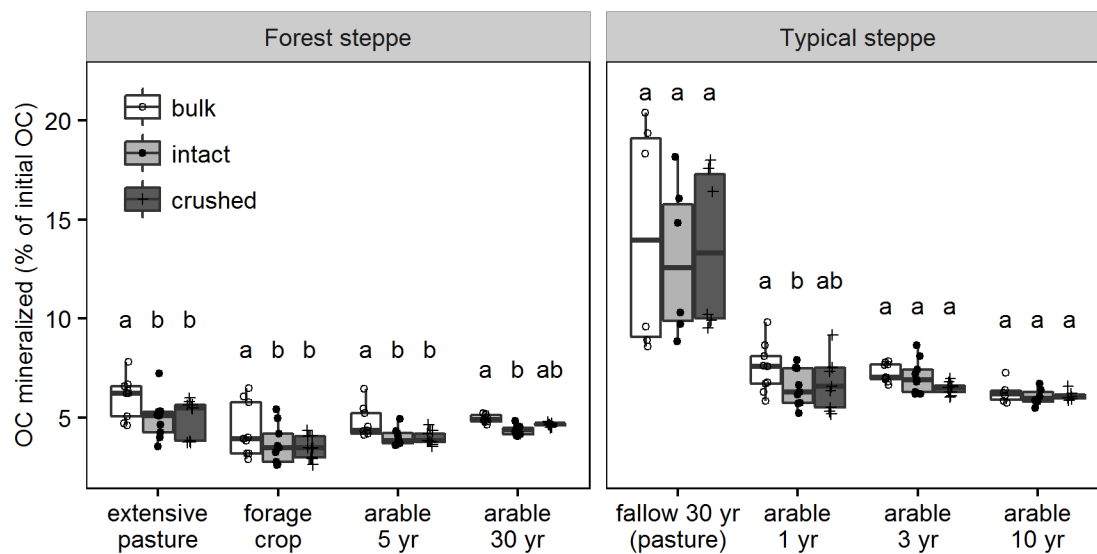
24

Figure 3: Percentage of soil OC mineralized during 401 days of incubation for eight plots within two steppe types and for the three fractions bulk soil, intact macro-aggregates, and crushed macro-aggregates. Different lowercase letters indicate significant differences between fractions within plots at p<0.05.

5
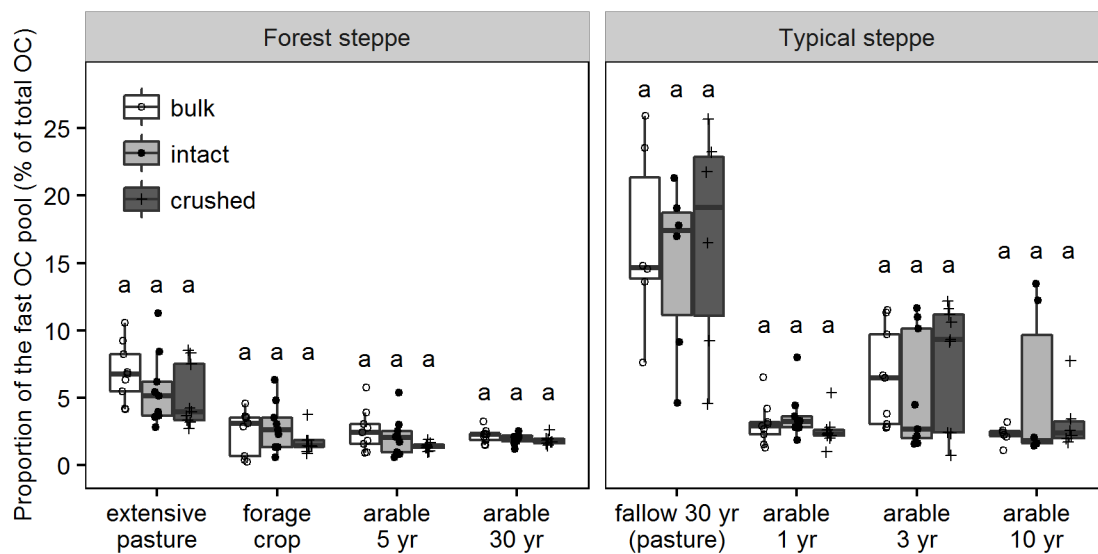
Figure 4: Proportion of the fast OC pool (% of total OC) for eight plots within two steppe types and for the three fractions bulk soil, intact macro-aggregates, and crushed macro-aggregates as derived from two-pool model fits to incubation data (Eq. 2 and 3). Significant differences (p<0.05) between fractions within plots were not detected, which is indicated by same lowercase letters.
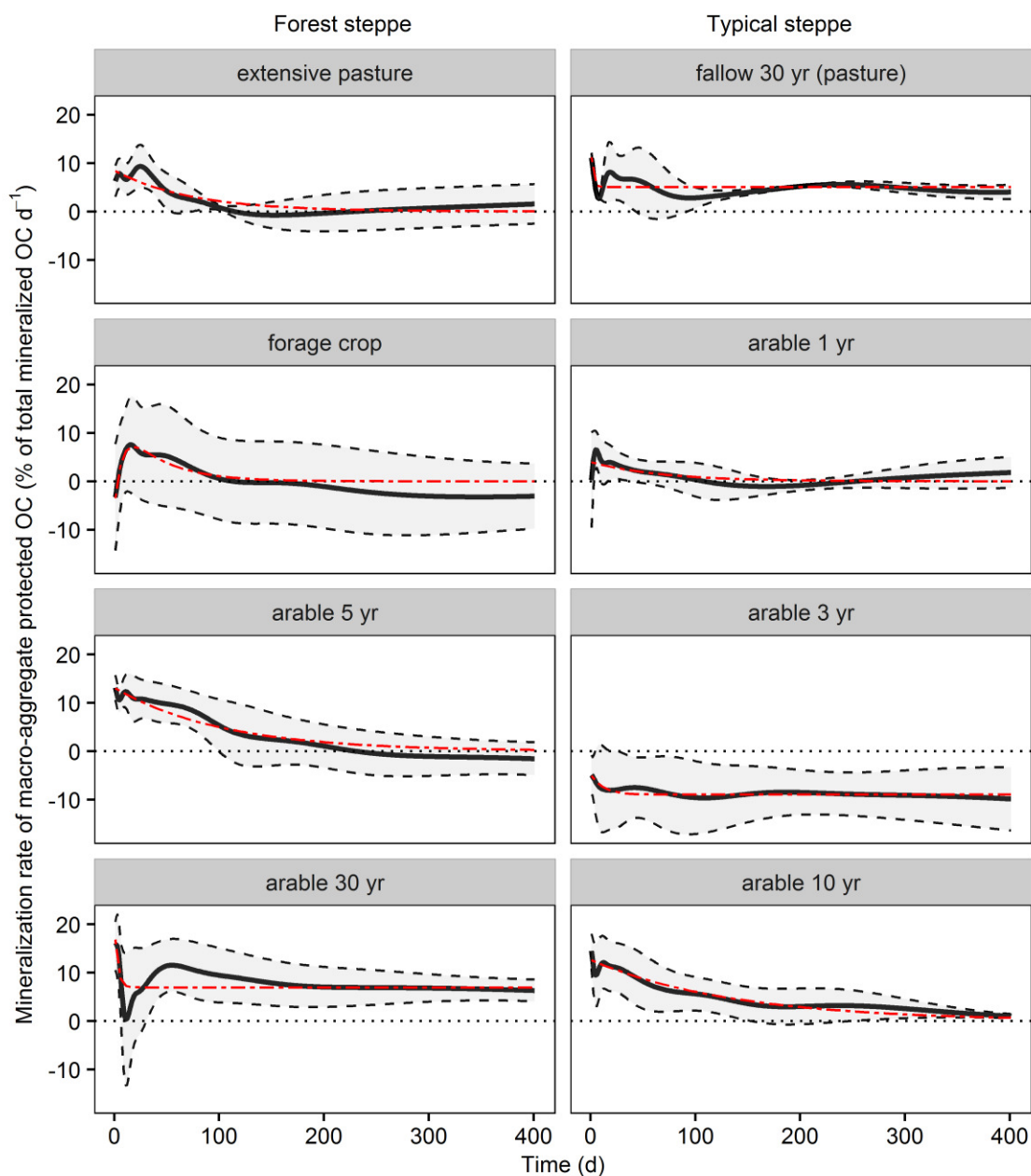
5

Figure 5: Mineralization rate of macro-aggregate protected OC (% of total mineralized OC d^{-1}) during 401 days of incubation for eight plots within two steppe types. The black solid line shows the mean mineralization rate per plot and the shaded grey area (confined by the black dashed lines) shows the corresponding standard error. The red dot-dashed line shows the fit of an exponential decay model (either 1-pool model, 2-pool model, or asymptotic 2-pool model according to the best fit). Since the mineralization rates were calculated by subtracting the OC mineralization rates of intact macro-aggregates from that of crushed macro-aggregates, negative values occur when the OC mineralization was smaller in crushed than in intact macro-aggregates.
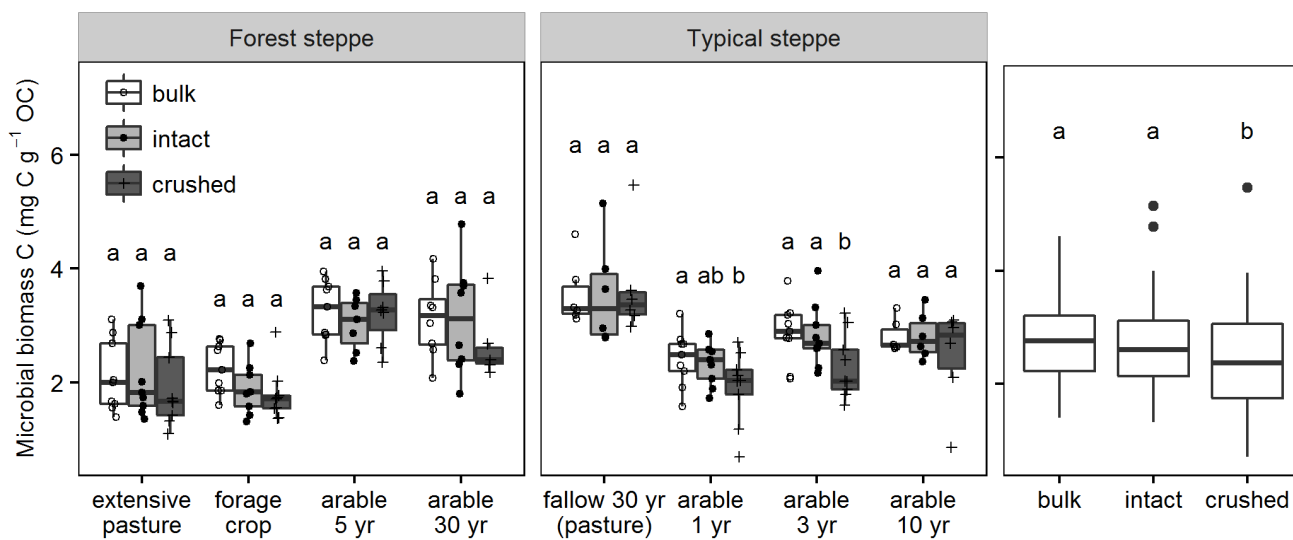
Figure 6: Microbial biomass C (mg C g^{-1} OC) for eight plots within two steppe types and the three fractions bulk soil, intact macro-aggregates, and crushed macro-aggregates. Different lowercase letters indicate significant differences between fractions within plots at p<0.05. The right panel shows differences between the three fractions averaged over all plots.

Supplement of

Limited protection of macro-aggregate occluded organic carbon in Siberian steppe soils

5   **N. Bischoff et al.**

Correspondence to: N. Bischoff (bischoff@ifbk.uni-hannover.de)

Supplements

Calculation of the share of steppe soils in the global soil OC stocks down to 1m depth

Steppe soils are typically the group of Kastanozems (KS), Chernozems (CH) and Phaeozems (PH; FAO, 2001). Average OC stocks of these soils are found in Batjes (1996) and their global area is estimated in the IUSS

5 Working Group WRB (2014). By multiplying the average OC stock of these soil types by their global area and dividing the result by the global soil OC stock of about 1505 Pg OC (Batjes, 1996), we can estimate the share of steppe soils in the global soil OC stock down to 1m depth. This was done as, to our knowledge, there is no study yet, which modelled the portion of steppe soils on the global soil OC stock. The equation is as following:

$$y = \frac{\text{average OC stock (KS)} \times \text{area (KS)} + \text{average OC stock (CH)} \times \text{area (CH)} + \text{average OC stock (PH)} \times \text{area (PH)}}{\text{OC stock (worldwide)}}$$

10
where y is the share of steppe soils in the global soil OC stock.

Tables

Table S 1: Geographical coordinates and vegetation cover (pastures only) for the studied plots.

Steppe	Land use	Coordinates		Vegetation (pastures only)
		latitude	longitude	Dominant species (from most to least dominant)
Forest steppe	extensive pasture	53°44'19.53"N	80°41'2.88"E	*Festuca valesiaca - Fillipendula vulgaris - Bromopsis inermis*
	forage crop	53°44'24.92"N	80°40'58.73"E	
	arable 5 yr	53°45'0.19"N	80°40'12.68"E	
	arable 30 yr	53°45'3.32"N	80°40'2.97"E	
Typical steppe	fallow 30 yr (pasture)	52°30'1.43"N	80°44'41.68"E	*Agropyron pectinatum - Bromopsis inermis - Artemisia glauca*
	arable 1 yr	52°30'5.43"N	80°44'25.57"E	
	arable 3 yr	52°30'10.92"N	80°44'44.44"E	
	arable 10 yr	52°29'30.56"N	80°45'5.21"E	

3

Table S 2: Organic carbon (OC) and total nitrogen (TN) of the three fractions bulk soil, intact macro-aggregates and crushed macro-aggregates for the respective land-use and steppe type.

| Steppe	Land-use	Fraction	n	OC mg g^{-1}			TN mg g^{-1}			C : N -		
Forest steppe	extensive pasture	bulk	3	54.6	±	5.4	4.5	±	0.4	12.2	±	0.2
		intact	3	53.3	±	6.5	4.4	±	0.5	12.0	±	0.2
		crushed	3	52.2	±	5.7	4.4	±	0.4	11.8	±	0.2
	forage crop	bulk	3	49.3	±	1.7	4.1	±	0.2	12.1	±	0.0
		intact	3	48.7	±	1.2	4.1	±	0.1	12.0	±	0.1
		crushed	3	45.5	±	1.1	3.9	±	0.1	11.6	±	0.1
	arable 5 yr	bulk	3	39.1	±	1.4	3.3	±	0.1	11.7	±	0.2
		intact	3	39.2	±	2.4	3.3	±	0.2	12.0	±	0.1
		crushed	3	38.4	±	2.6	3.2	±	0.1	11.8	±	0.3
	arable 30 yr	bulk	3	40.4	±	1.6	3.4	±	0.1	11.8	±	0.1
		intact	3	39.1	±	2.3	3.4	±	0.2	11.6	±	0.0
		crushed	3	37.4	±	1.4	3.3	±	0.1	11.3	±	0.0
Typical steppe	fallow 30 yr (pasture)	bulk	2	21.6	±	2.3	2.0	±	0.2	10.9	±	0.1
		intact	2	20.6	±	2.8	1.9	±	0.2	10.6	±	0.3
		crushed	2	20.4	±	2.6	2.0	±	0.2	10.3	±	0.3
	arable 1 yr	bulk	3	13.3	±	0.3	1.3	±	0.0	10.0	±	0.1
		intact	3	14.1	±	0.9	1.4	±	0.1	10.0	±	0.2
		crushed	3	13.3	±	0.5	1.3	±	0.0	10.2	±	0.2
	arable 3 yr	bulk	3	14.9	±	1.6	1.5	±	0.2	9.8	±	0.2
		intact	3	16.6	±	2.6	1.7	±	0.3	9.9	±	0.2
		crushed	3	15.6	±	2.5	1.6	±	0.2	9.8	±	0.2
	arable 10 yr	bulk	2	18.8	±	1.5	1.8	±	0.1	10.6	±	0.2
		intact	2	20.0	±	0.7	1.9	±	0.0	10.6	±	0.3
		crushed	2	18.5	±	0.9	1.8	±	0.0	10.5	±	0.2

Figures
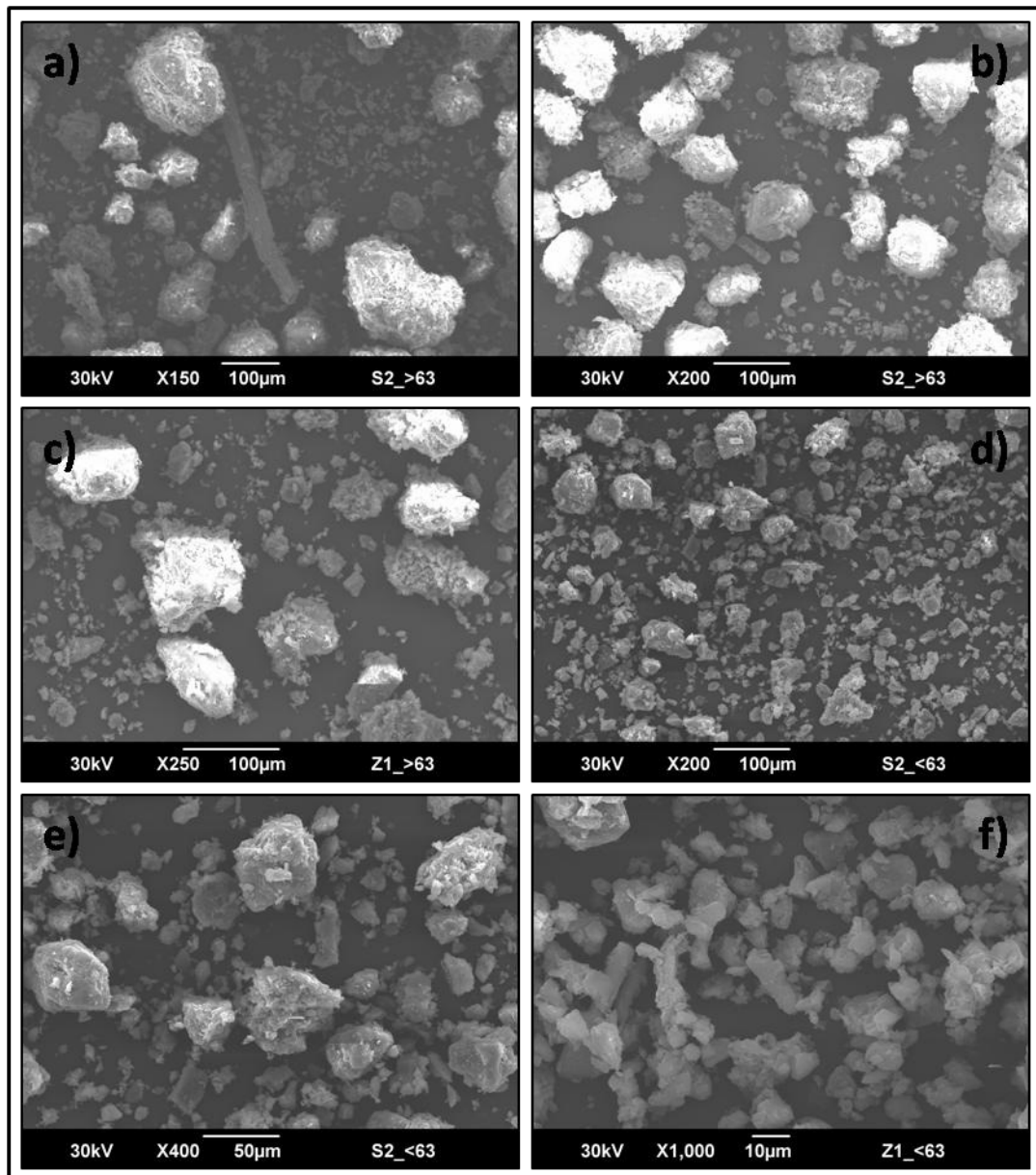
Fig. S 1: Scanning electron micrographs of crushed macro-aggregates (<250 µm). a) fallow 30 yr (pasture) 63–250 µm, b) fallow 30 yr (pasture) 63–250 µm, c) arable 5 yr 63–250 µm, d) fallow 30 yr (pasture) <63 µm, e) fallow 30 yr (pasture) <63 µm, f) arable 5 yr <63 µm.
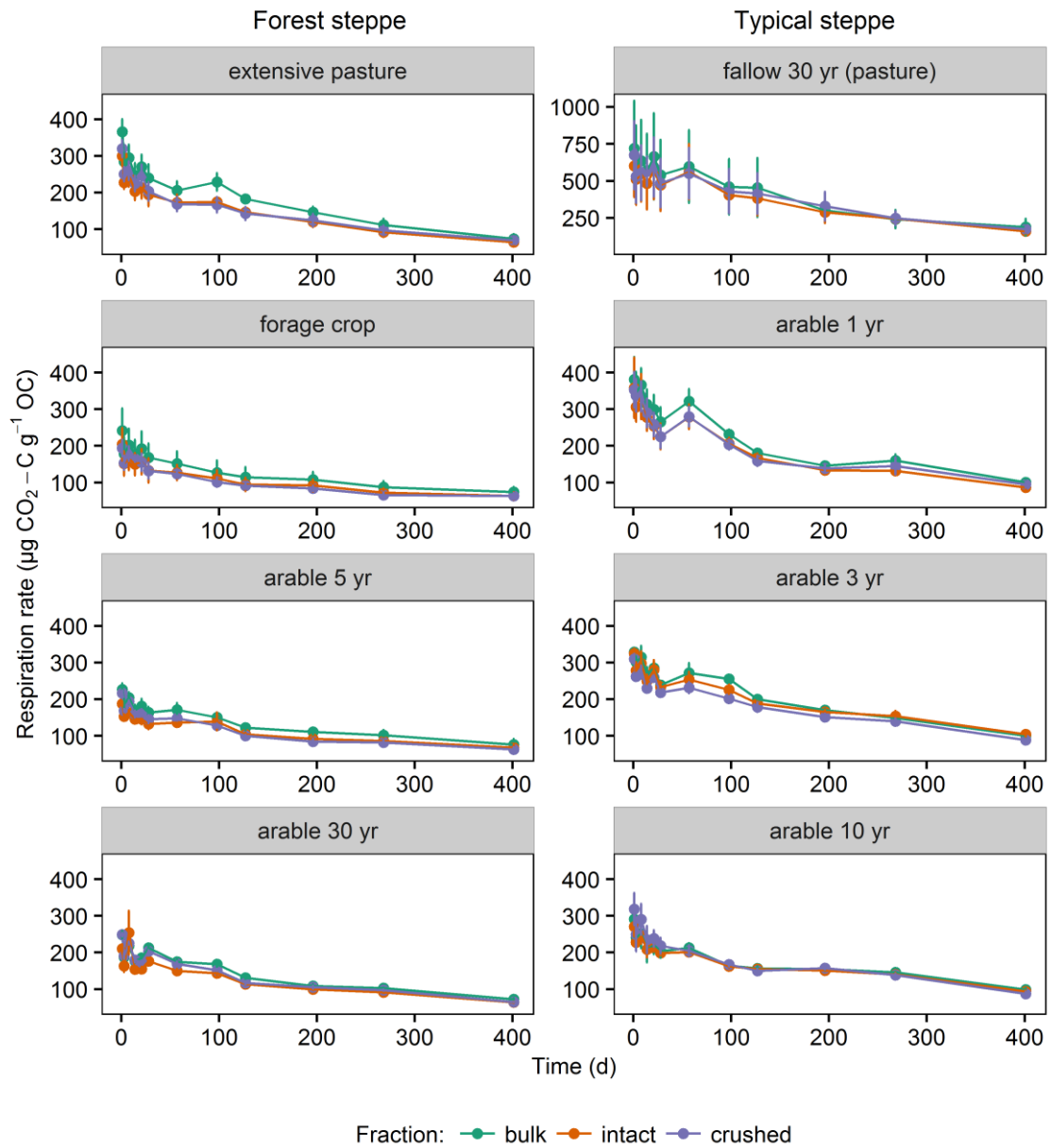
5

Fig. S 2: Time course of respiration rates (µg CO_2-C g^{-1} OC) for eight plots within two steppe types and for the three fractions bulk soil, intact macro-aggregates and crushed macro-aggregates. Shown are arithmetic means ± SE for all 12 time points where CO_2 gas samples were taken. Note the different scale for the fallow 30 yr (pasture).
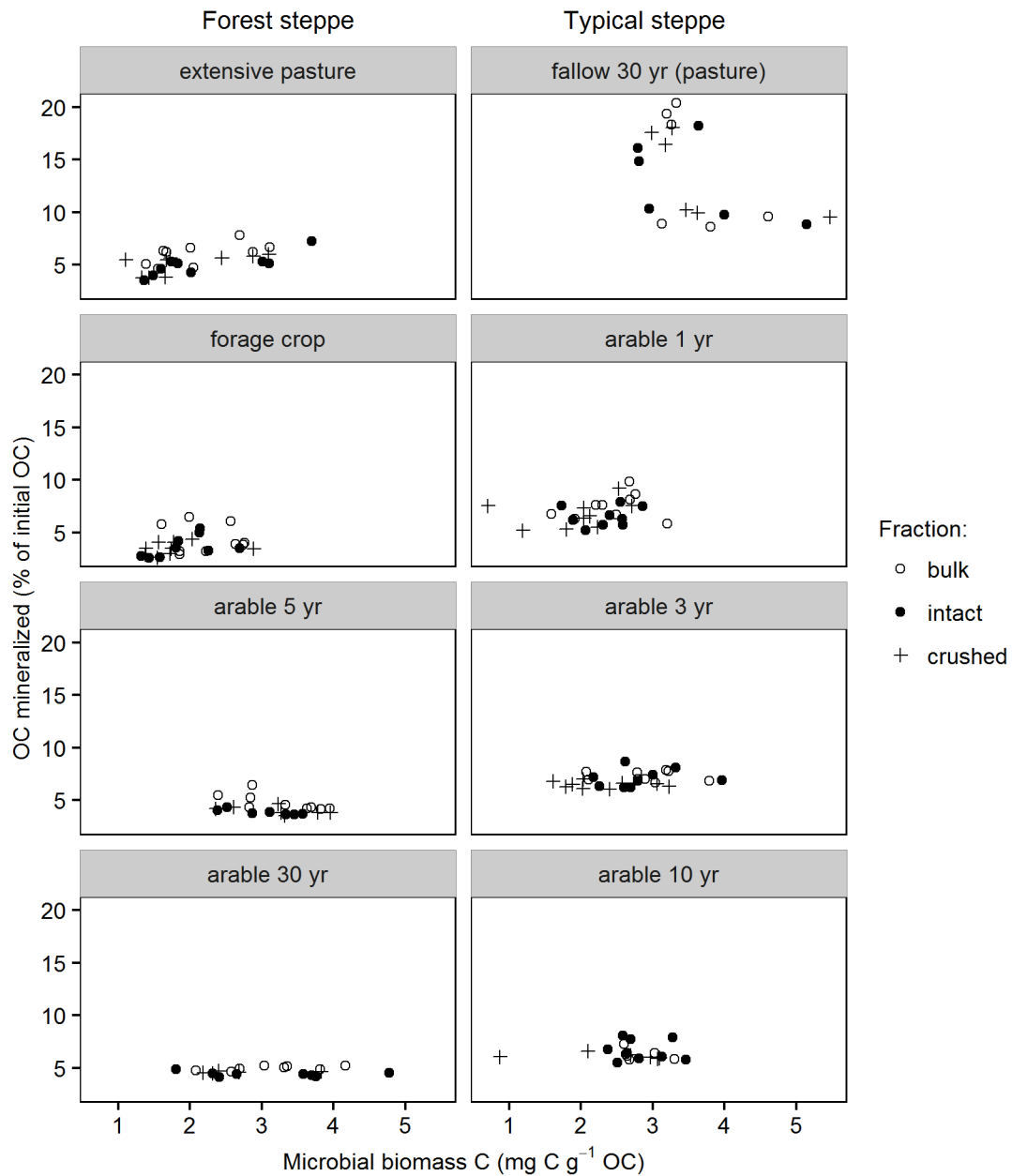
5

Fig. S 3: Mineralized OC (% of initial OC) plotted against the microbial biomass C normalized to total OC (mg C g^{-1} OC) for eight plots within two steppe types and the three fractions bulk soil, intact macro-aggregates, and crushed macro-aggregates.

7

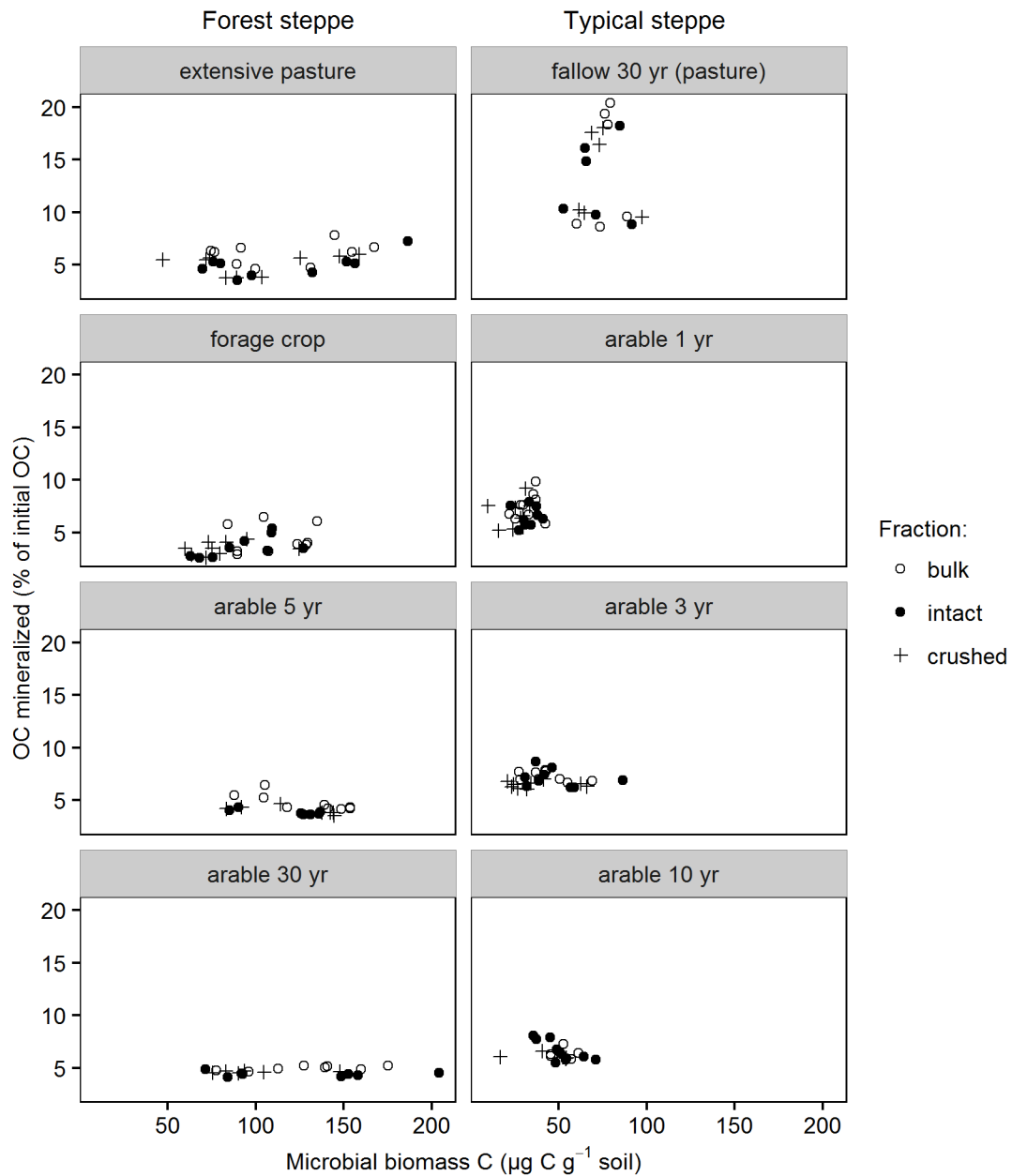**Fig. S 4: Mineralized OC (% of initial OC) plotted against the microbial biomass C per soil mass (µg C g^{-1} soil) for eight plots within two steppe types and the three fractions bulk soil, intact macro-aggregates, and crushed macro-aggregates.**

5

References

Batjes, N. H.: Total carbon and nitrogen in the soils of the world, Eur. J. Soil Sci., 47(2), 151–163, doi:10.1111/j.1365-2389.1996.tb01386.x, 1996.

5   FAO: Lecture notes on the major soils of the world, edited by P. Driessen, J. Deckers, O. Spaargaren, and F. Nachtergaele, World soil Resour. reports, 94, 336, doi:10.1136/gut.27.11.1400-b, 2001.

IUSS Working Group WRB: World reference base for soil resources 2014. International soil classification system for naming soils and creating legends for soil maps, World Soil Resour. Reports No. 106, 1–191, doi:10.1017/S0014479706394902, 2014.

10

4 Study III

Organic matter dynamics along a salinity gradient in Siberian steppe soils

Contribution: I did half of the field work, participated in the laboratory work, collected and analyzed the data, compiled tables and graphs, and wrote the manuscript.

Publication status: published and under review in

Biogeosciences Discussions (2017).

DOI: 10.5194/bg-2017-53

Permission for publication in the dissertation:

Biogeosciences is an open access journal and it is allowed to include the article in a dissertation.

Organic matter dynamics along a salinity gradient in Siberian steppe soils

Norbert Bischoff[1], Robert Mikutta[2], Olga Shibistova[1,3], Reiner Dohrmann[4], Daniel Herdtle[1], Lukas Gerhard[1], Franziska Fritzsche[1], Alexander Puzanov[5], Marina Silanteva[6], Anna
5   Grebennikova[6], Georg Guggenberger[1]

[1]Institute of Soil Science, Leibniz University Hannover, Herrenhäuser Straße 2, 30419 Hannover, Germany
[2]Soil Science and Soil Protection, Martin Luther University Halle-Wittenberg, Von-Seckendorff-Platz 3, 06120 Halle (Saale), Germany
10   [3]VN Sukachev Institute of Forest, Siberian Branch of the Russian Academy of Sciences, Akademgorodok 50, 660036 Krasnoyarsk, Russian Federation
[4]Federal Institute for Geosciences and Natural Resources, Stilleweg 2, 30655 Hannover, Germany
[5]Institute for Water and Environmental Problems, Siberian Branch of the Russian Academy of Sciences, Molodezhnaya Street 1, 656038 Barnaul, Russian Federation
15   [6]Faculty of Biology, Altai State University, Prospekt Lenina 61a, 656049 Barnaul, Russian Federation

Correspondence to: Norbert Bischoff (bischoff@ifbk.uni-hannover.de)

Abstract

Salt-affected soils will become increasingly important in the next decades as arid and semi-arid ecosystems are predicted to expand as a result of climate change. Nevertheless, little is known about organic matter (OM) dynamics in these soils, though OM is largely controlling soil fertility and represents an important C sink. We aimed at investigating OM dynamics along a salinity and sodicity gradient in soils of the south-western Siberian Kulunda steppe (Kastanozem, Non-sodic Solonchak, Sodic Solonchak) by assessing the organic carbon (OC) stocks, the quantity and quality of particulate and mineral-associated OM in terms of non-cellulosic neutral sugar contents and carbon isotopes ($\delta^{13}C$, ^{14}C activity), and the microbial community composition based on phospholipid fatty acid (PLFA) patterns. Our hypotheses were that (i) soil OC stocks decrease along the salinity gradient, (ii) the proportion and stability of particulate OM is larger in salt-affected Solonchaks as compared to non-salt-affected Kastanozems, and (iii) sodicity reduces the proportion and stability of mineral-associated OM. Against our first hypothesis, OC stocks increased along the salinity gradient with most pronounced differences between topsoils. In contrast to our second hypothesis, the proportion of particulate OM was unaffected by salinity, thereby accounting for only <10% in all three soil types, while mineral-associated OM contributed to >90%. Isotopic data ($\delta^{13}C$, ^{14}C activity) and neutral sugars in the OM fractions indicated a comparable degree of OM transformation along the salinity gradient, thus particulate OM was not more persistent under saline conditions. This we attribute to a resilient microbial community composition and function, which was nearly unaffected by salt occurrence, and capable of decomposing OM at a similar rate in salt-affected and non-salt-affected soils. Also our third hypothesis was rejected, as saline-sodic soils contained more than twice as much mineral-bound OC than non-salt-affected soils, what we ascribe to the flocculation of OM and mineral components under higher ionic strength conditions. We conclude that salt-affected soils contribute significantly to the OC storage in the semi-arid soils of the Kulunda steppe while most of the OC is associated to minerals and therefore effectively sequestered in the long-term.

Introduction

Salt-affected soils occur predominantly in arid and semi-arid environments where rainfall is insufficient to leach salts from the soil (Mavi et al., 2012). They form either anthropogenically as a result of agricultural mismanagement or naturally due to the accumulation of salts from mineral weathering, dust deposition,

5   precipitation or capillary rise of shallow groundwater tables (Essington, 2004). According to FAO (2001), salt-affected soils include Solonchaks and Solonetzes. While Solonchaks contain high loads of water-soluble salts, Solonetzes are primarily distinguished by Na^+ as a dominant cation present on the exchange sites and usually a pH > 8.5. This difference in the composition of salts within both soil types leads to contrasting physico-chemical properties. Solonchaks have a compact soil aggregation, whereas soil particles tend to disperse in Solonetzes,

10 causing a poor soil structure and the translocation of clay (lessivation) and organic matter (OM) as well as clogging of pores which results in reduced water infiltration, increased surface run-off, and the risk of erosion (Qadir and Schubert, 2002; Sumner, 1993). Salt-affected soils, i.e. both Solonchaks and Solonetzes, respectively, are harsh environments for plants as high salt contents reduce the osmotic potential and subsequently limit plant water uptake (Läuchli and Grattan, 2007). Nutrient uptake is impeded due to ion competition and the high pH,

15 while the poor soil structure particularly in Solonetzes has adverse effects on soil water balance and plant development (Qadir and Schubert, 2002). As a result, plant residue inputs into the soil are reduced and, thus, lead to small soil OM contents (Wong et al., 2010). However, OM is a key component of soils, being a reservoir for nutrients and determining a soil's agricultural productivity, while, at the same time, it is an important C repository and plays a pivotal role in the course of climate change (Lal, 2004). Particularly by improving soil

20 structure and increasing the selectivity of exchange sites for Ca^{2+}, soil OM can ameliorate sodic soils (Nelson and Oades, 1998; Sumner, 1993).

Independent from soil genesis, salt-affected soils are classified according to their electrical conductivity (EC; in dS m^{-1}) and sodium adsorption ratio (SAR) of the saturated paste extract into saline (EC >4 and SAR <13), sodic (EC <4 and SAR >13), and saline-sodic (EC >4 and SAR >13; U.S. Salinity Laboratory Staff, 1954). Both

25 parameters control the soil structure due to their impact on the dispersion of clay and OM significantly. Numerous studies showed that the desorption of OM from clay particles increases with SAR, while a rise in EC or the proportion of divalent cations counterbalances the dispersing effect of Na^+ by inducing flocculation (Mavi et al., 2012; Nelson and Oades, 1998; Setia et al., 2014). High soil pH is likewise supposed to increase losses of organic C (OC) through solubilization of OM (Pathak and Rao, 1998). Peinemann et al. (2005) concluded that in

30 salt-affected soils mineral-associated OM can be rapidly lost through dispersion and subsequent leaching as dissolved OM, while particulate OM represents a relatively stable fraction as its decomposition is reduced due to an inhibited microbial activity. In line with this, previous work revealed in incubation and field-studies that the microbial decomposition of soil OM is reduced along salinity gradients (Rath and Rousk, 2015; Rietz and Haynes, 2003). However, little is known about microbial functioning in salt-affected soils, and particularly for

35 Solonchaks and Solonetzes, there are so far no studies available that characterized microbial community compositions.

Though, based on conclusions from sorption-desorption experiments, previous studies noted the sensitivity of mineral-organic associations in salt-affected soils, to date, no study quantified the amount and properties of mineral-associated and particulate OM in these soils. This is surprising, as the occurrence of salt-affected soils is

40 predicted to increase as a result of climate change due to enhanced aridity (Amini et al., 2016). To date, these soils cover already an area of 831 Mio. ha worldwide (Martinez-Beltran and Manzur, 2005), of which

Solonchaks and Solonetzes constitute about 260 Mio. ha and 135 Mio. ha, respectively (IUSS Working Group WRB, 2014). Thus, our objectives were to (i) elucidate the effect of salinity and sodicity on soil OC stocks, (ii) determine the quantities and properties of functionally different soil OM fractions (particulate *vs.* mineral-associated OM), and (iii) relate our results to changes of the microbial community composition. We approached this by comparing soil OC stocks, the amount and properties of density-separated OM fractions (contents of hydrolysable non-cellulosic neutral sugars; $\delta^{13}C$ and ^{14}C activity), and the PLFA-based microbial community composition of three soil types representing an increasing impact of salinity and sodicity along a transect in the south-western Siberian Kulunda steppe. Non-cellulosic sugars were chosen as an OM quality parameter, as they enter the soil in large amounts with litter, root residues and plant rhizodeposits as well as by products of microbial and faunal metabolism and represent a major energy source for heterotrophic soil microbial communities (Cheshire, 1979; Gunina and Kuzyakov, 2015). Additionally, soil aggregate stability was determined to assess the effect of salts, particularly Na^+, on the structural stability of the soils. We hypothesized that (i) soil OC stocks decrease along the salinity gradient, because high salinity decreases plant growth and subsequently lowers soil OC inputs, (ii) the proportion and stability of particulate OM is larger in salt-affected soils as compared to non-salt-affected soils since microbial decomposition and transformation of OM is reduced under high salinity levels, and (iii) sodicity reduces the proportion and stability of mineral-associated OM.

Material & Methods

Study site and soil sampling

The study site is located in the south-western Siberian Kulunda steppe which is part of the Altaysky Kray (Russian Federation). The area belongs to the dry steppe type with a mean annual temperature of 2.6 °C and a mean annual precipitation of 285 mm (climate data from "WorldClim" data base; Hijmans et al., 2005). The studied transect (52°3'36.51"N, 79°36'0.71"E) ranged from a lake over a terraced hillslope to about 5 m upslope the lake (Figure 1). The groundwater table varied from ca. 140 cm next to the lake to >300 cm at the highest point of the transect. Three different soil types developed along the transect primarily as function of the groundwater table. At shallow groundwater depth close to the lake, Sodic Solonchaks dominated, while Mollic Solonchaks (non-sodic) prevailed backslope with slightly higher groundwater at about 170–180 cm. Upslope the groundwater table reached >300 cm and capillary rise did not reach the soil surface, thus, Haplic Kastanozems and Calcic Kastanozems occurred which were generally grouped as Kastanozems. A detailed soil type classification according to IUSS Working Group WRB (2014) of the analyzed profiles is given in Table S1. We sampled the soils at plane areas along the terraced slope to avoid the influence of erosion on the soil profiles. Three plots, each with a soil profile down to the groundwater table and locations for plant analyses, were established per soil type; only in the Kastanozems the groundwater was too deep to be reached. Four plots were analyzed on the footslope next to the lake, where site heterogeneity was larger, but one of the four soils was not classified as Sodic Solonchak but as Haplic Solonchak. This soil profile was grouped together with the Mollic Solonchaks since these soils corresponded to a lower level of sodicity and they were referred to as Non-sodic Solonchaks. Therefore, Kastanozems and Sodic Solonchaks were represented by three soil profiles, while Non-sodic Solonchaks were characterized by four soil profiles. Composite soil samples were taken according to generic horizons in the profiles. Plant samples (shoots and roots) were taken within the plots 5 m distant from around each profile for determination of OC, total nitrogen (TN), and $\delta^{13}C$. The above-ground biomass was

4

determined in triplicate around each profile by cutting off plants in a 40 cm x 40 cm square and subsequent drying (70°C) and weighing of plant material. The major plant species are listed in Table 1.

Sample preparation and basic soil analyses

Samples from generic horizons of the profiles were air-dried and sieved to <2 mm. Visible plant materials were removed and big clods were gently broken to pass the sieve. An aliquot of the fine earth fraction was dried at 105°C to determine the residual soil water content. Soil bulk density was determined gravimetrically in triplicate for generic horizons by use of a soil sample ring. Soil pH was measured in a 1 : 2.5 (w : v) soil-to-water suspension after equilibration for one day. Carbonate content was analyzed by the Scheibler volumetric method (Schlichting et al., 1995). The texture of the soils was determined according to the standard sieve-pipette method (DIN ISO 11277, 2002) and the content of oxalate- and dithionite-extractable Fe was analyzed as described in McKeague and Day (1966). Soil aggregate stability was measured based on a method modified from Hartge and Horn (1989) and explained in detail in Bischoff et al. (2016). It was calculated as the difference between the mean weight diameter (MWD) of aggregates of a dry- and a wet-sieving method, expressed as ΔMWD, with a large ΔMWD corresponding to low aggregate stability and a small ΔMWD relating to high aggregate stability.

Soil salinity parameters

The content and composition of water-soluble salts was determined by shaking the soil in a 1 : 5 (w : v) soil-to-water suspension at 15 rpm during 1 h and leaving the sample for one day to reach equilibrium. After measuring the EC the extract was centrifuged at 3,000 g for 15 min and filtered through 0.45-µm syringe filters (Cellulose acetate). An aliquot of the extract was measured for Na^+, K^+, Ca^{2+}, and Mg^{2+} with an inductively coupled plasma optical emission spectrometer (Varian 725-ES; Agilent Technologies, Santa Clara, USA) while another aliquot was analyzed for Cl^-, NO_3^-, and SO_4^{2-} with an ion chromatograph (ICS-90; Dionex Corp., Sunnyvale, USA). The concentrations of Na^+, Ca^{2+}, and Mg^{2+} (mmol l^{-1}) in the extract were used to calculate the SAR according to Eq. (1).

$$SAR = \frac{Na^+}{(Ca^{2+} + Mg^{2+})^{0.5}}$$

(1)

Soil mineralogical composition

X-ray diffractograms of ball-milled <2-mm fractions were recorded with an X'Pert PRO MPD Θ–Θ diffractometer (PANalytical, Almelo, Netherlands) equipped with a Cu anode producing Kα radiation. The powder samples were scanned from 2° to 85° 2Θ with a step size of 0.02° 2Θ and 3 s per step. A subset of samples was evaluated at the micro-scale using a Quanta 600 FEG environmental scanning electron microscope (ESEM; FEI Company, Hillsboro, USA) with an acceleration voltage of 20 keV. As the analysis was carried out in low-vacuum mode (0.6 mbar), sputtering of the samples with gold or carbon was not necessary. The microscope was equipped with an Apollo XL EDX detector (Ametek Inc., Berwyn, USA).

Clay mineralogical analyses were carried out for one representative soil profile of each soil type. Clay fractions (<2 µm) were obtained by pre-treating the soil with acetic acid (removal of carbonates), H_2O_2 (removal of OM), and dithionite-citrate (removal of iron oxides), subsequent separation by sedimentation (Stoke's law) and final Mg^{2+} saturation to cause flocculation and thus easier handling of samples. X-ray diffraction patterns were recorded using the same system and settings as for the powder analyses of bulk soil but with Co-Kα radiation

5

generated at 40 kV and 40 mA. Oriented mounts were prepared on porous ceramic tiles to avoid segregation of fine particles during sedimentation (Dohrmann et al., 2009) and scanned from 2° to 35° 2Θ with a step size of 0.02° 2Θ and 4 s per step. Sample quantity allowed only for two treatments for qualitative analysis: (i) Mg^{2+}, (ii) Mg^{2+} + ethylene glycol. The ethylene glycol treatment was used as it detects expandable clay minerals like smectite, which strongly affect the physical properties of sodic soils.

Determination of organic carbon, $\delta^{13}C$, and total nitrogen

Ball-milled <2-mm fractions were measured for OC and TN as well as for $\delta^{13}C$ via dry combustion in an Elementar vario MICRO cube C/N Analyzer (Elementar Analysensysteme GmbH, Hanau, Germany) coupled to an IsoPrime IRMS (IsoPrime Ltd, Cheadle Hulme, UK) after removing inorganic C by fumigation with HCl and subsequent neutralization over NaOH pellets (modified from Walthert et al., 2010). The measured $\delta^{13}C$ values were corrected by calculating response factors from standard compounds ($CaCO_3$, cellulose, caffein) and expressed in the delta notation related to the Vienna Peedee-Belemnite-Standard (0‰). The complete removal of inorganic C from all samples was confirmed by $\delta^{13}C$ values which are in the typical range of soil OM (-22.5‰ to -28.1‰).

Density fractionation and ^{14}C analysis

Density fractionation (modified after Golchin et al., 1994) separated the soil into a light fraction (LF), containing mostly particulate OM, and a heavy fraction (HF), consisting of mineral-associated OM as well as mineral components free of OM. As particulate OM contents are mostly very low in the subsoil, we fractionated the soil only until the first C horizon of each profile. In brief, 25g soil was weighted in duplicate into beakers and 125ml sodium polytungstate (SPT; ρ = 1.6 g cm^{-3}) was added, gently stirred with a glass rod and ultra sonification was applied with an energy input of 60 J ml^{-1}during 8 min to break down aggregates. After centrifugation at 3,000 g for 20 min the LF was separated from the HF by decanting the floating LF on polyethersulfone filters and repeating the procedure if the separation between both fractions was insufficient. LF remaining on the filter was washed with deionized water to remove residual SPT until the washing solution had an EC <60 µS cm^{-1}. The HF remaining in the beaker was washed with deionized water until the EC of the washing solution was <100 µS cm^{-1}, but at maximum four times in the salt-affected soils, as no residual SPT was detected afterwards by ESEM–EDX analysis, which was carried out with a Quanta 200 FEG environmental scanning electron microscope (FEI Company, Hillsboro, USA) coupled to an XL–30 EDX detector (Ametek Inc, Berwyn, USA). The washing solutions of both LF and HF, respectively, were collected, filtered through 0.45-µm syringe filters (PVDF), and measured for non-purgeable OC with a LiquiTOC (Elementar Analysensysteme GmbH, Hanau, Germany) to account for the loss of OC during washing of the samples (mobilized OC, MobC; Gentsch et al., 2015). The LF and HF were freeze-dried, weighted, homogenized in a mortar, and subsequently measured for OC and TN as well as $\delta^{13}C$ as described in Sect. 2.5, after removal of inorganic C. The mobilized OC was added to the OC content of the LF or HF, respectively.

Three representative soil profiles were selected, one per soil type, for analysis of ^{14}C activities of OM fractions at the Max Planck Institute for Biogeochemistry Jena (Germany). Inorganic C was removed by 2M HCl until pH remained <3.5 and samples were subsequently neutralized with 2M NaOH to pH 6. After freeze-drying ^{14}C analysis was performed with a 3MV Tandetron^{TM} AMS ^{14}C system (Steinhof et al., 2011) and ^{14}C isotope

activities were converted to percent modern carbon (pMC) according to Steinhof (2013), while pMC was defined according to Stuiver and Polach (1977), see Eq. (2):

$$pMC = \frac{A_{SN}}{A_{abs}} \times 100\% \tag{2}$$

where A_{SN} is the normalized sample activity and A_{abs} corresponds to the activity of the absolute international standard; both activities were background-corrected and $\delta^{13}C$-normalized. OxCal 4.2 software (University of Oxford) was used to calculate conventional ^{14}C ages by selecting the IntCal13 calibration curve (Reimer et al., 2013), if pMC was <100%, and the calibration curve from Hua et al. (2013), if pMC was >100%.

Biomarker analyses

Non-cellulosic neutral sugars

Non-cellulosic neutral sugars were analyzed in the LF and HF from generic horizons of each soil profile. In the LF neutral sugars were only analyzed in some of the topmost horizons, as its content was too low in most samples to provide sufficient material. Additionally, neutral sugars were determined in plant material (shoots and roots). Neutral sugars were analyzed slightly modified according to Rumpel and Dignac (2006), including the EDTA purification step from Eder et al. (2010). In brief, 600mg of HF and 50mg of LF or plant material was hydrolyzed in 4M trifluoroacetic acid (TFA) at 105°C during 4 h after 1.5ml myo-inositol was added as an internal standard. After cooling to room temperature the extract was filtered through glassfiber filters (Whatman™ GF6) and TFA was removed in a rotary evaporator. The samples were redissolved in ultrapure water and the pH was adjusted to 4–5 by adding NH_3. Ferric Fe was complexed by adding 4ml EDTA and incubating the samples in the dark during 10min. From now on darkened glassware was used to prevent photolysis of Fe(III) ligand complexes. After freeze-drying and adding two drops of NH_3 the reduction of aldoses to their corresponding alditols (derivatization) was performed at 40°C during 1.5 h with $NaBH_4$ dissolved in dimethyl sulfoxide. Acetylation was carried out by adding 2ml acetic anhydride and 0.2ml glacial acetic acid, thereby using methylimidazole as a catalyst. Ice-cold deionised water was added after 10 min to stop the reaction. Sugar monomers were extracted by liquid-liquid extraction with dichloromethane and subsequently measured by gas chromatography on a 7890A GC system (Agilent Technologies, Santa Clara, USA) equipped with a SGE forte GC capillary column (0.25mm diameter and 0.25µm film thickness; SGE Analytical Science, Melbourne, Australia) and a flame ionization detector, using He as a carrier gas. External standards were used to detect eight different sugars: arabinose, xylose and ribose (pentoses), galactose, glucose and mannose (hexoses), and fucose and rhamnose (desoxysugars).

Phospholipid fatty acids

Directly after sampling, sieving to <2 mm and removing visible plant materials, 1.0–1.5g field-moist soil was weighted into cryovials and 3ml RNAlater® was added to prevent sample degradation (Schnecker et al., 2012). An aliquot was dried at 105°C to determine the soil water content. The cryovials were kept cool until they were frozen to −20°C within 72 h. For PLFA analysis we used a modified method from Gunina et al. (2014). Briefly, samples were transferred from cryovials into test tubes and washed with ultrapure water to remove residual RNAlater®. Lipids were extracted twice with a chloroform-methanol-citrate buffer (1:2:0.8 v/v/v) and separated into glycolipids, neutral lipids, and phospholipids by solid phase extraction with activated Silica gel (Sigma Aldrich, pore size 60Å, 70–230 mesh). Phospholipids were derivatized into fatty acid methyl esters (FAME)

7

with 0.5M NaOH dissolved in methanol and with BF$_3$ as catalyst. FAME were analyzed with a 7890A GC system (Agilent Technologies, Santa Clara, USA) equipped with a 60m Zebron ZB-5MSi capillary GC column (0.25mm diameter and 0.25µm film thickness; Phenomenex, Torrance, USA) and a flame ionization detector, using He as a carrier gas. As an internal standard we used nonadecanoic acid (FA 19:0) and 17 fatty acids were used as external standards. Peak identification of the internal standard turned out as problematic in the salt-affected topsoils. Therefore we could not reliably quantify individual PLFA but only their relative proportion in the sample. As a result the sum of all PLFA was not used as a proxy of the microbial biomass contents but PLFA were used to characterize the composition of functional microbial groups. We applied a principal components analysis (PCA) on the relative distribution of all 17 PLFA to identify clusters of correlated PLFA, which presumably derive from identical microbial functional groups. The assignment of individual PLFA to certain microbial groups based on the PCA was in agreement with the literature (Frostegård et al., 2011; Olsson, 1999; Ruess and Chamberlain, 2010; Zelles, 1999). Thus, the following PLFA were used to distinguish functional microbial groups: 18:2ω6,9 and 18:1ω9c as marker for saprophytic fungi (SAP), 16:1ω5c to identify arbuscular mycorrhizal fungi (AMF), i15:0, a15:0, i16:0, i17:0 and a17:0 were related to gram-positive bacteria (Gram+), 10Me16:0 characterized actinomycetes (Actino), 16:1ω7c and 18:1ω7c identified gram-negative bacteria (Gram–), and 14:0, 15:0, 17:0 and 18:0 related to unspecific bacteria (UnspBact). The PLFA Cy19:0 and 20:4ω6c were not used as markers for microbial groups as they hardly reached the detection limit and were sometimes difficult to distinguish from other unspecific peaks in the gas chromatogram.

Calculation of organic carbon stocks

Organic C stocks (Mg ha^{-1}) were calculated according to Poeplau & Don (2013) for all horizons and the entire soil profile as well as until 1m depth using Eq. (3):

$$OCstock = \sum_{i=1}^{n} \frac{FSM_i}{V_i} \times C_i \times D_i \tag{3}$$

where *n* is the number of horizons, *FSM* is the fine-earth soil mass (g), *V* is the volume (cm^3), C is the OC content (% of soil mass) and *D* is the length of the horizon (cm).

Statistical analyses

Data analysis was performed in R, version 3.2.5 (R Core Team, 2016). From replicated measurements we calculated arithmetic means and standard errors. To test for the effect of soil type on above-ground plant biomass a linear mixed effects model was fitted (package lme4; Bates et al., 2012). We accounted for the nested structure of sampling, i.e. the soil type was used as fixed effect while the soil profiles (of each soil type) were included as random effects. Residuals and random effect estimates of the fitted model were visually assessed by Q-Q-normal plots but no deviations from normality were observed. The difference of the response variable between the soil types was tested based on the linear mixed effects model fit, including corrections for multiple comparisons (analogous to the Tukey test), with Satterthwaite degrees of freedom, on the basis of the R packages lsmeans (Lenth and Herve, 2015), lmerTest (Kuznetsova et al., 2015), and multcomp (Hothorn et al., 2008). Soil sample related parameters were analyzed descriptively, as their sample size was only 3–4 per soil type, which was insufficient for statistical hypothesis testing. Analysis of data from PLFA and neutral sugars involved the consideration of several response variables which was done by PCA, thereby adding confidence regions (68%) for the group centroids of the analyzed factor variables. Figure 1 was drawn in Inkscape, while the other graphs were generated using ggplot2 (Wickham, 2009).

8

Results

Basic soil and site properties

The soil moisture during sampling (% of dry weight) was very small in the Kastanozems (3.6–4.5%) and larger in the salt-affected soils with shallow groundwater table (Non-sodic Solonchaks: 14.9–20.5%, Sodic Solonchaks: 16.4–30.6%; Table 2). The pH in the Kastanozems increased from about 7 in the topsoil to 9 in the subsoil, while the Solonchaks revealed a nearly constant pH throughout the soil profile between 8.5 and 9. While Kastanozems had no carbonates in the topsoil, the carbonate content peaked in the Ck horizon with 51 ± 12 mg g^{-1} (Table 2). The salt-affected soils exhibited larger carbonate contents, between 53 ± 16 mg g^{-1} and 152 ± 34 mg g^{-1} in the Non-sodic Solonchaks and 115 ± 49 mg g^{-1} and 264 ± 22 mg g^{-1} in the Sodic Solonchaks. The aggregate stability was larger in Kastanozems and Sodic Solonchaks (ΔMWD: 0.41 ± 0.06 mm and 0.33 ± 0.03 mm, respectively) than in Non-sodic Solonchaks (1.02 ± 0.29 mm; Table 2). The Kastanozems consisted mostly of sandy loam, while the Solonchaks were more loamy with larger clay and silt contents. Oxalate- and dithionite-extractable Fe was consistently low in all three soil types (<0.4 mg g^{-1}Fe$_O$, <5 mg g^{-1}Fe$_D$; Table 2).

Soil salinity parameters

The EC$_{1:5}$ was small (<250 μS cm^{-1}) in the Kastanozems with a slight increase from top- to subsoil, while the largest EC$_{1:5}$ in the Solonchaks was found in the topsoil (Table 2). In the Non-sodic Solonchaks the EC$_{1:5}$ decreased from 3416 ± 1053 μS cm^{-1} in the topsoil to 796 ± 333 μS cm^{-1} in the subsoil, while the Sodic Solonchaks had the largest EC$_{1:5}$ with 5350 ± 1476 μS cm^{-1} in the topsoil and the smallest EC$_{1:5}$ with 1093 ± 702 μS cm^{-1} in the subsoil. The SAR$_{1:5}$ revealed a similar pattern, with small SAR$_{1:5}$ (<2) in the Kastanozems and larger values in the Solonchaks (Table 2). In the Non-sodic Solonchaks the SAR$_{1:5}$ dropped from 9.6 ± 2.2 in the topsoil to 3.9 ± 1.0 in the subsoil, while Sodic Solonchaks had the largest SAR$_{1:5}$ with 36.0 ± 10.4 in the topsoil and 8.0 ± 4.6 in the subsoil. The composition of water-soluble anions and cations was different in the two salt-affected soils (Figure S1). While the Non-sodic Solonchaks had an almost balanced concentration of SO_4^{2-} and Cl^- on the one hand, and Na^+, Ca^{2+} and Mg^{2+} on the other hand, the Sodic Solonchaks were dominated by SO_4^{2-} and Na^+, with smaller quantities of Cl^-.

Soil mineralogical composition

The three soil types had a quite homogenous mineralogical composition, dominated by quartz and feldspars as well as calcite and dolomite in the carbonate-rich horizons, whereas almost all samples showed small quantities of amphibole and muscovite (Figure S2). In the Solonchaks also gypsum was present. Calcite and dolomite XRD peaks were very broad, peak broadening is related to very fine crystallite sizes. The clay fraction showed small amounts of illite, kaolinite, and chlorite, while smectites were partially present in the subsoil, and in the Sodic Solonchak also in the topsoil. In the smectite-rich horizons, the quantities of smectite and illite exceeded those of chlorite and kaolinite significantly (Figure S3). In the Solonchaks, the quantities of water-soluble salts were small when related to the bulk soil. Mass balance calculations (data not shown) and analyses by ESEM–EDX (Figure S4) revealed that water-soluble salts mostly consisted of thenardite (α-Na$_2$SO$_4$) and halite (NaCl), but also bischofite (MgCl$_2 \cdot$ 6H$_2$O) could be present.

9

Soil organic carbon stocks

Soil OC stocks increased with salinity and sodicity from Kastanozems over Non-sodic Solonchaks to Sodic Solonchaks (Figure 2). Differences were most pronounced in the topsoils, while subsoil OC stocks were similar between the soil types. Down to a depth of 100 cm Kastanozems had 70.9 ± 2.8 Mg OC ha^{-1}, Non-sodic Solonchaks 94.2 ± 6.9 Mg OC ha^{-1} and Sodic Solonchaks 129.5 ± 25.6 Mg OC ha^{-1}. Thus, OC stocks in Non-sodic Solonchaks were 32.8 ± 9.7% larger than in Kastanozems and OC stocks of Sodic Solonchaks exceeded those of Kastanozems even by 82.6 ± 36.1%. The C : N ratios were comparable along the salinity gradient and ranged from about 10 in the topsoil to 5–8 in the subsoil (Table S2).

Soil organic matter fractions

Organic carbon contents and isotopic composition

All three soil types were dominated by HF–OC with >90% of bulk OC, while LF–OC accounted for <10% (Table 3). The proportion of HF–OC revealed no clear depth gradient within the soil profiles. The OC content of the HF increased in A horizons with salinity and sodicity from Kastanozems (7.7 ± 0.3 mg g^{-1}) to Non-sodic Solonchaks (18.3 ± 2.7 mg g^{-1}) to Sodic Solonchaks (19.3 ± 5.0 mg g^{-1}), while OC contents were similar in the subsoil (Table 3). OC contents in the LF were smaller in the Kastanozems (120–219 mg OC g^{-1}) than in Non-sodic Solonchaks (197–279 mg OC g^{-1}) and Sodic Solonchaks (247–265 mg OC g^{-1}; Table 3). Kastanozems and Non-sodic Solonchaks had the largest LF-OC contents in the subsoil but LF-OC contents were equal over depth in the Sodic Solonchaks. HF material was enriched in δ^{13}C as compared to LF material (Table 3). In the LF δ^{13}C ratios ranged from -27.5‰ to -26.4‰ (Kastanozems), -27.0‰ to -28.1‰ (Non-sodic Solonchaks) and -24.3‰ to -26.9‰ (Sodic Solonchaks). Remarkably, the δ^{13}C ratios in the LF decreased from top- to subsoil in the Solonchaks, while the Kastanozems revealed a typical increase of δ^{13}C ratios from top- to subsoil. The δ^{13}C ratios of the LF were similar to the root signals of the plants, while no relation to the shoot signals was apparent (Figure 4). Ratios of δ^{13}C in the HF were comparable between the three soil types and ranged from -23.8‰ to -23.0‰ in the Kastanozems, from -23.3‰ to -22.8‰ in the Non-sodic Solonchaks and from -23.4‰ to -22.5‰ in the Sodic Solonchaks (Table 3). As residual SPT had to be removed during density fractionation for subsequent determination of OC parameters, all samples were washed with deionized water (see Sect. 2.6). This resulted in a loss of HF material. About 8–29 mg HF g^{-1} soil was lost in Kastanozems, while the loss was larger in salt-affected soils due to the high solubility of salts and accounted for 61–86 mg HF g^{-1} soil in Non-sodic Solonchaks and 46–76 mg HF g^{-1} soil in Sodic Solonchaks, with larger losses in samples with high EC (Table 3). Despite larger HF losses were observed in Solonchaks, the percentage of MobC related to bulk OC was small in these soils (maximally 9.4 ± 1.6%), while Kastanozems had larger proportions of MobC (15.6 ± 0.5% to 45.7 ± 12.0%). This indicates that the water-soluble salts in the salt-affected soils were mostly not associated with OC. The quantities of MobC from the LF were larger in salt-affected soils and accounted for up to 258 mg OC g^{-1} LF, but maximally 3.4% of bulk OC in all three soil types (Table 3). The proportion of MobC increased with depth in both LF and HF, respectively. The ^{14}C activities in the LF were similar in the Kastanozem and the Sodic Solonchak and amounted mostly >100 pMC (Table 3), corresponding to recent C with ^{14}C ages of maximally 60 years B.P. In the Non-sodic Solonchak the ^{14}C activity was >100 pMC in the topmost horizon (Az1) but lower in the underlying horizons, i.e. 91.67 pMC (ca. 730 years B.P.) in the Az2 horizon and 93.86 pMC (ca. 580 years B.P.) in the Bkz horizon, respectively. This untypically high age of LF material indicated a possible

10

contamination with HF material. The ^{14}C activities in the HF were smaller than in the LF, corresponding to higher ^{14}C ages, and no trend related to the three soil types was apparent. Remarkably, ^{14}C activities increased from ca. 30 cm depth to 50–60 cm depth after a typical decrease from the topsoil. The ^{14}C activities in the HF corresponded to ^{14}C ages of 150–950 years B.P. in the topsoil horizons and 1200–2900 years B.P. in the underlying horizons, while the highest ^{14}C age occurred in the comparatively deep Cz horizon (ca. 90 cm) of the Non-sodic Solonchak with 4600 years B.P.

Non-cellulosic neutral sugars

The neutral sugar content of the LF from the topmost horizons was similar in the Kastanozems and the Non-sodic Solonchaks with 47 ± 5 mg g^{-1} and 46 mg g^{-1}, respectively, while Sodic Solonchaks contained more neutral sugars (105 ± 27 mg g^{-1}; Table 3). Related to the OC content, sugar contents were comparable between all soil types and ranged from 328–410 mg g^{-1} OC. The HF contained less sugars than the LF, thereby sugar contents decreased from top- to subsoil according to the decrease of OC contents (Table 3). In topsoils sugar contents of the HF increased from Kastanozems (1.0 ± 0.2 mg g^{-1}) over Non-sodic Solonchaks (3.1 ± 0.6 mg g^{-1}) to Sodic Solonchaks (5.7 ± 0.8 mg g-1), while sugar contents were similar in the subsoil. Based on the OC content, sugar contents were similar in the Kastanozems and Non-sodic Solonchaks and ranged between 136–172 mg g^{-1} OC, with no clear depth gradient. Sodic Solonchaks contained more sugar per g OC than the other two soil types, with 322 ± 61 mg g^{-1} OC in the topsoil and smaller sugar contents in the subsoil (165 mg sugar g^{-1} OC). The averaged proportion of each sugar in the total sugars was as following: xylose ($27 \pm 8\%$), glucose ($20 \pm 2\%$), arabinose ($19 \pm 2\%$), galactose ($18 \pm 3\%$), mannose ($7 \pm 3\%$), rhamnose ($5 \pm 1\%$), fucose ($3 \pm 1\%$), and ribose ($1 \pm 1\%$; data not shown).

The PCA of neutral sugars from plants, LF and HF material revealed two significant components (eigenvalue > 1), the first component (PC1) with 54.9% explained variance and the second component (PC2) related to 18.7% explained variance (Figure 5). The composition of neutral sugars was different between plants, LF material and HF material, while differences between the three soil types were smaller. Plants of all soil types were enriched in xylose and those of salt-affected soils also in arabinose, while HF material of all soils was augmented with mannose, galactose, fucose, ribose, and rhamnose. Differences between soil types were apparent with respect to arabinose and glucose. In the Kastanozems OM in the LF and HF became enriched in arabinose during decomposition of plant material, while the opposite was observed in the salt-affected soils (see also Figure S5). The relative proportion of glucose remained similar in the Kastanozems but increased in the salt-affected soils in the course of decomposition (see also Figure S6). However, on the whole, neutral sugars in LF but also HF material were similarly altered in all three soil types with respect to their initial composition in the plant tissue, as indicated by a comparable shift of the three fractions in all soil types along the first axis in the biplot, suggesting a comparable degree of soil OM alteration between the soil types.

Phospholipid fatty acids

The relative contribution of PLFA observed within the PLFA profiles was as follows: PLFA from unspecific bacteria ($36.7 \pm 2.2\%$), Gram+ ($25.6 \pm 0.7\%$), Gram– ($11.9 \pm 1.3\%$), SAP ($11.3 \pm 0.9\%$), AMF ($8.4 \pm 1.8\%$) and from actinomycetes ($6.1 \pm 0.6\%$). Thus, bacterial PLFA constituted $80.4 \pm 1.1\%$ while fungal PLFA represented $19.6 \pm 1.1\%$ of the analyzed fatty acids. The PCA of the PLFA-based microbial groups extracted two significant components (eigenvalue >1) and showed a clear differentiation between bacterial and fungal PLFA (Figure 6),

11

the former stretching along the first component (PC1) and the latter correlating with the second component (PC2). Accordingly, bacterial PLFA explained 57.8% of the variability of total PLFA, while fungal PLFA corresponded to 22.0% of the total variability. PLFA of Gram+, Gram– and actinomycetes were positively correlated with each other, but had a negative correlation to the group of unspecific PLFA. Among the fungal

5   PLFA, those of AMF correlated negatively to those of SAP. Differences in the microbial community composition existed between soil horizons and were largely explained by the variability of bacterial PLFA, with a larger abundance of Gram+, Gram– and actinomycetes in topsoil horizons and a larger abundance of unspecific PLFA in the subsoil (Figure 6). Changes of the microbial community composition between the three soil types were less pronounced and mostly due to a larger variability of fungal PLFA in the Solonchaks as compared to

10   the Kastanozems, whereas the composition of bacterial PLFA was similar between all soils. However, the fungi : bacteria ratio was rather constant between the three soil types and amounted to 0.22 ± 0.03 in Kastanozems, 0.28 ± 0.05 in Non-sodic Solonchaks, and 0.27 ± 0.03 in Sodic Solonchaks, with slightly larger fungi : bacteria ratios in the subsoils of the Solonchaks (data not shown).

Discussion

15   **Soil OC stocks along the salinity gradient**

Salt-affected soils, such as Solonchaks, are normally characterized by poor plant growth resulting in small soil OC inputs and subsequently low soil OC stocks (Wong et al., 2010). Muñoz-Rojas et al. (2012), for example, reported soil OC stocks in Solonchaks of southern Spain in 0–75cm depth of 53.6 Mg ha^{-1} (coefficient of variation (CV): 60%) under shrub and/or herbaceous vegetation. Batjes (1996) calculated in the framework of a

20   global meta-analysis average soil OC stocks of Solonchaks of 42 Mg ha^{-1} (CV: 67%) in 0–100 cm depth, while he noted that particularly Mollic Solonchaks had much larger soil OC stocks of 101 Mg ha^{-1} (CV: 44%). Kastanozems, on the other hand, contained on average 96 Mg ha^{-1} (CV: 50%) in the first meter, at which Haplic Kastanozems had soil OC stocks above that average of 138 Mg ha^{-1} (CV: 44%; Batjes, 1996). Based on data from Bischoff et al. (2016), we calculated soil OC stocks in Kastanozems of the dry steppe type of the Kulunda

25   steppe down to 60 cm, which accounted for 110 ± 6 Mg ha^{-1}. All of the previously published data confirm that salt-affected soils like Solonchaks have normally smaller OC stocks than the non-salt-affected Kastanozems. Contrary, in our study, salt-affected soils had larger OC stocks as compared to the nearby Kastanozems. With average OC stocks of 70.9 ± 2.8 Mg OC ha^{-1} in 0–100 cm depth of the Kastanozems, the values were clearly below those observed by Batjes (1996) and calculated from Bischoff et al. (2016). On the other hand, average

30   OC stocks of 94.2 ± 6.9 Mg OC ha^{-1} and 129.5 ± 25.6 Mg OC ha^{-1} in 0–100 cm of the Non-sodic Solonchaks and Sodic Solonchaks, respectively, were clearly above the values reported by Batjes (1996) and Muñoz-Rojas et al. (2012). Larger OC stocks in salt-affected soils than in Kastanozems are also in contrast to earlier work which found a negative effect of salinity on soil OC stocks (reviewed by Wong et al., 2010). Possible reasons for the observed differences are climatic variations between the studies (strong aridity in the Spanish Solonchaks from

35   Muñoz-Rojas et al., 2012) or alterations in soil texture (finer textured Kastanozems in the study from Bischoff et al., 2016) which may eventually change the soil water balance and thus plant growth and soil OC inputs. Moreover, during sampling we observed very dry conditions in the Kastanozems (only 4 ± 0.3% soil water related to dry soil mass), while the Solonchaks were generally wetter due to their shallow groundwater table (15–30% soil water, Table 2), such that in these soils water stress was mostly related to a small osmotic potential.

12

Overall, the water stress in the three soil types could have been similar, either as a result of matric stress or osmotic stress, leading to comparable moisture conditions for plant growth. Accordingly and in contrast to previous work, along our transect plant growth (as measured by above-ground biomass) was not reduced under high salinity (Table 1). As this was discussed as a prerequisite of reduced OC stocks at elevated salinity (Wong et al., 2010), it can be one reason why our study revealed different results. As the δ^{13}C ratios suggested that soil OM was mostly root-derived in the studied soils (Figure 4), one might argue that above-ground biomass is a poor proxy for soil OC input. However, under the assumption that root residue inputs are correlated with the above-ground biomass (evidence is given by Titlyanova et al. (1999) who observed significant correlations ($p <$ 0.01, R > 0.5) between the above-ground and below-ground biomass of typical plants in Siberian grasslands), we might conclude that both, above-ground and below-ground soil OC inputs, were comparable between all three soil types.

Moreover, Wong et al. (2010) argued that small OC stocks in salt-affected soils can also be the result of erosion-induced OC losses, as particularly sodic soils are prone to erosion. Since we paid particular attention to the fact that all soils were not affected by erosion, we can rule out erosion as a factor that modified OC stocks in our study. Summing up, our first hypothesis has to be rejected since soil OC stocks have not decreased along the salinity gradient in contrast to previous observations from comparable soils (Figure 2). As the quantity of plant biomass was not reduced under high salinity, we consider this as main reason for the large OC stocks in salt-affected soils.

Partitioning and composition of soil OM in different functional OM fractions

Considering processes of soil OC stabilization, semi-arid soils should have large proportions of particulate OC, as the formation of stable mineral-organic associations is attenuated due to low water availability and a high soil pH (Kleber et al., 2015). However, in the semi-arid soils of the studied transect particulate OC contributed <10% of bulk OC, while mineral-bound OC accounted for >90% (Table 3). This contrasts observations from steppe soils (mostly Chernozems) of European Russia (Breulmann et al., 2014; Kalinina et al., 2011), Canada (Plante et al., 2010), or China (Steffens et al., 2010), where particulate OC represented >20% of bulk OC. Nevertheless, our results are in line with Bischoff et al. (2016) who reported that maximally 10% of OC was present in particulate OM in Chernozems and Kastanozems of the Kulunda steppe. Thus, we support previous observations from this region and conclude that mineral-bound OM is the dominant OM fraction in both, salt- and non-salt-affected soils of the studied region.

Against our second hypothesis, salt-affected soils contained similar proportions of particulate OC like non-salt-affected soils, with 4–8% particulate OC in all three soil types (Table 3). Comparable ^{14}C activities in the LF of the three soil types (small ^{14}C activities in the Non-sodic Solonchak were probably due to a contamination with HF material) indicated a similar turnover of particulate OM, thus contradicting our hypothesis of increased stabilization of particulate OM under high salinity levels. Peinemann et al. (2005) concluded, based on OC determinations in particle-size separates and analyses of lignin components along a salinity gradient in the Argentinian Pampa, that particulate OM is a relatively stable fraction in salt-affected soils due to a reduced microbial transformation of the plant-derived residue inputs. This is not corroborated by our results. The isotopic C composition (^{14}C activity, δ^{13}C) and the composition of neutral sugars suggest a comparable alteration of OM (i.e. degree of OM decomposition) between the three soil types (Figure 3-5). Furthermore, Peinemann et al. (2005) supposed that mineral-bound OM is relatively susceptible to losses in salt-affected soils due to weak

13

chemical bonding and subsequently weak OM stabilization. Against our third hypothesis, the OC content of the HF of the salt-affected soils was more than twice as large as of the non-salt-affected Kastanozems (Table 3). Moreover, during washing of the density-separates (SPT removal) relatively less OC was mobilized from the HF of the salt-affected soils (3–10% MobC) than from the HF of the Kastanozems (16–46% MobC, Table 3), suggesting a lower chemical stabilization of mineral-bound OM in the non-salt-affected soils.

We explain the large contents of mineral-associated OC under high salinity levels by consideration of basic chemical principles. According to Sumner (1993), dispersion of clay minerals is only possible below their critical flocculation concentration (CFC). This concept relates the dispersive effect of Na^+ on the soil structure to the corresponding salt concentration of the soil solution (Rengasamy et al. 1984; Sumner et al. 1998). The authors classified soils into *flocculated*, *potentially dispersive* and *dispersive* depending on the EC and SAR of the soil water extract. Sumner et al. (1998) classified soils with large proportions of non-swelling illitic clays, while Rengasamy et al. (1984) considered soils with swelling 2:1 clays, similar to the smectite-rich soils of our study. According to their classification, all of the salt-affected soils of our study fall into the category *flocculated*; even A horizons of the Sodic Solonchaks with an average SAR of 36 ± 10 remain flocculated, presumably due to the high electrolyte concentration as indicated by a large EC of 5350 ± 1476 µS cm^{-1} (Table 2). This is underpinned by the large aggregate stability of the Sodic Solonchaks (Table 2) and the lack of clay lessivation or OM translocation, processes for which the dispersion of clays and OM is one prerequisite. Similarly, Setia et al. (2013, 2014) confirmed that the dispersive effect of Na^+ on OM and mineral components is only evident at low electrolyte concentrations, particularly at low concentrations of divalent cations like Ca^{2+}. Nelson and Oades (1998) showed that the solubility of Na^+–coated OM is larger than that of OM coated with Ca^{2+}. Thus, particularly in the Non-sodic Solonchaks where Ca^{2+} is a dominant cation in the soil solution (Figure S1), the solubility of OM can be reduced. In summary, mineral-bound OM is stabilized in the studied salt-affected soils as the large electrolyte concentration in the soil solution promotes the flocculation of OM and minerals. On the other hand, particulate OM is not as stable in salt-affected soils as previously assumed, as the degree of decomposition of this OM fraction was similar between salt-affected and non-salt-affected soils.

Microbial community composition along the salinity gradient

Microbial communities are sensitive to environmental changes and react to differences in the osmotic and matric potential (Rath and Rousk, 2015; Schimel et al., 2007). Particularly fungi but also Gram+ are thought to be more resistant against drought than Gram– due to their ability to produce osmolytes (Schimel et al., 2007). However, previous work on differences of the microbial community composition along salinity gradients could not support the view that fungi are superior to bacteria under water stress, i.e. high salinity, as several studies observed even a negative relationship between fungal abundance and salinity (Baumann and Marschner, 2011; Chowdhury et al., 2011; Pankhurst et al., 2001). This suggests that in salt-affected soils not only drought dictates the abundance of certain microbial groups but that also toxic effects of certain ions or impeded nutrient uptake as a result of ion competition may exist. In our study, the fungi : bacteria ratio was not related to the salinity gradient and was similar between the three soil types. Moreover, the fungal PLFA composition revealed a larger variability in the salt-affected soils, indicating that these soils have a more variable fungal community composition. Both results can have consequences, if we consider that fungi are thought to be the primary decomposers of particulate OM (evidence is given by Bossuyt et al., 2001; Frey et al., 2000; Six et al., 2006): a fungal community whose abundance and diversity is unaffected by salinity is capable of decomposing particulate OM at the same rate in

14

salt-affected and non-salt-affected soils. Thus, the decomposition of particulate OM proceeds also in the salt-affected soils, explaining the comparatively low contents of particulate OM and the observation that the proportion of particulate OM was unrelated to salinity.

Conclusions

This study aimed at investigating OM dynamics along a salinity gradient in soils of the south-western Siberian Kulunda steppe. Based on previous research, three hypotheses were tested: (i) soil OC stocks decrease along the salinity gradient, because high salinity decreases plant growth and subsequently lowers soil OC inputs, (ii) the proportion and stability of particulate OM is larger in salt-affected soils as compared to non-salt-affected soils as microbial decomposition and transformation of OM is reduced under high salinity levels, and (iii) sodicity reduces the proportion and stability of mineral-associated OM as the presence of Na^+ and a high pH causes dispersion of OM and mineral components. Based on our results, all three hypotheses were rejected. Against our first hypothesis, soil OC stocks increased along the salinity gradient with the most pronounced differences in the topsoil. Contrary to previous studies, plant growth (as determined by above-ground biomass) was not reduced under high salinity levels, suggesting that the soil OC input was similar between salt-affected and non-salt-affected soils. In contrast to our second hypothesis, the abundance and stability of particulate OM was not related to salinity levels. Remarkably, most of soil OC (>90%) existed in mineral-organic associations (HF >1.6 g cm^3) and only a small proportion (<10%) was present in particulate OM (LF <1.6 g cm^3). The composition of C isotopes ($\delta^{13}C$, ^{14}C activity) and neutral sugars in the density separates suggested a similar degree of OM alteration in salt-affected and non-salt-affected soils. This let´s assume that the microbial activity was not reduced under high salinity levels. We ascribe this to a functionally diverse and resilient microbial community, as indicated by a fungi : bacteria ratio unaffected by salinity and an even larger fungal PLFA variability under saline conditions, which is capable of decomposing particulate OM at a similar rate in salt-affected and non-salt-affected soils. Contrary to our third hypothesis, the proportion and stability of mineral-bound OM was not reduced under high sodicity levels. High ionic strength of the soil solution fosters the flocculation of soil constituents and, hence, increases the stability of mineral-organic associations. This, in conclusion, can be the reason for the larger OC stocks in the salt-affected soils: at similar soil OC inputs along the transect and a similar rate of particulate OM decomposition, mineral-associated OM accumulated in the salt-affected soils due to the high ionic strength of the soil solution. In summary, salt-affected soils contribute significantly to the OC storage in the semi-arid soils of the Kulunda steppe. Most of the OC was present in stable mineral-organic associations and, thus, effectively sequestered in the long-term.

Acknowledgements

15

References

Amini, S., Ghadiri, H., Chen, C. and Marschner, P.: Salt-affected soils, reclamation, carbon dynamics, and biochar: a review, J. Soils Sediments, 16(3), 939–953, doi:10.1007/s11368-015-1293-1, 2016.

Bates, D., Mächler, M. and Bolker, B.: Fitting linear mixed-effects models using lme4, J. Stat. Softw., 1–51

5 [online] Available from: http://arxiv.org/abs/1406.5823%5Cnhttp://listengine.tuxfamily.org/lists.tuxfamily. org/eigen/2011/06/pdfKU_S0z6LjT.pdf, 2012.

Batjes, N. H.: Total carbon and nitrogen in the soils of the world, Eur. J. Soil Sci., 47(2), 151–163, doi:10.1111/j.1365-2389.1996.tb01386.x, 1996.

Baumann, K. and Marschner, P.: Effects of salinity on microbial tolerance to drying and rewetting,

10 Biogeochemistry, 112(1–3), 71–80, doi:10.1007/s10533-011-9672-1, 2011.

Bischoff, N., Mikutta, R., Shibistova, O., Puzanov, A., Reichert, E., Silanteva, M., Grebennikova, A., Schaarschmidt, F., Heinicke, S. and Guggenberger, G.: Land-use change under different climatic conditions: Consequences for organic matter and microbial communities in Siberian steppe soils, Agric. Ecosyst. Environ., 235, 253–264, doi:10.1016/j.agee.2016.10.022, 2016.

15 Bossuyt, H., Denef, K., Six, J., Frey, S. D., Merckx, R. and Paustian, K.: Influence of microbial populations and residue quality on aggregate stability, Appl. Soil Ecol., 16(3), 195–208, doi:10.1016/S0929-1393(00)00116-5, 2001.

Breulmann, M., Masyutenko, N. P., Kogut, B. M., Schroll, R., Dörfler, U., Buscot, F. and Schulz, E.: Short-term bioavailability of carbon in soil organic matter fractions of different particle sizes and densities in grassland

20 ecosystems., Sci. Total Environ., 497–498, 29–37, doi:10.1016/j.scitotenv.2014.07.080, 2014.

Cheshire, M. V.: Nature and origin of carbohydrates in soils, Academic Press, London., 1979.

Chowdhury, N., Marschner, P. and Burns, R.: Response of microbial activity and community structure to decreasing soil osmotic and matric potential, Plant Soil, 344(1), 241–254, doi:10.1007/s11104-011-0743-9, 2011.

25 DIN ISO, 11277: Soil quality – determination of particle size distribution in mineral soil material – method by sieving and sedimentation, 2002.

Dohrmann, R., Rüping, K. B., Kleber, M., Ufer, K. and Jahn, R.: Variation of preferred orientation in oriented clay mounts as a result of sample preparation and composition, Clays Clay Miner., 57(6), 686–694, doi:10.1346/CCMN.2009.0570602, 2009.

30 Eder, E., Spielvogel, S., Kölbl, A., Albert, G. and Kögel-Knabner, I.: Analysis of hydrolysable neutral sugars in mineral soils: Improvement of alditol acetylation for gas chromatographic separation and measurement, Org. Geochem., 41(6), 580–585, doi:10.1016/j.orggeochem.2010.02.009, 2010.

Essington, M. E.: Soil and water chemistry - An integrative approach, CRC Press, Boca Raton., 2004.

FAO: Lecture notes on the major soils of the world, edited by P. Driessen, J. Deckers, O. Spaargaren, and F.

35 Nachtergaele, World soil Resour. reports, 94, 336, doi:10.1136/gut.27.11.1400-b, 2001.

Frey, S. D., Elliott, E. T., Paustian, K. and Peterson, G. A.: Fungal translocation as a mechanism for soil nitrogen inputs to surface residue decomposition in a no-tillage agroecosystem, Soil Biol. Biochem., 32(5), 689–698, doi:10.1016/S0038-0717(99)00205-9, 2000.

Frostegård, Å., Tunlid, A. and Bååth, E.: Use and misuse of PLFA measurements in soils, Soil Biol. Biochem.,

40 43(8), 1621–1625, doi:10.1016/j.soilbio.2010.11.021, 2011.

Gentsch, N., Mikutta, R., Alves, R. J. E., Barta, J., Capek, P., Gittel, A., Hugelius, G., Kuhry, P., Lashchinskiy,

16

N., Palmtag, J., Richter, A., Santruckova, H., Schnecker, J., Shibistova, O., Urich, T., Wild, B. and Guggenberger, G.: Storage and turnover of organic matter fractions in cryoturbated permafrost soils across the Siberian Arctic, Biogeosciences, 12, 4525–4542, doi:10.5194/bg-12-4525-2015, 2015.

Golchin, A., Oades, J. M., Skjemstad, J. O. and Clarke, P.: Study of free and occluded particulate organic matter in soils by solid state 13C CP/MAS NMR spectroscopy and scanning electron microscopy, Aust. J. Soil Res., 32, 285–309, doi:10.1071/SR9940285, 1994.

Gunina, A. and Kuzyakov, Y.: Sugars in soil and sweets for microorganisms: Review of origin, content, composition and fate, Soil Biol. Biochem., 90, 87–100, doi:10.1016/j.soilbio.2015.07.021, 2015.

Gunina, A., Dippold, M. A., Glaser, B. and Kuzyakov, Y.: Fate of low molecular weight organic substances in an arable soil: From microbial uptake to utilisation and stabilisation, Soil Biol. Biochem., 77, 304–313, doi:10.1016/j.soilbio.2014.06.029, 2014.

Hartge, K. H. and Horn, R.: Die physikalische Untersuchung von Böden, 2nd ed., F. Enke Verlag, Stuttgart., 1989.

Hijmans, R. J., Cameron, S. E., Parra, J. L., Jones, P. G. and Jarvis, A.: Very high resolution interpolated climate surfaces for global land areas, Int. J. Climatol., 25(15), 1965–1978, doi:10.1002/joc.1276, 2005.

Hothorn, T., Bretz, F. and Westfall, P.: Simultaneous inference in general parametric models, Biometrical J., 50(3), 346–363, doi:10.1002/bimj.200810425, 2008.

Hua, Q., Barbetti, M. and Rakowski, A. Z.: Atmospheric radiocarbon for the period 1950-2010, Radiocarbon, 55(4), 2059–2072, doi:10.2458/azu_js_rc.v55i2.16177, 2013.

IUSS Working Group WRB: World reference base for soil resources 2014. International soil classification system for naming soils and creating legends for soil maps, World Soil Resour. Reports No. 106, 1–191, doi:10.1017/S0014479706394902, 2014.

Kalinina, O., Krause, S.-E., Goryachkin, S. V., Karavaeva, N. a., Lyuri, D. I. and Giani, L.: Self-restoration of post-agrogenic chernozems of Russia: Soil development, carbon stocks, and dynamics of carbon pools, Geoderma, 162(1–2), 196–206, doi:10.1016/j.geoderma.2011.02.005, 2011.

Kleber, M., Eusterhues, K., Keiluweit, M., Mikutta, C., Mikutta, R. and Nico, P. S.: Mineral-organic associations: formation, properties, and relevance in soil environments, Adv. Agron., 130, 1–140, doi:10.1016/bs.agron.2014.10.005, 2015.

Kuznetsova, A., Brockhott, P. B. and Christensen, R. H. B.: lmerTest: Tests in linear mixed effects models. R package version 2.0-25, [online] Available from: http://cran.r-project.org/package=lmerTest, 2015.

Lal, R.: Soil carbon sequestration impacts on global climate change and food security, Science., 304(June), 1623–1627, doi:10.1126/science.1097396, 2004.

Läuchli, A. and Grattan, S. R.: Plant growth and development under salinity stress, in Advances in molecular breeding toward drought and salt tolerant crops, edited by M. A. Jenks, P. M. Hasegawa, and S. Mohan Jain, pp. 1–32, Springer, Dordrecht., 2007.

Lenth, R. V. and Herve, M.: lsmeans: Least-squares means. R package version 2.17, [online] Available from: http://cran.r-project.org/package=lsmeans, 2015.

Martinez-Beltran, J. and Manzur, C. L.: Overview of salinity problems in the world and FAO strategies to address the problem, in Proceedings of the international salinity forum, pp. 311–313, Riverside., USA., 2005.

Mavi, M. S., Sanderman, J., Chittleborough, D. J., Cox, J. W. and Marschner, P.: Sorption of dissolved organic matter in salt-affected soils: effect of salinity, sodicity and texture., Sci. Total Environ., 435–436, 337–44,

doi:10.1016/j.scitotenv.2012.07.009, 2012.

McKeague, J. A. and Day, J. H.: Dithionite- and oxalate-extractable Fe and Al as aids in differentiating various classes of soils, Can. J. Soil Sci., 46(154), 1966.

Muñoz-Rojas, M., Jordán, A., Zavala, L. M., De la Rosa, D., Abd-Elmabod, S. K. and Anaya-Romero, M.: Organic carbon stocks in Mediterranean soil types under different land uses (Southern Spain), Solid Earth, 3(2), 375–386, doi:10.5194/se-3-375-2012, 2012.

Nelson, P. N. and Oades, J. M.: Organic matter, sodicity, and soil structure, in Sodic soils: Distribution, properties, management, and environmental consequences, edited by E. Sumner, Malcolm, R. Naidu, and M. E. Sumner, pp. 51–75, Oxford University Press Inc, New York., 1998.

Olsson, P. A.: Signature fatty acids provide tools for determination of the distribution and interactions of mycorrhizal fungi in soil, FEMS Microbiol. Ecol., 29(4), 303–310, doi:10.1111/j.1574-6941.1999.tb00621.x, 1999.

Pankhurst, C. E., Yu, S., Hawke, B. G. and Harch, B. D.: Capacity of fatty acid profiles and substrate utilization patterns to describe differences in soil microbial communities associated with increased salinity or alkalinity at three locations in South Australia, Biol. Fertil. Soils, 33(3), 204–217, doi:10.1007/s003740000309, 2001.

Pathak, H. and Rao, D. L. N.: Carbon and nitrogen mineralization from added organic matter in saline and alkali soils, Soil Biol. Biochem., 30(6), 695–702, doi:10.1016/S0038-0717(97)00208-3, 1998.

Peinemann, N., Guggenberger, G. and Zech, W.: Soil organic matter and its lignin component in surface horizons of salt-affected soils of the Argentinian Pampa, Catena, 60(2), 113–128, doi:10.1016/j.catena.2004.11.008, 2005.

Plante, A. F., Virto, I. and Malhi, S. S.: Pedogenic, mineralogical and land-use controls on organic carbon stabilization in two contrasting soils, Can. J. Soil Sci., 90(1), 15–26, doi:10.4141/CJSS09052, 2010.

Poeplau, C. and Don, A.: Sensitivity of soil organic carbon stocks and fractions to different land-use changes across Europe, Geoderma, 192, 189–201, doi:10.1016/j.geoderma.2012.08.003, 2013.

Qadir, M. and Schubert, S.: Degradation processes and nutrient constraints in sodic soils, L. Degrad. Dev., 13(4), 275–294, doi:10.1002/ldr.504, 2002.

R Core Team: R: A language and environment for statistical computing, [online] Available from: http://www.r-project.org/, 2016.

Rath, K. M. and Rousk, J.: Salt effects on the soil microbial decomposer community and their role in organic carbon cycling: A review, Soil Biol. Biochem., 81, 108–123, doi:10.1016/j.soilbio.2014.11.001, 2015.

Reimer, P. J., Bard, E., Bayliss, A., Beck, J. W., Blackwell, P. G. and Ramsey, C. B.: IntCal13 and Marine13 radiocarbon age calibration curves 0–50,000 years cal BP, Radiocarbon, 55(4), 1869–1887, doi:10.2458/azu_js_rc.55.16947, 2013.

Rengasamy, P., Greene, R. S. B., Ford, G. W. and Mehanni, A. H.: Identification of dispersive behaviour and the management of red-brown earths, Soil Res., 22(4), 413–431, doi:Doi 10.1071/Sr9840413, 1984.

Rietz, D. N. and Haynes, R. J.: Effects of irrigation-induced salinity and sodicity on soil microbial activity, Soil Biol. Biochem., 35(6), 845–854, doi:10.1016/S0038-0717(03)00125-1, 2003.

Ruess, L. and Chamberlain, P. M.: The fat that matters: Soil food web analysis using fatty acids and their carbon stable isotope signature, Soil Biol. Biochem., 42(11), 1898–1910, doi:10.1016/j.soilbio.2010.07.020, 2010.

Rumpel, C. and Dignac, M.-F.: Gas chromatographic analysis of monosaccharides in a forest soil profile: Analysis by gas chromatography after trifluoroacetic acid hydrolysis and reduction–acetylation, Soil Biol.

18

Biochem., 38(6), 1478–1481, doi:10.1016/j.soilbio.2005.09.017, 2006.

Schimel, J., Balser, T. C. and Wallenstein, M.: Microbial stress-response physiology and its implications for ecosystem function, Ecology, 88(6), 1386–1394, doi:10.1890/06-0219, 2007.

Schlichting, E., Blume, H.-P. and Stahr, K.: Bodenkundliches Praktikum – Eine Einführung in pedologisches Arbeiten für Ökologen, insbesondere Land- und Forstwirte, und für Geowissenschaftler, 2nd ed., Blackwell Wissenschafts-Verlag Berlin, Wien., 1995.

Schnecker, J., Wild, B., Fuchslueger, L. and Richter, A.: A field method to store samples from temperate mountain grassland soils for analysis of phospholipid fatty acids., Soil Biol. Biochem., 51(2), 81–83, doi:10.1016/j.soilbio.2012.03.029, 2012.

Setia, R., Rengasamy, P. and Marschner, P.: Effect of exchangeable cation concentration on sorption and desorption of dissolved organic carbon in saline soils, Sci. Total Environ., 465, 226–232, doi:10.1016/j.scitotenv.2013.01.010, 2013.

Setia, R., Rengasamy, P. and Marschner, P.: Effect of mono- and divalent cations on sorption of water-extractable organic carbon and microbial activity, Biol. Fertil. Soils, 50(5), 727–734, doi:10.1007/s00374-013-0888-1, 2014.

Six, J., Frey, S. D., Thiet, R. K. and Batten, K. M.: Bacterial and fungal contributions to carbon sequestration in agroecosystems, Soil Sci. Soc. Am. J., 70(2), 555–569, doi:10.2136/sssaj2004.0347, 2006.

Steffens, M., Kölbl, A., Schörk, E., Gschrey, B. and Kögel-Knabner, I.: Distribution of soil organic matter between fractions and aggregate size classes in grazed semiarid steppe soil profiles, Plant Soil, 338(1–2), 63–81, doi:10.1007/s11104-010-0594-9, 2010.

Steinhof, A.: Data analysis at the Jena ^{14}C laboratory, Radiocarbon, 55(3–4), 282–293, doi:10.2458/azu_js_rc.55.16350, 2013.

Steinhof, A., Baatzsch, A., Hejja, I. and Wagner, T.: Ion source improvements at the Jena ^{14}C-AMS facility, Nucl. Instruments Methods Phys. Res. Sect. B Beam Interact. with Mater. Atoms, 269(24), 3196–3198, doi:10.1016/j.nimb.2011.04.018, 2011.

Stuiver, M. and Polach, H. A.: Reporting of ^{14}C data, Radiocarbon, 19(3), 355–363, doi:10.1016/j.forsciint.2010.11.013, 1977.

Sumner, M. E.: Sodic soils: New perspectives, Aust. J. Soil Res., 31(6), 683–750, doi:10.1071/SR9930683, 1993.

Sumner, M. E., Rengasamy, P. and Naidu, R.: Sodic soils: a reappraisal, in Sodic soils: Distribution, properties, management, and environmental consequences, edited by E. Sumner, Malcolm, R. Naidu, and M. E. Sumner, pp. 3–17, Oxford University Press Inc, New York., 1998.

Titlyanova, A. A., Romanova, I. P., Kosykh, N. P. and Mironycheva-Tokareva, N. P.: Pattern and process in above-ground and below-ground components of grassland ecosystems, J. Veg. Sci., 10(3), 307–320, doi:10.2307/3237060, 1999.

U.S. Salinity Laboratory Staff: Diagnosis and improvement of saline and alkaline soils, edited by L. A. Richards, Government Printing Office, Washington D.C., 1954.

Walthert, L., Graf, U., Kammer, A., Luster, J., Pezzotta, D., Zimmermann, S. and Hagedorn, F.: Determination of organic and inorganic carbon, δ^{13} C, and nitrogen in soils containing carbonates after acid fumigation with HCl, J. Plant Nutr. Soil Sci., 173(2), 207–216, doi:10.1002/jpln.200900158, 2010.

Wickham, H.: ggplot2: Elegant graphics for data analysis, [online] Available from:

19

papers2://publication/uuid/DE806F9A-5AD0-450B-AC68-5164EDBA8787, 2009.

Wong, V. N. L., Greene, R. S. B., Dalal, R. C. and Murphy, B. W.: Soil carbon dynamics in saline and sodic soils: A review, Soil Use Manag., 26(1), 2–11, doi:10.1111/j.1475-2743.2009.00251.x, 2010.

Zelles, L.: Fatty acid patterns of phospholipids and lipopolysaccharides in the characterisation of microbial
5   communities in soil: a review, Biol. Fertil. Soils, 29(2), 111–129, doi:10.1007/s003740050533, 1999.

20

Tables

Table 1: Vegetation (dominant species) and above-ground biomass on each soil type. Given are arithmetic means and the standard error of the mean in parentheses. Significant differences (p <0.05) were not present and are denoted as same lowercase letters.

Soil type	Vegetation / dominant species (from most to least dominant)	Above-ground biomass $g\ m^{-2}$	
Kastanozem	*Festuca valesiaca – Thymus maschallianus – Koeleria glauca*	164.8 (37.7)	a
Non-sodic Solonchak	*Leymus poboanus – Artemisia nitrosa – Atriplex verrucifera*	133.7 (17.6)	a
Sodic Solonchak	*Atriplex verrucifera – Leymus poboanus – Hordeum brevisubulatum*	139.5 (21.7)	a

5

21

Table 2: Basic soil parameters as function of soil type and horizon. Given are arithmetic means and the standard error of the mean in parentheses. Abbreviations: n = sample size, BD = bulk density, EC = electrical conductivity, SAR = sodium adsorption ratio, Aggstab = aggregate stability, MWD = mean weight diameter, Fe_O = oxalate-extractable Fe, Fe_D = dithionite-extractable Fe.

Soil type	Horizon	n	Depth cm	BD g cm^{-3}	Moisture % of dry weight	$pH_{H2O,1:2.5}$ -	$EC_{1:5}$ µS cm^{-1}	$SAR_{1:5}$ -	$CaCO_3$ mg g^{-1}	Aggstab Δ MWD (mm)	Clay mg g^{-1}	Silt mg g^{-1}	Sand mg g^{-1}	Fe_O mg g^{-1}	Fe_D mg g^{-1}	$Fe_O : Fe_D$ -
Kastanozem	Ah	3	23.3 (1.5)	1.47 (0.07)	3.6 (0.3)	7.1 (0.1)	27 (3)	0.4 (0.1)	0 (0)	0.41 (0.06)	127 (7)	230 (20)	643 (24)	0.21 (0.20)	4.9 (0.1)	0.04 (0.04)
	AC	3	48.3 (2.8)	1.52 (0.07)	4.5 (0.2)	8.0 (0.2)	26 (1)	0.4 (0.0)	0 (0)		170 (8)	219 (33)	611 (35)	0.16 (0.16)	4.9 (0.2)	0.03 (0.03)
	Ck	3	114.7 (8.0)	1.60 (0.07)	3.6 (0.3)	8.8 (0.1)	152 (35)	0.9 (0.5)	51 (12)		95 (13)	121 (22)	784 (35)	0.04 (0.04)	3.0 (0.2)	0.01 (0.01)
	C	2	175.0 (15.0)	1.70 (0.05)	4.3 (0.4)	9.0 (0.1)	236 (101)	1.7 (0.3)	29 (1)		91 (5)	125 (22)	784 (27)	0.07 (0.07)	2.9 (0.4)	0.03 (0.03)
Non-sodic Solonchak	Az	4	27.3 (7.1)	1.44 (0.06)	20.5 (1.9)	8.5 (0.2)	3416 (1053)	9.6 (2.2)	53 (16)	1.02 (0.29)	174 (14)	330 (17)	497 (26)	0.31 (0.04)	2.8 (0.7)	0.13 (0.02)
	B	4	62.0 (6.4)	1.58 (0.02)	17.8 (1.4)	8.8 (0.1)	1378 (372)	7.0 (0.3)	102 (28)		207 (12)	313 (21)	481 (32)	0.14 (0.07)	3.7 (0.5)	0.03 (0.01)
	C	4	107.3 (6.1)	1.78 (0.03)	14.9 (1.7)	8.8 (0.1)	1016 (343)	5.3 (0.9)	152 (34)		203 (32)	320 (56)	477 (87)	0.07 (0.03)	3.7 (0.3)	0.02 (0.01)
	Cl	4	175.0 (8.7)	1.76 (0.03)	16.5 (0.6)	8.7 (0.1)	796 (333)	3.9 (1.0)	82 (26)		157 (34)	250 (81)	593 (114)	0.24 (0.08)	3.9 (0.4)	0.06 (0.02)
Sodic Solonchak	Az	3	22.0 (1.5)	1.23 (0.04)	30.6 (4.1)	8.7 (0.1)	5350 (1476)	36.0 (10.4)	207 (22)	0.33 (0.03)	192 (55)	308 (81)	500 (64)	0.02 (0.01)	1.0 (0.3)	0.02 (0.01)
	ACz	3	50.0 (6.1)	1.29 (0.06)	29.2 (3.0)	8.8 (0.0)	3880 (1590)	23.8 (8.7)	264 (22)		230 (41)	307 (45)	464 (47)	0.01 (0.00)	0.9 (0.5)	0.02 (0.01)
	C	2	94.5 (10.5)	1.65 (0.11)	20.0 (4.4)	9.0 (0.1)	911 (639)	11.7 (9.7)	213 (17)		190 (34)	308 (47)	502 (81)	0.03 (0.01)	2.6 (0.3)	0.01 (0.00)
	Cl	3	140.7 (5.2)	1.78 (0.01)	16.4 (0.9)	8.9 (0.0)	1093 (702)	8.0 (4.6)	115 (49)		166 (22)	250 (43)	584 (60)	0.32 (0.14)	3.3 (0.2)	0.10 (0.05)

23

Table 3: Parameters of OM fractions as function of soil type and horizon. Given are arithmetic means and the standard error of the mean in parentheses. Where n differs for a certain parameter from those indicated in the third column, it is indicated by a separate n in brackets. Abbreviations: OC = organic carbon, MobC = mobilized organic carbon.

| Soil type	Horizon	n	mg fraction g⁻¹ soil	mg fraction lost (HF) g⁻¹ soil	mg OC g⁻¹ fraction	C : N	δ¹³C (‰)	mg MobC g⁻¹ fraction	% MobC of total OC	% OC of total OC	mg sugar g⁻¹ fraction	mg sugar g⁻¹ OC
Light fraction (LF)												
Kastanozem	Ah	3	5.3 (0.6)		119.6 (3.4)	14.6 (0.4)	-27.48 (0.06)	17.6 (1.5) [2]	1.50 (0.05) [2]	7.30 (0.59) [2]	46.5 (5.0)	409.6 (38.2) [1]
	AC	3	1.4 (0.1)		151.4 (7.0)	14.2 (0.3)	-27.12 (0.26)	33.3 (7.4) [2]	1.25 (0.06) [2]	4.54 (0.31) [2]		
	Ck	2	0.9 (0.2)		218.6 (24.8)	13.8 (0.8)	-26.42 (0.48)	75.9 (10.6)	3.38 (0.89)	8.29 (2.42)		
Non-sodic Solonchak	Az	4	3.1 (1.1)		196.9 (30.8)	16.7 (1.8)	-26.99 (0.42)	34.8 (5.3) [2]	0.71 (0.13) [2]	3.62 (0.50) [2]	46.1 - [1]	328.4 - [1]
	B	4	0.9 (0.1)		261.4 (14.2)	17.2 (1.0)	-27.40 (0.28)	161.0 (13.0) [2]	1.64 (0.28) [2]	5.51 (1.08) [2]		
	C	3	0.3 (0.1)		279.2 (37.5)	16.0 (1.1)	-28.08 (0.29)	236.4 (84.2) [2]	3.05 (0.52) [2]	7.26 (0.57) [2]		
Sodic Solonchak	Az	3	4.5 (0.6)		265.1 (31.5)	13.1 (0.9)	-24.27 (1.33)	46.7 (3.3) [2]	0.67 (0.18) [2]	6.91 (2.77) [2]	104.6 (27.2)	379.1 (65.2)
	ACz	3	1.1 (0.3)		246.5 (26.9)	13.8 (1.0)	-25.11 (0.44)	130.3 (37.7) [2]	0.79 (0.20) [2]	4.18 (2.09) [2]		
	C	2	0.4 (0.1)		246.9 (22.4)	14.7 (1.5)	-26.61 (0.03)	258.3 (62.7)	1.93 (0.12)	4.96 (0.06)		
Heavy fraction (HF)												
Kastanozem	Ah	3	994.7 (0.6)	7.7 (3.2)	7.7 (0.3)	9.1 (0.2)	-23.79 (0.09)	1.5 (0.1) [2]	15.56 (0.51) [2]	92.70 (0.59) [2]	1.0 (0.2)	135.6 (22.1)
	AC	3	998.6 (0.1)	28.7 (1.5)	4.4 (0.3)	7.5 (0.1)	-23.02 (0.04)	2.0 (0.4) [2]	29.41 (1.36) [2]	95.46 (0.31) [2]	0.7 (0.1)	150.7 (15.7)
	Ck	2	999.2 (0.2)	8.8 (6.4)	2.1 (1.1)	6.6 (0.7)	-23.04 - [1]	1.7 (0.1)	45.71 (12.02)	91.71 (2.42)	0.5 -	171.0 - [1]
Non-sodic Solonchak	Az	4	996.9 (1.1)	85.8 (19.8)	18.3 (2.7)	9.8 (0.1)	-23.26 (0.54)	0.7 (0.1) [2]	3.72 (0.63) [2]	96.38 (0.50) [2]	3.1 (0.6)	169.3 (27.5)
	B	4	999.1 (0.1)	64.7 (5.6)	4.7 (0.8)	8.2 (0.4)	-22.79 (0.36) [3]	0.2 (0.1) [2]	5.84 (1.04) [2]	94.49 (1.08) [2]	1.0 (0.4)	171.8 (33.8)
	C	4	999.7 (0.1)	60.7 (6.3)	2.0 (0.4)	7.0 (0.3)	-23.04 - [1]	0.2 (0.1) [2]	9.43 (1.60) [2]	92.74 (0.57) [3]	0.2 - [1]	136.4 - [1]
Sodic Solonchak	Az	3	995.5 (0.6)	76.4 (14.0)	19.3 (5.0)	8.4 (1.7)	-23.40 (0.30)	0.5 (0.3) [2]	3.35 (0.95) [2]	93.09 (2.77) [2]	5.7 (0.8)	322.0 (60.8)
	ACz	3	998.9 (0.3)	53.9 (10.0)	10.6 (2.7)	10.1 (0.1)	-23.05 (0.13)	0.1 (0.1) [2]	2.89 (0.63) [2]	95.82 (2.09) [2]	2.6 (0.6)	244.8 (3.5)
	C	2	999.6 (0.1)	45.8 (4.1)	3.1 (0.8)	9.2 (0.1)	-23.20 (0.22)	0.1 (0.1)	5.75 (0.38)	95.04 (0.06)		
	Cl	1	997.2 -	66.6 -	1.6 -	7.9 -	-22.52 -	0.2 -			0.3 -	164.8 -

Figures
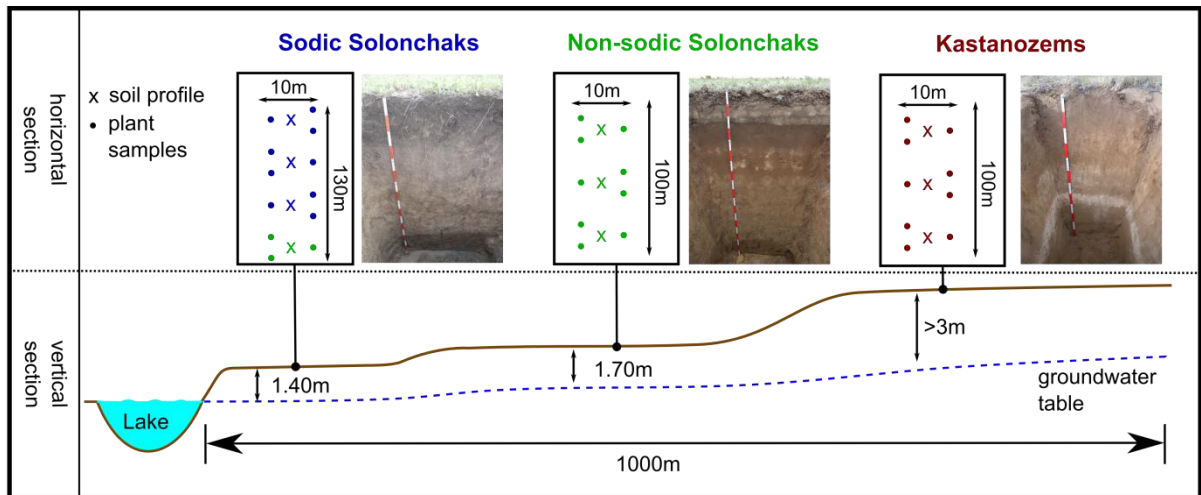
Figure 1: Schematic representation of study sites and the experimental design. Same colors of the soil profiles and plant samples mark the same soils. A detailed soil type classification of the grouped soils is given in Table S1.
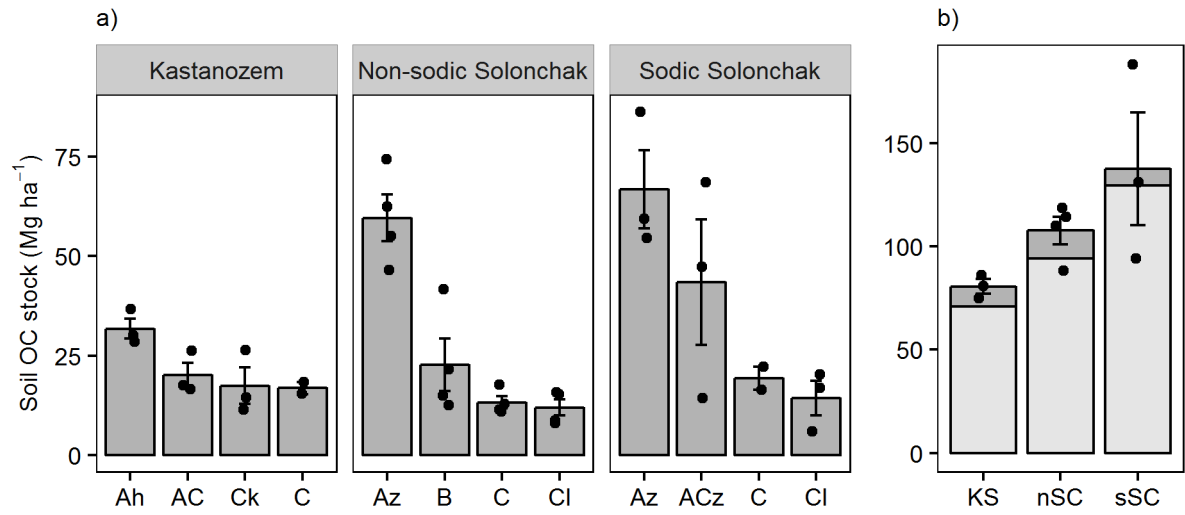
5

Figure 2: Soil OC stocks (Mg ha^{-1}) for three soil types, (a) as function of horizon and (b) for a depth of 100 cm and the entire soil profile (light and dark grey). Mean depths of the profiles were 157 ± 20 cm (KS), 175 ± 9 cm (nSC) and 141 ± 5 cm (sSC). Given are arithmetic means ± SE, while dots show individual measurements (in plot b) for the entire soil profile. Abbreviations: KS = Kastanozem, nSC = Non-sodic Solonchak, sSC = Sodic Solonchak.
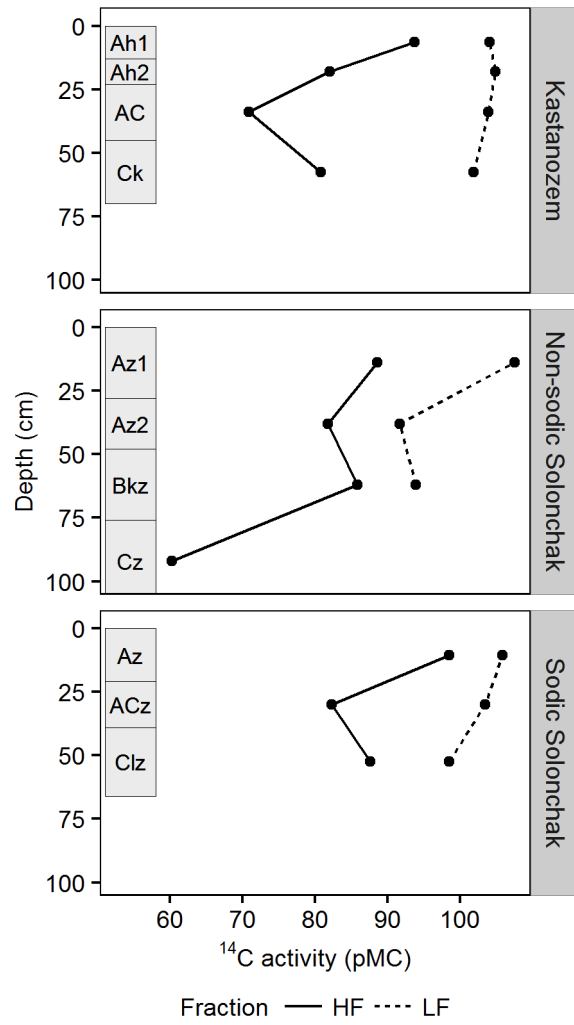
25

Figure 3: ^{14}C activity (pMC) for three soil types and two OM fractions as function of soil depth. Rectangles on the left of each panel indicate diagnostic horizons. Abbreviations: LF = light fraction, HF = heavy fraction.
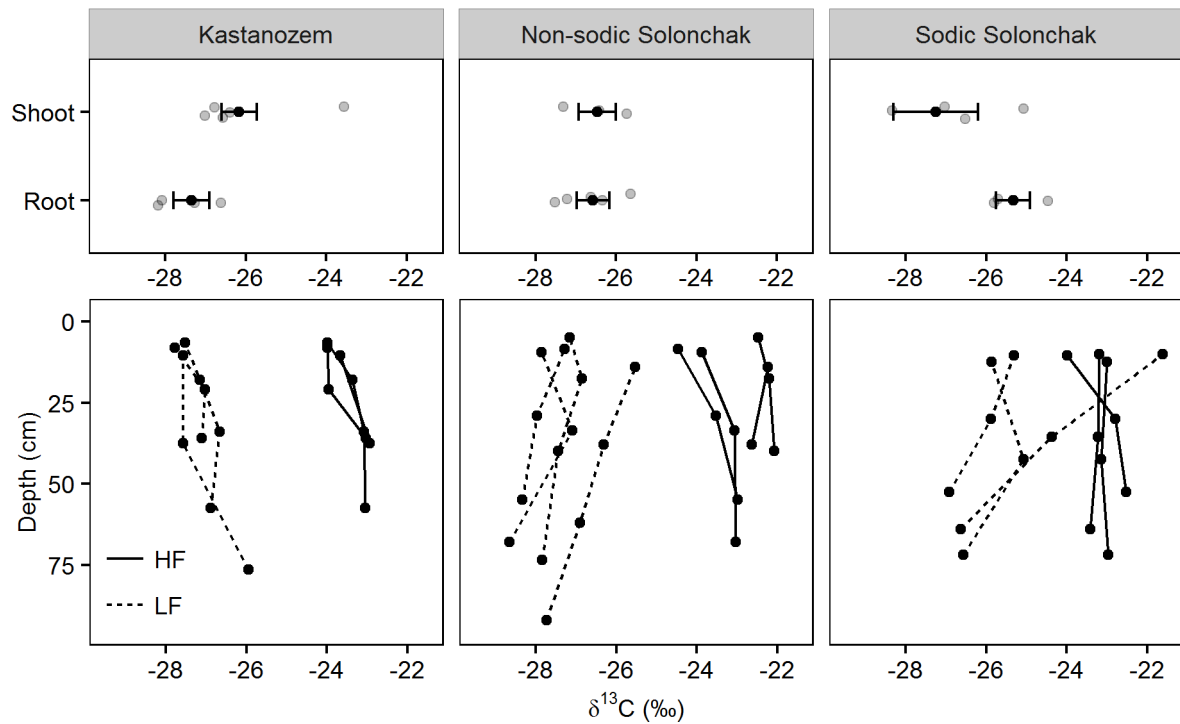
26

Figure 4: δ¹³C ratios of plant components (upper three panels) and of OM present in the light fraction (LF) and the heavy fraction (HF) as function of soil depth (lower three panels) for three soil types. Grey dots in the upper three panels show individual measurements, while the black dots show arithmetic means ± standard error of the mean. In the lower three panels, the three and four replicates per soil type are shown.
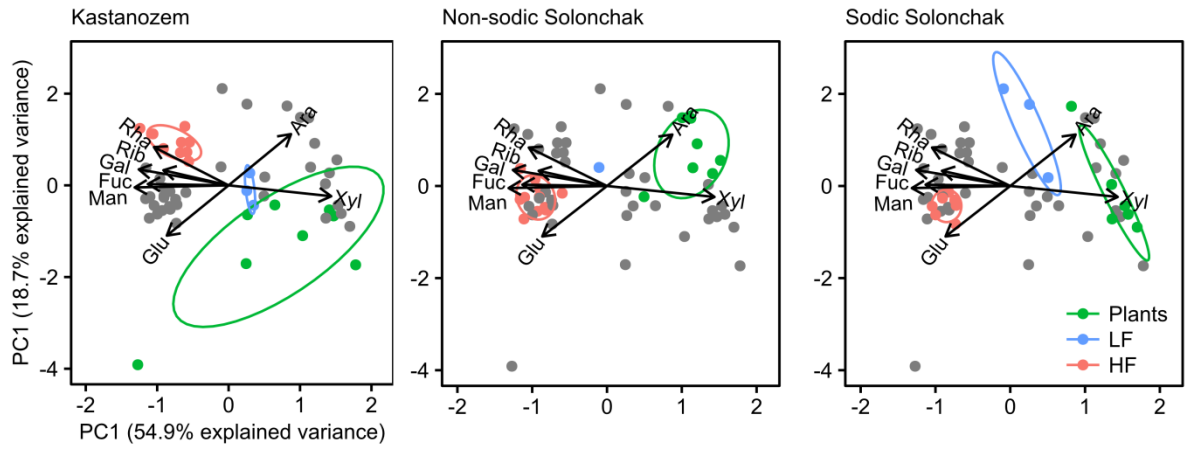
5

Figure 5: Biplots derived from a principal components analysis of non-cellulosic neutral sugars from plants, the light fraction (LF) and the heavy fraction (HF), plotted for each soil type separately. The grey dots belong to those samples not considered for the particular soil type. Abbreviations: Man = mannose, Ara = arabinose, Rha = rhamnose, Rib = ribose, Glu = glucose, Fuc = fucose, Xyl = xylose, Gal = galactose.

28
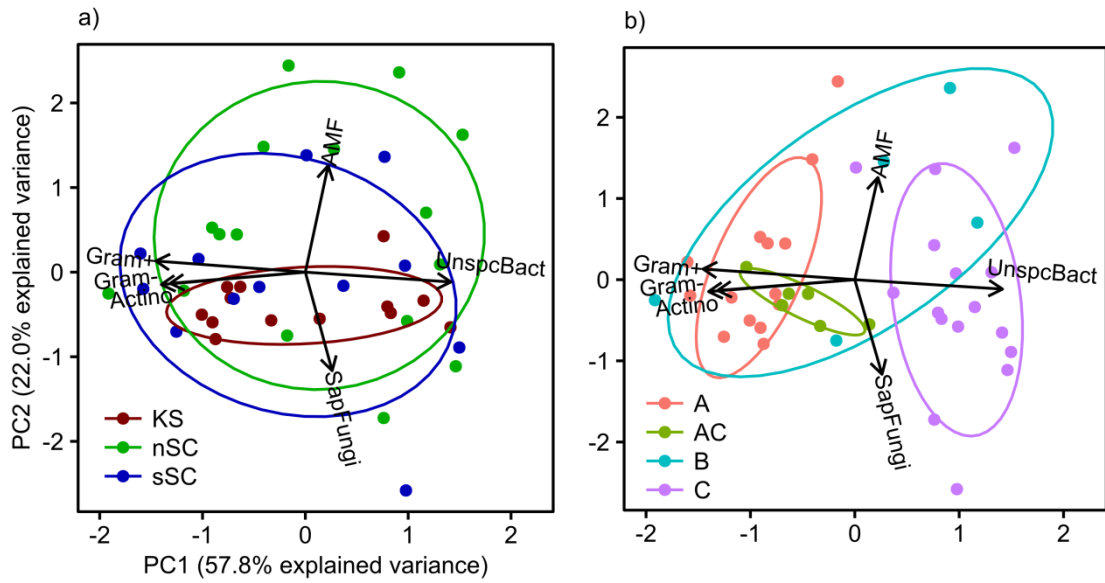
Figure 6: Biplots derived from a principal components analysis of functional microbial groups as identified from PLFA analysis. Colors and 68% confidence regions are grouped by a) soil type and b) horizon. Abbreviations: KS = Kastanozem, nSC = Non-sodic Solonchak, sSC = Sodic Solonchak, Gram+ = gram-positive bacteria, Gram– = gram-negative bacteria, Actino = actinomycetes, SapFungi = saprotrophic fungi, UnspcBact = unspecific bacteria, AMF = arbuscular mycorrhizal fungi.

29

Supplement of

Organic matter dynamics along a salinity gradient in Siberian steppe soils

N. Bischoff et al.

5   *Correspondence to:* N. Bischoff (bischoff@ifbk.uni-hannover.de)

1

Tables

Table S 1: Assignment of soil types according to IUSS Working Group WRB (2014) to groups and soil types, respectively, used in the present study.

Group / Soil type	Plot	Soil type according to IUSS Working Group WRB (2014)
Kastanozem	I	Calcic Kastanozem (Loamic)
	II	Haplic Kastanozem (Arenic, Loamic)
	III	Haplic Kastanozem (Arenic, Loamic)
Non-sodic Solonchak	IV	Mollic Solonchak (Loamic)
	V	Mollic Solonchak (Loamic)
	VI	Mollic Solonchak (Alcalic, Loamic)
	VII	Haplic Solonchak (Alcalic, Loamic)
Sodic Solonchak	VIII	Gleyic Sodic Solonchak (Alcalic, Loamic)
	IX	Sodic Solonchak (Alcalic, Loamic, Humic)
	X	Sodic Solonchak (Alcalic, Loamic, Humic)

Table S 2: Organic carbon (OC), total nitrogen (TN), and C : N ratio of OM as function of soil type and horizon. Given are arithmetic means and the standard error of the mean in parentheses. Abbreviation: n = sample size.

| Soil type	Horizon	n	OC mg g^{-1}		TN mg g^{-1}		C : N -	
Kastanozem	Ah	3	9.28	(0.34)	0.96	(0.03)	9.8	(0.1)
	AC	3	5.33	(0.27)	0.63	(0.03)	8.2	(0.3)
	Ck	3	2.05	(0.28)	0.30	(0.06)	8.2	(0.7)
	C	2	1.27	(0.28)	0.25	(0.05)	5.7	(1.0)
Non-sodic Solonchak	Az	4	17.38	(2.90)	1.78	(0.31)	9.8	(0.1)
	B	4	4.04	(0.62)	0.52	(0.07)	7.7	(0.2)
	C	4	1.74	(0.13)	0.29	(0.01)	6.1	(0.4)
	Cl	4	1.10	(0.18)	0.24	(0.02)	4.8	(0.6)
Sodic Solonchak	Az	3	24.53	(2.34)	2.53	(0.24)	9.7	(0.2)
	ACz	3	11.07	(2.77)	1.10	(0.29)	10.0	(0.1)
	C	2	3.46	(1.04)	0.40	(0.10)	8.8	(0.4)
	Cl	3	1.34	(0.36)	0.24	(0.03)	6.0	(1.0)

3
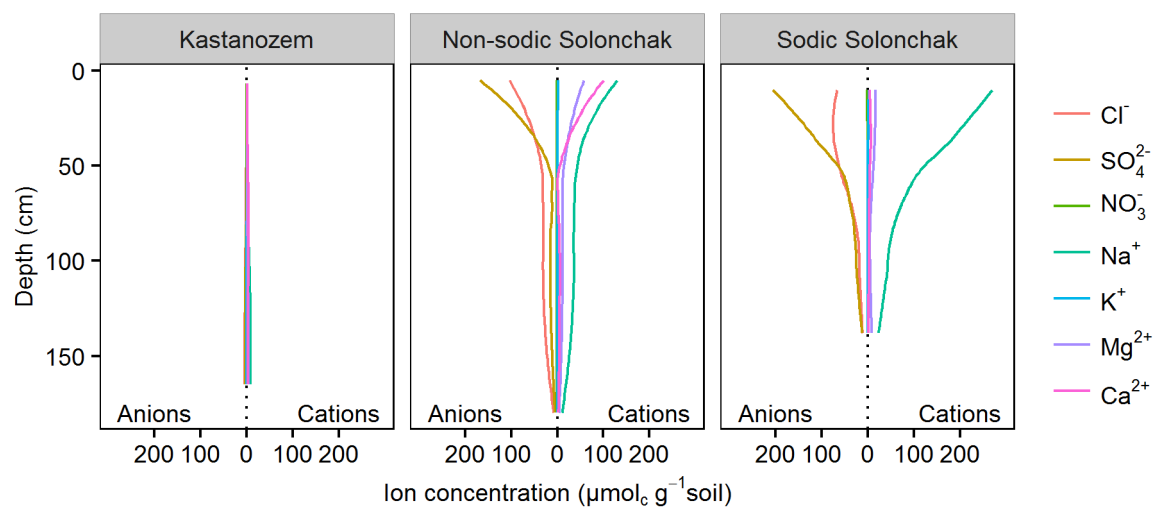
Figures

Figure S 1: Concentration of water-soluble anions and cations (μmol_c g^{-1} soil) for three soil types as a function of soil depth. For better visualization measured data are omitted and only the local polynomial regression fits (LOESS) are shown.
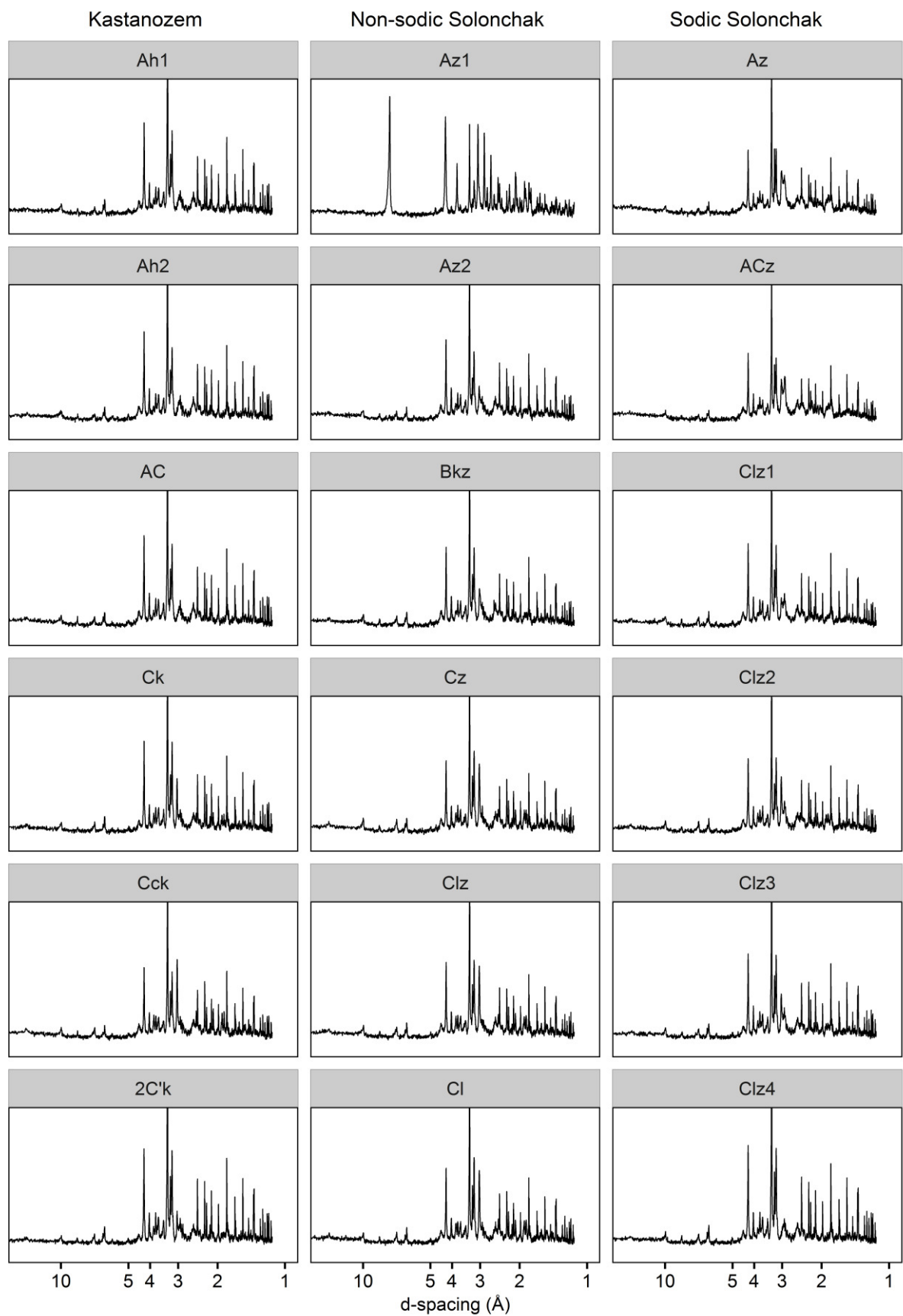
Figure S 2: X-ray powder diffractograms of bulk soil from three profiles and respective horizons. Intensities are square root transformed for better visualization of trace mineral phases.
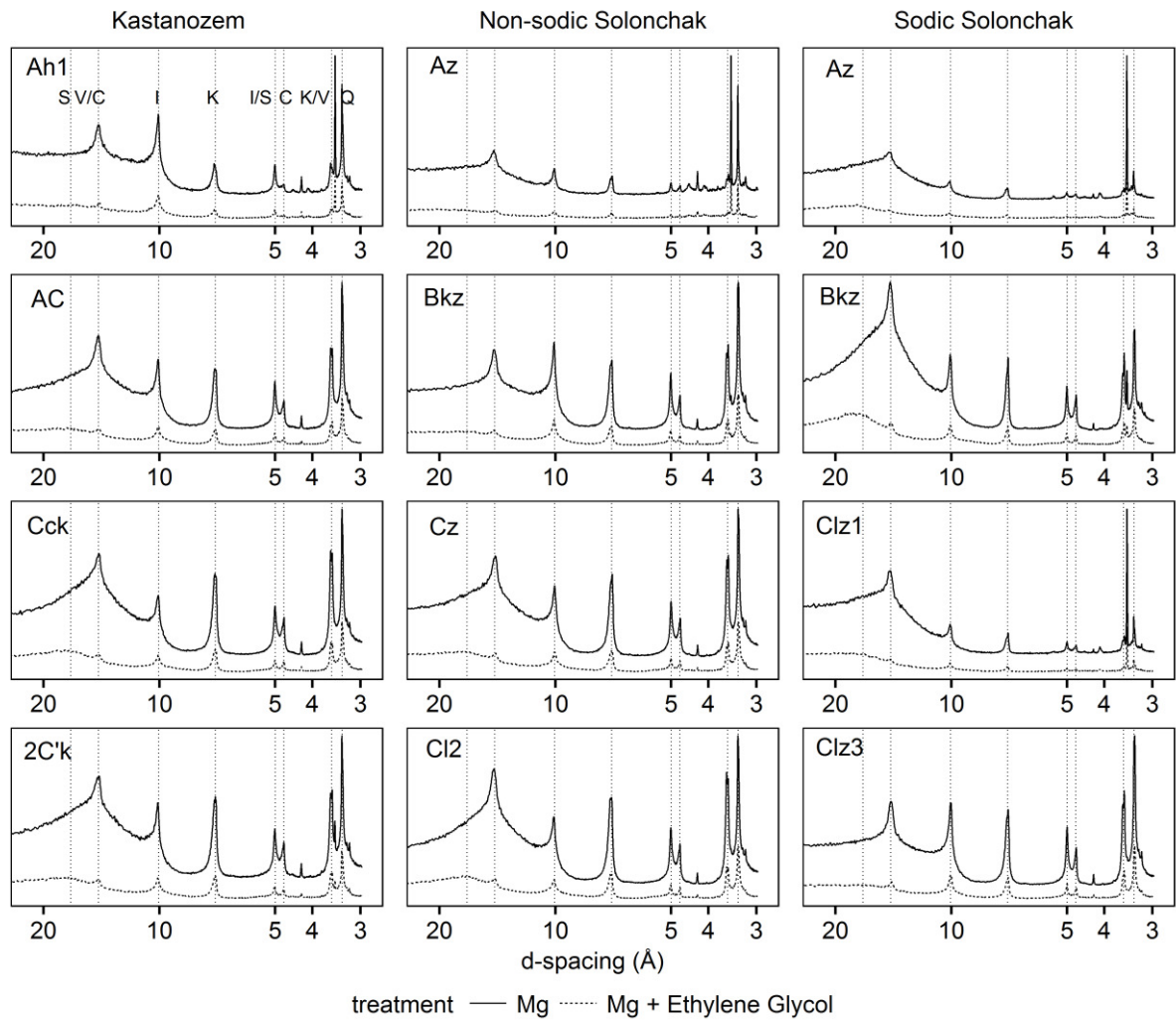
5

Figure S 3: -ray diffractograms of clay fractions from two treatments of three soil types and four different horizons. Abbreviations: S = smectite, V = vermiculite, C = chlorite, I = illite, K = kaolinite, and Q = quartz.
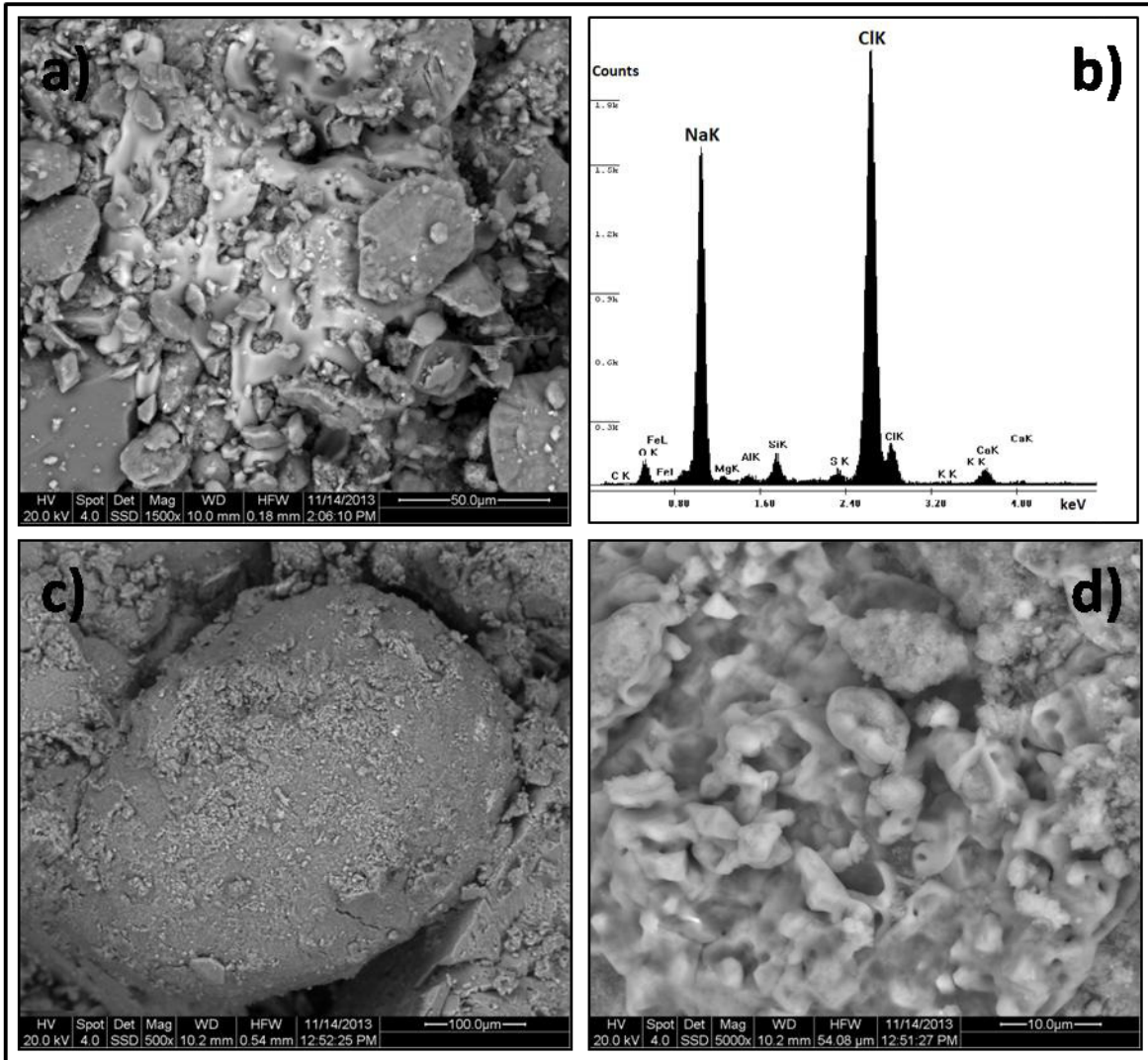
6

Figure S 4: Scanning electron micrographs (a, c, d) and EDX spectra (b) of the fine earth fraction of Solonchaks. The two common salt minerals halite (a, b) and thenardite (c, d) are shown. In a), halite is represented by the white region embedded in gypsum crystals. In c), thenardite is the finely textured coating on the larger mineral, d) is the enlargement of c).
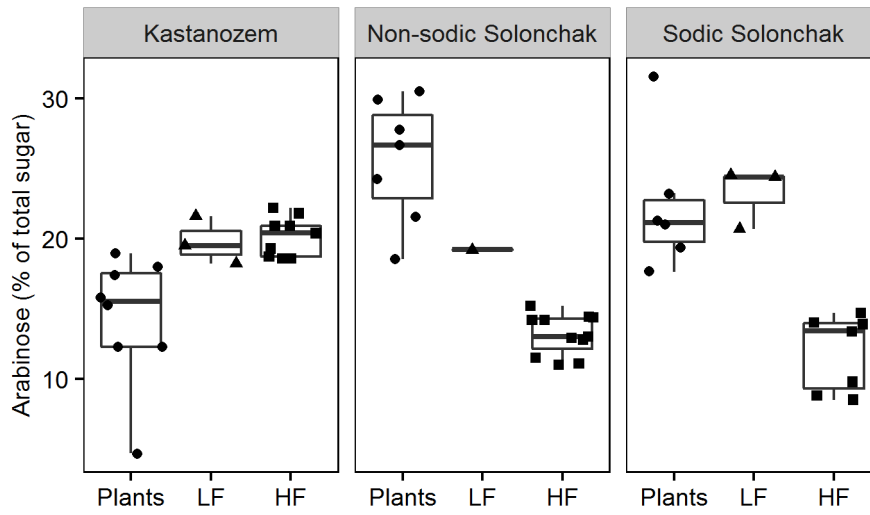
5

Figure S 5: Percentage contribution of arabinose to the total non-cellulosic neutral sugars of three soil types, separated for plants, light fraction (LF) and heavy fraction (HF).
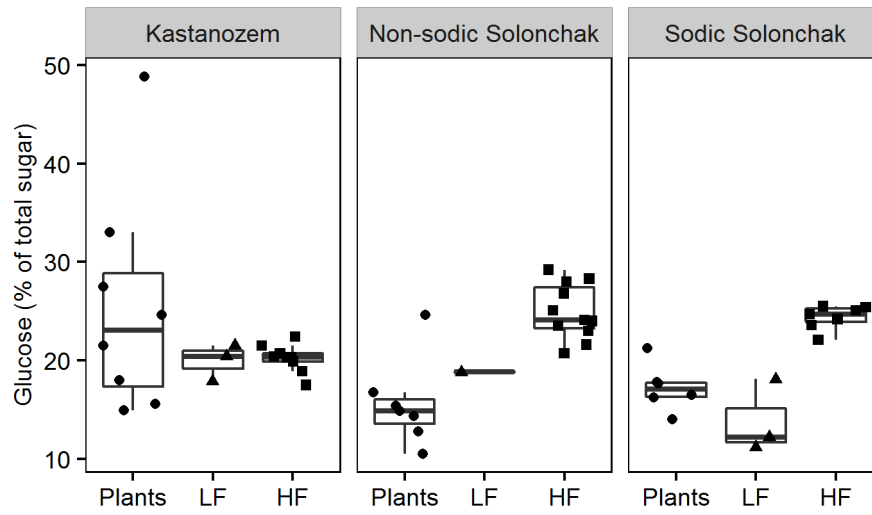
Figure S 6: Percentage contribution of glucose to the total non-cellulosic neutral sugars of three soil types, separated for plants, light fraction (LF) and heavy fraction (HF).

9

References

IUSS Working Group WRB: World reference base for soil resources 2014. International soil classification system for naming soils and creating legends for soil maps, World Soil Resour. Reports No. 106, 1–191, doi:10.1017/S0014479706394902, 2014.

5

10

5 Synopsis

5.1 Climate-dependent OC stocks and partitioning of OM into functionally different OM fractions

Organic C stocks in steppe biomes were shown to correlate negatively with aridity, e.g. in the North American prairies, European Russia, or the steppes of northern China (Burke *et al.*, 1989; Schimel *et al.*, 1994; Kalinina *et al.*, 2011; Dang *et al.*, 2014; Follett *et al.*, 2015). This is explained by lower net primary productivity (NPP) under arid conditions and, hence, smaller soil OM inputs which consequently result in smaller soil OC stocks (Jenkinson *et al.*, 1992; Bazilevich, 1993; Burke *et al.*, 1997; Jobbagy *et al.*, 2002). Thus, we hypothesized that OC stocks would decrease with aridity also in soils of the Kulunda steppe, which was corroborated by our results (Study I). While OC stocks in grasslands amounted 218 ± 17 Mg ha^{-1} in 0-60cm depth in the forest steppe, it was only 153 ± 10 Mg ha^{-1} in the typical steppe, and 134 ± 11 Mg ha^{-1} in the dry steppe. A comparison of studies investigating OM dynamics in steppe soils worldwide shows that OC stocks in steppes of Siberia or European Russia are relatively large when compared to soil OC stocks e.g. of the Great Plains (Table 1). A possible explanation is a slightly wetter climate in the Siberian or Russian steppes resulting in larger NPP and, hence, larger soil OC stocks. According to the climate classification system by Lauer & Frankenberg (1987) the Siberian steppes are more humid than the North American prairies, giving evidence for the explanation.

Soil OC is partitioned between functionally different soil OM fractions (i.e. particulate OM and mineral-associated OM) depending on environmental factors such as soil moisture, pH or soil texture (Christensen, 1992; Kleber *et al.*, 2015). In steppe soils, particulate OM comprises generally a considerable portion of total soil OC, as the formation of mineral-associated OM is attenuated due to a deficit of soil moisture and a relatively high soil pH (Kleber *et al.*, 2015). Particulate OM accounted for >20% of the total soil OC storage in steppe soils of the Great Plains, European Russia or northern China, (Plante *et al.*, 2010; Steffens *et al.*, 2010; Kalinina *et al.*, 2011; Breulmann *et al.*, 2014). Hence, we expected that particulate OM would also contribute considerably to the total OC stocks in the soils of the Kulunda steppe, while its portion would increase with aridity. Remarkably, in soils of the Kulunda steppe the share of particulate OM in the total soil OC storage was small and comprised maximally 10% (Study I and III). More than 90% of soil OC was stored in mineral-organic associations, which is much more than previously observed in steppe soils. Possible reasons for the smaller quantity of particulate OM in the Siberian steppe soils are (i) a smaller soil OM input by plant residues, or (ii) a moister climate fostering the formation of mineral-organic associations, which in turn decreases proportions of particulate OM. Gulde *et al.* (2008) and Brown *et al.* (2014) showed that the proportion of particulate OM increased linearly with soil OM inputs, indicating that

differences in soil OM inputs between the steppe regions could explain differences in particulate OM quantities. However, as indicated above by the climate classification system of Lauer & Frankenberg (1987), the Siberian steppes are more humid than those of northern China or the Great Plains and under these conditions smaller soil OM inputs are unlikely. More likely appears that the wetter climate has fostered the decomposition of particulate OM while enhancing the formation of mineral-organic associations, thus, reducing the proportion of particulate OM (Kleber *et al.,* 2015). The negative relationship between humidity and particulate OM quantity was already shown by Amelung *et al.* (1998) for soils in the Great Plains. In Study I, we demonstrate this also for the Siberian steppe soils, as we observed a small but considerable increase of particulate OM from the forest steppe over the typical steppe to the dry steppe. While particulate OM comprised $6.9 \pm 0.9\%$ of total soil OC in A horizons of the forest steppe, it was $9.8 \pm 0.9\%$ in the dry steppe, corresponding to a relative increase with aridity of 42%.

Table 1: Studies dealing with soils of different steppe regions of the world and their respective OC stocks. n.d. = not determined.

Study	Region	Vegetation subzone	Soil type	MAP (mm)	MAT (°C)	Depth (cm)	OC stock (Mg ha^{-1})
this thesis	Siberia	Forest steppe	Chernozem	350-450	1.0	0-10	51.5
						0-25	124.9
						0-60	218.4
		Typical steppe	Chernozem/ Kastanozem	300-350	1.5	0-10	41.2
						0-25	89.9
						0-60	152.8
		Dry steppe	Kastanozem/ Chernozem	250-300	2.0	0-10	36.2
						0-25	75.7
						0-60	133.7
Meyer *et al.* 2006	Siberia	Typical steppe	Chernozem	270	1.6	0-18 (A horizon)	110.4
		Forest steppe	Chernozem	319	0.8	0-37 (A horizon)	250.4
Kalinina *et al.* 2011	European Russia	Steppe	Chernozem	350-570	5.4	0-50	260.0
Mikhailova *et al.* 2000	European Russia	Steppe	Chernozem	587	5.4	0-103	339.0
Li *et al.* 2015	Central Asia	Typical steppe	n.d.	n.d.	n.d.	0-100	88.4
Follett *et al.* 2015	Great Plains	n.d.	n.d.	633	9.4	0-10	29.6
Doran *et al.* 1998	Great Plains	n.d.	Kastanozem	446	10.0	0-30	62.8
Ingram *et al.* 2008	Great Plains	n.d.	Kastanozem	425	8.0	0-60	80.5
Beniston *et al.* 2014	Great Plains	Tall-grass prairie	n.d.	730	13.2	0-100	153.0

In summary, Siberian steppe soils exhibit larger OC stocks than soils from other steppe regions of the world, while more OC is stored within mineral-organic associations. Thus, the large amounts of OC are sequestered in the long-term, since mineral-bound OC was shown to have high ^{14}C ages (Study I and III). The large soil OC stocks result possibly from a moister climate which leads to enhanced NPP and higher soil OM inputs, while the formation of mineral-organic associations is increased due to the enhanced water availability. However,

similar to other steppe regions of the world, Siberian steppe soils reveal decreasing OC stocks and increasing quantities of particulate OC along aridity gradients.

5.2 Climate-dependent effect of LUC from grassland to cropland on OC stocks

Land-use change from grassland to cropland is generally associated with smaller soil OM inputs (due to crop harvest) and enhanced soil OM decomposition, both resulting in a decrease of soil OC stocks (reviewed by Poeplau *et al.*, 2011). Losses of soil OC due to LUC were also observed in the Siberian steppe soils, and the amount of OC lost was similar to that inspected in soils of the Great Plains or steppe soils of European Russia (Study I). Less consensus exists on the effect of LUC under different climatic conditions and how the effect of LUC on soil OM is affected by climate change. While Burke *et al.* (1989) and Guo & Gifford (2002) found a positive relationship between MAP and the relative OC loss until MAP of ca. 600 mm, Poeplau *et al.* (2011) inspected MAT to be positively related to OC losses, though none of these studies revealed reasons for this findings. Considering processes of soil OC stabilization, the amount of OC lost should be larger in soils with large quantities of particulate OM, as this represents a labile fraction and was shown to be readily lost upon cultivation of grasslands in the North American prairies (Cambardella & Elliot, 1992; Six *et al.*, 1998). Combined with the assumption that the amount of particulate OM is larger under arid conditions, we hypothesized that LUC-induced OC losses were larger under arid than under humid conditions. This was not corroborated by our results and we showed that OC losses upon cultivation of grasslands were independent from climatic conditions (Study I). Thus, under a predicted drier climate, in the course of climate change, losses of OC as a result of LUC are expected to remain at the same critical level as is observed now. This was attributed to the small share of particulate OC in the total soil OC and the climate-independent vulnerability of mineral-bound OC, to which most LUC-induced losses were assigned (see Study I). Remarkably, 80–90% of OC losses originated from mineral-organic associations, indicating that mineral-bound OM in Siberian steppe soils is susceptible to LUC. A possible reason is that the soils are weakly weathered and have a high pH which consequently results in weak adsorption of OM on mineral surfaces and, thus, large vulnerability to disturbances (Kleber *et al.*, 2015). However, high ^{14}C ages of mineral-bound OM in croplands (500–2,900 years B.P.) suggest that mineral-organic associations contain also stable OM components.

Nevertheless, questions arise whether factors other than climate affect the relative loss of soil OC upon LUC. In order to reveal possible relations, I plotted the relative OC loss in A horizons against various soil parameters, based on data of Study I (Figure 5). Remarkably, none of the investigated parameters showed a clear relation to the relative soil OC loss. Only a slight relation was evident with respect to the soil depth of A horizons and clay content, with smaller OC losses in deep A horizons or samples with large clay contents. Smaller OC losses in deep A horizons could be attributed to the fact, that the negative effect of tillage decreases with soil depth (see Study I). The relation between clay content and LUC-induced OC losses

is consistent with observations from Poeplau *et al.* (2011), who inspected an attenuating effect of clay on OC losses upon cultivation of natural grasslands in temperate soils, probably because OC is stabilized on clay-sized minerals.

Wiesmeier *et al.* (2015) investigated degraded cropland soils in the steppes of northern China and evaluated their C sequestration potential after improved land management. They detected that wind erosion leads particularly in degraded soils to substantial (>50%) losses of silt- and clay-sized particles, which are decisive for OC stabilization and sequestration. Thus, in steppes of northern China soil OC losses induced by intensive land management are irreversible and the C sequestration potential is limited due to improved land management. In soils of the Kulunda steppe very small losses of silt- and clay-sized minerals are detectable after LUC in the typical steppe and in the dry steppe, but with only 3–5% at a much lower level than observed by Wiesmeier *et al.* (2015) (Figure 6). This indicates, that the negative effect of LUC on the C sequestration potential is not as severe as detected in the steppes of northern China. A reason might be, that the Kulunda steppe is not as arid as the steppes in northern China, thus lowering the risk of wind erosion. This is confirmed by the similar percentage of silt- and clay-sized particles under grassland and cropland in the more humid forest steppe, suggesting that wind erosion has not occurred in these soils.

Improved land management may refer to sustainable soil tillage systems, such as conservative tillage practices like no-tillage (no-till) or mini-tillage (mini-till). Along two transects of different tillage systems in the dry steppe we could assess the effect of tillage on soil OC stocks. The losses of OC were larger under intensive tillage systems (mini-till *vs.* no-till, plough *vs.* mini-till), indicating that reduced soil tillage has the potential to sequester OC (Figure 7). This is in line with many studies from North American prairie soils, which found larger OC stocks under no-tillage as compared to conventional tillage (reviewed by West & Post, 2002). Six *et al.* (2000a) found that the frequent disruption of macro-aggregates in intensive tillage systems and the concomitant increased macro-aggregate turnover inhibits the formation of stable micro-aggregates within macro-aggregates, in which OC is sequestered in the long-term, hence, reducing OC stocks under conventional tillage systems. Moreover, macro-aggregate occluded OM is released upon the tillage-induced macro-aggregate disruption and preferentially mineralized by microorganisms, resulting in a decrease of soil OC (Elliott, 1986; Cambardella & Elliott, 1993, 1994). In soils of the Kulunda steppe the latter process is probably not decisive, since OM mineralization rates were similar between intact and crushed macro-aggregates in the incubation experiment of Study II. In contrast, the stabilization of OC in micro-aggregates, as proposed by Six *et al.* (2000a), or by association with mineral-surfaces appears to be more important.
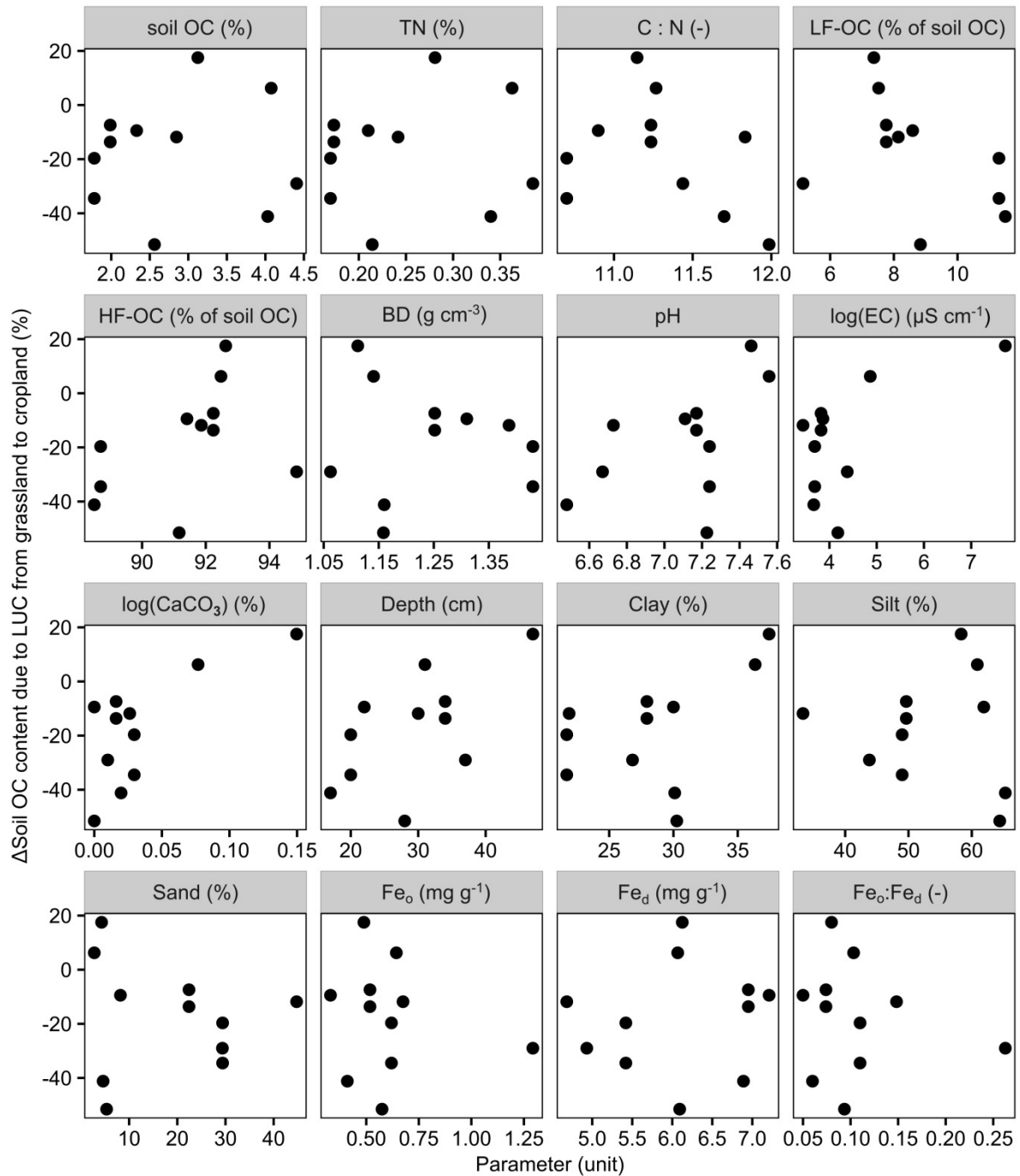
Figure 5: Change (Δ) of soil OC contents due to LUC from grassland to cropland in A horizons as a function of 16 parameters. Each panel highlights the relation to a certain parameter, with the parameter and its unit given in the panel title. The parameter values reflect soil conditions before LUC, i.e. from the grassland soils. Abbreviations: LUC = land-use change, OC = organic carbon, TN = total nitrogen, LF-OC = light fraction organic carbon, HF-OC = heavy fraction organic carbon, BD = bulk density, EC = electrical conductivity, Depth = A horizon depth, Fe$_o$ = oxalate-extractable Fe, Fe$_d$ = dithionite-extractable Fe.
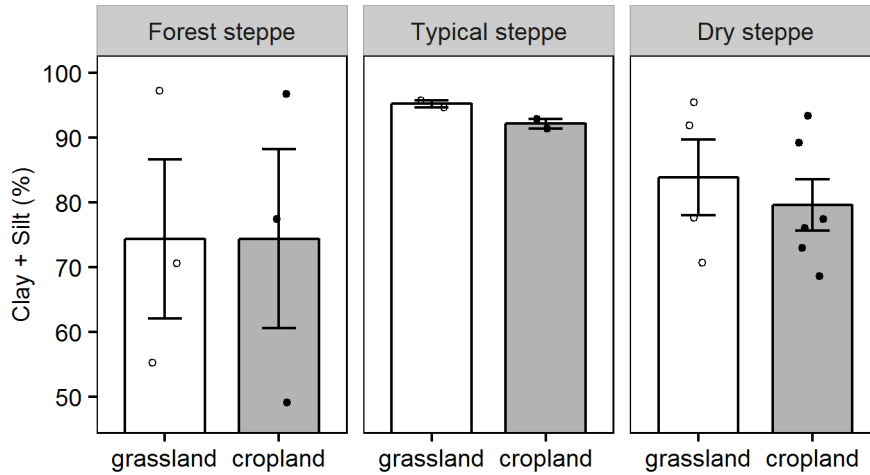
Figure 6: Percentage of clay and silt under paired grassland and cropland plots of three steppe types. Shown are arithmetic means ± standard error of the mean.
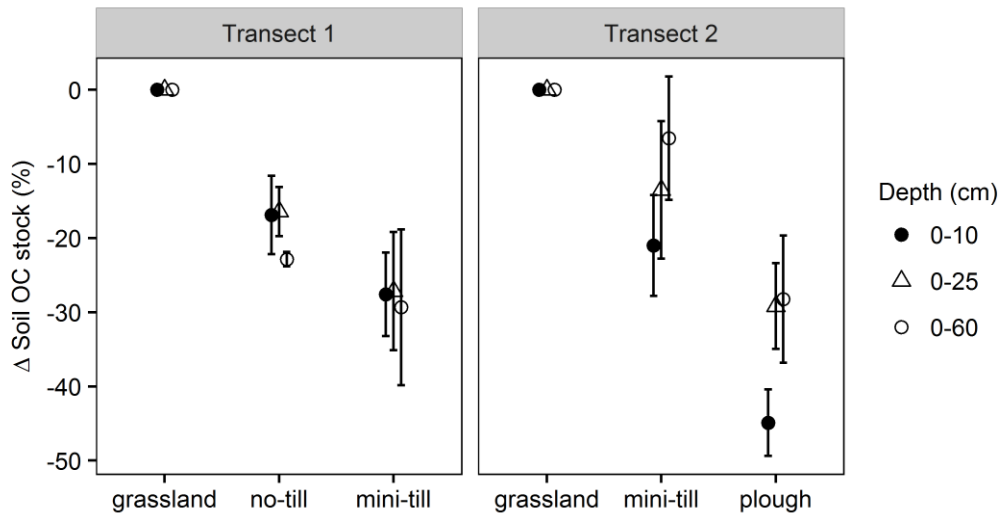

Figure 7: Soil OC stock change after LUC from grassland to cropland as function of soil management in three depths along two transects.

Summing up, in soils of the Kulunda steppe losses of OC due to LUC from grassland to cropland are in the same order of magnitude as observed in other steppe regions of the world. Remarkably, most of OC-losses originated from mineral-organic associations but not from the disruption of macro-aggregates and the subsequent mineralization of particulate OM. LUC-induced OC losses were not related to climate and, thus, are not expected to change in the course of climate change. Improved soil management has the potential to sequester OC and, hence, ameliorate degraded soils. Most of OC is thereby stabilized in micro-aggregates and/or on mineral-surfaces.

5.3 Protection of macro-aggregate occluded OM against decomposition

There is much evidence that macro-aggregate occluded OM is protected against decomposition, particularly in weakly weathered steppe soils where the formation of mineral-organic associations is thought to be limited. Evidence is given by the long mean residence time of macro-aggregate occluded OM, ranging between 10 and 150 years (Six *et al.*, 2002), or increased OM mineralization rates after macro-aggregate disruption (Gupta & Germida, 1988; Beare *et al.*, 1994; Bossuyt *et al.*, 2002; Pulleman & Marinissen, 2004). Thus, we hypothesized that macro-aggregate occluded OM is also protected against decomposition in the weakly weathered steppe soils of Siberia. However, our results suggest that the protection of OM within macro-aggregates plays a minor role in the studied soils and the LUC-induced OC decline is not attributed to the mineralization of macro-aggregate occluded OC (Study II). It appears that the stabilization of OM within micro-aggregates and/or on mineral surfaces is more decisive. Hence, the relative importance of OM stabilization mechanisms in the Siberian steppe soils seems to be different than those observed in other steppe regions of the world, where macro-aggregate protection was shown to be relevant. Two reasons can be considered for the observed differences to other steppe regions: (i) soil OM inputs by plant residues are smaller in the Siberian soils, or (ii) the climate in Siberian steppes is more humid than in comparable steppe regions. While small soil OM inputs can result in small quantities of particulate OM (Gulde *et al.*, 2008; Brown *et al.*, 2014), the decomposition of particulate OM is accelerated under more humid conditions with increased formation of mineral-organic associations (Kleber *et al.*, 2015). Thus, both factors result in smaller proportions of particulate OM, which is the dominant OM fraction protected against decomposition by occlusion within macro-aggregates. This means, if there is no particulate OM in these soils, there is nothing to protect. In Study I we showed, that the proportion of particulate OM is indeed very small when compared to other steppe regions of the world. Moreover, the percentage of macro-aggregate occluded OM which was mineralized during the long-term incubation in Study II (up to $8 \pm 4\%$ in the forest steppe, and up to $5 \pm 1\%$ in the typical steppe) corresponded well to the proportion of particulate OM determined in Study I ($7 \pm 1\%$ *vs.* $8 \pm 1\%$). This suggests that it was preferably particulate OM which was mineralized during the incubation, though accurate statements can only be made if the source of emitted CO_2 was measured, e.g. by analyzing $^{14}CO_2$ where it is possible to distinguish between old C (mineral-bound OM) and young C (particulate OM). However, these results propose that the stabilization of macro-aggregate occluded OM is of less importance in the Siberian steppes, since these soils exhibit only small proportions of particulate OM.

5.4 Microbial community composition along climatic, land-use and salinity gradients

The microbial community composition was shown to be affected along climate or land-use gradients (Frey *et al.*, 2008; Li *et al.*, 2014), but little is known about the interaction between

both factors. In soils of the Kulunda steppe, climate had a larger effect on the microbial community composition than LUC, while the microbial community composition was more similar under croplands than under grasslands of varying climate (Study I). This indicates, that climate change would result in an alteration of microbial communities but this alteration is attenuated by LUC. As the area of cropland soils clearly exceeds that of grassland soils in the study area (>90% of the area is cropland; Frühauf, 2011), the overall effect of climate change on microbial communities in the Kulunda steppe is expected to be small.

Salinity was shown to affect microbial communities as a result of osmotic stress or ion toxicity (Schimel *et al.*, 2007; Rath & Rousk, 2015). Our results from a soil salinity gradient in the dry steppe indicate only little alteration of the microbial community composition with increasing salinity (Study III). In contrast, microbial communities were different between soil horizons and, thus, affected by soil depth. This was also observed in temperate soils, where fungi : bacteria ratios decreased with depth, which was assigned to larger quantities of particulate OM and more readily available C sources in topsoils, at which fungi are superior over bacteria (Fierer *et al.*, 2003). However, in the Kulunda steppe fungi : bacteria ratios were similar between soil horizons while subsoils were enriched in PLFA from unspecific bacteria. In this regard it is problematic that the PLFA-method yielded not enough resolution to conclude to what extend bacterial communities were affected by different soil horizons. Nevertheless, our results suggest that the PLFA-based microbial communities in the studied soils were quite resistant to salinity stress.

One should consider that the PLFA method is not as resolutive as e.g. molecular methods such as DNA or rRNA extraction (Kaur *et al.*, 2005; Frostegård *et al.*, 2011). While the analysis of PLFA aims particularly at distinguishing microbes according to their cell wall properties, hence, allowing for a distinction on a phenotype level, molecular methods provide insights about the genetic variation of microorganisms resulting in a distinction of genotypes (Kaur *et al.*, 2005). This can be important, as the distinction of functional microbial groups occurs very likely on family or phyla levels (Schimel & Schaeffer, 2012). Thus, one should note that, though changes in the PLFA-based microbial community composition were small along the salinity gradient, they may be larger when using DNA or rRNA methods and differences between soils or horizons can be more prominent.

In summary, PLFA-based microbial community compositions in soils of the Kulunda steppe are not expected to change much in the course of climate change. Though, changes along the climatic gradient were detected, these changes were attenuated by the effect of grassland to cropland conversion. Given the much larger area of croplands in the region, the overall effect of climate change is expected to be small. Also salinity is not expected to change PLFA-based microbial groups considerably.

5.5 The effect of fungi on aggregate stability

Fungal hyphae entangle soil particles and, hence, promote the formation of stable soil aggregates (Tisdall & Oades, 1982; Six *et al.*, 2004). Previous studies showed that fungal abundance was positively related to aggregate formation and stability in prairie soils of the Great Plains (Guggenberger *et al.*, 1999; Bossuyt *et al.*, 2001). Thus, we hypothesized also a positive effect of fungi on aggregate stability in soils of the Kulunda steppe. In contrast, our results revealed no correlation between fungal PLFA abundance and aggregate stability, indicating that the formation of stable aggregates was unaffected by the occurrence of fungi (Study I). Kiem & Kandeler (1997) concluded that aggregate stability is less mediated by microbial abundance in soils with large clay (>35%) and OM contents. Soils in the Kulunda steppe had clay contents between 26% and 34% and were rich in OM, thus, the stabilization of aggregates by fungi can be of less importance according to Kiem & Kandeler (1997). Also De Gryze *et al.* (2005) found no aggregate-stabilizing effect of fungi in a silty clay loam soil with 24% clay, while a positive effect of fungi on aggregate stability was prominent in sandy and silty loams, thus the authors concluded that fungi are less important for aggregate formation in more clayey soils. Moreover, Blankinship *et al.* (2016) assessed the contribution of plant growth and rooting on aggregate stability and found that particularly in dry ecosystems the stabilizing effect of plant roots on aggregates is decisive.

Summing up, fungi were not a critical driver for the formation of stable aggregates in soils of the Kulunda steppe, since clay-sized minerals, the presence of OM, and the enmeshing of aggregates by plant roots are probably more decisive for aggregate formation and stability.

5.6 OM dynamics along salinity gradients

Soil salinity has detrimental effects on plant growth as it causes water stress by lowering the osmotic potential and as it impedes the uptake of nutrients due to ion competition (Qadir & Schubert, 2002; Läuchli & Grattan, 2007). As a result, soil OM inputs by plant residues are generally reduced in salt-affected soils, which is thought to be the main reason for the concomitant small OC stocks in these soils (Wong *et al.*, 2010). Thus, we hypothesized that also in soils of the Kulunda steppe OC stocks would decrease with salinity. In contrast, we determined increasing OC stocks along a salinity gradient in soils of the dry steppe type in the Kulunda steppe (Study III). This was assigned to (i) the similar plant growth, as determined by above-ground biomass, along the salinity gradient which presumably results in similar soil OM inputs, and (ii) the large quantity of mineral-associated OM in salt-affected soils, whose formation is fostered due to the high ionic strength of the soil solution under saline soil conditions. By that, our results challenge previous studies which found smaller OC stocks in saline soils due to smaller soil OM inputs (Wong *et al.*, 2010). On the other hand, previous studies showed that sodicity results in a smaller percentage of mineral-associated OM due to the dispersing effect of Na^+ on OM and mineral components (Peinemann *et al.*, 2005). Along the studied salinity transect in the Kulunda steppe, sodicity increased concurrently, thus the

effect of sodicity was superimposed by the salinity effect. Since higher ionic strength in the largely saline soils fostered flocculation and, hence, the formation of mineral-organic associations, the dispersing effect of large sodicity was not evident (Study III).

To summarize, soil OC stocks in the studied soils increased with salinity, thus salt-affected soils contributed significantly to the soil OC storage in the Kulunda steppe. Most of OC was in association with mineral-surfaces and, as indicated by the high ^{14}C ages of mineral-bound OM, effectively sequestered in the long-term.

5.7 The contribution of IC to total C stocks and its role in terms of C sequestration

Soil IC contributes substantially to total C stocks in semi-arid environments (Lal, 2004a). It was estimated that IC comprised >90% of total C down to 1m depth in grassland and cropland soils of the semi-arid Loess Plateau in China (Shaoxuan *et al.*, 2016). Mi *et al.* (2008) analyzed IC and OC stocks across soils of entire China and concluded that IC storage exceeded that of OC where MAP is <400mm. As this is the precipitation range also observed in the Kulunda steppe, I seek to determine the contribution of soil IC to total C as function of soil type and climate also in the Kulunda soils.

Soil IC was calculated by multiplying the gravimetrical carbonate content ($CaCO_3$), as determined by the Scheibler volumetric method (Schlichting *et al.*, 1995), with 12/100 as this represents the molar mass ratio of C in $CaCO_3$. By multiplying soil IC contents with the respective bulk density IC stocks were obtained, according to the calculation of OC stocks in Study I (see Study I, Material & Methods). Soil IC stocks were determined down to 1m depth across all investigated sites from Study I, II and III. To account for the tillage-induced change of soil bulk density in croplands and the subsequent alteration of soil mass within 1m soil depth, soil IC stocks under cropland were mass-corrected according to Ellert & Bettany (1995), using the adjacent grassland as reference. This was only necessary for soils from Study I, as Study II comprised only one soil profile at a grassland and Study III did not consider arable soils. Moreover, mass-correction could only be done for paired plots, while it was not feasible for single cropland plots, thus, for these plots soil IC stocks had to be taken as measured. The mass correction was done in the same way for soil OC and total C stocks. This resulted in total in 42 profiles which could be considered in the analysis, 27 from paired plots which were subject to mass correction, 4 which could not be mass-corrected, and 11 where mass correction was not necessary. For a detailed description about the definition and use of paired plots in this thesis, please refer to the method description in Study I.

The results show that IC stocks were slightly larger in the more arid dry steppe, as compared to the more humid typical and forest steppe types, mostly due to the consideration of Solonchaks which exhibited large IC stocks (Figure 8). In terms of percentage contribution, IC comprised about 30 ± 5% of total C in forest steppe soils, 42 ± 5% in typical steppe soils,

and 48 ± 5% in dry steppe soils. When compared between soil types, IC accounted for 31 ± 3% of total C in Chernozems, while it was 46 ± 4% in Kastanozems, and even 71 ± 2% in Solonchaks. This indicates the large relative importance of IC as part of total C stocks particularly in soils developing under dry climates also in the Kulunda steppe, and corroborates previous research (Mi *et al.*, 2008).
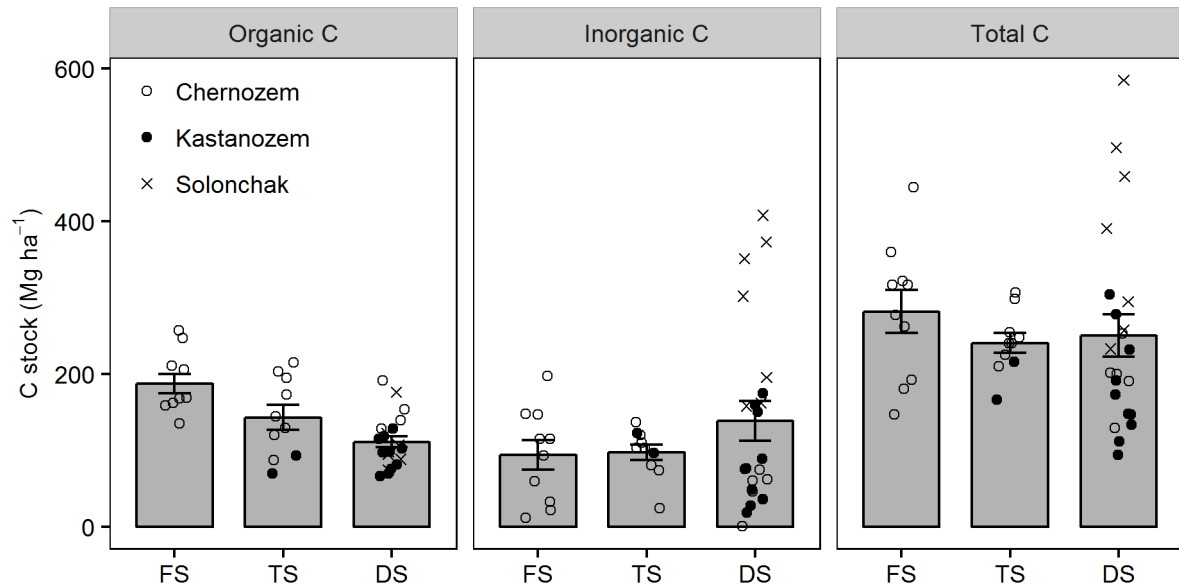

Figure 8: Carbon stocks in 0-100 cm partitioned between OC, IC and total C dependent on steppe type and soil type. Shown are arithmetic means ± standard error, and individual measurements as dots. Abbreviations: FS = forest steppe, TS = typical steppe, DS = dry steppe.

In the last decades increasing attention was paid to the fate of C after dissolution of carbonates and the subsequent leaching as DIC (Hamilton *et al.*, 2007; Liu *et al.*, 2010, 2011). Carbonate is dissolved in the soil due to reaction with acids, for example carbonic acid (H_2CO_3) or nitric acid (HNO_3). At pH >5, the carbonate dissolution by H_2CO_3 is more relevant than that by strong acids like HNO_3 (Hamilton *et al.*, 2007) and occurs according to the following reaction:

$$CaCO_3 + H_2CO_3 = Ca^{2+} + 2HCO_3^- \qquad \qquad (eq.1)$$
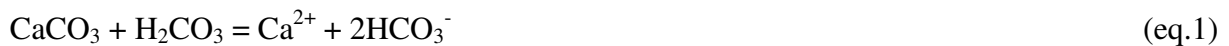
Thus, the dissolution of $CaCO_3$ consumes H_2CO_3 while Ca^{2+} and HCO_3^- (bicarbonate) is produced. The bicarbonate ions are, together with CO_2 and CO_3^{2-}, referred to as DIC. The formation of H_2CO_3, in turn, consumes CO_2 according to equation 2:

$$CO_2 + H_2O = H_2CO_3 \qquad \qquad (eq.2)$$

If the bicarbonate ions from eq.1 are leached from the soil to the groundwater and are subsequently discharged into rivers, they eventually end up in the oceans, where they may precipitate again to carbonate, thereby releasing the previously uptaken soil CO_2 (Milliman, 1993). Hamilton *et al.* (2007) noted that the two processes of (i) carbonate dissolution (CO_2

consumption) in the soil and (ii) carbonate formation (CO_2 release) in the ocean act on two different time scales. They suggested, that the dissolution of carbonate in the soil and the subsequent transport of DIC in groundwater and rivers to the oceans act as C sink on a decadal time scale, as the subsequent precipitation of DIC as carbonate minerals occurs with a time lag of centuries. Moreover, some of the precipitated oceanic carbonate sinks down to the ocean floor, becomes buried and, thus, removed from the contemporary C cycle (Milliman, 1993). Furthermore, Liu *et al*. (2010) remarked that not all of the DIC which is discharged into the oceans becomes subject to carbonate precipitation but that some of it is also used by aquatic organisms to carry out photosynthesis and, hence, becomes incorporated in organic tissues. Since part of the dead biota and feces fall down to the ocean floor, they become buried and removed from the contemporary C cycle, similarly as precipitated carbonate minerals. Thus, we may conclude that once DIC, derived from carbonate dissolution by carbonic acid, is leached from the soil into the groundwater, it resembles a C sink removing CO_2 from the atmosphere. In contrast, if the DIC is not leached from the soil but remains within the soil column, for example due to reduced groundwater recharge as a result of dry climate, it neither acts as a sink nor as a source, as it is solely redistributed within the soil. This means that, under a predicted drier climate in the Kulunda steppe, the potential C sink of the soils, as originating from the dissolution of the large IC stocks, becomes less important. Drier climate, therefore, is not only expected to decrease the C sequestration potential of the soils by lowering OC stocks, but also by limiting the potential of the soils to act as C sink via dissolution and subsequent leaching of IC.

6   Conclusions and Outlook

Soils of the Siberian Kulunda steppe exhibited large OC stocks, both in the non-salt-affected soils like Chernozems and Kastanozems as well as in the salt-affected Solonchaks. The observed OC stocks were generally larger than those determined in other steppe regions of the world, possibly due to a more humid climate which results in enhanced NPP and consequently large soil OM inputs. Soil OC stocks followed a climatic gradient and were larger in the more humid forest steppes than in the more arid dry steppes. This implies, that future drier climate conditions are expected to result in smaller soil OC stocks in this region. In all investigated soil types (Chernozems, Kastanozems, Solonchaks) >90% of OC was stored in mineral-organic associations, which is much more than previously observed in comparable steppe regions of the world, while particulate OM accounted for maximally 10% of total OC. The differences to other steppe regions on earth were probably assigned to a more humid climate in the Siberian steppes.

Mineral-bound OM revealed high ^{14}C ages in all soil types, indicating that it represents a stable OM fraction with relatively slow turnover times. However, the majority of OM which was lost upon cultivation of grasslands originated from mineral-organic associations, suggesting that this OM fractions comprised also vulnerable OM components with fast turnover times. The quantity of particulate OM increased slightly with aridity, in turn, the amount of mineral-bound OM decreased concomitantly, promoting the observation that sufficient water is needed for the formation of mineral-organic associations.

Land-use change from grassland to cropland resulted in a loss of OC by about 31% in 0–25 cm, which corresponds to observations from other steppe regions on earth. The quantity of lost OC was independent from climatic conditions, implying that climate change is not expected to alter the effect of LUC on soil OC quantities. The decline of OC after LUC was not attributed to the tillage-induced break-down of macro-aggregates and the subsequent mineralization of previously occluded particulate OM, but most of the OC loss originated from mineral-organic associations. Thus, macro-aggregate occluded OM is not stabilized against decomposition in these soils, while the stabilization of soil OM on mineral surfaces (as indicated by high ^{14}C ages of mineral-bound OM) and/or by occlusion within micro-aggregates appeared decisive. For future research, the study of the role of hydrophobicity could be promising to unravel the entire palette of OM stabilization mechanisms in steppe soils, since previous work suggested that reduced surface wettability limits OM accessibility by microorganisms and is therefore crucial for OM stabilization (von Lützow *et al.*, 2006). Particularly in the frequently dry steppe soils hydrophobic surfaces could restrain the access of microorganisms to the organic substrate and, hence, stabilize soil OM.

In most steppe regions on earth the majority of grasslands is already converted into croplands. Thus the implementation of improved land management systems, such as no-tillage or mini-tillage, deserves great attention in the future when analyzing the C sequestration potential of steppe soils. Based on a comparison of different management practices and the assessment of the loss of silt- and clay-sized particles due to wind erosion, it can be concluded that in the Kulunda steppe degraded croplands may be ameliorated by improved land management, thus bearing the potential to sequester previously lost OC.

Moreover, the application of nutrients by fertilization could add to the strategies of improved land management and increase crop yields. The majority of farmers in the Kulunda steppe does not apply fertilizers (neither organic nor mineral) so far, since the application is too costly (own interviews with farmers of the region). Thus, there is still a large potential for improving management strategies. From the point of view of C sequestration, nutrient application could be beneficial as previous studies showed that an increased nutrient availability enhanced the stock of mineral-bound OM (Kirkby *et al.*, 2013, 2014, 2016). This was explained by the concurrent increase of soil microbial biomass which is the parent material for mineral-organic associations. Hence, future studies should also consider the nutrient status of the soils in the studied region.

The analysis of PLFA revealed that fungal abundance was not related to aggregate stability. This was assigned to the large OM contents and the relatively high clay contents (26–34%) as well as the aggregate promoting effect of plant roots. Future drier climate conditions are expected to alter PLFA-based microbial community compositions with a smaller abundance of fungi and a larger abundance of gram-positive bacteria, while LUC will attenuate the climatic effect. Increasing salinity caused only small changes in the composition of PLFA-based microbial communities with a larger variability of fungal PLFA under saline conditions. However, since PLFA analysis is not as resolutive as e.g. rRNA analysis, molecular methods could be a promising tool to gain deeper insights into possible changes of the microbial community even on a genotype level. Moreover, recent research indicated the importance of soil food web analysis to elucidate the role of soil biota on OC dynamics, e.g. by accounting for predator-prey relationships and including the role of the meso- and macrofauna in the OM decomposition process (de Vries *et al.*, 2013). Thus, future research in the Siberian steppes could benefit from advanced molecular methods and soil food web analysis which are expected to provide deeper insights into the role of certain functional microbial groups in soil OM dynamics.

The determination of OC stocks along a salinity gradient showed that the OC storage increased with salinity, hence, challenging observations from previous studies. This was assigned to an adaptive plant community whose productivity, as expressed by above-ground biomass, was unaffected by salinity stress, thus maintaining soil OM inputs constant along the salinity gradient. At the same time, the formation of mineral-organic associations was fostered in salt-affected soils by the high ionic strength of the soil solution. Therefore, soil OM became

stabilized under high salinity which resulted in large OC stocks. Concurrently, the dispersing effect of sodicity on OM and mineral components became attenuated by the salinity-induced flocculation of soil constituents. Accordingly, even saline-sodic soils exhibited large mineral-bound OM contents with high ^{14}C ages, indicating a slow OM turnover in the mineral fraction. By separating soil OM into functionally different OM fractions, we showed in Study III for the first time that in salt-affected soils particulate OM is not as stable as previously assumed. On the other hand, mineral-associated OM is more stable as yet expected. We demonstrate that salt-affected soils contribute significantly to the OC storage in Siberian steppe soils, while most of OC is associated to minerals and thus effectively sequestered in the long-term.

When also accounting for IC, existing in form of carbonates, the salt-affected Solonchaks contained the largest C stocks in the entire Kulunda steppe. Based on theoretical considerations, carbonate dissolution in the Kulunda soils acts as a C sink. However, due to the increase of aridity in the course of climate change carbonate dissolution becomes limited. Thus, future drier climate conditions in the Siberian steppes are not only expected to decrease the soil C sequestration potential by lowering soil OC stocks in the region, but also by lowering the potential to sequester IC via carbonate dissolution.

Finally, I like to cite Powlson *et al.* (2011), who concluded that combating climate change by solely focusing on soil C sequestration may distract from other essential mitigation measures, such as reducing N_2O emissions from arable soils or the extend of deforestation in tropical regions. Albeit the reduction of fossil fuel combustion is of particular importance. The mitigation of climate change is a multifactorial task and the implementation of many measures is the only way to keep global warming as little as possible. However, enhancing soil OM has not only the potential to mitigate climate change, but it is particularly important to keep our soils fertile and suitable for agricultural use.

7 References

Amelung W, Flach KW, Zhang X, Zech W (1998) Climatic effects on C pools of native and cultivated prairie. *Advances in GeoEcology*, **31**, 217–224.

Amini S, Ghadiri H, Chen C, Marschner P (2016) Salt-affected soils, reclamation, carbon dynamics, and biochar: a review. *Journal of Soils and Sediments*, **16**, 939–953.

Batjes NH (2016) Harmonized soil property values for broad-scale modelling (WISE30sec) with estimates of global soil carbon stocks. *Geoderma*, **269**, 61–68.

Bazilevich NI (1993) *Biological productivity of ecosystems of northern europe and asia*. Nauka Publishing House, Moscow, Russia.

Beare MH, Hendrix PF, Cabrera ML, Coleman DC (1994) Aggregate-protected and unprotected organic matter pools in conventional- and no-tillage soils. *Soil Science Society of America Journal*, **58**, 787–795.

Beniston JW, DuPont ST, Glover JD, Lal R, Dungait JAJ (2014) Soil organic carbon dynamics 75 years after land-use change in perennial grassland and annual wheat agricultural systems. *Biogeochemistry*, **120**, 37–49.

Blankinship JC, Fonte SJ, Six J, Schimel JP (2016) Plant versus microbial controls on soil aggregate stability in a seasonally dry ecosystem. *Geoderma*, **272**, 39–50.

Blume H-P, Brümmer GW, Horn R et al. (2010) *Scheffer/Schachtschabel - Lehrbuch der Bodenkunde*, 16th edn. Spektrum Akademischer Verlag GmbH, Heidelberg, Berlin, Germany, 593 pp.

Bossuyt H, Denef K, Six J, Frey SD, Merckx R, Paustian K (2001) Influence of microbial populations and residue quality on aggregate stability. *Applied Soil Ecology*, **16**, 195–208.

Bossuyt H, Six J, Hendrix PF (2002) Aggregate-protected carbon in no-tillage and conventional tillage agroecosystems using carbon-14 labeled plant residue. *Soil Science Society of America Journal*, **66**, 1965–1973.

Breulmann M, Masyutenko NP, Kogut BM, Schroll R, Dörfler U, Buscot F, Schulz E (2014) Short-term bioavailability of carbon in soil organic matter fractions of different particle sizes and densities in grassland ecosystems. *The Science of the total environment*, **497–498**, 29–37.

Brown KH, Bach EM, Drijber RA, Hofmockel KS, Jeske ES, Sawyer JE, Castellano MJ (2014) A long-term nitrogen fertilizer gradient has little effect on soil organic matter in a high-intensity maize production system. *Global Change Biology*, **20**, 1339–1350.

Burke IC, Yonker CM, Parton WJ, Cole CV, Flach K, Schimel DS (1989) Texture, climate, and cultivation effects on soil organic matter content in US grassland soils. *Soil Science Society of America Journal*, **53**, 800–805.

Burke IC, Lauenroth WK, Parton WJ (1997) Regional and temporal variation in net primary

production and nitrogen mineralization in grasslands. *Ecology*, **78**, 1330–1340.

Burns RG, Dick RP (2002) Enzymes in the environment: Activity, ecology and applications. *Books in soils, plants, and the environment series*, **86**, 1–640.

Cambardella CA, Elliot ET (1992) Particulate soil organic-matter changes across a grassland cultivation sequence. *Soil Science Society of America Journal*, **56**, 777–783.

Cambardella CA, Elliott ET (1993) Carbon and nitrogen distribution in aggregates from cultivated and native grassland soils. *Soil Science Society of America Journal*, **57**, 1071–1076.

Cambardella CA, Elliott ET (1994) Carbon and nitrogen dynamics of soil organic matter fractions from cultivated grassland soils. *Soil Science Society of America Journal*, **58**, 123–130.

Castellano MJ, Mueller KE, Olk DC, Sawyer JE, Six J (2015) Integrating plant litter quality, soil organic matter stabilization, and the carbon saturation concept. *Global Change Biology*, **21**, 3200–3209.

Christensen BT (1992) Physical fractionation of soil and organic matter in primary particle size and density separates. *Advances in Soil Science*, **20**, 2–76.

Ciais P, Sabine C, Bala G et al. (2013) Carbon and other biogeochemical cycles. In: *Climate Change 2013: The Physical Science Basis. Contribution of Working Group I to the Fifth Assessment Report of the Intergovernmental Panel on Climate Change.* (eds Stocker TF, Qin D, Plattner G-K, Tignor M, Allen SK, Boschung J, Nauels A, Xia Y, Bex V, Midgley PM), pp. 465–570. Cambridge University Press, Cambridge, United Kingdom and New York, NY, USA.

Dang Y, Ren W, Tao B et al. (2014) Climate and land use controls on soil organic carbon in the Loess Plateau region of China. *PLoS ONE*, **9**, 1–11.

Doran JW, Elliott ET, Paustian K (1998) Soil microbial activity, nitrogen cycling, and long-term changes in organic carbon pools as related to fallow tillage management. *Soil and Tillage Research*, **49**, 3–18.

Ellert BH, Bettany JR (1995) Calculation of organic matter and nutrients stored in soils under contrasting management regimes. *Canadian Journal of Soil Science*, **75**, 529–538.

Elliott ET (1986) Aggregate structure and carbon, nitrogen, and phosphorus in native and cultivated soils. *Soil Science Society of America Journal*, **50**, 627–633.

Essington ME (2004) *Soil and water chemistry - An integrative approach*. CRC Press, Boca Raton, USA, 534 pp.

FAO (2001) Lecture notes on the major soils of the world (eds Driessen P, Deckers J, Spaargaren O, Nachtergaele F). *World soil resources reports*, **94**, 336pp.

FAO (2013) *FAO Statistical yearbook 2013 - World food and agriculture*. Rome, Italy, 289 pp.

Fierer N, Schimel JP, Holden PA (2003) Variations in microbial community composition through two soil depth profiles. *Soil Biology and Biochemistry*, **35**, 167–176.

Flessa H, Amelung W, Helfrich M et al. (2008) Storage and stability of organic matter and

fossil carbon in a Luvisol and Phaeozem with continuous maize cropping: A synthesis. *Journal of Plant Nutrition and Soil Science*, **171**, 36–51.

Follett RF, Stewart CE, Pruessner EG, Kimble JM (2015) Great Plains climate and land-use effects on soil organic carbon. *Soil Science Society of America Journal*, **79**, 261.

Fontaine S, Henault C, Aamor A et al. (2011) Fungi mediate long term sequestration of carbon and nitrogen in soil through their priming effect. *Soil Biology and Biochemistry*, **43**, 86–96.

Frey SD, Elliott ET, Paustian K, Peterson GA (2000) Fungal translocation as a mechanism for soil nitrogen inputs to surface residue decomposition in a no-tillage agroecosystem. *Soil Biology and Biochemistry*, **32**, 689–698.

Frey SD, Drijber R, Smith H, Melillo J (2008) Microbial biomass, functional capacity, and community structure after 12 years of soil warming. *Soil Biology and Biochemistry*, **40**, 2904–2907.

Frostegård Å, Bååth E (1996) The use of phospholipid fatty acid analysis to estimate bacterial and fungal biomass in soil. *Biology and Fertility of Soils*, **22**, 59–65.

Frostegård Å, Tunlid A, Bååth E (2011) Use and misuse of PLFA measurements in soils. *Soil Biology and Biochemistry*, **43**, 1621–1625.

Frühauf M (2011) Landnutzungs- und Ökosystementwicklung in den südsibirischen Agrarsteppen. *Geografische Rundschau*, **1**, 46–53.

De Gryze S, Six J, Brits C, Merckx R (2005) A quantification of short-term macroaggregate dynamics: Influences of wheat residue input and texture. *Soil Biology and Biochemistry*, **37**, 55–66.

Guggenberger G, Elliott ET, Frey SD, Six J, Paustian K (1999) Microbial contributions to the aggregation of a cultivated grassland soil amended with starch. *Soil Biology and Biochemistry*, **31**, 407–419.

Gulde S, Chung H, Amelung W, Chang C, Six J (2008) Soil carbon saturation controls labile and stable carbon pool dynamics. *Soil Science Society of America Journal*, **72**, 605–612.

Guo LB, Gifford RM (2002) Soil carbon stocks and land use change: a meta analysis. *Global Change Biology*, **8**, 345–360.

Gupta VVSR, Germida JJ (1988) Distribution of microbial biomass and its activity in different soil aggregate size classes as affected by cultivation. *Soil Biology and Biochemistry*, **20**, 777–786.

Hamilton SK, Kurzman AL, Arango C, Jin L, Robertson GP (2007) Evidence for carbon sequestration by agricultural liming. *Global Biogeochemical Cycles*, **21**, 1–12.

ten Have R, Teunissen PJM (2001) Oxidative mechanisms involved in lignin degradation by white-rot fungi. *Chemical Reviews*, **101**, 3397–3413.

Hijoka Y, Lin E, Pereira JJ et al. (2014) Asia. In: *Climate Change 2014: Impacts, Adaptation, and Vulnerability. Part B: Regional Aspects. Contribution of Working Group II to the Fifth Assessment Report of the Intergovernmental Panel on Climate Change* (eds Barros VR, Field CB, Dokken DJ, Mastrandrea MD, Mach KJ, Bilir TE, Chatterjee M, Ebi KL,

Estrada YO, Genova RC, Girma B, Kissel ES, Levy AN, MacCracken S, Mastrandrea PR, White LL), pp. 1327–1370. Cambridge University Press, Cambridge, United Kingdom and New York, NY, USA.

Houghton RA (2003) The contemporary carbon cycle. In: *Treatise on geochemistry, Volume 8*, 2nd edn (eds Schlesinger WH, Holland HD, Turekian KK), pp. 473–513. Elsevier, Oxford, United Kingdom.

Ingram LJ, Stahl PD, Schuman GE et al. (2008) Grazing impacts on soil carbon and microbial communities in a mixed-grass ecosystem. *Soil Science Society of America Journal*, **72**, 939–948.

IPCC (2014) *Climate Change 2014: Synthesis Report. Contribution of Working Groups I, II and III to the Fifth Assessment Report of the Intergovernmental Panel on Climate Change* (eds Team CW, Pachauri RK, Meyer LA). IPCC, Geneva, Switzerland, 151 pp.

IUSS Working Group WRB (2014) World reference base for soil resources 2014. International soil classification system for naming soils and creating legends for soil maps. *World Soil Resources Reports No. 106*, FAO, Rome, Italy, 191pp.

Jenkinson DS, Harkness DD, Vance ED, Adams DE, Harrison AF (1992) Calculating net primary production and annual input of organic matter to soil from the amount and radiocarbon content of soil organic matter. *Soil Biology & Biochemistry*, **24**, 295–308.

Jobbagy EG, Sala OE, Paruelo JM (2002) Patterns and controls of primary production in the patagonian steppe : A remote sensing approach. *Ecology*, **83**, 307–319.

Kalbitz K, Solinger S, Park J-H, Michalzik B, Matzner E (2000) Controls on the dynamics of dissolved organic matter in soils: A review. *Soil Science*, **165**, 277–304.

Kalinina O, Krause S-E, Goryachkin SV, Karavaeva NA, Lyuri DI, Giani L (2011) Self-restoration of post-agrogenic chernozems of Russia: Soil development, carbon stocks, and dynamics of carbon pools. *Geoderma*, **162**, 196–206.

Kaur A, Chaudhary A, Kaur A, Choudhary R, Kaushik R (2005) Phospholipid fatty acid - A bioindicator of environment monitoring and assessment in soil ecosystem. *Current Science*, **89**, 1103–1112.

Kharlamova NF, Revyakin VS (2006) Regional climate and environmental change in Central Asia. In: *Environmental Security and Sustainable Land Use - with Special Reference to Central Asia*, 1st edn (eds Vogtmann H, Dobretsov N), pp. 19–26. Springer Netherlands.

Kiem R, Kandeler E (1997) Stabilization of aggregates by the microbial biomass as affected by soil texture and type. *Applied Soil Ecology*, **5**, 221–230.

Kirkby CA, Richardson AE, Wade LJ, Batten GD, Blanchard C, Kirkegaard JA (2013) Carbon-nutrient stoichiometry to increase soil carbon sequestration. *Soil Biology and Biochemistry*, **60**, 77–86.

Kirkby CA, Richardson AE, Wade LJ, Passioura JB, Batten GD, Blanchard C, Kirkegaard JA (2014) Nutrient availability limits carbon sequestration in arable soils. *Soil Biology and Biochemistry*, **68**, 402–409.

Kirkby CA, Richardson AE, Wade LJ, Conyers M, Kirkegaard JA (2016) Inorganic nutrients increase humification efficiency and C-sequestration in an annually cropped soil. *PloS*

one, **11**, 1–17.

Kleber M, Eusterhues K, Keiluweit M, Mikutta C, Mikutta R, Nico PS (2015) Mineral-organic associations: formation, properties, and relevance in soil environments. *Advances in Agronomy*, **130**, 140pp.

Klotzbücher T, Kaiser K, Guggenberger G, Gatzek C, Kalbitz K (2011) A new conceptual model for the fate of lignin in decomposing plant litter. *Ecology*, **92**, 1052–1062.

Köchy M, Hiederer R, Freibauer A. (2015) Global distribution of soil organic carbon – Part 1: Masses and frequency distributions of SOC stocks for the tropics, permafrost regions, wetlands, and the world. *Soil*, **1**, 351–365.

Kögel-Knabner I (2002) The macromolecular organic composition of plant and microbial residues as inputs to soil organic matter. *Soil Biology and Biochemistry*, **34**, 139–162.

Kuzyakov Y, Domanski G (2000) Carbon input by plants into the soil. Review. *Zeitschrift für Pflanzenernährung und Bodenkunde*, **163**, 421–431.

Lal R (2004a) Soil carbon sequestration to mitigate climate change. *Geoderma*, **123**, 1–22.

Lal R (2004b) Soil carbon sequestration impacts on global climate change and food security. *Science*, **304**, 1623–1627.

Lal R, Follett RF, Stewart BA, Kimble JM (2007) Soil carbon sequestration to mitigate climate change and advance food security. *Soil Science*, **172**, 943–956.

Läuchli A, Grattan SR (2007) Plant growth and development under salinity stress. In: *Advances in molecular breeding toward drought and salt tolerant crops* (eds Jenks MA, Hasegawa PM, Mohan Jain S), pp. 1–32. Springer, Dordrecht, Netherlands.

Lauer W, Frankenberg P (1987) Klimaklassifikation. In: *Diercke Weltatlas*, 5th edn, pp. 220–221. Westermann, Braunschweig, Germany.

Lehmann J, Kleber M (2015) The contentious nature of soil organic matter. *Nature*, **528**, 60–68.

Li N, Yao S-H, You M-Y et al. (2014) Contrasting development of soil microbial community structure under no-tilled perennial and tilled cropping during early pedogenesis of a Mollisol. *Soil Biology and Biochemistry*, **77**, 221–232.

Li C, Zhang C, Luo G et al. (2015) Carbon stock and its responses to climate change in Central Asia. *Global Change Biology*, **21**, 1951–1967.

Liu Z, Dreybrodt W, Wang H (2010) A new direction in effective accounting for the atmospheric CO_2 budget: Considering the combined action of carbonate dissolution, the global water cycle and photosynthetic uptake of DIC by aquatic organisms. *Earth-Science Reviews*, **99**, 162–172.

Liu Z, Dreybrodt W, Liu H (2011) Atmospheric CO_2 sink: Silicate weathering or carbonate weathering? *Applied Geochemistry*, **26**, S292–S294.

von Lützow M, Kögel-Knabner I, Ekschmitt K, Matzner E, Guggenberger G, Marschner B, Flessa H (2006) Stabilization of organic matter in temperate soils: Mechanisms and their relevance under different soil conditions - A review. *European Journal of Soil Science*, **57**, 426–445.

References

Maire V, Alvarez G, Colombet J et al. (2013) An unknown oxidative metabolism substantially contributes to soil CO_2 emissions. *Biogeosciences*, **10**, 1155–1167.

Meyer H, Kaiser C, Biasi C et al. (2006) Soil carbon and nitrogen dynamics along a latitudinal transect in Western Siberia, Russia. *Biogeochemistry*, **81**, 239–252.

Mi N, Wang S, Liu J, Yu G, Zhang W, Jobbágy E (2008) Soil inorganic carbon storage pattern in China. *Global Change Biology*, **14**, 2380–2387.

Mikhailova EA, Bryant RB, Vassenev II, Schwager SJ, Post CJ (2000) Cultivation effects on soil carbon and nitrogen contents at depth in the Russian Chernozem. *Soil Science Society of America Journal*, **64**, 738–745.

Milliman JD (1993) Production and accumulation of calcium carbonate in the ocean: Budget of a nonsteady state. *Global Biogeochemical Cycles*, **7**, 927–957.

Moyano FE, Manzoni S, Chenu C (2013) Responses of soil heterotrophic respiration to moisture availability: An exploration of processes and models. *Soil Biology and Biochemistry*, **59**, 72–85.

Myhre G, Shindell D, Bréon F-M et al. (2013) Anthropogenic and natural radiative forcing. In: *Climate Change 2013: The Physical Science Basis. Contribution of Working Group I to the Fifth Assessment Report of the Intergovernmental Panel on Climate Change* (eds Stocker TF, Qin D, Plattner G-K, Tignor M, Allen SK, Boschung J, Nauels A, Xia Y, Bex V, Midgley PM), pp. 659–740. Cambridge University Press, Cambridge, United Kingdom and New York, NY, USA.

Peinemann N, Guggenberger G, Zech W (2005) Soil organic matter and its lignin component in surface horizons of salt-affected soils of the Argentinian Pampa. *Catena*, **60**, 113–128.

Persson T (1989) Role of soil animals in C and N mineralisation. **245**, 241–245.

Plante AF, Virto I, Malhi SS (2010) Pedogenic, mineralogical and land-use controls on organic carbon stabilization in two contrasting soils. *Canadian Journal of Soil Science*, **90**, 15–26.

Poeplau C, Don A, Vesterdal L, Leifeld J, Van Wesemael B, Schumacher J, Gensior A (2011) Temporal dynamics of soil organic carbon after land-use change in the temperate zone - carbon response functions as a model approach. *Global Change Biology*, **17**, 2415–2427.

Powlson DS, Smith P, Smith JU (1996) *Evaluation of soil organic matter models - using existing long-term datasets*, 1st edn. Springer-Verlag Berlin Heidelberg, 425 pp.

Powlson DS, Whitmore AP, Goulding KWT (2011) Soil carbon sequestration to mitigate climate change: A critical re-examination to identify the true and the false. *European Journal of Soil Science*, **62**, 42–55.

Pulleman MM, Marinissen JCY (2004) Physical protection of mineralizable C in aggregates from long-term pasture and arable soil. *Geoderma*, **120**, 273–282.

Qadir M, Schubert S (2002) Degradation processes and nutrient constraints in sodic soils. *Land Degradation and Development*, **13**, 275–294.

Ramankutty N, Foley JA (1999) Estimating historical changes in global land cover: Croplands from 1700 to 1992. *Global Biogeochemical Cycles*, **13**, 997–1027.

Rath KM, Rousk J (2015) Salt effects on the soil microbial decomposer community and their role in organic carbon cycling: A review. *Soil Biology and Biochemistry*, **81**, 108–123.

Schimel JP, Schaeffer SM (2012) Microbial control over carbon cycling in soil. *Frontiers in Microbiology*, **3**, 1–11.

Schimel JP, Weintraub MN (2003) The implications of exoenzyme activity on microbial carbon and nitrogen limitation in soil: A theoretical model. *Soil Biology and Biochemistry*, **35**, 549–563.

Schimel DS, Braswell BH, Holland EA et al. (1994) Climatic, edaphic, and biotic controls over storage and turnover of carbon in soils. *Global Biogeochemical Cycles*, **8**, 279–293.

Schimel J, Balser TC, Wallenstein M (2007) Microbial stress-response physiology and its implications for ecosystem function. *Ecology*, **88**, 1386–1394.

Schlichting E, Blume H-P, Stahr K (1995) *Bodenkundliches Praktikum – Eine Einführung in pedologisches Arbeiten für Ökologen, insbesondere Land- und Forstwirte, und für Geowissenschaftler*, 2nd edn. Blackwell Wissenschafts-Verlag Berlin, Wien, Austria, 144-147 pp.

Shaoxuan H, Zongsuo L, Ruilian H, Yong W, Guobin L (2016) Soil carbon dynamics during grass restoration on abandoned sloping cropland in the hilly area of the Loess Plateau, China. *Catena*, **137**, 679–685.

Six J, Elliott ET, Paustian K, Doran JW (1998) Aggregation and soil organic matter accumulation in cultivated and native grassland soils. *Soil Science Society of America Journal*, **62**, 1367–1377.

Six J, Elliott E., Paustian K (2000a) Soil macroaggregate turnover and microaggregate formation: a mechanism for C sequestration under no-tillage agriculture. *Soil Biology and Biochemistry*, **32**, 2099–2103.

Six J, Paustian K, Elliott ET, Combrink C (2000b) Soil structure and organic matter: I. Distribution of aggregate-size classes and aggregate-associated carbon. *Soil Science Society of America Journal*, **64**, 681–689.

Six J, Feller C, Denef K, Ogle SM, Moraes, J.C., Albrecht A (2002) Soil organic matter, biota and aggregation in temperate and tropical soils - effects of no-tillage. *Agronomie*, **22**, 755–775.

Six J, Bossuyt H, Degryze S, Denef K (2004) A history of research on the link between (micro)aggregates, soil biota, and soil organic matter dynamics. *Soil & Tillage Research*, **79**, 7–31.

Six J, Frey SD, Thiet RK, Batten KM (2006) Bacterial and fungal contributions to carbon sequestration in agroecosystems. *Soil Science Society of America Journal*, **70**, 555–569.

Steffens M, Kölbl A, Schörk E, Gschrey B, Kögel-Knabner I (2010) Distribution of soil organic matter between fractions and aggregate size classes in grazed semiarid steppe soil profiles. *Plant and Soil*, **338**, 63–81.

Sumner ME (1993) Sodic soils: New perspectives. *Australian Journal of Soil Research*, **31**, 683–750.

Tisdall J, Oades J (1982) Organic matter and water-stable aggregates in soils. *Journal of soil science*, **33**, 141–163.

Trumbore SE (1997) Potential responses of soil organic carbon to global environmental change. *Proceedings of the National Academy of Sciences*, **94**, 8284–8291.

United Nations, Department of Economic and Social Affairs, Population Division (2015). World population prospects: The 2015 revision, key findings and advance tables. Working Paper No. ESA/P/WP.241.

de Vries FT, Thébault E, Liiri M et al. (2013) Soil food web properties explain ecosystem services across European land use systems. *Proceedings of the National Academy of Sciences*, **110**, 14296–14301.

West TO, Post WM (2002) Soil organic carbon sequestration rates by tillage and crop rotation: A global data analysis. *Soil Science Society of America Journal*, **66**, 1930–1946.

Wiesmeier M, Munro S, Barthold F, Steffens M, Schad P, Kögel-Knabner I (2015) Carbon storage capacity of semi-arid grassland soils and sequestration potentials in northern China. *Global Change Biology*, **21**, 3836–3845.

Wolters V (2000) Invertebrate control of soil organic matter stability. *Biology and Fertility of Soils*, **31**, 1–19.

Wong VNL, Greene RSB, Dalal RC, Murphy BW (2010) Soil carbon dynamics in saline and sodic soils: A review. *Soil Use and Management*, **26**, 2–11.

Wu Z, Dijkstra P, Koch GW, Peñuelas J, Hungate BA (2011) Responses of terrestrial ecosystems to temperature and precipitation change: A meta-analysis of experimental manipulation. *Global Change Biology*, **17**, 927–942.

Yang J, Yang Y, Wu WM, Zhao J, Jiang L (2014) Evidence of polyethylene biodegradation by bacterial strains from the guts of plastic-eating waxworms. *Environmental Science and Technology*, **48**, 13776–1378